รายงานวิจัยฉบับสมบูรณ์

คาลิก[4]ซารีนควิโนนไดเมอร์สำหรับเป็นตัวตรวจจับไอออนของโลหะแอลคาไลและแอลคาไลน์เอิร์ธ

โดย ผู้ช่วยศาสตราจารย์ ดร. ธวัชชัย ตันฑุลานิ

ภาควิชาเคมี คณะวิทยาศาสตร์ จุฬาลงกรณ์มหาวิทยาลัย

พฤษภาคม 2547

สัญญาเลขที่ RSA/06/2544

รายงานวิจัยฉบับสมบูรณ์

คาลิก[4]ซารีนควิโนนไดเมอร์สำหรับเป็นตัวตรวจจับไอออนของโลหะแอลคาไลและแอลคาไลน์เอิร์ธ

ผู้ช่วยศาสตราจารย์ ดร. ธวัชชัย ตันฑุลานิ

ภาควิชาเคมี คณะวิทยาศาสตร์ จุฬาลงกรณ์มหาวิทยาลัย

สนับสนุนโดยสำนักงานกองทุนสนับสนุนการวิจัย

กิตติกรรมประกาศ

ผู้วิจัยขอขอบคุณสำนักงานกองทุนสนับสนุนการวิจัยที่ได้ให้เงินทุนอุดหนุนโครงการวิจัยชิ้นนี้จนสำเร็จลงด้วยดี ขอขอบพระคุณรองศาสตราจารย์ ดร. นวลพรรณ จันทรศิริ และผู้ช่วยศาสตราจารย์ ดร. อรวรรณ ชัยลภากุล ที่ได้ให้คำแนะนำและอนุญาตให้ใช้เครื่องมือทางเคมีไฟฟ้า ทำให้งานวิจัยชิ้นนี้สมบูรณ์ขึ้น

ขอขอบคุณท่านผู้ดูแลเครื่องนิวเคลียร์แมกเนติกเรโซแนนซ์และแมสสเปกโตรมิเตอร์ ศูนย์เทคโนโลยีชีวภาพแห่งชาติ ที่ได้ให้ความอนุเคราะห์ในการพิสูจน์เอกลักษณ์ของสารบางอย่าง ขอขอบคุณศูนย์เครื่องมือวิทยาศาสตร์และเทคโนโลยีแห่งจุฬาลงกรณ์มหาวิทยาลัยที่ให้ความอนุเคราะห์ในการวิเคราะห์หาธาตุองค์ประกอบและดำเนินการทดลองเอ็นเอ็มอาร์ที่อุณหภูมิต่างๆ และขอขอบคุณภาควิชาเคมี คณะวิทยาศาสตร์ ที่ได้อุดหนุนค่าใช้จ่ายในการทำวิจัยบางส่วน

ขอขอบคุณ Professor Michael B. Hurthouse และ Dr. Simon Cole แห่งภาควิชาเคมี University of Southampton ประเทศสหราชอาณาจักรที่ให้ความช่วยเหลือในการหาโครงสร้างผลึกของสารที่สังเคราะห์ได้ในงานวิจัยชิ้นนี้บางชนิด

ท้ายที่สุดนี้ขอขอบคุณคณาจารย์และข้าราชการในภาควิชาเคมีทุกๆท่านที่ได้อำนวยความสะดวกให้แก่งานวิจัยชิ้นนี้ ตลอดจนนิสิตทุกท่านในหน่วยวิจัยเคมีซุปราโมเลคิวลาร์ ภาควิชาเคมี คณะวิทยาศาสตร์ จุฬาลงกรณ์มหาวิทยาลัยในความวิริยะอุตสาหะช่วยเหลือจนงานวิจัยชิ้นนี้สำเร็จลงได้ด้วยดี

บทคัดย่อ

เลขที่สัญญา: RSA/06/2544

ชื่อโครงการ: คาลิก[4]ซารีนควิโนนไดเมอร์สำหรับเป็นตัวตรวจจับไอออนของโลหะแอลคาไลและแอลคาไลน์เอิร์ธ

ผู้ดำเนินการวิจัย:
หัวหน้าโครงการ: ผู้ช่วยศาสตราจารย์ ดร. ธวัชชัย ตันฑุลานิ
ภาควิชาเคมี คณะวิทยาศาสตร์ จุฬาลงกรณ์มหาวิทยาลัย

E-mail Address: tthawatc@chula.ac.th

ระยะเวลาดำเนินโครงการ: 1 ธันวาคม 2543 ถึง 30 พฤศจิกายน 2546

วัตถุประสงค์: เพื่อสังเคราะห์คาลิก[4]ซารีนควิโนนไดเมอร์และคาลิก[4]ซารีนที่มีเฟอร์โรซีนเอไมด์เป็นองค์ประกอบ และเพื่อศึกษาสมบัติการจับกับไอออนของโลหะแอลคาไลและแอนไอออนตามลำดับ จากนั้นวัดความสามารถในการเป็นเซนเซอร์ของสารที่สังเคราะห์ได้ด้วยไซคลิกโวลแทมเมทรีและสแควร์เวฟโวลแทมเมทรี

ระเบียบวิธีวิจัย: คาลิก[4]ซารีนควิโนนไดเมอร์สามารถสังเคราะห์ได้จากการคัปปลิงคาลิก[4]ซารีนสองหน่วยกับสายโซ่เอธีลีนไกลคอลที่มีความยาวต่างกัน จากนั้นหมู่ฟีนอลจะถูกออกซิไดซ์ด้วยทริสไทรฟลูออโรอะซีทาโททาลเลียมให้เป็นควิโนน ส่วนคาลิก[4]ซารีนที่มีเฟอร์โรซีนเอไมด์เป็นองค์ประกอบสังเคราะห์จากการคัปปลิงเททระแอลคิลไดอะมิโนคาลิก[4]ซารีนและบิส(คลอโรคาร์บอนิล)เฟอร์โรซีนในไดคลอโรมีเทนโดยใช้เอธิลเอมีนเป็นเบส สมบัติการจับของสารที่สังเคราะห์ได้ต่อไอออนของโลหะแอลคาไลและแอนไอออนสามารถศึกษาได้โดยวิธีโปรตอนเอ็นเอ็มอาร์ไทเทรชัน สมบัติการตรวจวัดไอออนของโลหะแอลคาไลและแอนไอออนสามารถวัดได้โดยวิธีไซคลิกโวลแทมเมทรีและสแควร์เวฟโวลแทมเมทรี

ผลการทดลอง: ได้สังเคราะห์คาลิก[4]ซารีนควิโนนซึ่งมีสะพานเชื่อมเป็นไกลคอลและจำนวนหมู่ควิโนนที่แตกต่างกัน และได้สังเคราะห์คาลิก[4]ซารีนที่มีเฟอร์โรซีนเอไมด์เป็นองค์ประกอบซึ่งมีหมู่แทนที่ที่แนโรวริมแตกต่างกันอย่างละสามชนิด พบว่าคาลิก[4]ซารีนควิโนนไดเมอร์เกิดสารประกอบเชิงซ้อนกับไอออนของโลหะแอลคาไลแบบ 1:1 และสามารถเลือกจับกับไอออนของโลหะแอลคาไลเช่นลิเธียม โซเดียม โพแทสเซียม และซีเซียมได้แตกต่างกัน ผลจากไซคลิกและสแควร์เวฟโวลแทมเมทรีแสดงให้เห็นว่าคาลิก[4]ซารีนควิโนนสามารถตรวจวัดไอออนของโลหะแอลคาไลได้ต่างกัน ในกรณีของคาลิก[4]ซารีนที่มีเฟอร์โรซีนเอไมด์เป็นองค์ประกอบพบว่าสามารถเกิดสารประกอบเชิงซ้อนกับแอนไอออนต่างๆ เช่น อะซีเทต เบนโซเอต ไดไฮโดรเจนฟอสเฟต และคลอไรด์ เป็นแบบ 1:1 และความสามารถในการเป็นตัวตรวจวัดแอนไอออนสามารถวัดได้โดยไซคลิกและสแควร์เวฟโวลแทมเมทรี

อภิปรายและสรุปผลการทดลอง: ขนาดของโพรงของลิแกนด์มีบทบาทสำคัญอย่างยิ่งต่อการเลือกจับไอออนของโลหะแอลคาไลของคาลิก[4]ซารีนควิโนนไดเมอร์ การเปลี่ยนแปลงของโวลแทมโมแกรมของคาลิก[4]ซารีนควิโนนแสดงให้เห็นถึงผลกระทบจากความเป็นฮาร์ดซอฟท์แอซิดของไอออนโลหะแอลคาไลอันมีผลทำให้สมบัติทางไฟฟ้าเคมีของลิแกนด์เปลี่ยนไปด้วย เนื่องจากโครงสร้างที่จำเพาะของคาลิก[4]ซารีนที่มีเฟอร์โรซีนเอไมด์เป็นองค์ประกอบทำให้สารเหล่านี้จับกับคาร์บอกซิเลทแอนไอออนได้ดีกว่าแอนไอออนชนิดอื่น ผลจากโวลแทมเมทรีแสดงให้เห็นว่าหมู่แทนที่แอลคิลบนแนโรวริมทำให้สมบัติการตรวจวัดแอนไอออนของสารทั้งสามมีความแตกต่างกัน

คำสำคัญ: คาลิก[4]ซารีน ควิโนน เอ็นเอ็มอาร์ไทเทรชัน โวลแทมเมทรี เซนเซอร์

Abstract

Project Code: RSA/06/2544

Project Title: Calix[4]arenequinone dimers as sensing agents for alkali and alkaline earth metal ions

Investigator:
Project head: Assistant Professor Dr. Thawatchai Tuntulani
Department of Chemistry, Faculty of Science, Chulalongkorn University

E-mail Address: tthawatc@chula.ac.th

Project Period: December 1, 2000 to November 30, 2003

Objectives: To synthesize calix[4]arenequinone dimers and calix[4]arenes containing ferrocene amides and to study binding properties of the compounds towards alkali metal ions and anions, respectively. Abilities of the synthesized compounds as alkali metal ion sensors and anion sensors have been measured by cyclic voltammetry and square wave voltammetry.

Methodology: Calix[4]arenequinone dimers were synthesized by coupling two calix[4]arene units with various ethylene glycol chains. Phenol groups were then oxidized to quinones by tristrifluoroacetato thallium(III). Calix[4]arenes containing ferrocene amide were synthesized by coupling tetraalkyldiaminocalix[4]arenes and bis(chlorocarbonyl)ferrocene in dichlormethane with triethylamine as base. Binding properties of the synthesized compounds towards alkali metal ions and anions were studied by ^{1}H NMR titrations. Alkali metal ion and anion sensing properties of the synthesized compounds were investigated by cyclic voltammetry and square wave voltammetry.

Results: Three calix[4]arenequinones possessing different glycol bridges and numbers of quinone groups have been synthesized. Three calix[4]arenas containing ferrocene amide with different alkyl substituents at the narrow rim were prepared. Calix[4]arenequinone dimers were found to form 1:1 complexes with alkali metal ions and able to bind alkali metal ions such as Li^+, Na^+, K^+ and Cs^+ to a different extent. Cyclic voltammetry and square wave voltammetry showed that the three calix[4]arenequinones detected alkali metal ions to a different extent. In the case of calix[4]arenes containing ferrocene amide, they were found to form 1:1 complexes with various anions such as acetate, benzoate, dihydrogenphosphate and chloride and their anion sensing abilities were verified by cyclic voltammetry and square wave voltammetry.

Discussion and Conclusion: Sizes of the ligand cavity play an important role in alkali metal binding abilities of calix[4]arenequinone dimers. Shifts of voltammograms of calix[4] arenequinones signified the effect of hard-soft acid of alkali metal ions upon changing of electrochemical properties of the three ligands. Due to structures of calix[4]arenes containing ferrocene amide, they preferred to bind carboxylate anions over others. Voltammetry showed that different alkyl substituents on the narrow rim lead to different sensing properties of the three compounds.

Keywords: calix[4]arene, quinone, NMR titration, voltammetry, sensor

Content

Page

New Calix[4]arenequinone Dimers as Alkali Metal Ion Sensors

Anion Sensory Studies of Amide Ferrocene Calix[4]arene Derivatives

New Calix[4]arenequinone Dimers as Alkali Metal Ion Sensors

1. Introduction

Electrochemical sensor is perhaps the most important application of electrochemistry in the field of supramolecular chemistry. This concept, whose use has been widespread in the past two decades, has been exploited to such an extent that a through examination of its use is well beyond the scope. The early focus of this concept in supramolecular research was primarily cation recognition. During the 1980's much interest centered on redox-switchable cation binding systems as potential mimics of biological cation transport or the emphasis has broadened to include anion and molecular recognition. Without a doubt however, the predominant interest in this field has shifted toward the development of sensored molecular devices.[1]

1.1 The concept of electrochemical sensor

The IUPAC Commission on General Aspects of Analytical Chemistry has defined chemical sensors as follows.

'*A chemical sensor is a device that transforms chemical information, ranging from the concentration of a specific sample component to total composition analysis, into a useful analytical signal'*

On the basis of this definition the whole device is the sensor, for without immobilisation of the host and transduction of the interaction, it would not be possible to convert the host-guest interaction into a useful analytical signal. The physical immobilisation of the selective agent, and the transduction process have distinct effects on the performance of a sensing device, espescially in relation to selectivity, sensitivity and response time.[2] However, excellent chemical sensors that possess highly selective complexation properties and highly response time require

1. Size of the receptor should be complementary with the size of the ion to be complexed.
2. The receptor should be closed to the reporter group (signalling group) to enhance signals.[3]

Cation recognition is undoubtedly the most studied and best developed application of calixarenes in sensing devices. Molecules such as derivatives of calix[4]arene in its *cone* conformation with, for example, ester [4], ether [5], ketone [6], carboxylic acid [7], amide [8], crown ether[9], and hemispherand[10] substituents, have been extensively studied over the years.

1.2 Calix[4]arenes

Condensations of *p*-substituted phenols with formaldehyde under base-catalyzed condition afford a new class of oligophenolic macrocyclic compounds called calixarenes (in Greek, calix means *chalice* or Eucharistic cup). Calixarenes are defined as $[1_n]$ metacyclophanes comprising phenol units liked by methylene bridges.[11-13] Most common calixarenes have a number of phenol groups either 4, 6 or 8 while odd-number ring calixarenes are less studied due to the difficulty of their syntheses. Rotation of phenol units around methylene carbons causes many conformational isomers that give a great number of cavities with different size and shape.[14] Since synthetic methods were reported by Gutsche[15-16] , Calixarenes have become one of the most attractive building blocks in supramolecular chemistry. They can be modified to gain numerous types of molecular receptors by many chemical reactions. The modification can be introduced at oxygen atoms (that called ‘lower rim or narrow rim’), methylene bridge carbon or *para* position of aromatic rings (which named ‘upper rim or wide rim’).[12,17-19] Among the calixarene family, calix[4]arene is the smallest member and served as the most popular building block in syntheses of new compound which have high selectivity towards ionic and neutral molecules. It is known that unmodified calix[4]arene exists in ‘cone’ conformation due to its strong intramolecular hydrogen bonding. However, chemically modified calix[4]arene can adopt other conformations as ‘partial cone’, ‘1,2-alternate’ and ‘1,3-alternate’. All four conformation of calix[4]arene can be immobilized in only one of them by different reaction condition. Determination of conformational differences should be deduced from ^{1}H-NMR spectra because each isomer has its unique methylene proton signals pattern.[20-21]

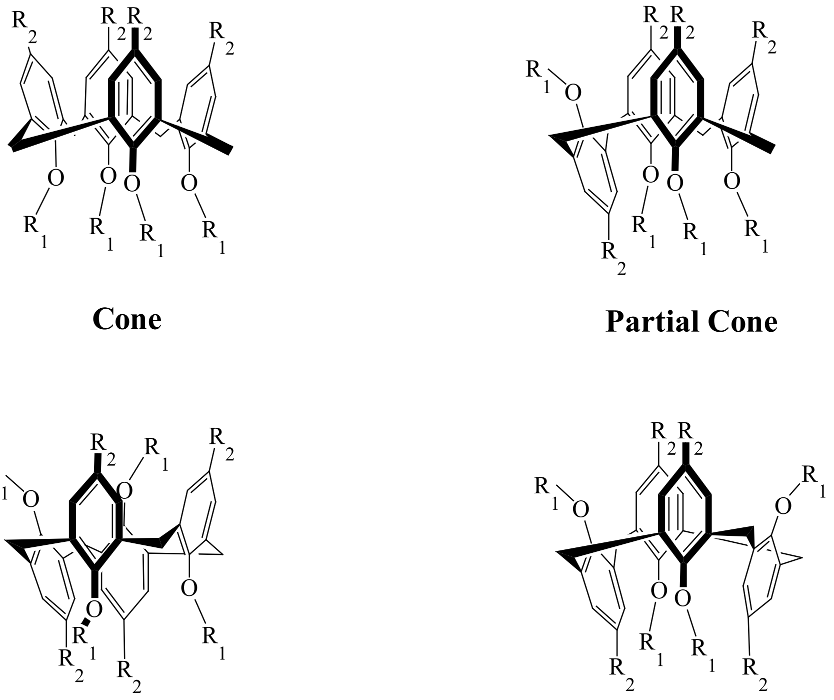

Cone

Partial Cone

1, 2-Alternate

1, 3-Alternate

Figure 1.1: Conformational isomers of calix[4]arene

1.3 Calix[4]arene dimers

Calix[4]arenes are easily (and often selectively) functionalized and therefore they can be combined in various ways to larger molecules containing more than one calixarene substructure. Their connection can be separated into three types, the first type is connected via the narrow rim (also called tail-to-tail), the second type is connected via the wide rim (also called head-to-head) and the last is connected via the narrow and the wide rim (also called tail-to-head). Some examples of each type are shown in Figure 1.2. Moreover, double calix[4]arenes can be separated by the connection into three types, first is connected via single bridge, second is connected via double bridge and the last is connected via more than two bridges.

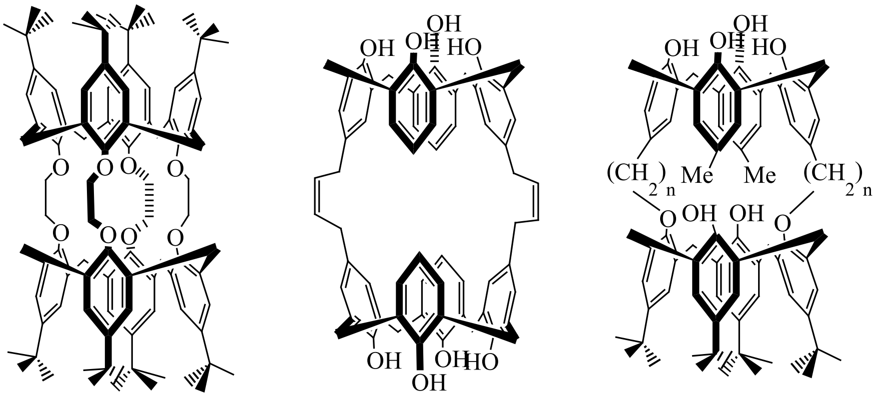

1 **2** **3**

tail-to-tail **head-to-head** **tail-to-head**

Figure 1.2: Example of double calix[4]arene, connected via double bridge

A rather rigid double calix[4]arene (calix[4]tube) **1** connecting by four ethylene bridges was obtained in 51% yield by the reaction of the tetrakis(tosyloxyethoxy)-*p-tert*-butylcalix[4]arene with *p-tert*-butylcalix[4]arene in the presence of K_2CO_3.[22] Obviously the K^+-ion acts as a template, since **1** is a selective ligand for K^+, forming kinetically and thermodynamically stable complexes, in which the K^+ is coordinated by the eight oxygens in a cubic fashion. Molecular mechanic simulations suggest that complexation occurs via a two-stage mechanism in which the intermediate involves an intracavity K^+-π complex (Figure 1.3). This is of interest as a model system for a K^+ transport by gated ion channels

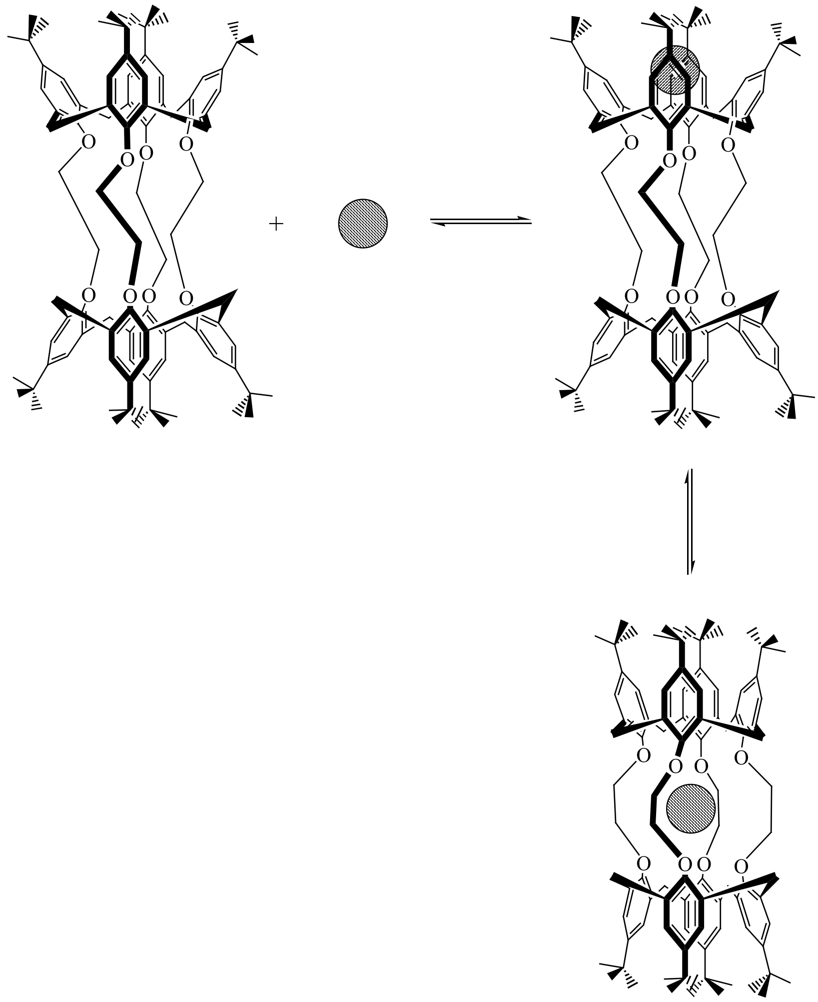

Figure 1.3: Potassium ion complexation by double calix[4]arene **1** cage host

With the larger biscalix[4]arene **4** which has two metal complexing site.[23] , two dynamic processes are observed. The intermolecular association/dissociation equilibrium in which the complex equilibrates with the uncomplexed ligand and free metal cation is slow on the NMR time scale. The complex also exhibits a faster intramolecular exchange of the metal cation such as Na^+ or K^+ from one binding site to another (Figure 1.4).

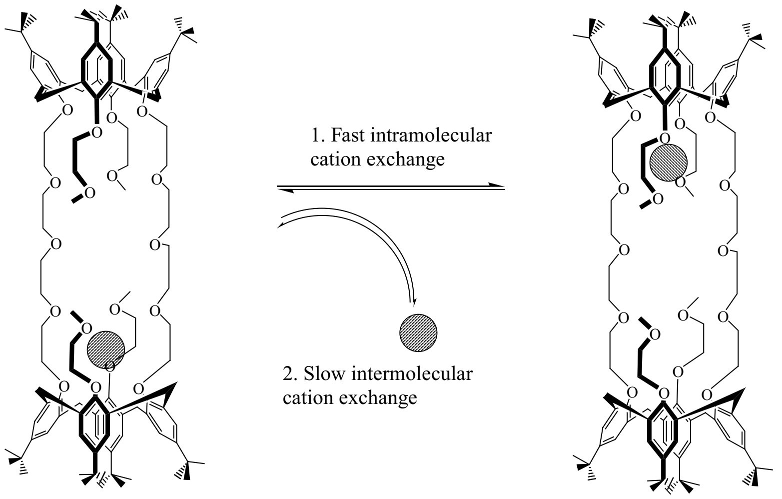

4 **4**

Figure 1.4: Intra- and intermolecular metal exchange processes in biscalix[4]arene **4**

1.4 Calix[4]arenequinone based electrochemical sensors

The reaction of calix[4]arenes with strong oxidizing agents may afford derivatives in which one or several phenolic moieties have been oxidized to quinone groups (‘calix-quinones’).[24-25] The selective oxidation of some of the phenol rings of a calix[4]arene can be achieved by protection of one or more of the phenolic OH groups by etherification or esterification prior to the oxidation step.Using this strategy calix[4]arene with one, two or three quinone groups and four groups **5-8** have been prepared[26] (Figure 1.5) Tl-$(CF_3COO)_3$ is the reagent most commonly used for oxidation.[27]

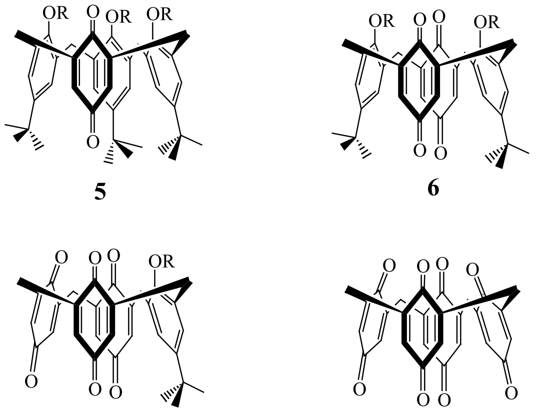

5 **6** **7** **8**

Figure 1.5: A series of calix[4]arenequinones

In recent years, the most popular signaling unit used by chemists are ferrocene and quinone.[1] An increasing interest in the synthesis of redox-active calixarenes has centered on the appropriate functionalization of phenol units since the possibility of calixarenes as enzyme mimics was suggested.[11] Calix[4]arenequinone compounds have espescially attracted chemist's attention because of their selectivity toward certain cations and electrochemical properties.[28-29] The study on the effect of electron transfer processes in spatially constrained syntems with multiple redox units of quinone made calix[4] arenequinone one of the molecular devices in redox switching studies.

Some examples of calix[4]arenequinone are shown in Figure 1.6. The tertiary amide substituents **9** have been synthesized by treatment of the respective 1,3-bis-substituted *p-tert*-butylcalix[4]arene with $Tl(OCOCF_3)_3$ in trifluoroacetic acid.[30] The electrochemical properties and its complexes have been studied using cyclic and square wave voltammetric techniques. The result showed that addition of 1 equiv. or more of sodium perchlorate or potassium hexafluorophosphate to electrochemical solutions of **5** resulted in the disappearance of waves 1 and 2 and the evolution of reversible new wave couples at more anodic potentials.(Figure 1.6)

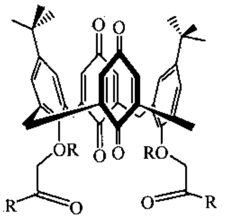

9 : R = NEt_2
10 : R = OEt
11 : R = OMe

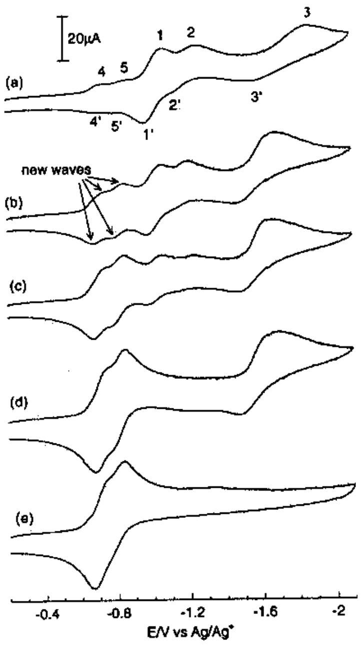

Figure 1.6: Cyclic voltammogram of **9** ($1.17x10^{-3}M$) in a 1/1 mixture of CH_3CN and CH_2Cl_2 in the presence of different concentrations (equiv.) of sodium cations (a) 0 ; (b) 0.21 ; (c) 0.42 ; (d) 0.63 ; (e) 2.7. Scan rate : 100 mV/s

The electrochemical properties of calix[4]arenediquinone **10** and **11** have been studied.[31] Figure 1.7a and 1.7b showed voltammetric responses of variously charged metal ions. ΔE_p value of the compound **10** and **11** after complexation with a series of metal ions exhibits the trend $La^{3+} > Mg^{2+} > Ca^{2+} > Li^{+} > Na^{+} > K^{+}$.

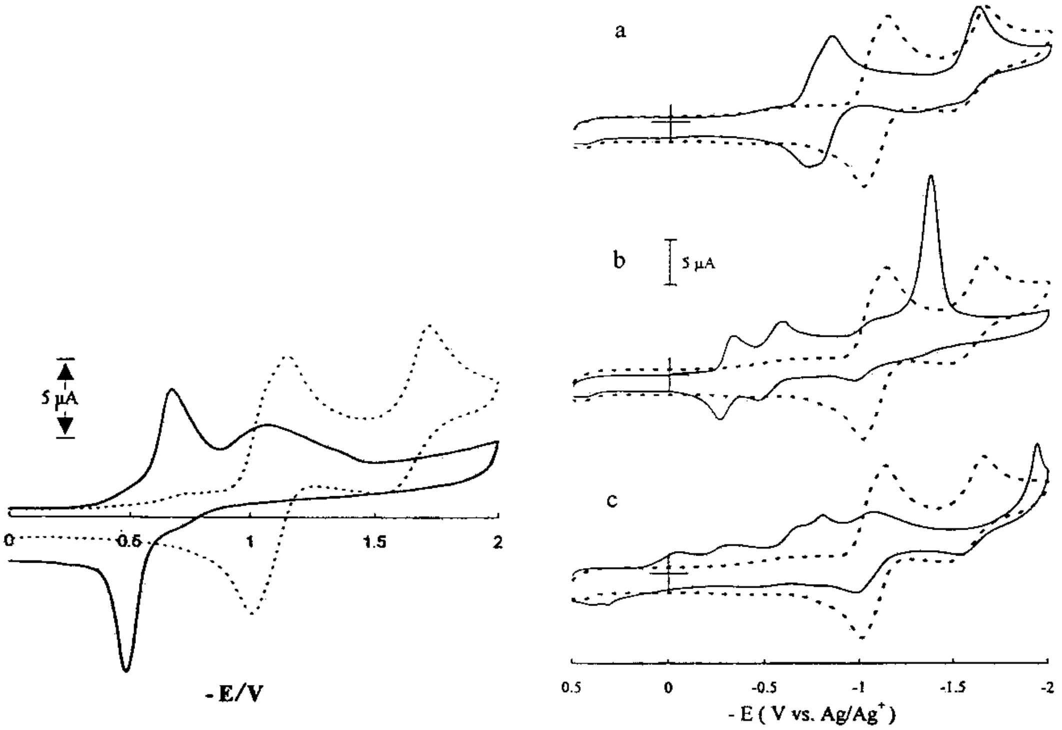

A **B**

Figure 1.7: **A.** Cyclic voltammogram of 0.5 mM compound **10** in the absence (-------) and presence (____) of one equiv. of Li^{+}

B. Cyclic voltammogram of 0.5 mM compound **11** in the absence (-------) and presence (____) of one equiv. of (a) Li^{+}, (b) Ca^{2+} and (c) La^{3+}

1.5 Calix[4]arenequinone dimer based electrochemical sensor

A few studies of double calix[4]arenequiones has been reported. In 1996 double calix[4]arenes bridged with bpy (2,2′-bipyridine) subunits **12** (Figure 1.8) has been synthesized.[32] Spectroscopic titrations have shown that **12** form more stable complexes with K^+ with association constant of 0.8x10^5 than with NH_4^+ 0.7x10^4. Cyclic Voltammetry of **12** with K^+ showed the first reduction wave shifted to more positive potentials by the addition of K^+ (Figure 1.8). The addition of one equivalent of metal cation caused a potential shift to a more positive direction by 200 mV (Figure 1.8, curve (C)). Further addition of K^+ produced no change. Thus, K^+ was considered to form a 1:1 complex with **12**.

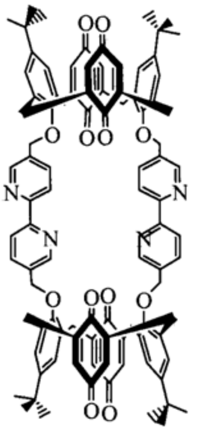

12

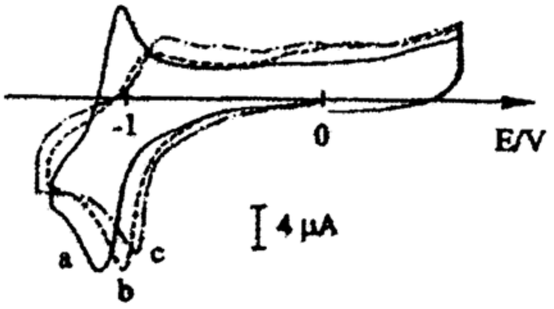

Figure 1.8: Cyclic voltammograms for 0.2 mM of compound **12** in CH_3CN, the absence of K^+ (curve (a), ___), and in the presence of 0.4 equiv. of K^+ (curve (b), -----) and one equiv. of K^+ (curve (c), ._._.)

In 2001 Beer synthesized novel bis(calix[4]diquinone) receptors **13**, **14** and **15** from *p-tert*-butylcalix[4]arene in acetonitrile with propane-1,3-ditosylate, 1,4-dibrobutane and

1,5-dibromopentane, respectively in the presence of potassium carbonate and then oxidized with $Tl(OCOCF_3)_3$ in trifluoroacetic acid (Figure 1.9).[33] Receptors **13** and **14** display a high selectivity for Rb^+ ($K = 6.3x10^4$) and Cs^+($K = 1.6x10^3$), respectively. The electrochemical properties of **13** and **14** with group I metal ions were studied by cyclic voltammetry (CV) and square-wave voltammetry (SWV, Figure 1.9) Both receptors exhibited essentially two broad redox waves, which implied a multielectron transfer. The two redox waves corresponded to a quasi-reversible reduction and an irreversible redox process which occurred at a more cathodic potential. The addition of Group I metal cations to electrochemical solutions of **13** and **14** led in all cases to the evolution of two new redox waves at potentials that were substantially positively shifted.

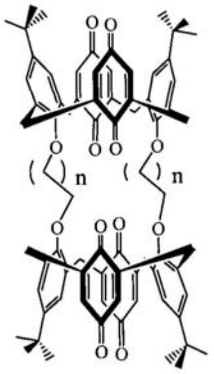

13 : n = 2
14 : n = 3
15 : n = 4

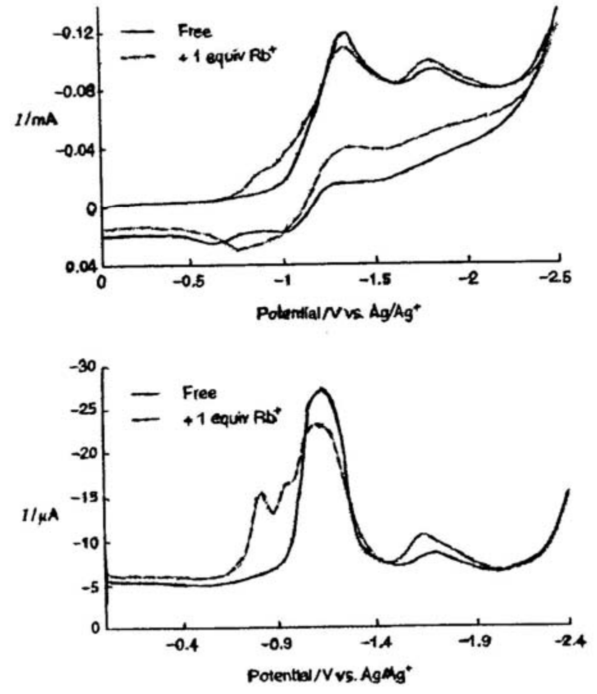

Figure 1.9: Cyclic voltammogram (top) and square wave voltammogram (bottom) of **13** + 1.0 equiv. of Rb^+ in CH_2Cl_2 : CH_3CN (4:1)

1.6 Cyclic voltammetry

Cyclic voltammetry is the most widely use technique for acquiring qualitative information about electrochemical reactions. The power of cyclic voltammetry results from its ability to rapidly provide considerable information on the thermodynamics of redox processes and the kinetics of heterogeneous electron transfer reactions, and on coupled chemical reactions or adsorption processes. Cyclic voltammetry is often the first experiment performed in an electroanalytical study. In particular, it offers a rapid location of redox potentials of the electroactive species, and convenient evaluation of the effect of media upon the redox process.[34]

Rapid-voltage-scan technique in which the direction of voltage scan is reversed are called cyclic technique. In these technique, a ramp is applied over the full voltage-scan range and then reversed so that a descending ramp returns, almost invariably to the original potential. The scan rate in the forward and reverse directions is normally the same, so that the excitation waveform is actually an isosceles triangle. (Figure 1.10) Cyclic voltammetry can be used in single-cycle (Figure 1.11) or in multicycle modes, depending upon the electrode, the reaction in question, and the information sought. In most cases the first and later scans are not identical.[35]

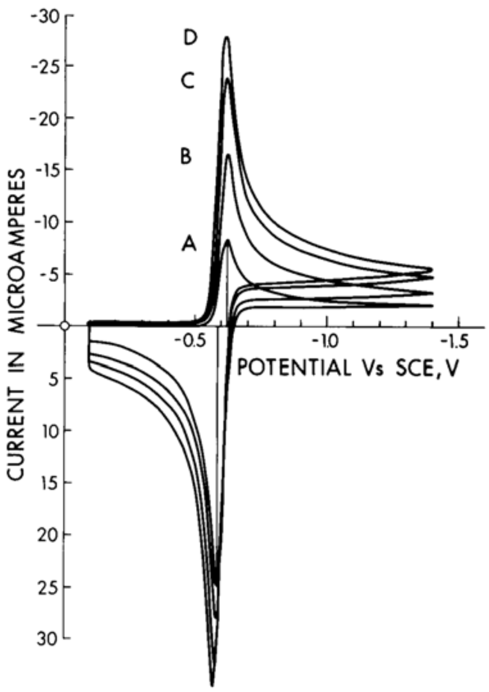

Figure 1.10: Cyclic voltammetry of a reversible process. Aqueous solution, 1.0 mol/m^3 Cd(II) in 100 mol/m^3 KCl, HMDE. Curve A, 20 mV/s; curve B, 50 mV/s; curve C, 100 mV/s; curve D, 200 mV/s. Initial scan cathodic

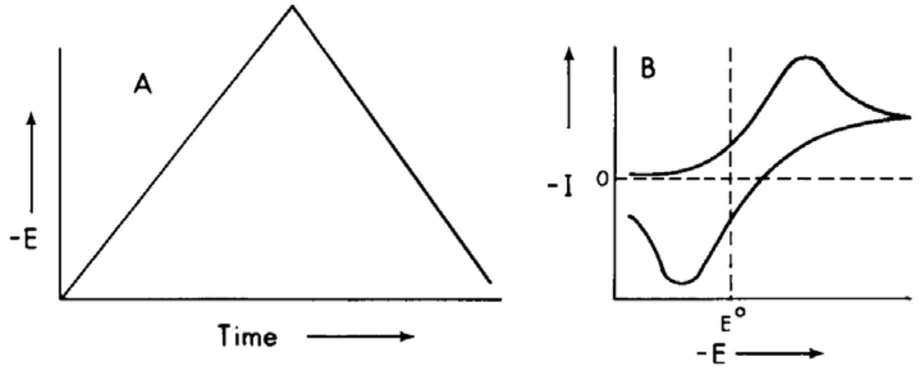

Figure 1.11: Cyclic voltammetry. (A) Excitation signal; (B) response is obtained for a single reversible reduction when the voltage-time excitation signal extends considerably on both sides of the E^o for the reversible process.

The important parameters of a cyclic voltammogram are: anodic peak current (i_{pa}) and anodic peak potential (E_{pa}) taken from the peak position of anodic current and the respective parameters i_{pc} and E_{pc} from the peak position of cathodic current. If the redox couple is reversible the half-wave potential is centered between E_{pa} and E_{pc}.

$$E_{1/2} = (E_{pa} + E_{pc}) / 2$$

Frequently $E_{1/2}$ calculated in this way is considered simply as the formal potential because the diffusion coefficients have a small effect. The difference between peak potentials is related with the number of electrons transferred in the electrode reaction.[36]

$$\Delta E_p = E_{pa} - E_{pc} = 0.059 / n$$

Electrochemical 'reversibility' means that the electrode reaction is fast enough to maintain the surface concentrations of the oxidized and reduced forms at equilibrium with each other, which is an indispensable condition for the validity of the Nernst equation.

1.7 Square wave voltammetry

Square wave voltammetry is a large-amplitude differential technique in which a waveform composed of a symmetrical square wave, superimposed on a base staircase potential, is applied to the working electrode (Figure 1.12). The current is sampled twice during each square-wave cycle, once at the end of the forward pulse and once at the end of the reverse pulse. Since the square wave modulation amplitude is very large, the reverse pulses cause the reverse reaction of the product (of the forward pulse). The difference between the two measurements is plotted vs. the base staircase potential. A dimensionless plot of the theoretical forward, reverse, and difference currents is given in Figure 1.13 for a rapid reversible redox system. The resulting peak-shaped voltammogram is symmetrical about the half-wave potential, and the peak current is proportional to the concentration.[34]

The major advantage of square wave voltammetry is its speed. The effective scan rate is given by $f\Delta E_s$. The term f is square wave frequency (in Hz), and ΔE_s is the step height. Frequencies of 1 to 100 cycles per second permit the use of extremely fast potential scan rates. As a result, the analysis time is drastically reduced; a complete voltammogram can be recorded within a few seconds, as compared with about 2-3 minutes in differential-pulse voltammetry.

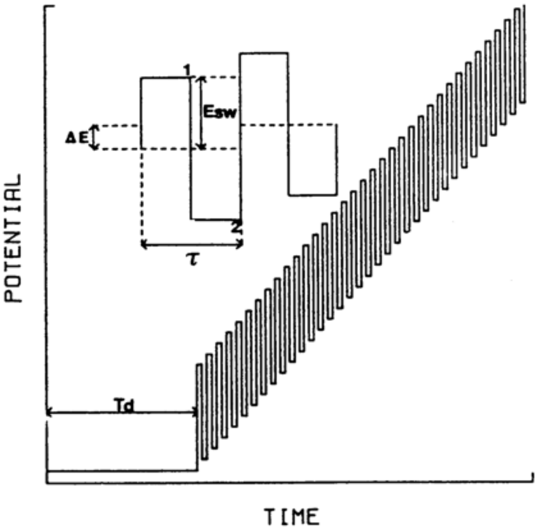

Figure 1.12: Square wave waveform showing the amplitude, E_{sw} : step height, ΔE : square wave period, τ : delay time : T_d, and current measurement times, 1 and 2.

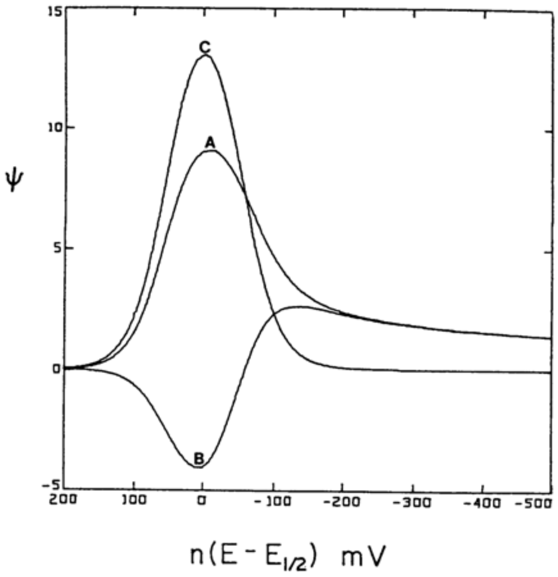

Figure 1.13: Square wave voltammogram for reversible electron transfer : (A) forward current; (B) reverse current; (C) net current. ψ is a dimensionless current function.

1.8 Objective of this research

The main goals of this research are to synthesize double calix[4]arenequinone **5a**, **5b**, **5c** (Figure 1.14) by combining the lower-rim cation binding properties of calixarenes with ethylene glycol linkages similar to those found in crown ethers. Compounds **5a**, **5b** and **5c** are in cone conformation and provide oxygen donor atoms from glycol linkages that served to bind cation *via* ion-dipole interactions. The complexation studied of these compounds with alkaline cations such as Li^+, Na^+, K^+, Cs^+ are also studied by means of ^{1}H-NMR titrations. Results of this research should give information about their binding abilities toward alkaline cations. The effect of size and shape of host molecules to metal ion recognition will also be obtained.

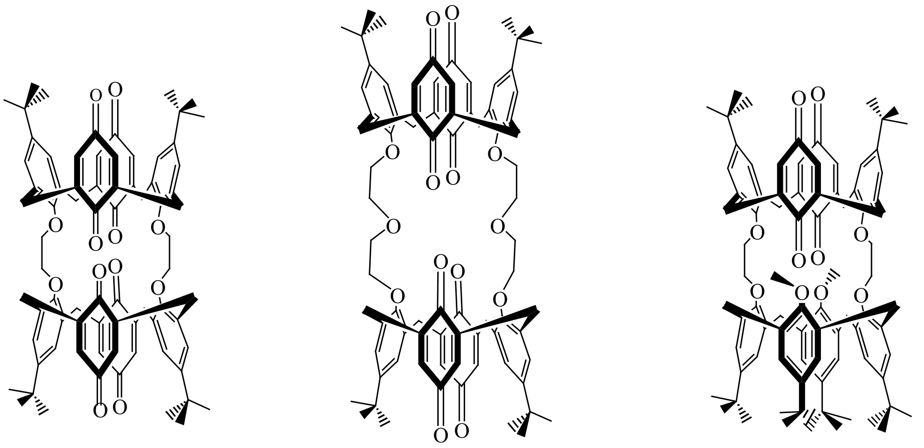

5a **5b** **5c**

Figure 1.14: Structures of double calix[4]arenequinone **5a**, **5b**, **5c**

Another aim of this work is to investigate the redox chemistry of double calix[4] arenequinones **5a**, **5b**, **5c** in non-aqueous solution in the absence and in the presence of alkaline cations by cyclic voltammetry and square wave voltammetry and at last, to explore the possibility to use them as alkali metal ion sensors.

2. Experimental section

2.1 General procedures

2.1.1 Analytical instruments

Nuclear Magnetic Resonance (NMR) spectra were recorded on a Varian 200, 400 and a Brucker ACF 200 MHz nuclear magnetic resonance spectrometers. In all cases, samples were dissolved in deuterated chloroform and chemical shifts were recorded in part per million (ppm) using a residual proton or carbon signals in deuterated solvents as internal reference. Elemental analysis were carried out on a CHNS/O analyzer (Perkin Elmer PE2400 series II). ESI and FAB Mass spectra were recorded on a Bruker Mass spectrometer and a GCQ Finigan Mass spectrometer. Infrared spectra were obtained on a Nicolet Impact 410 using KBr pellet. All melting points were obtained on an Electrothermal 9100 apparatus and uncorrected.

2.1.2 Materials

All materials were standard analytical grade, purchased from Fluka, Aldrich, BHD, Carlo Erba, Merck or J.T. Baker and used without further purification. Commercial grade solvents such as acetone, hexane, dichloromethane, methanol and ethyl acetate were distilled before used. Acetonitrile was dried over CaH_2 and freshly distilled under nitrogen prior to use. THF was dried with Na in benzophenone under nitrogen atmosphere and distrilled before used.

Column chromatography was carried out using silica gel (Kieselgel 60, 0.063-0.200 mm, Merck). Thin layer chromatography (TLC) was performed on silica gel plates (Kieselgel 60 F_{254}, 1 mm, Merck).

Starting materials such as *p-tert*-butylcalix[4]arene were prepared according to the literature procedure.[37] . Synthesis of compound **1**, **3a**, **3b**, **3c** and **3d** was adapted from the literature procedure.[38-39] All compounds were characterized by ^{1}H-NMR spectroscopy, ^{13}C-NMR spectroscopy, mass spectrometry and elemental analysis.

2.2 Synthesis

2.2.1 Preparation of 25,27-di(ethyleneglycol)-bis-*p*-*tert*-butylcalix[4]arene (1)

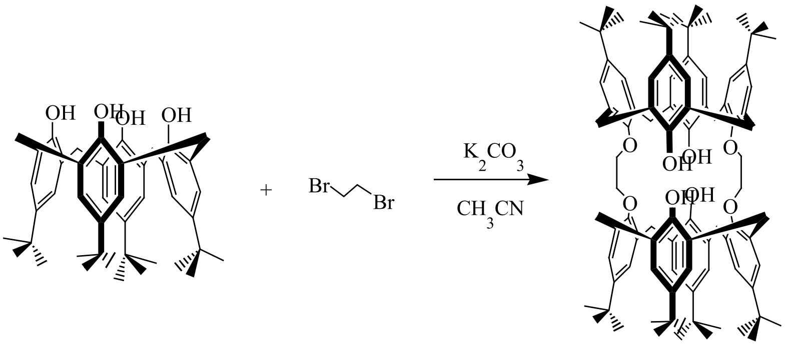

1

In a 100 mL two-necked round bottom flask, *p*-*tert*-butylcalix[4]arene (3.24 g, 5 mmol) and potassium carbonate (0.69 g, 5 mmol) were suspended in dried acetonitrile (50 mL). After the mixture was stirred for 30 minutes, 1,2-dibromoethane (5 mL, 58 mmol) was then added. The mixture was stirred overnight and heated at 70 ^{o}C under nitrogen atmosphere. The solution was allowed to cool to room temperature and evaporated to dryness under reduced pressure. The residue was dissolved in dichloromethane (50 mL) and stirred with an aqueous solution of 3 M hydrochloric acid (50 mL) for 30 minutes and then extracted with dichloromethane (2x50 mL). The organic layer was dried over anhydrous sodium sulfate, filtered and evaporated to dryness. The residue was dissolved in a minimum amount of dichloromethane and methanol was added to precipitate a white crystalline solid (0.42 g, 12% yield). The product was dried in *vacuo* and kept in a desiccator.

Characterization data for 25,27-di(ethyleneglycol)-bis-*p*-*tert*-butylcalix[4]arene (1)

mp. > 300 ^{o}C (decompose)

^{1}H-NMR spectrum ($CDCl_3$, 200 MHz) : δ (in ppm) 7.65 (s, 4H, $O\underline{H}$), 7.00 (s, 8H, m-$\underline{H}ArOH$), 6.82 (s, 8H, m-$\underline{H}ArOCH_2CH_2OAr\underline{H}$), 4.55 (s, 8H, $ArOC\underline{H}_2C\underline{H}_2OAr$), 3.35, 4.50 (dd, J = 14.0 Hz, 16H, $ArC\underline{H}_2Ar$), 1.25 (s, 36H, HOAr-t-$C_4\underline{H}_9$), 0.99 (s, 36H, t-$C_4\underline{H}_9$-ArOH)

^{13}C-NMR spectrum ($CDCl_3$, 50 MHz) : δ (in ppm) 151.16, 150.42, 147.08, 141.27, 132.34, 127.78, 127.70, 125.54, 124.62, 75.88, 33.74, 33.48, 32.13, 31.26, 30.73

FAB mass (m/z) : 1367.8 [$M^+ + NH_4^+$]

Elemental analysis :	Calculate ($C_{92}H_{116}O_8$)	C, 81.86 ; H, 8.66
	Found	C, 81.86 ; H, 8.86

2.2.2 Preparation of diethyleneglycol ditosylate (2a)

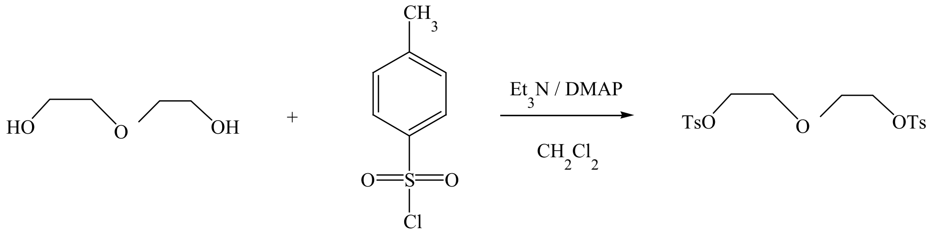

2a

In a 250 mL two-necked round bottom flask, a dichloromethane solution (50 mL) of diethyleneglycol (3 g, 28.28 mmol), triethylamine (11.76 mL, 84.84 mmol) and a catalytic amount of DMAP was chilled to 10 °C with an ice bath and stirred under nitrogen for 30 minutes. The solution of tosylchloride (11.86 g, 62.22 mmol) in dichloromethane (100 mL) was then added dropwise. The reaction mixture was allowed to stir overnight at room temperature under nitrogen. After the reaction was completed, the mixture was then poured into an aqueous solution of 3 M hydrochloric acid (100 mL) and stirred for 30 minutes and then extracted with dichloromethane (2x50 mL). The organic layer was dried over anhydrous sodium sulfate, filtered and evaporated to dryness. The residue was dissolved in a minimum amount of dichloromethane and methanol was added to precipitate a white crystalline solid (7.66 g, 65% yield). The product was dried in *vacuo* and kept in a desiccator.

Characterization data for preparation of diethyleneglycol ditosylate (2a)

^{1}H-NMR spectrum (CDCl$_3$, 200 MHz) : δ (in ppm) 7.76 (d, *J* = 8.3 Hz, 4H, Ar$\underline{\mathrm{H}}$), 7.33 (d, *J* = 8.3 Hz, 4H, Ar$\underline{\mathrm{H}}$), 4.07 (t, J = 4.6 Hz, 4H, TsOC$\underline{\mathrm{H}}_2$CH$_2$), 3.59 (t, *J* = 4.8 Hz, 4H, CH$_2$C$\underline{\mathrm{H}}_2$OH), 2.43 (s, 6H, ArC$\underline{\mathrm{H}}_3$)

2.2.3 Preparation of 25,27-di(diethyleneglycol)-bis-*p-tert*-butylcalix[4]arene (2b)

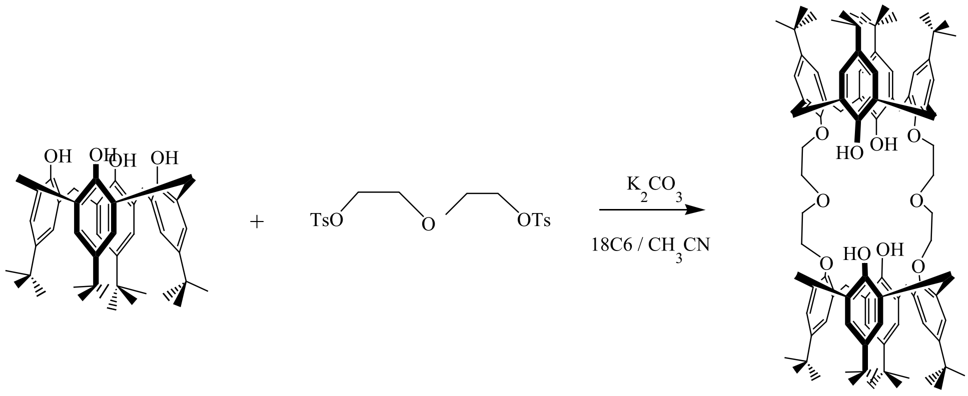

2a **2b**

In a high pressure tube equipped with valves and a pressure gauge, *p-tert*-butylcalix [4]arene (3 g, 4.62 mmol), diethyleneglycol ditosylate, **2a** (1.91 g, 4.62 mmol), catalytic amount of 18-crown-6 and potassium carbonate (1.28 g, 9.24 mmol) were suspened in dried acetonitrile (10 mL). The tube was then pressurized with N$_2$ at 50 psi. The mixture was stirred and heated at 70 °C for 2 days. The solution was allowed to cool to room temperature and evaporated to dryness under reduced pressure to yield a crude product. The residue was dissolved in dichloromethane (50 mL) and stirred with an aqueous solution of 3 M hydrochloric acid (2x50 mL) for 30 minutes, and then extracted with dichloromethane (2x50 mL). The organic layer was dried over anhydrous sodium sulfate, filtered and evaporated to dryness. The residue was dissolved in a minimum amount of dichloromethane and methanol was added to precipitate a white crystalline solid (0.44 g, 14% yield). The product was dried in *vacuo* and kept in a desiccator.

Characterization data for 25,27-di(diethyleneglycol)-bis-*p-tert*-butylcalix[4]arene (2b)

mp. > 300 °C (decompose)

^{1}H-NMR spectrum ($CDCl_3$, 200 MHz) : δ (in ppm) 8.09 (s, 4H, O<u>H</u>), 7.00 (s, 8H, *m*-<u>H</u>ArOH), 6.85 (s, 8H, *m*-<u>H</u>ArOCH$_2$CH$_2$OAr<u>H</u>), 4.50-4.10 (m, 24H, ArOC<u>H</u>$_2$C<u>H</u>$_2$OAr, ArC<u>H</u>$_2$Ar), 3.18, (dd, *J* = 14.0 Hz, 8H, ArC<u>H</u>$_2$Ar), 1.25 (s, 36H, HOAr-*t*-C$_4$<u>H</u>$_9$), 1.05 (s, 36H, *t*-C$_4$<u>H</u>$_9$-ArOH)

^{13}C-NMR spectrum ($CDCl_3$, 50 MHz) : δ (in ppm) 150.49, 149.51, 147.20, 141.43, 133.45, 127.76, 125.62, 125.10 , 74.82, 70.44, 34.04, 33.78, 31.64, 31.11

FAB mass (m/z) : 1437 [$M^+ + H^+$]

Elemental analysis :	Calculate ($C_{96}H_{124}O_{10}$)	C, 80.18 ; H, 8.69
	Found	C, 80.21 ; H, 8.43

2.2.4 Preparation of 25,27-di(methoxy)-*p-tert*-butylcalix[4]arene (3a)

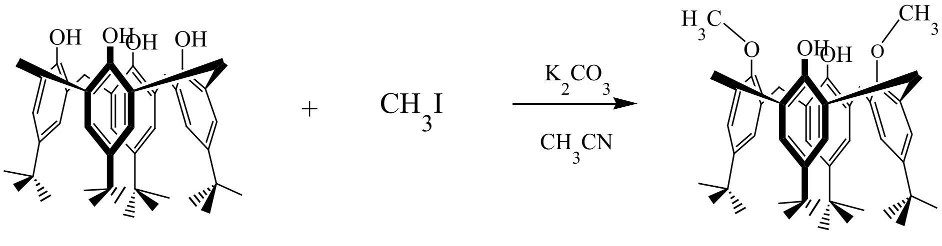

3a

In a 100 mL two-necked round bottom flask, *p-tert*-butylcalix[4]arene (5 g, 7.70 mmol) and potassium carbonate (1.60 g, 11.55 mmol) were suspended in dried acetonitrile (50 mL). The mixture was stirred at room temperature for 30 minutes. Methyl iodide (1.20 mL, 19.25 mmol) was then added by syringe. The mixture was stirred overnight and heated at 70 °C under nitrogen. The solution was allowed to cool to room temperature and evaporated to dryness under reduced pressure. The residue was dissolved in dichloromethane (50 mL) and stirred with aqueous solution of 3 M hydrochloric acid

(50 mL) for 30 minutes and then extracted with dichloromethane (2x50 mL). The organic layer was dried over anhydrous sodium sulfate, filtered and evaporated to dryness. The residue was dissolved in a minimum amount of dichloromethane and methanol was added to precipitate a white powder (4.75 g, 91% yield). The product was dried in *vacuo* and kept in a desiccator.

Characterization data for 25,27-di(methoxy)-*p-tert*-butylcalix[4]arene (3a)

^{1}H-NMR spectrum (CDCl$_3$, 200 MHz) : δ (in ppm) 7.25 (s, 2H, ArOH), 7.08 (s, 4H, *m*-ROArH), 6.77 (s, 4H, *m*-HOArH), 3.94 (s, 6H, ArOCH$_3$), 4.25 and 3.29 (dd, *J* = 13 Hz, 8H, ArCH$_2$Ar), 1.30 (s, 18H, ROAr-*t*-C$_4$H$_9$), 0.94 (s, 18H, HOAr-*t*-C$_4$H$_9$)

2.2.5 Preparation of 25,27-di(carboethoxymethoxy)-*p-tert*-butylcalix[4]arene (3b)

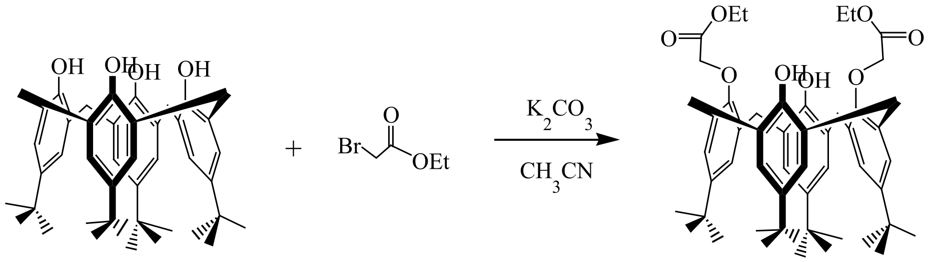

3b

In a 250 mL two-necked round bottom flask, *p-tert*-butylcalix[4]arene (3 g, 4.62 mmol) and potassium carbonate (1.6 g, 11.35 mmol) were suspended in dried acetonitrile (100 mL). The mixture was stirred for 30 minutes. Ethyl bromoacetate (1.03 mL, 9.24 mmol) was then added by syringe. The mixture was stirred and heated at 70 ^{o}C under nitrogen atmosphere for 4 hours. The solution was allowed to cool to room temperature and evaporated to dryness under reduced pressure. The residue was dissolved in dichloromethane (50 mL) and the saturated solution of ammonium chloride (50 mL) was subsequently added to destroy excess ethyl bromoacetate, followed by washing with saturated sodium chloride solution (50 mL). Water (50 mL) was added and the mixture was stirred for 30 minutes and extracted with dichloromethane (2x50 mL). The organic layer was dried over anhydrous sodium sulfate, filtered and evaporated to dryness. The residue was dissolved in a minimum amount of dichloromethane and methanol was added to precipitate a white powder (2.55 g, 67% yield). The product was dried in *vacuo* and kept in a desiccator.

Characterization data for 25,27-di(carboethoxymethoxy)-*p-tert*-butylcalix[4]arene (3b)

^{1}H-NMR spectrum ($CDCl_3$, 200 MHz) : δ (in ppm) 7.09 (s, 2H, ArO$\underline{H}$), 7.01 (s, 4H, *m*-HOAr$\underline{H}$), 6.81 (s, 4H, *m*-ROAr$\underline{H}$), 4.70 (s, 4H, OC$\underline{H}_2$CO), 4.30 (q, *J* = 7.8 Hz, 4H, OC$\underline{H}_2$CH$_3$), 3.34 and 4.40 (dd, *J* = 14.0 Hz, 8H, ArC$\underline{H}_2$Ar), 1.30 (t, 6H, OCH$_2$C$\underline{H}_3$), 1.24 (s, 18H, HOAr-*t*-C$_4\underline{H}_9$), 0.97 (s, 18H, ROAr-*t*-C$_4\underline{H}_9$)

2.2.6 Preparation of 25,27-di(2-hydroxyethoxy)-*p-tert*-butylcalix[4]arene (3c)

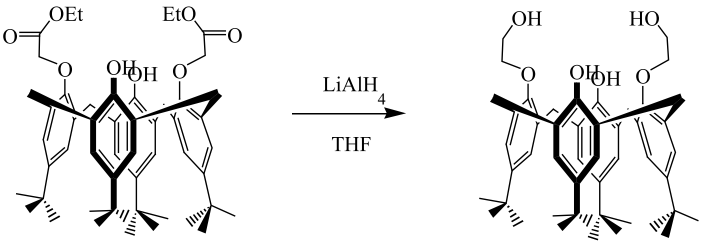

3b **3c**

In a 100 mL two-necked round bottom flask, a solution of 25,27-di (carboethoxymethoxy)-*p-tert*-butylcalix[4]arene (**3b**) (2 g, 2.44 mmol) in dried tetrahydrofuran (50 mL) was stirred for 10 minutes at 10 °C under nitrogen atmosphere. $LiAlH_4$ (0.4 g, 10.54 mmol) was then added gradually. The mixture was allowed to stir overnight at room temperature under nitrogen atmosphere. An aqueous solution of 3 M hydrochloric acid was subsequently added until a precipitate of lithium had formed which was then filtered. Water (30 mL) was added and stirred for 30 minutes and extracted with dichloromethane (2x30 mL). The organic layer was dried over anhydrous sodium sulfate, filtered and evaporated to dryness under reduced pressure. The residue was dissolved in a minimum amount of dichloromethane and methanol was added to precipitate a white powder (1.58 g, 88% yield). The product was dried in *vacuo* and kept in a desiccator.

Characterization data for 25,27-di(2-hydroxyethoxy)-*p-tert*-butylcalix[4]arene (3c)

^{1}H-NMR spectrum ($CDCl_3$, 200 MHz) : δ (in ppm) 9.23 (s, 2H, ArO<u>H</u>), 7.07 (s, 4H, *m*-<u>H</u>OArH), 7.01 (s, 4H, *m*-ROAr<u>H</u>), 5.25 (s, 2H, $CH_2O\underline{H}$), 4.25 (t, 8H, $ArOC\underline{H}_2C\underline{H}_2OH$), 4.30 and 3.43 (dd, $J = 14.0$ Hz, 8H, $ArC\underline{H}_2Ar$), 1.20 (s, 18H, ROAr-*t*-$C_4\underline{H}_9$), 1.19 (s, 18H, HOAr-*t*-$C_4\underline{H}_9$)

2.2.7 Preparation of 25,27-di(methanesulfonyloxyethoxy)-*p-tert*-butylcalix[4] arene (3d)

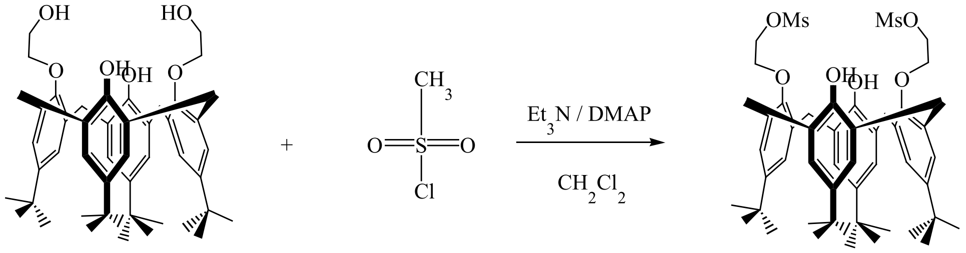

3c **3d**

In a 50 mL two-necked round bottom flask, a dichloromethane solution (30 mL) of 25,27-di(2-hydroxyethoxy)-*p-tert*-butylcalix[4]arene (**3c**) (0.5 g, 0.68 mmol), triethylamine (0.37 mL, 2.71 mmol) and a catalytic amount of DMAP was chilled to 10 °C with an ice bath and stirred under nitrogen for 30 minutes. MsCl (0.21 mL, 2.71 mmol) was then added by syringe. The reaction mixture was stirred at room temperature under nitrogen for 4 hours. After the reaction was completed, an aqueous solution of 3 M hydrochloric acid (30 mL) was added and stirred for 30 minutes and extracted with dichloromethane (2x30 mL). The organic layer was dried over anhydrous sodium sulfate, filtered and evaporated to dryness. The residue was dissolved in a minimum amount of dichloromethane and methanol was added to precipitate a white powder (0.54 g, 87% yield). The product was dried in *vacuo* and kept in a desiccator.

Characterization data for 25,27-di(methanesulfonyloxyethoxy)-*p-tert*-butylcalix[4] arene (3d)

^{1}H-NMR spectrum ($CDCl_3$, 200 MHz) : δ (in ppm) 7.06 (s, 4H, RAr<u>H</u>), 6.75 (s, 4H, HOAr<u>H</u>), 6.67 (s, 2H, ArO<u>H</u>), 4.64 (m, 4H, $MsC\underline{H}_2C\underline{H}_2O$), 3.36 (m, 8H, $ArC\underline{H}_2Ar$ and

$MsC\underline{H}_2C\underline{H}_2O$), 4.24 (d, J = 13 Hz, 4H, $ArC\underline{H}_2Ar$), 3.23 (s, 6H, $SO_2C\underline{H}_3$), 1.28 (s, 18H, HOAr-*t*-$C_4\underline{H}_9$), 0.90 (s, 18H, ROAr-*t*-$C_4\underline{H}_9$).

2.2.8 Attempt to synthesize 25,27-di(methoxy)-26,28-di(ethyleneglycol)-bis-*p*-*tert*-butylcalix[4]arene (3e)

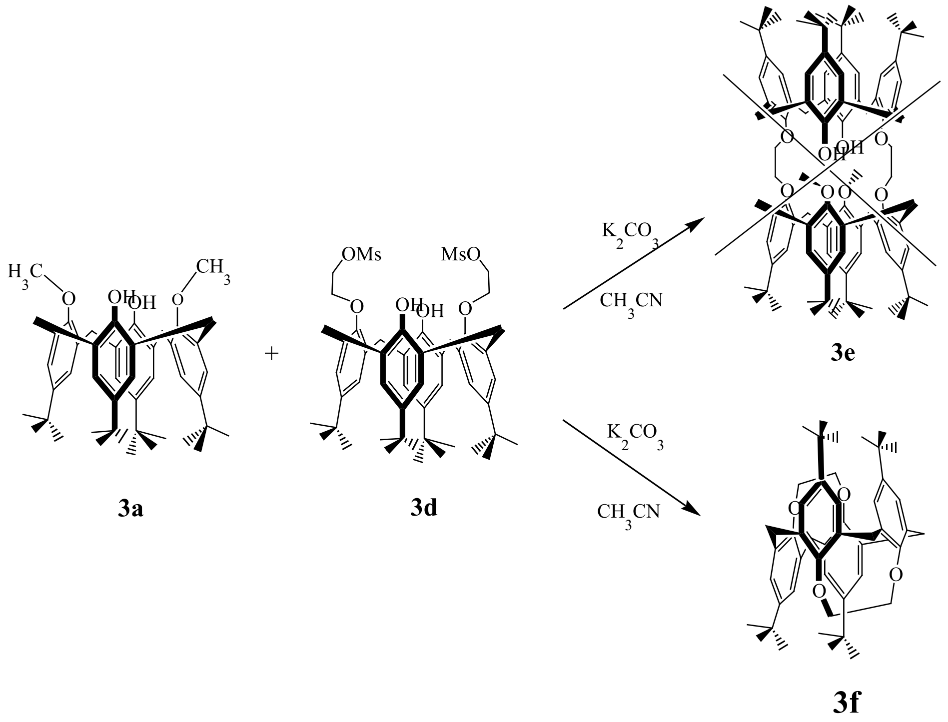

In a 100 mL two-necked round bottom flask, 25,27-di(methoxy)-*p*-*tert*-butylcalix[4]arene **(3a)** (0.4 g, 0.6 mmol) and potassium carbonate (0.34 g, 2.4 mmol) were suspended in dried acetonitrile (50 mL). The mixture was stirred at room temperature for 1 hour. A solution of 25,27-di(methanesulfonyloxyethoxy)-*p*-*tert*-butylcalix[4]arene **(3d)** (0.54 g, 0.6 mmol) in dried acetonitrile (10 mL) was then added. The mixture was stirred and heat at 70 °C under nitrogen atmosphere for 3 days. After the reaction was completed, the solution was allowed to cool to room temperature and evaporated to dryness under reduced pressure. The residue was dissolved in dichloromethane (50 mL) and stirred with an aqueous solution of 3 M hydrochloric acid (50 mL) for 30 minutes and then extracted with dichloromethane (2x30 mL). The organic layer was dried over anhydrous sodium sulfate, filtered and evaporated to dryness. The residue was dissolved in a minimum amount of dichloromethane and methanol was added to precipitate a white crystalline solid (0.33 g, 78% yield). The product was characterized by ^{1}H-NMR and the result indicated that the desired product (**3e**) was not obtained. However, the intramolecular alkylated product (**3f**) was obtained instead.

Characterization data for (3f)

mp. > 300 °C (decompose)

^{1}H-NMR spectrum ($CDCl_3$, 400 MHz) : δ (in ppm) 7.06, 6.96 (m, 8H, RAr$\underline{H}$), 4.57 (d, 2H, ArC$\underline{H}_2$Ar axial), 4.05 (s, 4H, ArC$\underline{H}_2$Ar), 3.58 (m, 4H, ArOC$\underline{H}_2$-C$\underline{H}_2$O), 3.32 (d, 2H, ArC$\underline{H}_2$Ar equatorial), 3.14 (m, 4H, ArOC$\underline{H}_2$-C$\underline{H}_2$O), 1.25 (s, 36H, HOAr-*t*-$C_4\underline{H}_9$).

^{13}C-NMR spectrum ($CDCl_3$, 50 MHz) : δ (in ppm) 153.10, 144.88, 134.73, 132.80, 125.21, 70.64, 34.19, 34.08, 31.46

FAB mass (m/z) : 701 [$M^+ + H^+$]

2.2.9 Preparation of 25,27-di(methoxy)-26,28-di(carbomethoxymethoxy)-*p-tert*-butylcalix[4]arene (4a)

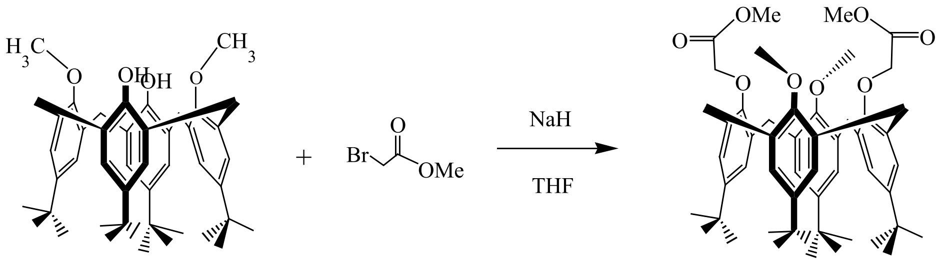

3a **4a**

In a 100 mL two-necked round bottom flask, 25,27-di(methoxy)-*p-tert*-butylcalix [4]arene **(3a)** (3 g, 4.32 mmol) and sodium hydride (0.31 g, 12.96 mmol) were suspended in dried tetrahydrofuran (60 mL). The mixture was stirred for 30 minutes. Methyl bromoacetate (1.23 mL, 12.96 mmol) was then added by syringe. The mixture was stirred overnight and heated at 70 °C under nitrogen. After the reaction was completed, the solution was allowed to cool to room temperature and evaporated to dryness under reduced pressure. The residue was dissolved in dichloromethane (50 mL) and the saturated solution of ammonium chloride (50 mL) was subsequently added to destroy excess methyl bromoacetate and followed by washing with saturated sodium chloride solution (50 mL). Water (50 mL) was added and the mixture was stirred for 30 minutes and extracted with dichloromethane (2x50 mL). The organic layer was dried over anhydrous sodium sulfate, filtered and evaporated to dryness. The residue was dissolved in a minimum amount of dichloromethane and methanol was added to precipitate a white powder (2.82 g, 80% yield). The product was dried in *vacuo* and kept in a desiccator.

Characterization data for 25,27-di(methoxy)-26,28-di(carbomethoxymethoxy)-*p-tert*-butylcalix[4]arene (4a)

mp. 170-172 °C

^{1}H-NMR spectrum ($CDCl_3$, 400 MHz) : δ (in ppm) 7.13 (br, 4H, *m*-ROAr$\underline{H}$), 6.95-6.42 (br, 4H, *m*-ROAr$\underline{H}$), 4.03 (s, 4H, $OC\underline{H}_2CO$), 3.82 (br, 6H, $ArOC\underline{H}_3$), 3.40-3.10 and 4.70-4.10 (br, 8H, $ArC\underline{H}_2Ar$), 1.37 (s, 18H, ROAr-*t*-$C_4\underline{H}_9$), 1.03 (2s, 18H, ROAr-*t*-$C_4\underline{H}_9$), 0.8 (s, 6H, $OC\underline{H}_3$)

^{13}C-NMR spectrum ($CDCl_3$, 50 MHz) : δ (in ppm) 169.87, 155.74, 153.74, 145.15, 144.73, 135.70, 131.87, 127.66, 125.38, 124.57, 72.04, 70.84, 60.43, 58.11, 51.61, 37.62, 34.05, 33.60, 31.63, 31.17

FAB mass (m/z) : 821 [$M^+ + H^+$]

Elemental analysis :	Calculate ($C_{52}H_{68}O_8$)	C, 76.06 ; H, 8.35
	Found	C, 76.14 ; H, 8.18

2.2.10 Preparation of 25,27-di(methoxy)-26,28-di(2-hydroxyethoxy)-*p-tert*-butylcalix[4]arene (4b)

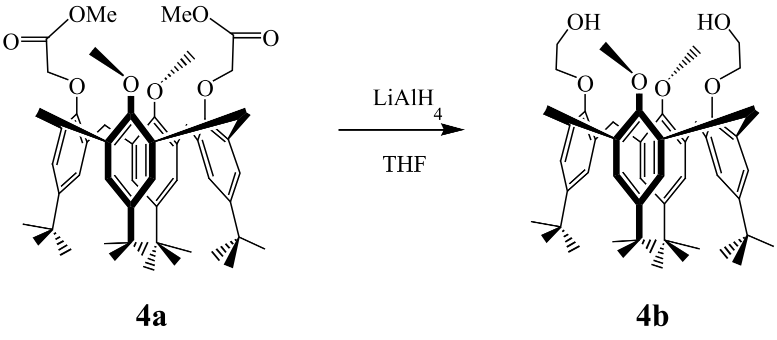

In a 100 mL two-necked round bottom flask, a solution of 25,27-di(methoxy)-26, 28-di(carbomethoxymethoxy)-*p-tert*-butylcalix[4]arene **(4a)** (1.6 g, 1.95 mmol) in dried tetrahydrofuran (40 mL) was stirred for 10 minutes at 10 °C under nitrogen atmosphere. $LiAlH_4$ (0.37 g, 9.75 mmol) was then added gradually. The mixture was allowed to stir overnight at room temperature under nitrogen atmosphere. After the reaction was completed, an aqueous solution of 3 M hydrochloric acid was subsequently added until a precipitate had formed which was then filtered. Water (30 mL) was added and stirred for 30 minutes and extracted with dichloromethane (2x30 mL). The organic layer was dried over anhydrous sodium sulfate, filtered and evaporated to dryness under reduced pressure. The residue was dissolved in a minimum amount of dichloromethane and methanol was added to precipitate a white powder (1.23 g, 82% yield). The product was dried in *vacuo* and kept in a desiccator.

Characterization data for 25,27-di(methoxy)-26,28-di(ethoxyl)-*p-tert*-butylcalix[4] arene (4b)

mp. 135 °C

^{1}H-NMR spectrum ($CDCl_3$, 400 MHz) : δ (in ppm) 7.20-6.50 (m, 8H, *m*-ROAr$\underline{H}$), 5.30-4.90 (m, 2H, $CH_2O\underline{H}$), 4.07 (m, 8H, $ArOC\underline{H}_2C\underline{H}_2OH$), 3.72 (s, 6H, $ArOC\underline{H}_3$), 4.30 and 3.20 (dd, J = 12.0 Hz, 8H, $ArC\underline{H}_2Ar$), 1.25 (s, 18H, ROAr-*t*-$C_4\underline{H}_9$), 0.82 (s, 18H, HOAr-*t*-$C_4\underline{H}_9$)

^{13}C-NMR spectrum ($CDCl_3$, 50 MHz) : δ (in ppm) 153.74, 153.39, 151.90, 146.23, 145.67, 145.04, 135.29, 133.65, 133.32, 132.15, 131.72, 126.35, 125.64, 124.94, 75.74, 62.86, 61.72, 61.46, 58.76, 38.36, 33.94, 33.87, 33.57, 31.58, 31.49, 30.97, 30.43

FAB mass (m/z) : 765 [$M^+ + H^+$]

Elemental analysis :	Calculate ($C_{50}H_{68}O_6$)	C, 78.49 ; H, 8.96
	Found	C, 78.41 ; H, 8.88

2.2.11 Preparation of 25,27-di(methoxy)-26,28-di(methanesulfonyloxyethoxy)-*p-tert*-butylcalix[4]arene (4c)

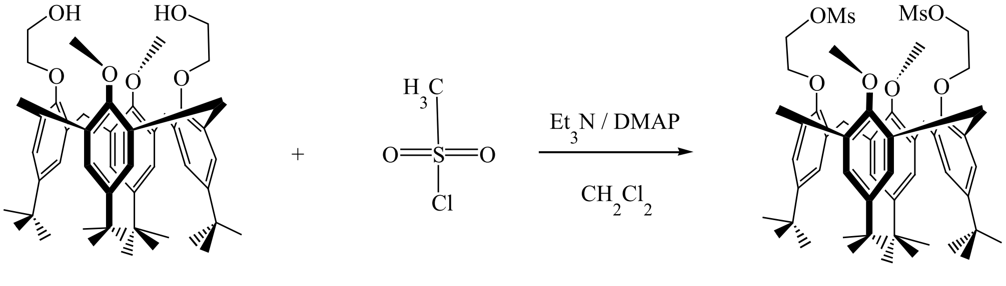

4b **4c**

In a 50 mL two-necked round bottom flask, dichloromethane solution (30 mL) of 25,27-di(methoxy)-26,28-di(2-hydroxyethoxy)-*p-tert*-butylcalix[4]arene (**4b**) (0.5 g, 0.65 mmol), triethylamine (1.02 mL, 6.5 mmol) and a catalytic amount of DMAP was chilled to 10°C with an ice bath and stirred under nitrogen for 30 minutes. MsCl (0.45 mL, 6.5 mmol) was then added by syringe. The reaction mixture was stirred at room temperature under nitrogen for 3 hours. After the reaction was complete, an aqueous solution of 3 M hydrochloric acid (30 mL) was added and stirred for 30 minutes and extracted with dichloromethane (2x30 mL). The organic layer was dried over anhydrous sodium sulfate, filtered and evaporated to dryness. The residue was dissolved in a minimum amount of dichloromethane and methanol was added to precipitate a white powder (0.52 g, 88% yield). The product was dried in *vacuo* and kept in a desiccator.

Characterization data for 25,27-di(methoxy)-26,28-di(methanesulfonyloxyethoxy)-*p*-*tert*-butylcalix[4]arene (4c)

mp. 234-236 °C

^{1}H-NMR spectrum (CDCl$_3$, 400 MHz) : δ (in ppm) 7.05 (br, 4H, RAr$\underline{H}$), 6.54 (br, 4H, HOAr$\underline{H}$), 4.61 (br, 2H, MsC$\underline{H}_2$C$\underline{H}_2$O), 4.30 (br, 2H, MsC$\underline{H}_2$C$\underline{H}_2$O), 3.95 (br, 6H, ArOC$\underline{H}_3$), 3.18 (br, 6H, SO$_2$C$\underline{H}_3$), 4.10 and 3.03 (br, 8H, ArC$\underline{H}_2$Ar), 1.32 (br, 18H, ROAr-*t*-C$_4\underline{H}_9$), 1.10-0.90 (br, 18H, ROAr-*t*-C$_4\underline{H}_9$).

^{13}C-NMR spectrum (CDCl$_3$, 75 MHz) : δ (in ppm) 155.21, 152.63, 145.02, 134.74, 132.33, 125.39, 71.46, 68.15, 60.23, 33.99, 33.63, 37.58, 31.55, 31.14

FAB mass (m/z) : 921 [M$^+$ + H$^+$]

Elemental analysis : Calculate (C$_{52}$H$_{72}$O$_{10}$S$_2$) C, 67.79 ; H, 7.88
Found C, 67.83 ; H, 7.84

2.2.12 Preparation of 25,27-di(methoxy)-26,28-di(ethyleneglycol)-bis-*p*-*tert*-butylcalix[4]arene (4d)

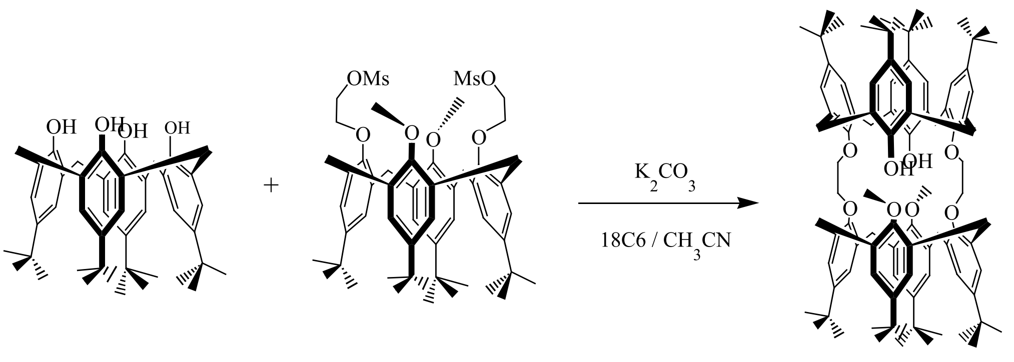

4c **4d**

In a high pressure tube equipped with valves and a pressure gauge, *p*-*tert*-butylcalix[4]arene (0.21 g, 0.33 mmol), 25,27-di(methoxy)-26,28-di(methanesulfonyloxyethoxy)-*p*-*tert*-butylcalix[4]arene **(4c)** (0.3 g, 0.33 mmol), catalytic amount of 18-crown-6 and potassium carbonate (0.11 g, 0.82 mmol) were suspended in dried acetonitrile (5 mL). The tube was then pressurized with N$_2$ at 50 psi. The mixture was stirred and heated at 80 °C for 4 days. The solution was allowed to cool to room temperature and evaporated to dryness under reduce pressure. The residue was dissolved in dichloromethane (50 mL) and an aqueous solution of 3 M hydrochloric acid (50 mL) was subsequently added and stirred for 30 minutes and then extracted with dichloromethane (2x50 mL). The organic layer was dried over anhydrous sodium sulfate, filtered and evaporated to dryness. The residue was dissolved in a minimum amount of dichloromethane and methanol was added to precipitate a white crystalline solid (0.23 g, 52% yield). The product was dried in *vacuo* and kept in a desiccator.

Characterization data for 25,27-di(methoxy)-26,28-di(ethyleneglycol)-bis-*p-tert*-butylcalix[4]arene (4d)

mp. > 300 °C (decompose)

^{1}H-NMR spectrum ($CDCl_3$, 200 MHz) : δ (in ppm) 10.37 (s, 2H, $ArO\underline{H}$), 7.09-6.70 (m, 16H, $\underline{H}Ar$), 4.78-4.12 (m, 22H, $OC\underline{H}_2C\underline{H}_2O$, $ArC\underline{H}_2Ar$ and $–OC\underline{H}_3$), 3.40-3.15 (m, 8H, $ArC\underline{H}_2Ar$), 1.30 (s, 18H, Ar-*t*-$C_4\underline{H}_9$), 1.25 (s, 18H, Ar-*t*-$C_4\underline{H}_9$), 0.95 (s, 36H, Ar-*t*-$C_4\underline{H}_9$)

^{13}C-NMR spectrum ($CDCl_3$, 50 MHz) : δ (in ppm) 154.56, 144.45, 144.26, 141.33, 134.47, 132.98, 132.56, 127.91, 127.67, 125.82, 125.17, 124.89, 75.42, 72.81, 62.52, 33.92, 33.80, 33.61, 32.67, 32.45, 31.58, 31.48, 31.38, 31.29, 31.13, 30.96

ESI mass (m/z) : 1395.2 ($M^+ + NH_4^+$)

Elemental analysis :	Calculate ($C_{94}H_{120}O_8$)	C, 80.01 ; H, 8.43
	Found	C, 80.40 ; H, 8.43

2.2.13 Preparation of 25,27-di(ethyleneglycol)-bis-*p*-*tert*-butylcalix[4] tetraquinone (5a)

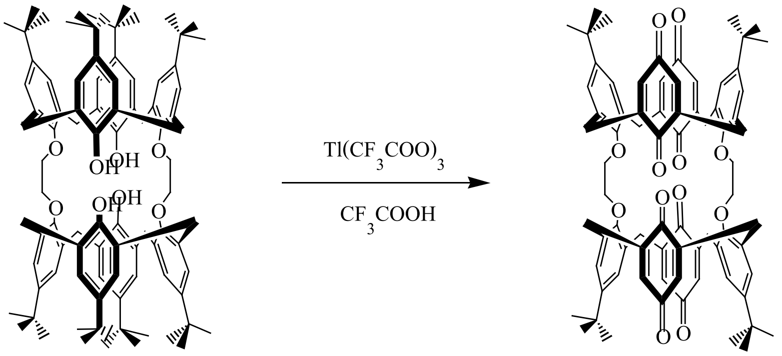

1 **5a**

In a 50 mL two-necked round bottom flask, a suspension of thallium trifluoroacetate (0.8 g, 1.48 mmol) in trifluoroacetic acid (5 mL) was stirred in the dark under nitrogen for 1 hour. 25,27-Di(ethyleneglycol)-bis-*p*-*tert*-butylcalix[4]arene **(1)** (0.2 g, 0.15 mmol) was then added. The mixture was stirred in the dark for another 2 hours. The solution was then poured into ice. Chloroform (50 mL) was added and stirred with water until the organic phase having pH 7 and then extracted with chloroform (2x30 mL). The organic layer was dried over anhydrous magnesium sulfate, filtered and evaporated to dryness. The residue was dissolved in a minimum amount of chloroform and methanol was added to precipitate a yellow crystalline solid (0.091 g, 52% yield). The product was dried in *vacuo* and kept in a desiccator.

Characterization data for 25,27-di(ethyleneglycol)-bis-*p*-*tert*-butylcalix[4] tetraquinone (5a)

mp. > 260 ^{o}C (decompose)

^{1}H-NMR spectrum ($CDCl_3$, 200 MHz) : δ (in ppm) 7.10 (s, 8H, ROAr$\underline{H}$), 5.86 (s, 8H, Hquinone), 4.39 (s, 8H, $OC\underline{H}_2C\underline{H}_2O$), 4.52, 3.00 (dd, J = 13.9 Hz, 16H, $ArC\underline{H}_2Ar$), 1.33 (s, 36H, Ar-*t*-$C_4\underline{H}_9$)

^{13}C-NMR spectrum ($CDCl_3$, 50 MHz) : δ (in ppm) 187.02, 184.97, 154.20, 149.66, 147.58, 133.97, 133.22, 126.67, 72.57, 33.61, 31.63, 30.84

ESI mass (m/z) : 1203.4 ($M^+ + 4H + NH_4^+$)

IR spectrum (KBr (cm^{-1})) : 1658 (C=O)

Elemental analysis :	Calculate ($C_{76}H_{76}O_{12}.2H_2O$)	C, 74.98 ; H, 6.62
	Found	C, 74.99 ; H, 6.20

2.2.14 Preparation of 25,27-di(diethyleneglycol)-bis-*p*-*tert*-butylcalix[4] tetraquinone (5b)

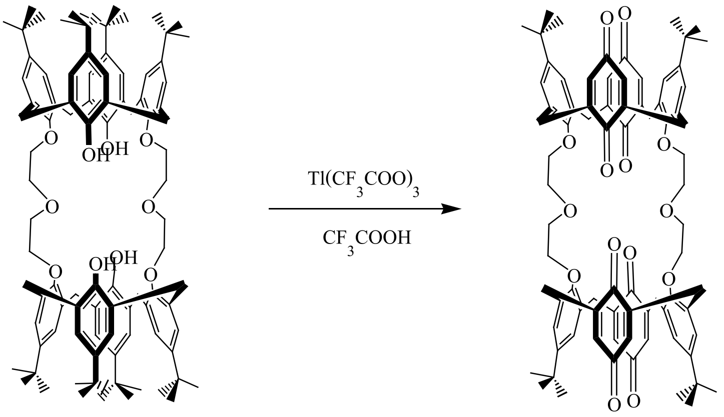

2b **5b**

In a 50 mL two-necked round bottom flask, a suspension of thallium trifluoroacetate (0.76 g, 1.39 mmol) in trifluoroacetic acid (5 mL) was stirred in the dark under nitrogen for 1 hour. 25,27-Di(diethyleneglycol)-bis-*p*-*tert*-butylcalix[4]arene **(2b)** (0.2 g, 0.14 mmol) was then added. The mixture was stirred in the dark for another 2 hours. The solution was then poured into ice. Chloroform (50 mL) was added and stirred with water until the organic phase having pH 7 and then extracted with chloroform (2x30 mL). The organic layer was dried over anhydrous magnesium sulfate, filtered and evaporated to dryness. The residue was dissolved in a minimum amount of chloroform and methanol was added to precipitate a yellow brown crystalline solid (0.12 g, 68% yield). The product was dried in *vacuo* and kept in a desiccator.

Characterization data for 25,27-di(diethyleneglycol)-bis-*p*-*tert*-butylcalix[4] tetraquinone (5b)

mp. > 260 °C (decompose)

^{1}H-NMR spectrum ($CDCl_3$, 200 MHz) : δ (in ppm) 6.95 (s, 8H, ROArH), 6.39 (s, 8H, Hquinone), 4.35-3.90 (m, 24H, $ArOCH_2CH_2OAr$, $ArCH_2Ar$), 3.12 (dd, J = 13.9 Hz, 8H, $ArCH_2Ar$), 1.20 (s, 36H, Ar-*t*-C_4H_9)

^{13}C-NMR spectrum ($CDCl_3$, 50 MHz) : δ (in ppm) 187.98, 185.27, 153.95, 148.79, 146.46, 132.77, 131.10, 126.58, 74.30, 71.29, 34.07, 31.37

IR spectrum (KBr (cm^{-1})) : 1661 (C=O)

Elemental analysis :	Calculate ($C_{80}H_{84}O_{14}.2H_2O$)	C, 72.60 ; H, 6.85
	Found	C, 72.86 ; H, 6.12

2.2.15 Preparation of 25,27-di(methoxy)-26,28-di(ethyleneglycol)-bis-*p*-*tert*-butylcalix[4]diquinone (5c)

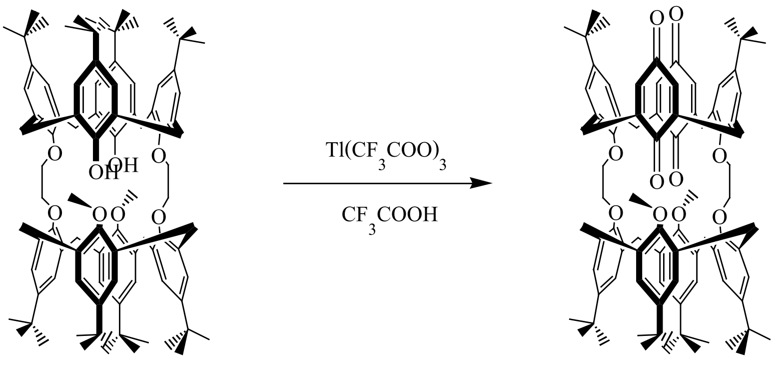

4d **5c**

In a 50 mL two-necked round bottom flask, a suspension of thallium trifluoroacetate (0.76 g, 1.39 mmol) in trifluoroacetic acid (5 mL) was stirred in the dark under nitrogen for 1 hour. 25,27-Di(methoxy)-26,28-di(ethyleneglycol)-bis-*p*-*tert*-butylcalix[4]arene **(4d)** (0.2 g, 0.14 mmol) was then added. The mixture was stirred in the dark for another 2 hours. The solution was then poured into ice. Chloroform (50 mL) was added and stirred with water until the organic phase having pH 7 and then extracted with chloroform (2x30 mL). The organic layer was dried over anhydrous magnesium sulfate, filtered and evaporated to dryness. The residue was dissolved in a minimum amount of chloroform and methanol was added to precipitate a yellow crystalline solid (0.036 g, 38% yield). The product was dried in *vacuo* and kept in a desiccator.

Characterization data for 25,27-di(methoxy)-26,28-di(ethyleneglycol)-bis-*p-tert*-butylcalix[4]diquinone (5c)

mp. > 260 °C (decompose)

^{1}H-NMR spectrum ($CDCl_3$, 200 MHz) : δ (in ppm) 7.15 (s, 8H, $\underline{H}$ArOR), 6.36 (s, 4H, $\underline{H}$ArOR), 5.68 (s, 4H, Hquinone), 4.60-4.40 (m, 16H, $OC\underline{H}_2C\underline{H}_2O$, $ArC\underline{H}_2Ar$), 4.17 (s, 6H, $-OC\underline{H}_3$), 3.30-2.90 (m, 8H, $ArC\underline{H}_2Ar$), 1.33 (s, 36H, Ar-*t*-$C_4\underline{H}_9$), 0.83 (s, 18H, Ar-*t*-C_4H_9)

^{13}C-NMR spectrum ($CDCl_3$, 50 MHz) : δ (in ppm) 187.00, 185.50, 155.73, 154.65, 154.23, 150.89, 146.84, 144.99, 144.15, 135.23, 134.50, 132.62, 130.93, 126.55, 125.73, 124.20, 73.65, 71.42, 63.02, 34.28, 33.99, 33.55, 31.63, 31.52, 31.22, 30.88, 29.65

ESI mass (m/z) : 1315.8 ($M^+ + 4H + NH_4^+$)

IR spectrum (KBr (cm^{-1})) : 1660 (C=O)

Elemental analysis :	Calculate ($C_{86}H_{100}O_{10}.3H_2O$)	C, 76.64 ; H, 7.93
	Found	C, 77.20 ; H, 8.52

2.3 Complexation studies

2.3.1 Complexation studies of ligands 5a, 5b and 5c with Li^+ ion

A solution of 0.005 M of ligands **5a**, **5b** and **5c** (2.5×10^{-6} mol) in $CDCl_3$ (0.5 mL) was prepared in NMR tubes. A solution of 0.05 M of $LiClO_4$ (5.32×10^{-3} g, 5×10^{-5} mol) in CD_3CN (1 mL) was prepared in a vial. The solution of $LiClO_4$ was added directly to the NMR tube by microsyringe to have cation : ligand ratios shown in Table 2.1. ^{1}H-NMR spectra were recorded after each addition.

2.3.2 Complexation studies of ligands 5a, 5b and 5c with Na^+ ion

A solution of 0.005 M of ligands **5a**, **5b** and **5c** (2.5×10^{-6} mol) in $CDCl_3$ (0.5 mL) was prepared in NMR tubes. A solution of 0.05 M of $NaClO_4$ (6.12×10^{-3} g, 5×10^{-5} mol) in CD_3CN (1 mL) was prepared in a vial. The solution of $NaClO_4$ was added directly to the NMR tube by microsyringe to have cation : ligand ratios shown in Table 2.1. ^{1}H-NMR spectra were recorded after each addition.

2.3.3 Complexation studies of ligands 5a, 5b and 5c with K^+ ion

A solution of 0.005 M of ligands **5a**, **5b** and **5c** (2.5×10^{-6} mol) in $CDCl_3$ (0.5 mL) was prepared in NMR tubes. A solution of 0.05 M of KPF_6 (9.2×10^{-3} g, 5×10^{-5} mol) in CD_3CN (1 mL) was prepared in a vial. The solution of KPF_6 was added directly to the NMR tube by microsyringe to have cation : ligand ratios shown in Table 2.1. ^{1}H-NMR spectra were recorded after each addition.

2.3.4 Complexation studies of ligands 5a, 5b and 5c with Cs^+ ion

A solution of 0.005 M of ligands **5a**, **5b** and **5c** (2.5×10^{-6} mol) in $CDCl_3$ (0.5 mL) was prepared in NMR tubes. A solution of 0.05 M of $CsPF_6$ (1.39×10^{-2} g, 5×10^{-5} mol) in CD_3CN (1 mL) was prepared in a vial. The solution of $CsPF_6$ was added directly to the NMR tube by microsyringe to have cation : ligand ratios shown in Table 2.1. ^{1}H-NMR spectra were recorded after each addition.

Table 2.1: Ratios of cation : ligand in $CDCl_3$: CD_3CN

Ratios of cation : ligand	Volumn cation added (mL)	Mole cation added (mol)	Total volumn in NMR tube(mL)
0.0 : 1.0	0	0	0.500
0.1 : 1.0	0.005	$2.5x10^{-7}$	0.505
0.2 : 1.0	0.005	$5.0x10^{-7}$	0.510
0.3 : 1.0	0.005	$7.5x10^{-7}$	0.515
0.4 : 1.0	0.005	$1.0x10^{-6}$	0.520
0.5 : 1.0	0.005	$1.25x10^{-6}$	0.525
0.6 : 1.0	0.005	$1.5x10^{-6}$	0.530
0.7 : 1.0	0.005	$1.75x10^{-6}$	0.535
0.8 : 1.0	0.005	$2.0x10^{-6}$	0.540
0.9 : 1.0	0.005	$2.25x10^{-6}$	0.545
1.0 : 1.0	0.005	$2.5x10^{-6}$	0.550
1.2 : 1.0	0.01	$3.0x10^{-6}$	0.560
1.4 : 1.0	0.01	$3.5x10^{-6}$	0.570
1.6 : 1.0	0.01	$4.0x10^{-6}$	0.580
1.8 : 1.0	0.01	$4.5x10^{-6}$	0.590
2.0 : 1.0	0.01	$5.0x10^{-6}$	0.600
3.0 : 1.0	0.05	$7.5x10^{-6}$	0.650
4.0 : 1.0	0.05	$1.0x10^{-5}$	0.700

2.4 Electrochemical studies

2.4.1 Apparatus

Cyclic voltammetry and square wave voltammetry was perfomed using an AUTOLAB PGSTAT 100 (Ecochemie, Netherlands) with a three electrode consisting of a glassy carbon electrode with a conducting area of 3mm diameter, a platinum wire counter electrode and a Ag/$AgNO_3$ reference electrode. All CV measurements were digitized using the GPES software (Version 4.7). All scans were carried out at room temperature and scan rates were varied.

2.4.2 Cleaning procedure for electrode

Cleaning of the glassy carbon electrode was done using a BAS polishing kit with stepwise finer abrasives down to 0.05 and 0.1 μm alumina powder slurry. The electrode was then sonicated in 0.005 M H_2SO_4 for 5 minutes and then soaked with dichloromethane. This cleaning procedure was repeated after each measurement. The platinum wire counter electrode was cleaned by immerged in 3 M HNO_3 for 30 minutes, rinsed with distilled water and wiped to dryness before use. The reference electrode was cleaned by immerging in 3 M HNO_3 for 30 minutes and by rinsing with distilled water.

2.4.3 Preparation of the main solution

Unless otherwise indicated, all experiments were carried out in an electrolyte solution of 0.1 M tetrabutyl ammonium hexafluorophosphate ($TBAPF_6$) in 20% acetonitrile in dichloromethane. The reference electrode contained 0.01 M $AgNO_3$ + 0.1 M $TBAPF_6$ in 20% acetonitrile in dichloromethane. The background solution contained only 0.1 M $TBAPF_6$ (0.19372 g, $5x10^{-4}$ mmol) in 5 mL of 20% acetonitrile in dichloromethane.

2.4.4 CV and SWV measurement

All CV and SWV measurements were carried out in a cell compartment enclosed with a build-in Teflon cap. To avoid the interference from O_2, All solution was bubbled with nitrogen at least 5 minutes before each measurement.

Cyclic voltammograms were recorded over a range of scan rate from 0.05 to 1.0 V/s. The values of E_p and i_p were determined graphically from the CV by plotting a tangent to the leading baseline of the peak to correct for the background current. At a scan rate of 0.050 V/s the half-wave potential $E_{1/2}$ was determined as $(E_{pa} + E_{pc})/2$

Square wave voltammograms were recorded in Frequency 60 Hz at amplitude 0.050 V.

2.4.5 CV and SWV measurements of ligands 5a, 5b and 5c with Li^+ ion

A solution of 0.001 M of ligands **5a**, **5b** and **5c** ($5x10^{-6}$ mol) + $TBAPF_6$ (0.19372 g, $5x10^{-4}$ mmol) in 5 mL of 20% acetonitrile in dichloromethane was prepared in a volumetric flask. $NaClO_4$ 0.1 M (0.05317 g, $5x10^{-4}$ mol) and $TBAPF_6$ (0.19372 g, $5x10^{-4}$ mmol) in 5 mL of acetonitrile was prepared in a volumetric flask. All solutions were sonicated for 30 minutes before used. The solution of $LiClO_4$ was added directly to the Cell by microsyringe to have cation : ligand ratios shown in Table 2.2. Redox currents were determined from CV scans of the complex solutions at a scan rate of 0.050 V/s using the method as described above.

2.4.6 CV and SWV measurements of ligands 5a, 5b and 5c with Na^+ ion

A solution of 0.001 M of ligands **5a**, **5b** and **5c** ($5x10^{-6}$ mol) + $TBAPF_6$ (0.19372 g, $5x10^{-4}$ mmol) in 5 mL of 20% acetonitrile in dichloromethane was prepared in a volumetric flask. $NaClO_4$ 0.1 M (0.06122 g, $5x10^{-4}$ mol) and $TBAPF_6$ (0.19372 g, $5x10^{-4}$ mmol) in 5 mL of acetonitrile was prepared in a volumetric flask. All solutions were sonicated for 30 minutes before used. The solution of $NaClO_4$ was added directly to the Cell by microsyringe to have cation : ligand ratios shown in Table 2.2. Redox currents were determined from CV scans of the complex solutions at a scan rate of 0.050 V/s using the method as described above.

2.4.7 CV and SWV measurements of ligands 5a, 5b and 5c with K^+ ion

A solution of 0.001 M of ligands **5a**, **5b** and **5c** ($5x10^{-6}$ mol) and $TBAPF_6$ (0.19372 g, $5x10^{-4}$ mmol) in 5 mL of 20% acetonitrile in dichloromethane was prepared in a volumetric flask. KPF_6 0.1 M (0.09203 g, $5x10^{-4}$ mol) and $TBAPF_6$ (0.19372 g, $5x10^{-4}$ mmol) in 5 mL of acetonitrile was prepared in a volumetric flask. All solutions were sonicated for 30 minutes before used. The solution of KPF_6 was added directly to the Cell by microsyringe to have cation : ligand ratios shown in Table 2.2. Redox currents were determined from CV scans of the complex solutions at a scan rate of 0.050 V/s using the method as described above.

2.4.8 CV and SWV measurements of ligand 5b with Cs^+ ion

A solution of 0.001 M of ligand **5b** ($5x10^{-6}$ mol) and $TBAPF_6$ (0.19372 g, $5x10^{-4}$ mmol) in 5 mL of 20% acetonitrile in dichloromethane was prepared in a volumetric flask. $CsPF_6$ 0.1 M (0.13894 g, $5x10^{-4}$ mol) and $TBAPF_6$ (0.19372 g, $5x10^{-4}$ mmol) in 5 mL of acetonitrile was prepared in a volumetric flask. All solutions were sonicated for 30 minutes before used. The solution of $CsPF_6$ was added directly to the Cell by microsyringe to have cation : ligand ratios shown in Table 2.2. Redox currents were determined from CV scans of the complex solutions at a scan rate of 0.050 V/s using the method as described above.

Table 2.2: Ratios of cation : ligand in CH_2Cl_2 : CH_3CN

Ratios of cation : ligand	Volumn cation added (mL)
0.0 : 1.0	0
0.2 : 1.0	0.010
0.4 : 1.0	0.010
0.6 : 1.0	0.010
0.8 : 1.0	0.010
1.0 : 1.0	0.010
1.5 : 1.0	0.025
2.0 : 1.0	0.025

3. Results and Discussion

3.1 Synthesis and characterization of double calix[4]arene derivatives

3.1.1 Synthesis and characterization of 25,27-di(ethyleneglycol)-bis-*p-tert*-butylcalix[4]arene (1)

The method to synthesized double calix[4]arene **1** was first reported by Tomapatanaget et. al. in 1998 by nucleophilic substitution reactions of *p-tert*-butylcalix [4]arene with bromoethyl tosylate using anhydrous potassium carbonate as base and yielded **1** in 41%.[40] In the year 2001, Tantrakarn applied high pressure in the same reaction and improved the yield of **1** to 69%.[41] However, the easier way to synthesize compound **1** was adapted from the report by Chen and coworkers as shown in Figure 3.1.[38] *p-tert*-Butylcalix[4]arene was prepared by the condensation of *p-tert*-butylphenol with formaldehyde in a minimum amount of sodium hydroxide as previously reported by Gutsche.[37] Treating *p-tert*-butylcalix[4]arene with 12 equiv. of 1,2-dibromoethane in acetonitrile in the presence of anhydrous potassium carbonate (1 equiv.) for one night. The white crystalline solid double calix[4]arene **1** was obtained in 12% yield. From ^{1}H-NMR spectrum, this compound is in cone conformation due to the presence of ArC$\underline{H}_2$Ar protons as two doublets at 4.50 and 3.35 ppm with coupling constant (*J*) = 13 Hz. The bridging glycolic protons (OC$\underline{H}_2$C$\underline{H}_2$O) appeared at 4.55 ppm. FAB mass spectra also supported the structure of this ligand showing an intense line at m/z 1367.8 due to the [M$^+$ + NH$_4^+$] and elemental analysis was in good agreement with the structure.

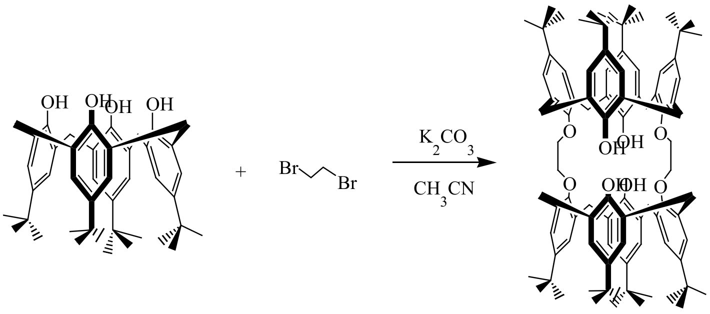

1 (12%)

Figure 3.1: Synthesis of double calix[4]arene (**1**)

3.1.2 Synthesis and characterization of 25,27-di(diethylene glycol)-bis-*p-tert*-butylcalix[4]arene (2b)

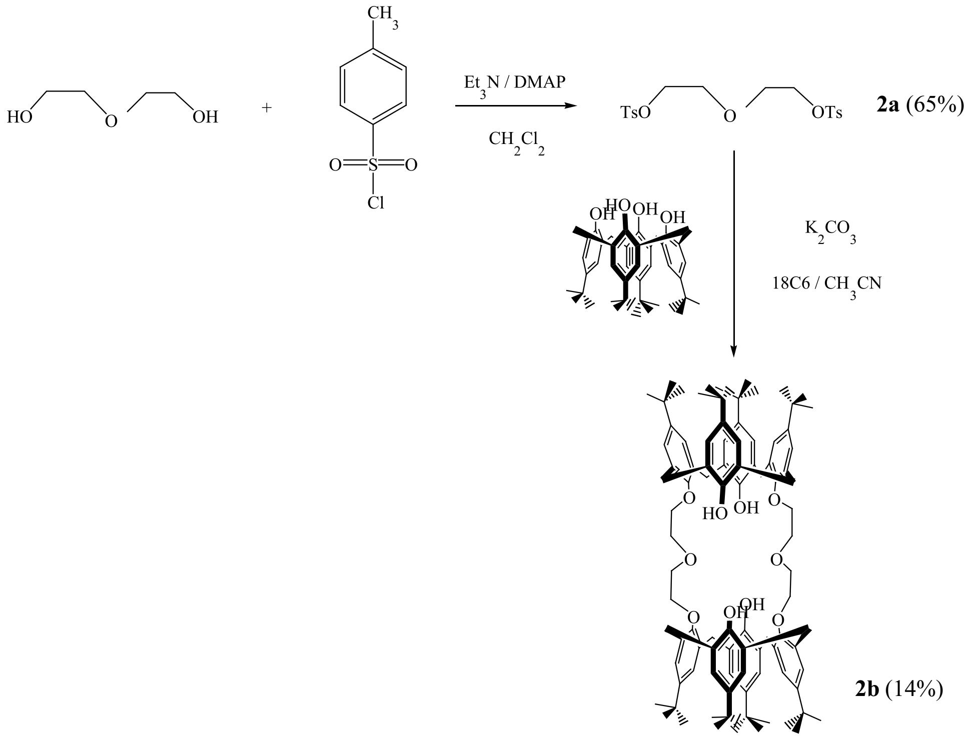

Figure 3.2: Synthetic pathway of double calix[4]arene **2b**

The synthetic pathway shown in Figure 3.2, adapted from Asfari's report, [42] started with a preparation of diethylene glycol ditosylate (**2a**) by tosylation of diethylene glycol in the presence of 3 equiv. of triethylamine and a catalytic amount of DMAP in dichloromethane at room temperature overnight. A white crystalline solid of compound **2a** was obtained in 65% yield. ^{1}H-NMR spectrum of compound **2a** showed the characteristic peaks of tosyl groups: singlet of $C\underline{H}_3$ at 2.43 ppm and two doublets of Ar$\underline{H}$ at 7.76 and 7.33 ppm with coupling constant (J) of 8 Hz. They are accordance with the structure of diethyleneglycol ditosylate (**2a**).

The coupling reaction of **2a** with *p-tert*-butylcalix[4]arene in acetonitrile (10 mL) using anhydrous potassium carbonate as base with a catalytic amount of 18-crown-6 as phase transfer was done by using high pressure technique which was reported by Tantrakarn K.[41] The tube was compressed with N_2 at 50 psi and heated at 70 °C for 2 days. After recrystallization with methanol, compound **2b** was obtained in 14% yield as a white crystalline solid. ^{1}H-NMR spectrum of compound **2b** indicated that it is in cone conformation due to the presence of ArC$\underline{H}_2$Ar protons as two doublets at 4.30 and 3.18 ppm with coupling constant (*J*) = 14.0 Hz. The bridging glycolic protons (OC$\underline{H}_2$C$\underline{H}_2$O) appeared at 4.50-4.10 ppm. FAB mass spectra also supported the structure of this ligand showing an intense line at m/z 1437 and elemental analysis was in good agreement with the structure.

3.1.3 Synthesis and characterization of 25,27-di(methoxy)-26,28-di(ethylene glycol)-bis-*p*-*tert*-butylcalix[4]arene (4d)

The synthesis of double calix[4]arene **4d** is more complicate than double calix[4] arene **1** and **2b** because the structure of compound **4d** was asymmetric. The only way to synthesize this compound was to coupling two units of calix[4]arene derivatives together. One unit must have a good leaving group that makes the coupling procudure more easily. By using this strategy, the synthesis of double calix[4]arene **4d** was carried out in two pathways as shown in Figure 3.3 and Figure 3.4.

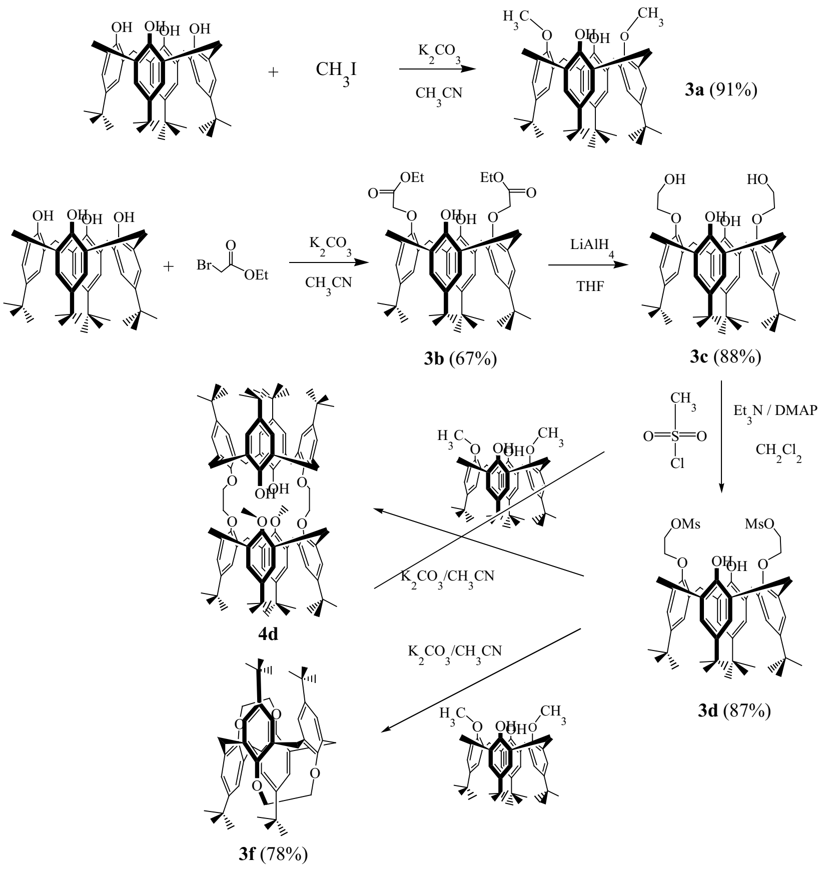

Figure 3.3: Synthetic pathway I of double calix[4]arene **4b**

In early attempt, we tried to synthesize compound **4d** by the synthetic pathway I shown in Figure 3.3. In the first step, compound **3a** was synthesized by a nucleophilic substitution reaction of *p-tert*-butylcalix[4]arene with methyliodide (2.5 equiv.) using anhydrous potassium carbonate as base in dried acetonitrile yielding dimethoxy derivative **3a** as white powder in 91% yield. The ^{1}H-NMR spectrum of **3a** showed singlet peak of the methyl proton at 3.94 ppm. In the second step, compound **3b** was synthesized by nucleophilic substitution reaction of *p-tert*-butylcalix[4]arene with ethylbromoacetate (2 equiv.) using anhydrous potassium carbonate as base in dried acetonitrile yielding diester product **3b** as white powder in 67% yield. The ^{1}H-NMR spectrum of **3b** showed quartet and triplet peaks of the ethylester proton at 4.30 and 1.30 ppm, respectively. After that diester product **3b** was then reduced by adding 4.3 equiv. of $LiAlH_4$ into the solution of **3b** in dried THF to afford an alcohol derivative **3c** as a white powder in 88% yield. The ^{1}H-NMR spectrum of **3c** exhibited two broader peaks due to phenolic hydroxy and alkyl hydroxy protons at 9.23 and 5.25 ppm, respectively with the integral ratio of 1:1. The hydroxy protons of alcohol derivative **3c** was then underwent nucleophilic substitution with methanesulfonyl groups (mesyl) by treating with 4.0 equiv. of triethylamine and a catalytic amount of DMAP in dichloromethane. A white powder product, **3d** was obtained in 87% yield. The ^{1}H-NMR spectrum of **3d** indicated methyl proton signals of methane sulfonyl groups at 3.23 ppm.

Finally, The coupling reaction between the methane sulfonyl derivative **3d** and dimethoxy derivative **3a** was done in the presence of 4.0 equiv. of anhydrous potassium carbonate as base in dried acetonitrile and heated at 70 ^{o}C for 3 days. The product was then characterized by ^{1}H-NMR, Mass spectrometry and the result indicated that the desired product **4d** was not obtained, but the product **3f** which its conformation was in 1,2-alternate was obtained instead. The compound **3f** resulted from an intramolecular alkylated reaction. ^{1}H-NMR spectrum of **3f** showed characteristic peaks due to 1,2 alternate conformation by the presence of a singlet at 4.05 ppm and two doublets at 4.57 and 3.32 ppm for the methylene bridge protons of the calixarene. In the mean time the four protons of the diethylene glycol units face the two opposite aromatic walls appear as a multiplet at 3.58 and 3.14 ppm.[43] In addition, there are 2 ^{13}C-NMR signals appear in the ^{13}C-NMR spectrum of **3f** at 34.2 and 34.1 ppm due to the anti orientation of the adjacent phenol rings.[44]

From the failure of coupling reaction of the pathway I, a new pathway was used. A new unit for the coupling reaction was employed. Figure 3.4 showed the pathway II for synthesize double calix[4]arene **4d**.

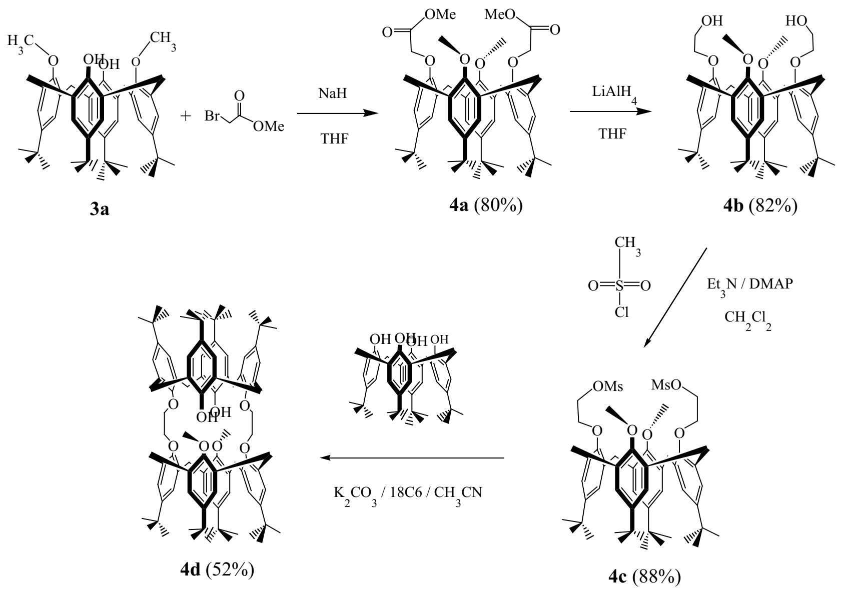

Figure 3.4: Synthetic pathway II of double calix[4]arene **4b**

The synthetic pathway II started with nucleophilic substition of dimethoxy *p-tert*-butylcalix[4]arene **3a** with 3.0 equiv. of methyl bromoacetate in the presence of 3.0 equiv. of sodium hydride as base in dried tetrahydrofuran. The tetra-substituted product **4a** was obtained as white powder in 80% yield. The ^{1}H-NMR spectrum of **4a** showed broad signals due to the phenyl ring inversion from the lack of intramolecular hydrogen bonding. FAB mass spectra supported the structure of this compound showing an intense line at m/z 821 and elemental analysis was in good agreement with the structure. Diester product **4a** was then reduced by adding 5 equiv. of $LiAlH_4$ into the solution of **4a** in dried THF to afford an alcohol derivative **4b** as white powder in 82% yield. As the same as **4a**, the ^{1}H-NMR spectrum of **4b** showed broad signals due to the phenyl ring inversion from the lack of intramolecular hydrogen bonding. FAB mass spectra also supported the structure of this compound showing an intense line at m/z 765 and elemental analysis was in good agreement with the structure. The hydroxy protons of alcohol derivative **4b** was then underwent nucleophilic substitution with methanesulfonyl groups (mesyl) by treating with 10 equiv. of triethylamine and a catalytic amount of DMAP in dichloromethane. A white powder product, **4c** was obtained in 88% yield. The ^{1}H-NMR spectrum of **4c** was not resolved due to the ring inversion from lacking of intramolecular hydrogen bonding.

However, FAB mass spectra supported the structure of this compound showing an intense line at m/z 921 and elemental analysis was in good agreement with the structure.

Finally, The coupling reaction between the tetra-substituted methane sulfonyl derivative **4c** and *p-tert*-butylcalix[4]arene in the presence of 2.5 equiv. of anhydrous potassium carbonate as base in dried acetonitrile (5 mL) with a catalytic amount of 18-crown-6 as phase transfer was done by using a high pressure technique. The reaction tube was compressed with nitrogen at 50 psi and heated at 80^{o}C for 4 days. After recrystallization with methanol, compound **4d** was obtained in 52% yield as a white crystalline solid. ^{1}H-NMR spectrum of compound **4d** at 4.78-4.12 and 3.40-3.15 ppm indicated that it existed in cone conformation with methyl group due to the presence of ArC$\underline{H}_2$Ar and –OC$\underline{H}_3$, respectively. The bridging glycolic protons (OC$\underline{H}_2$C$\underline{H}_2$O) appeared at 4.78-4.12 ppm. ESI mass spectra also supported the structure of this ligand showing an intense line at m/z 1395.2 due to the [M^{+} + NH_4^{+}] and elemental analysis was in good agreement with the structure.

3.1.4 Synthesis and characterization of double calix[4]arenequinone 5a, 5b and 5c

Double calix[4]arenes **1**, **2b** and **4d** were then transformed to their quinone derivatives. From Figure 3.5, compounds **5a**, **5b** and **5c** were synthesized by using $Tl(OCOCF_3)_3$ in CF_3COOH as oxidizing reagent in darkness under nitrogen. The final products, **5a**, **5b** and **5c** were obtained as yellow crystalline solid in 52%, 68% and 38% yield, respectively. ^{1}H-NMR spectrum of ligand **5a** showed the absence of the hydroxy proton signal at 7.65 ppm of compound **1** and a signal of quinone protons was found at 5.86 ppm instead. ESI mass spectra also supported the structure of this ligand showing an intense line at m/z 1203.4 due to the [M^{+} + 4H + NH_4^{+}] and elemental analysis was in good agreement with the structure. ^{1}H-NMR spectrum of ligand **5b** showed the same pattern as that of ligand **5a,** which a signal of quinone protons was found at 6.39 ppm. For ligand **5c**, ^{1}H-NMR spectrum showed absence of two hydroxy proton signals at 10.37 ppm of compound **4d** and a signal of quinone protons was found at 6.50 ppm instead. The methyl protons in structure appeared at 4.15 ppm. ESI mass spectra also supported the structure of this ligand showing an intense line at m/z 1315.8 due to the [M^{+} + 4H + NH_4^{+}] and elemental analysis was in good agreement with the structure. All three final products **5a**, **5b** and **5c** showed the CO stretching in their IR spectra at 1660 cm^{-1}.

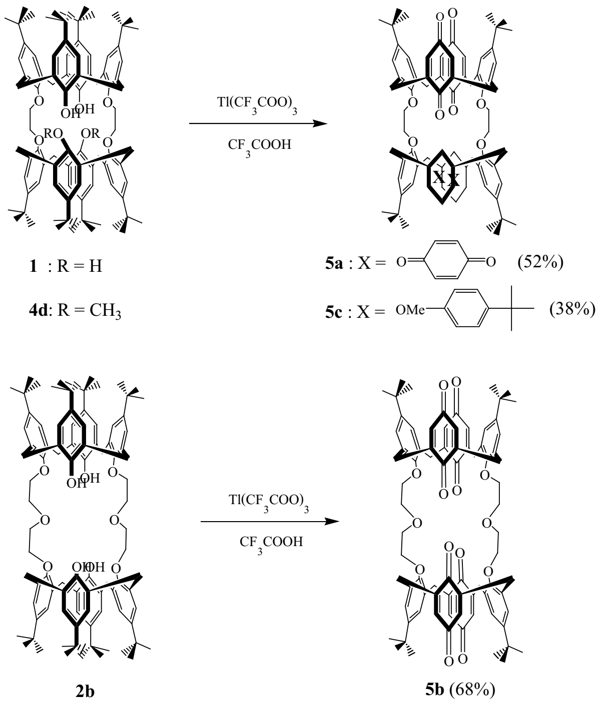

Figure 3.5: Synthetic pathway of double calix[4]arenequinones **5a**, **5b** and **5c**

3.2 Cation complexation studies

Ligands **5a**, **5b** and **5c** contain glycol linkages which have oxygen donor atoms for binding alkaline cations. Like the crown ether derivative calixarenes, they have different cavity size suitable for recognition studies with cations having various sizes. Thus, complexation studies of ligands **5a**, **5b** and **5c** with alkaline cations such as Li^+, Na^+, K^+ and Cs^+ were carried out.

3.2.1 Complexation studies of ligand 5a with Li^+, Na^+, K^+ and Cs^+ ions

Upon addition of $LiClO_4$ to the solutions, The signal of aromatic and quinone protons at 7.11 and 5.88 ppm in ^{1}H-NMR spectra (Figure 3.6) decreased rapidly and a new aromatic signal at 6.80 ppm increased significantly. The new doublet signal of methylene bridge protons of calixarene at 4.03 and 3.35 ppm was also found while doublet signals of the methylene bridge protons of the free ligand at 4.52 and 3.00 (dd, J = 13.9 Hz) decreased gradually. After adding 1.0 equiv. of $LiClO_4$, the signal of aromatic protons and quinone protons at 7.11 and 5.88 ppm of the free ligand totally disappeared and only a new signal of aromatic protons at 6.80 ppm of the complex was found instead. The signal of glycol linkage at 4.42 ppm shifted upfield to 4.31 ppm and the signal of methylene bridge protons of calixarenes at 4.52 and 3.00 (dd, J = 13.9 Hz) moved to 4.03 and 3.35 ppm for the complex. These results indicated that lithium cation bind oxygen atom of the glycol linkages and quinone moieties. The conformation of calixarene was changed, so that the lower rim of calixarene units were closely orientated to each other and suggested that the cavity of double calixarene **5a** was changed after complexation with lithium ion. Addition of more than 1.0 equiv. showed no change of the spectra, indicated that **5a** formed complex with lithium cation in a 1:1 stoichiometry.

When 1.0 equiv. of $NaClO_4$ was added to the $CDCl_3$ solution of **5a**, the signals of aromatic protons and quinone protons at 7.11 and 5.88 ppm disappeared and a new signal of aromatic protons at 6.76 ppm was found in the ^1H-NMR spectra (Figure 3.7). The signal of the glycolic chain at 4.42 ppm was shifted upfield to 4.31 ppm. The doublet signals of the methylene bridge protons of the free ligand at 4.52 and 3.00 (dd, J = 13.9 Hz) became a doublet signal at 4.42 and 3.20 ppm. From these results, suggested that the sodium cation bind oxygen atom of the glycol linkages and the cavity of double calixarene **5a** changed after complexation with sodium but compare with the case of lithium, the cavity after complexation was bigger due to a little shift of methylene bridge protons. Addition more than 1.0 equiv. showed no change of the spectra, indicated that **5a** formed complex with sodium cation in a 1:1 stoichiometry.

In the case of KPF_6, at 1.0 equiv of KPF_6, the signal of aromatic protons and quinone protons at 7.11 and 5.88 ppm disappeared from the ^1H-NMR spectra (Figure 3.7) and a new signal of aromatic protons at 6.66 ppm was found. The signal of the glycol chain at 4.42 ppm shifted upfield to 4.26 ppm. The doublet signal of methylene bridge protons of calixarenes at 4.52 and 3.00 (dd, J = 13.9 Hz) became a doublet signal at 4.35 and 3.10 ppm. From these results, suggested that the potassium cation bind oxygen atom of the glycol linkage and the cavity of double calixarene **5a** changed after complexation with potassium. Addition more than 1.0 equiv. showed no change of the spectra, indicated that **5a** formed complex with potassium ion in a 1:1 stoichiometry.

Upon addition of $CsPF_6$ to the solution, no new signal was observed in the ^1H-NMR spectra (Figure 3.8). The result shows that **5a** cannot form complexes with cesium ion. In conclusion, double calix[4]arene quinone **5a** can act as an alkali ion receptor. This ligand can bind Li^+, Na^+ and K^+ with oxygen donor atom in the ethylene glycol linkage and after binding cations, the cavity of double calix[4]arenequinone **5a** changed upon complexation. The quinone units can flip up and down to accommodate a particular cation (Li^+, Na^+ or K^+). In the case of Cs^+, no complexation between ligand **5a** and Cs^+ occurred due to the radius of Cs^+ is bigger than the cavity size. These results lead us to propose the structure of complexation between ligand **5a** with various cations as shown in Figure 3.10.

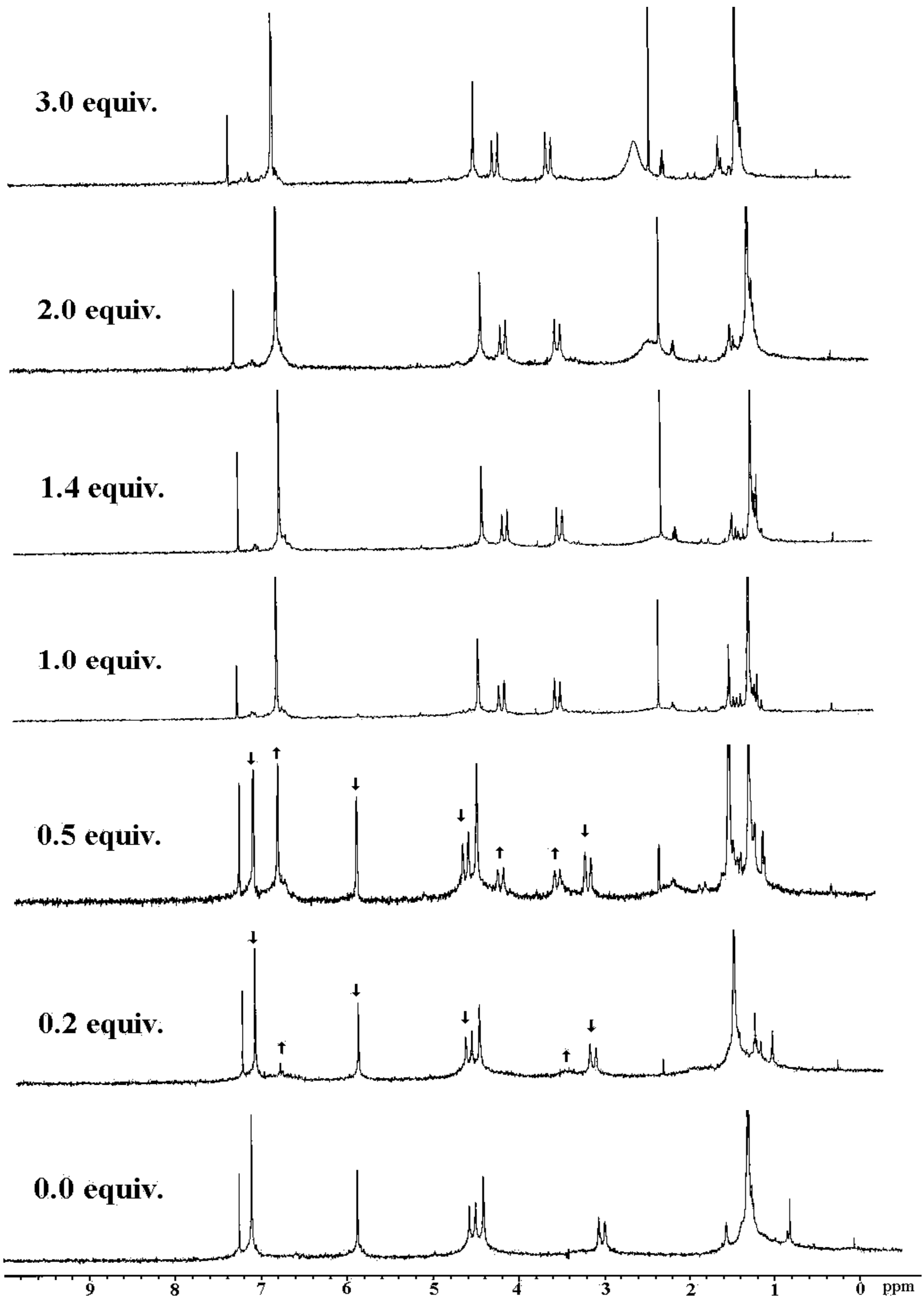

Figure 3.6 : ^{1}H-NMR ($CDCl_3$, 200 MHz) spectra of ligand **5a** with $LiClO_4$

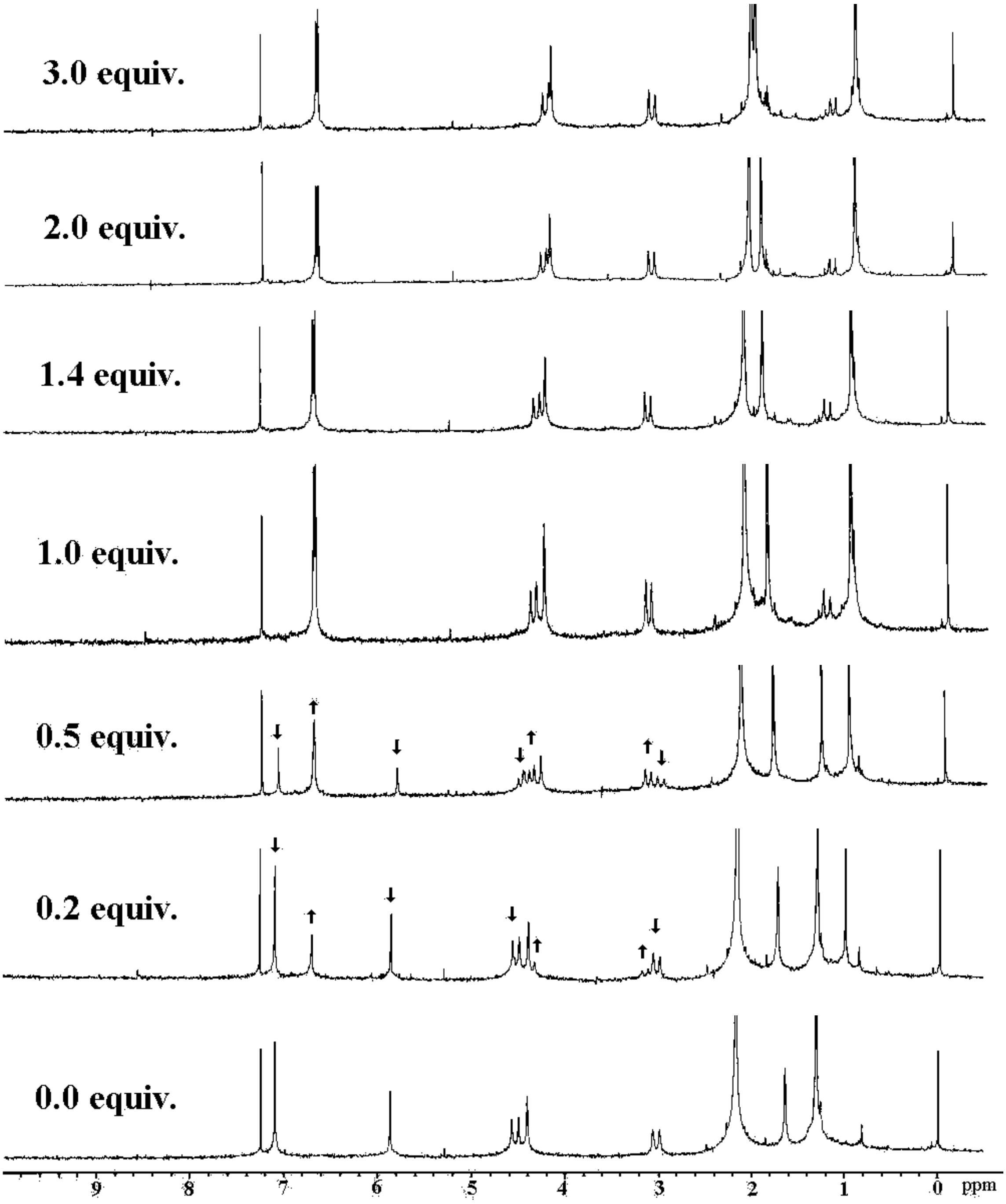

Figure 3.7 : ^{1}H-NMR ($CDCl_3$, 200 MHz) spectra of ligand **5a** with $NaClO_4$

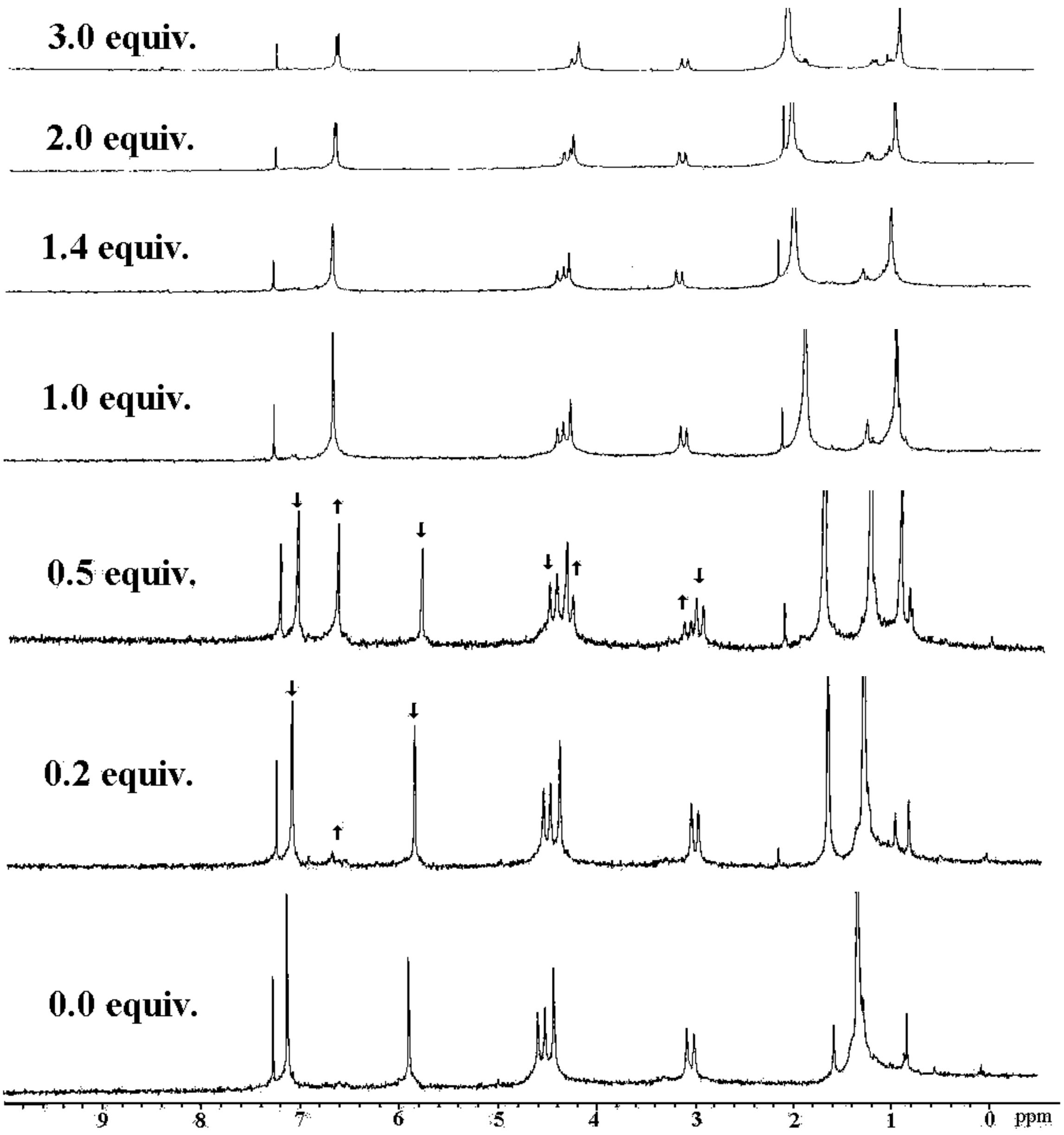

Figure 3.8 : ^{1}H-NMR ($CDCl_3$, 200 MHz) spectra of ligand **5a** with KPF_6

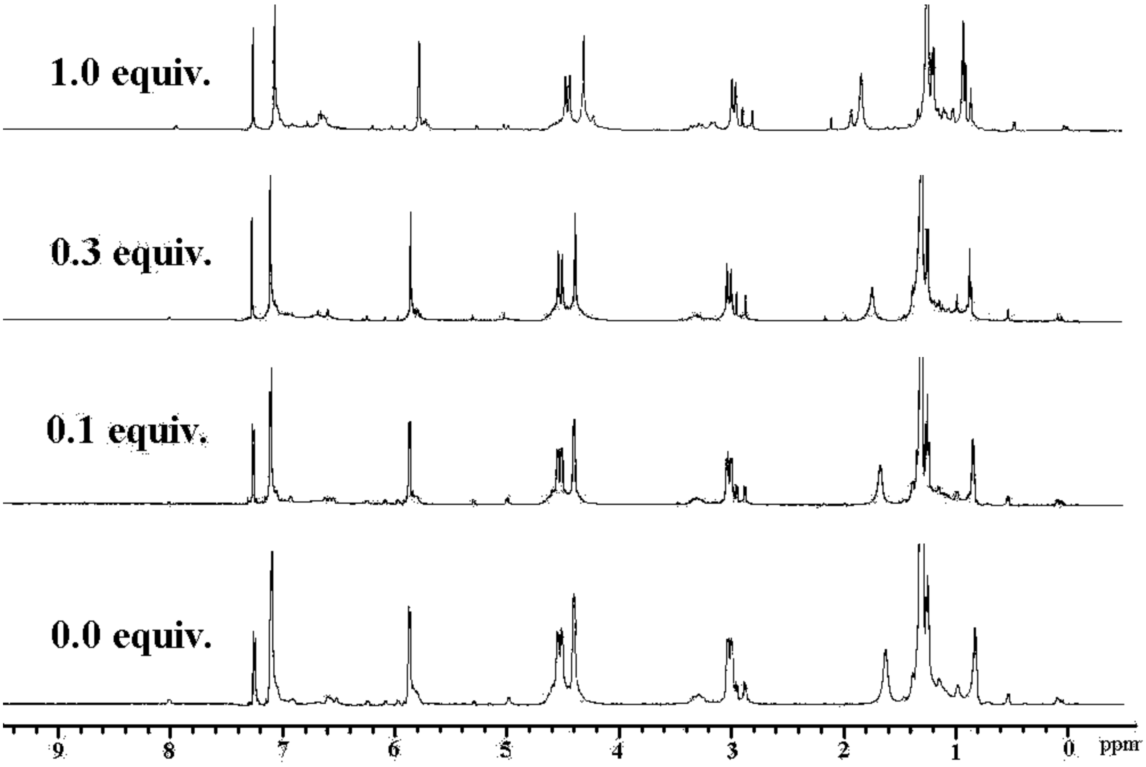

Figure 3.9 : ^{1}H-NMR ($CDCl_3$, 400 MHz) spectra of ligand **5a** with $CsPF_6$

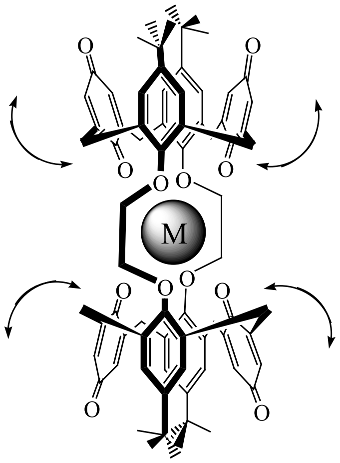

M = Li^+, Na^+ and K^+

Figure 3.10 : A proposed structure of complexation between ligand **5a** with various cations

3.2.2 Complexation studies of ligand 5b with Li^+, Na^+, K^+ and Cs^+ ions

Upon addition of $LiClO_4$ to the solutions, signals of aromatic and quinone protons at 6.95 and 6.37 ppm in ^{1}H-NMR spectra (Figure 3.11) decreased rapidly and a new aromatic signal at 6.66 ppm increased significantly. The signal of the diethylene glycol linkage at 4.01 ppm became a broad signal. Signals of methylene bridge protons of calixarene at 4.20 and 3.10 ppm were unchanged. After adding $LiClO_4$ to 1.0 equiv., signals of aromatic protons and quinone protons at 6.95 and 6.37 ppm of the free ligand totally disappeared and only a new signal of aromatic protons at 6.66 ppm of the complex was found instead. The signal of glycol linkage at 4.01 ppm shifted upfield to 3.90 ppm and signals of methylene bridge protons of calixarene were unchanged. These results indicated that lithium cation bind oxygen atom of the diethylene glycol linkages and the cavity of calixarene was unchanged. Addition more than 1.0 equiv. showed no change of the spectra, indicated that **5b** formed complex with lithium ion a in 1:1 stoichiometry.

When 1.0 equiv. of $NaClO_4$ was added to the $CDCl_3$ solution of **5b**. The signal of aromatic protons and quinone protons at 6.95 and 6.38 ppm disappeared and a new signal of aromatic protons at 6.65 ppm was found in the ^{1}H-NMR spectra (Figure 3.12). The signal of the glycolic chain at 4.01 ppm shifted upfield to 3.94 ppm and became a broad signal. Unlike with the case of lithium, new doublet signals of methylene bridge protons of calixarene at 4.14 and 3.06 ppm were found. From these results, suggested that the sodium cation bind oxygen atom of the diethylene glycol linkages and the cavity of the ligand changes a little due to a little shift of methylene bridge proton signals. Addition of more than 1.0 equiv. showed only changes at the diethylene glycol signal, indicated that **5b** formed complex with sodium ion in a 1:1 stoichiometry.

In the case of KPF_6 at 1.0 equiv. of KPF_6, signals of aromatic protons and quinone protons at 6.95 and 6.38 ppm disappeared and a new signal of aromatic protons at 6.65 ppm was found in the ^{1}H-NMR spectra (Figure 3.13). The signal of the glycolic chain at 4.01 ppm shifted upfield to 3.90 ppm. New doublet signals of methylene bridge protons of calixarenes at 4.14 and 3.04 ppm were found. From these results, suggested that the potassium cation bind oxygen atom of the diethylene glycol linkages and the cavity of double calixarene **5a** changes due to a little shift of methylene bridge proton signals. Addition of more than 1.0 equiv. showed no change of the spectra, indicated that **5b** formed complex with potassium cation in a 1:1 stoichiometry.

Upon addition of $CsPF_6$ to the solution at 1.0 equiv. of $CsPF_6$, signals of aromatic protons and quinone protons at 6.95 and 6.38 ppm disappeared and a new signal of aromatic protons at 6.65 ppm was found in the ^{1}H-NMR spectra (Figure 3.14). The signal of the glycol chain at 4.01 ppm shifted upfield to 3.90 ppm. New doublet signals of methylene bridge protons of calixarenes at 4.20 and 3.01 ppm were found. These results suggested that cesium ion binds oxygen atom of the diethylene glycol linkage and the cavity of double calixarene **5a** changes due to a little shift of methylene bridge protons to accommodate Cs^+. Addition of more than 1.0 equiv. showed no change of the spectra and indicated that **5b** formed complex with cesium ion in a 1:1 stoichiometry.

In conclusion, double calix[4]arene quinone **5b** can act as an alkali cation receptor. This ligand can bind Li^+, Na^+, K^+ and Cs^+ with oxygen donor atoms in diethylene glycol linkages and quinone units. Due to its large cavity size, ligand **5b** can bind Cs^+ and show a little change in calixarene conformation when bind with large alkali cations such as Na^+, K^+ and Cs^+. These results lead us to propose the structure of complexation between ligand **5b** with various cations as shown in Figure 3.15.

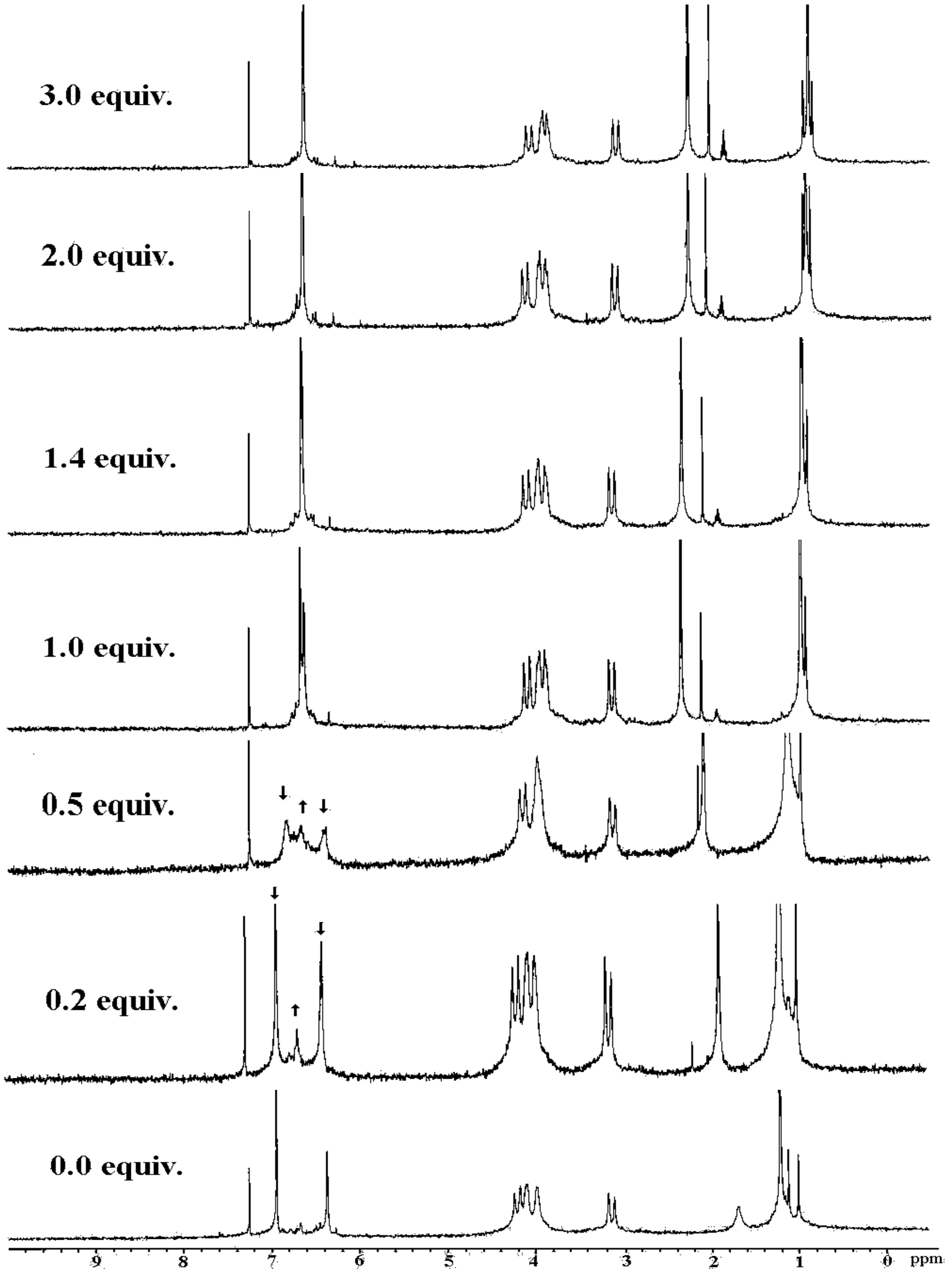

Figure 3.11 : ^{1}H-NMR ($CDCl_3$, 200 MHz) spectra of ligand **5b** with $LiClO_4$

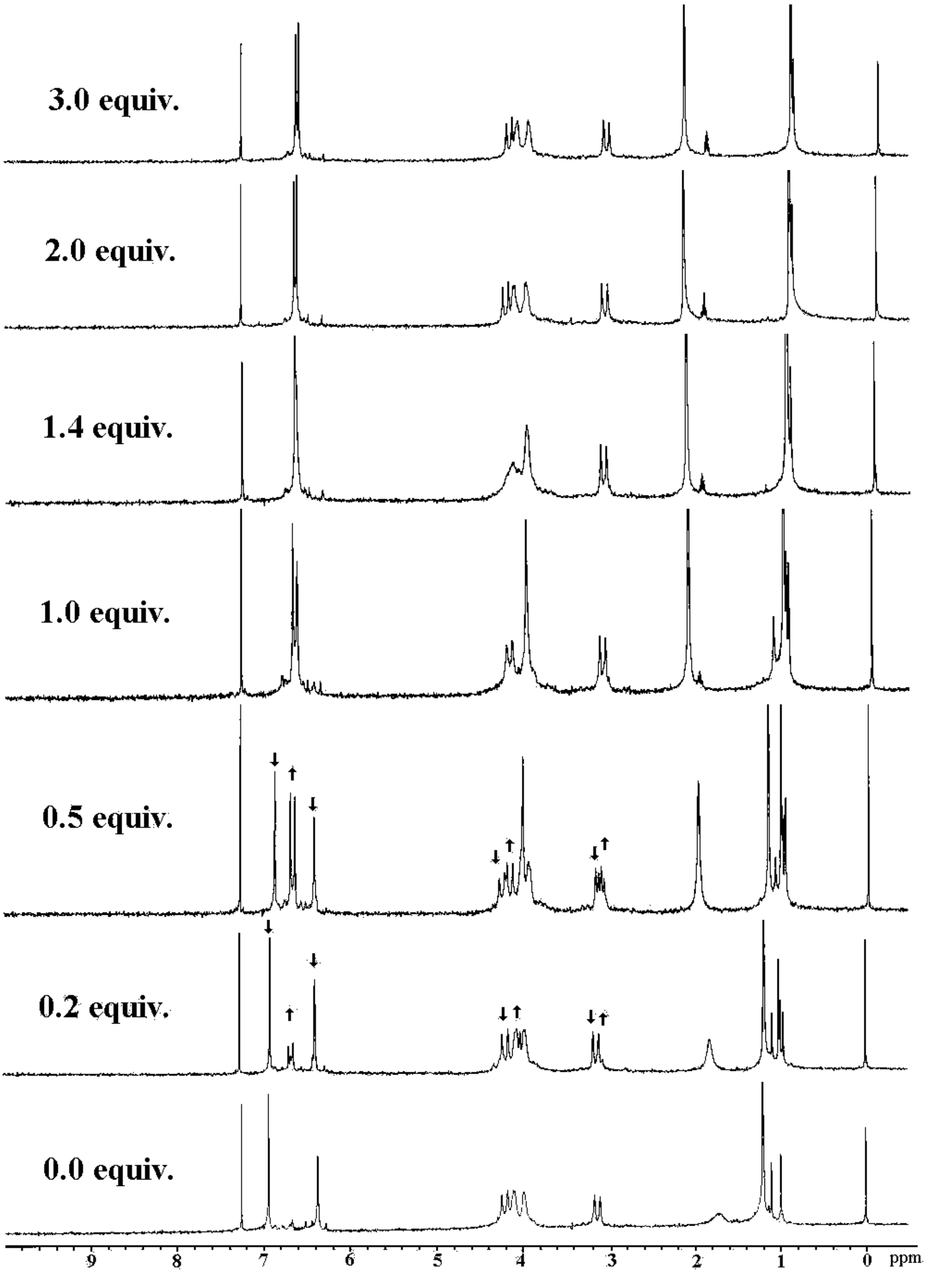

Figure 3.12 : ^{1}H-NMR ($CDCl_3$, 200 MHz) spectra of ligand **5b** with $NaClO_4$

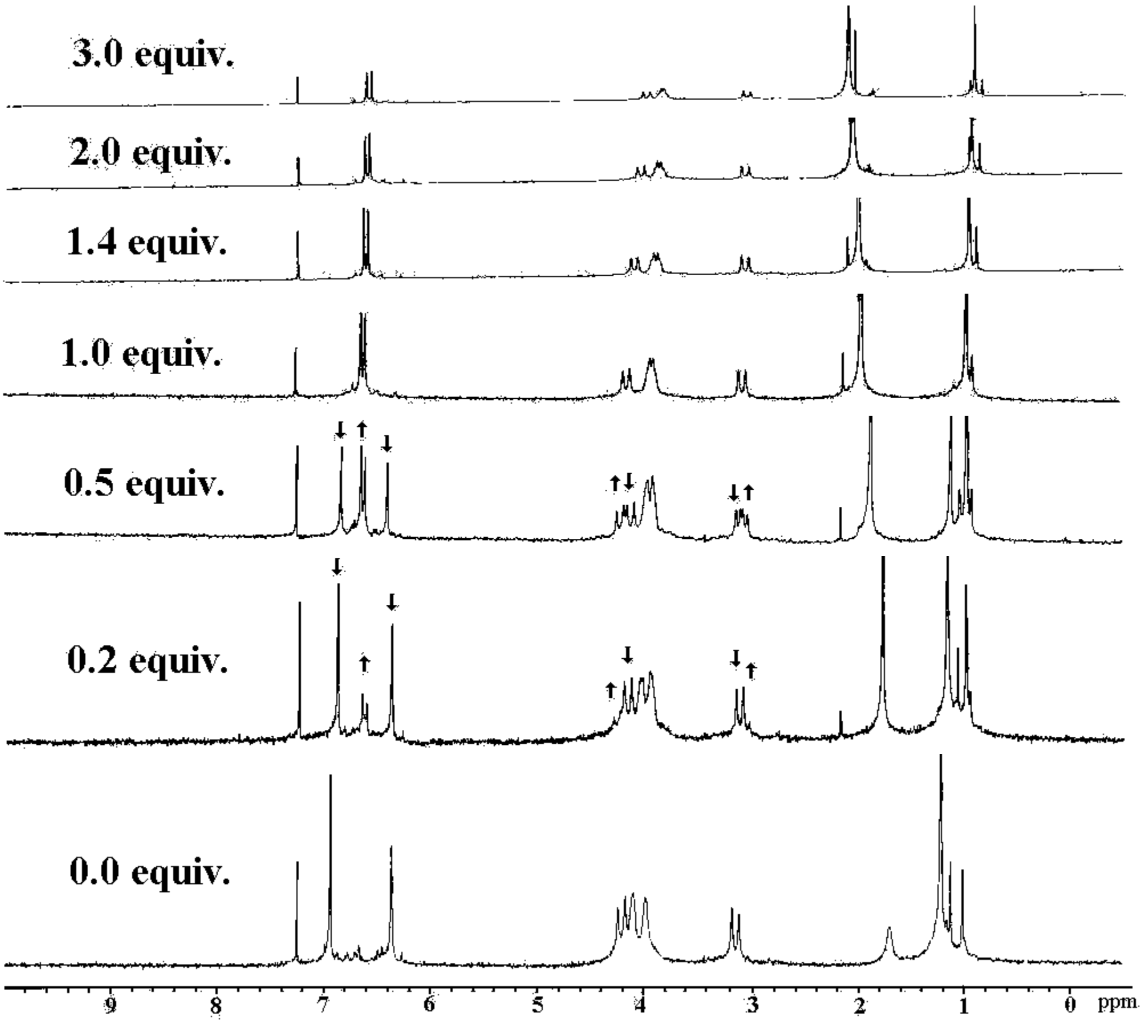

Figure 3.13 : ^{1}H-NMR ($CDCl_3$, 200 MHz) spectra of ligand **5b** with KPF_6

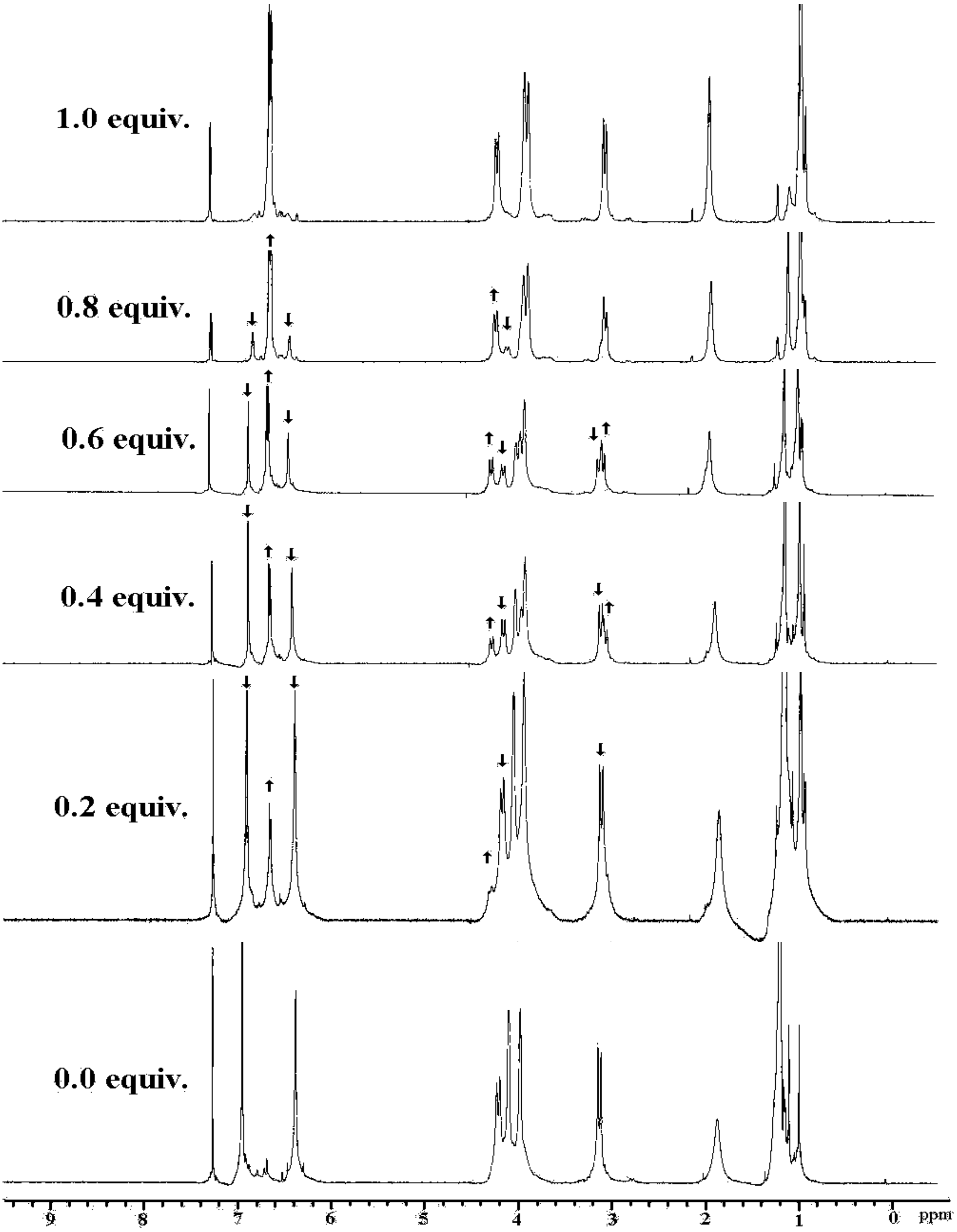

Figure 3.14 : ^{1}H-NMR ($CDCl_3$, 400 MHz) spectra of ligand **5b** with $CsPF_6$

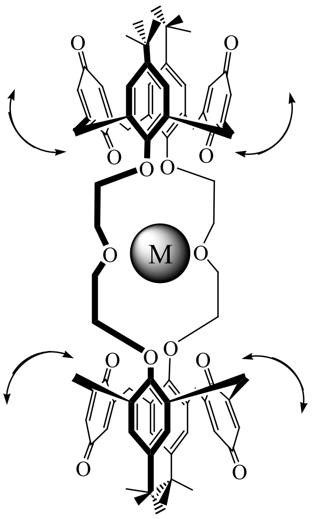

M = Li$^+$, Na$^+$, K$^+$ and Cs$^+$

Figure 3.15 : A proposed structure of complexation between ligand **5b** with various cations

3.2.3 Complexation studies of ligand 5c with Li$^+$, Na$^+$, K$^+$ and Cs$^+$ ions

Upon addition of $LiClO_4$ to the solutions, signals of aromatic and quinone protons at 7.15, 6.36 and 5.68 ppm in ^{1}H-NMR spectra (Figure 3.16) decreased rapidly and a new set of aromatic proton signals at 7.40-5.80 ppm increased significantly. These signals imply that upon complexing a cation the conformation of the methoxy phenyl units were frozen or their movement was prohibited and caused the phenyl ring moving slower than the NMR time scale. This results in various conformations appeared in the NMR spectrum of the complex. New doublet signals of methylene bridge protons of calixarene at 5.00-2.80 ppm was also found and increasing. After adding 1.4 equiv. of $LiClO_4$, the signal of aromatic protons and quinone protons at 6.36 and 5.68 ppm of the free ligand totally disappeared and a new set of aromatic proton signals at 7.40-6.50 ppm of the complex was found instead. New signals of glycolic linkages and methylene bridge protons were found at 5.00-2.80 ppm. The signal of methyl protons in the structure shifted downfield from 4.17 to 4.29 ppm. These results indicated that the cavity size of double calix[4]arene **5c** was small due to the steric from two methyl groups in the structure and when lithium cation bind oxygen atom of the ethylene glycol linkage, the conformation of calixarene changed (Figure 3.20) upon complexation. Addition of more than 1.4 equiv. showed no change of the spectra, suggested that **5c** formed complex with lithium cation in a 1:1 stoichiometry.

When 1 equiv. of $NaClO_4$ was added to the $CDCl_3$ solution of **5c**, signals of aromatic protons and quinone protons at 7.15, 6.36 and 5.68 ppm disappeared from the ^{1}H-NMR spectra (Figure 3.17) and new signals of aromatic protons at 7.40-6.50 ppm were found. Signals of methyl protons at 4.17 ppm shifted downfield to 4.24 ppm. New methylene bridge protons and ethylene glycol linkages signal were found at 5.00-3.40 ppm. From these results, as the same as lithium case, suggested that the sodium cation bind oxygen atom of the glycol linkages and the conformation of double calixarene **5a** changed for accommodating sodium ion. Addition of more than 1.0 equiv. showed no change of the spectra, indicated that **5c** formed complex with sodium ion in a 1:1 stoichiometry.

In the case of KPF_6, adding of more than 0.6 equiv of KPF_6 changed the spectra. From ^{1}H-NMR spectra (Figure 3.18) at 1.8 equiv., signals of aromatic protons and quinone protons at 6.36 and 5.68 ppm disappeared and a new signal of aromatic protons at 6.76 ppm was found. The signal of methyl protons at 4.17 ppm disappeared and became a signal at 3.52 ppm. New methylene bridge protons and ethylene glycolic linkages signal were found at 4.50-3.20 ppm. These results suggested that the potassium ion bind with oxygen atom of the glycol linkages moderately due to its large radius. Addition of more than 1.8 equiv. showed no change of the spectra, suggested that **5c** formed complex with potassium cation in a 1:1 stoichiometry.

Upon addition of $CsPF_6$ to the solution, no new signal was observed in the ^{1}H-NMR spectra (Figure 3.19). The result shows that **5c** cannot form a complex with cesium.

In conclusion, double calix[4]arene quinone **5c** can act as an alkali ion receptor. From the results, this ligand can bind Na^+, Li^+ and K^+ with oxygen donor atom in the ethylene glycol linkage and after binding cations, the conformation of double calix[4] arenequinone **5c** changed upon complexation. In the case of Cs^+, no complexation between ligand **5c** and Cs^+ occurred because the radius of Cs^+ is bigger than the cavity size. These results lead us to propose the structure of complexation between ligand **5c** with various cations as shown in Figure 3.20.

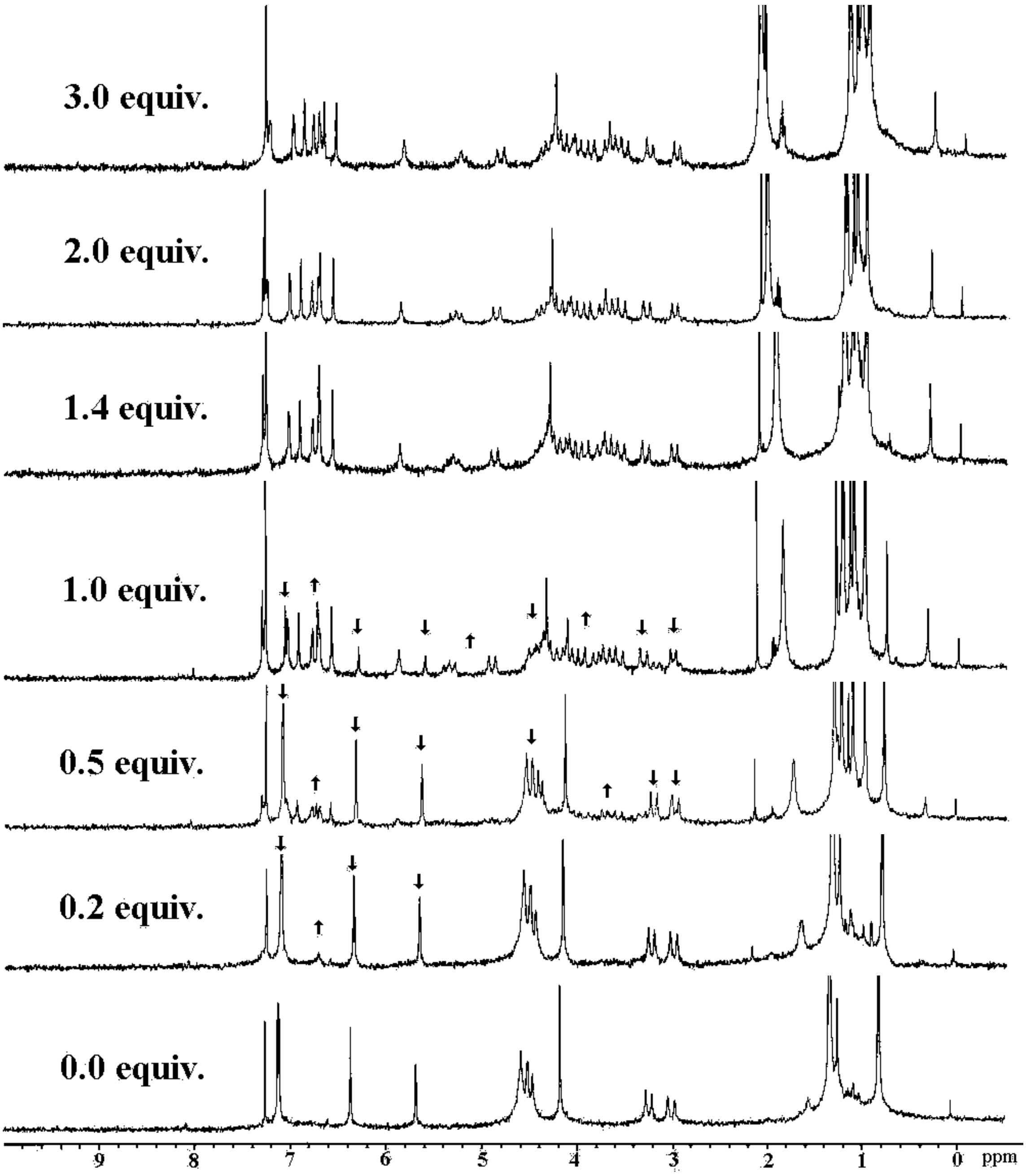

Figure 3.16 : ^{1}H-NMR (CDCl$_3$, 200 MHz) spectra of ligand **5c** with LiClO$_4$

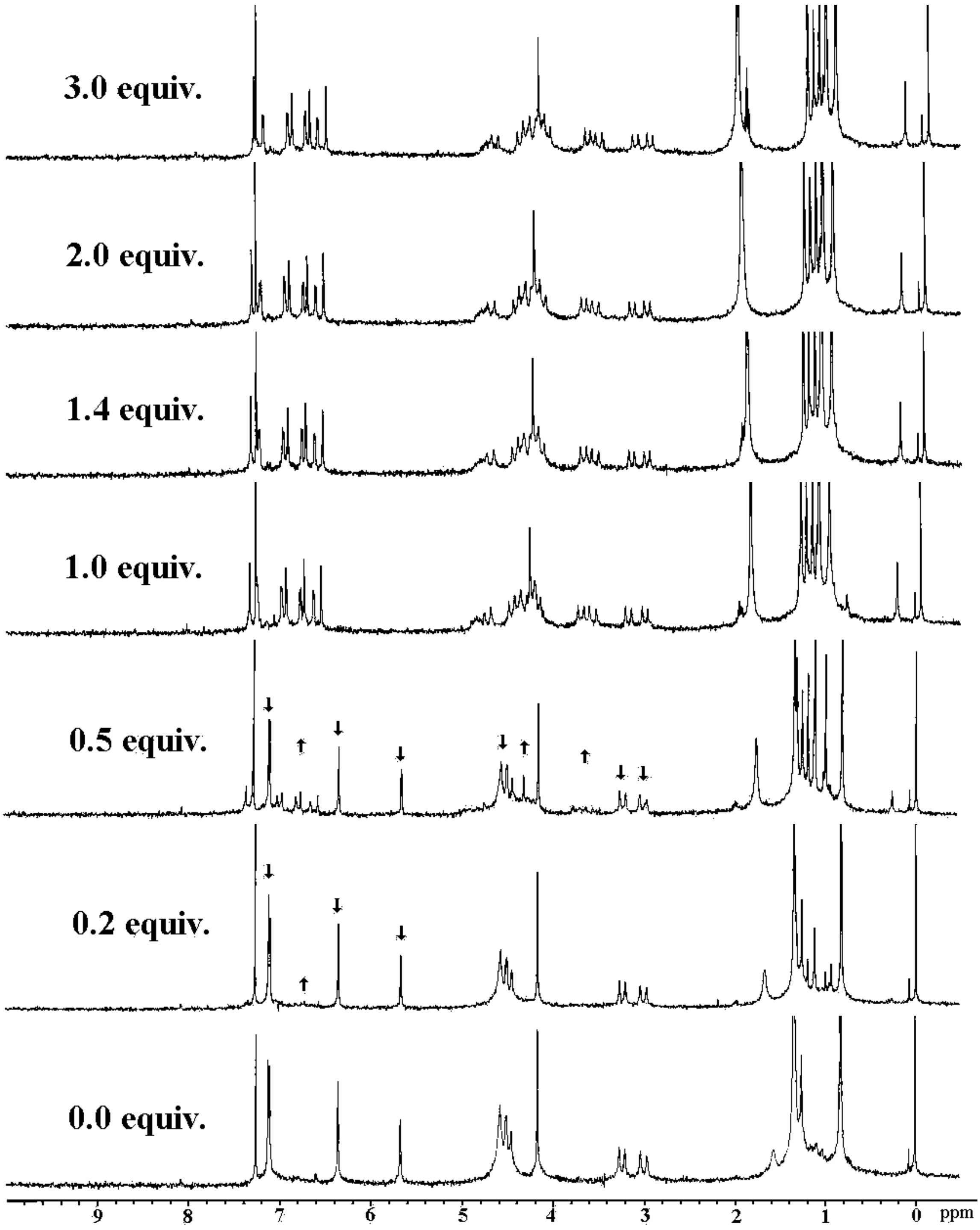

Figure 3.17 : ^{1}H-NMR ($CDCl_3$, 200 MHz) spectra of ligand **5c** with $NaClO_4$

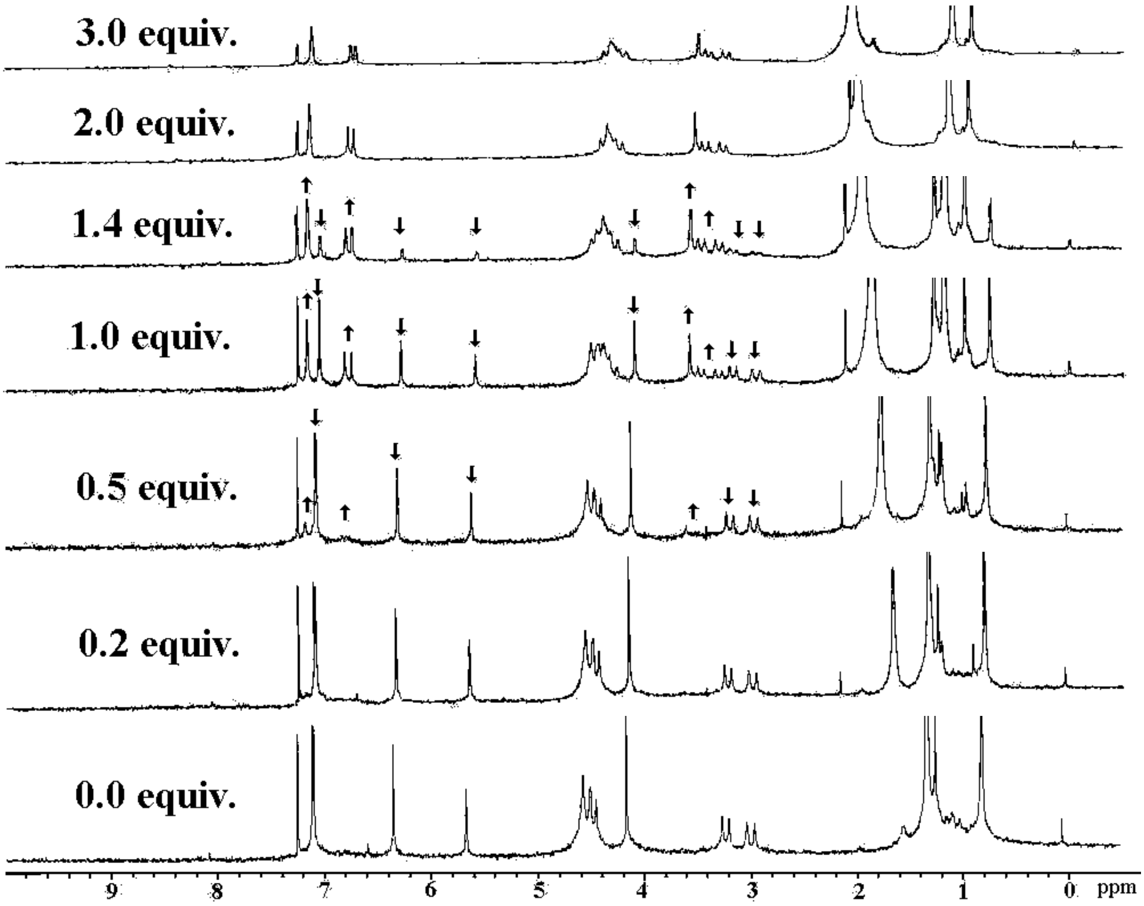

Figure 3.18 : ^{1}H-NMR ($CDCl_3$, 200 MHz) spectra of ligand **5c** with KPF_6

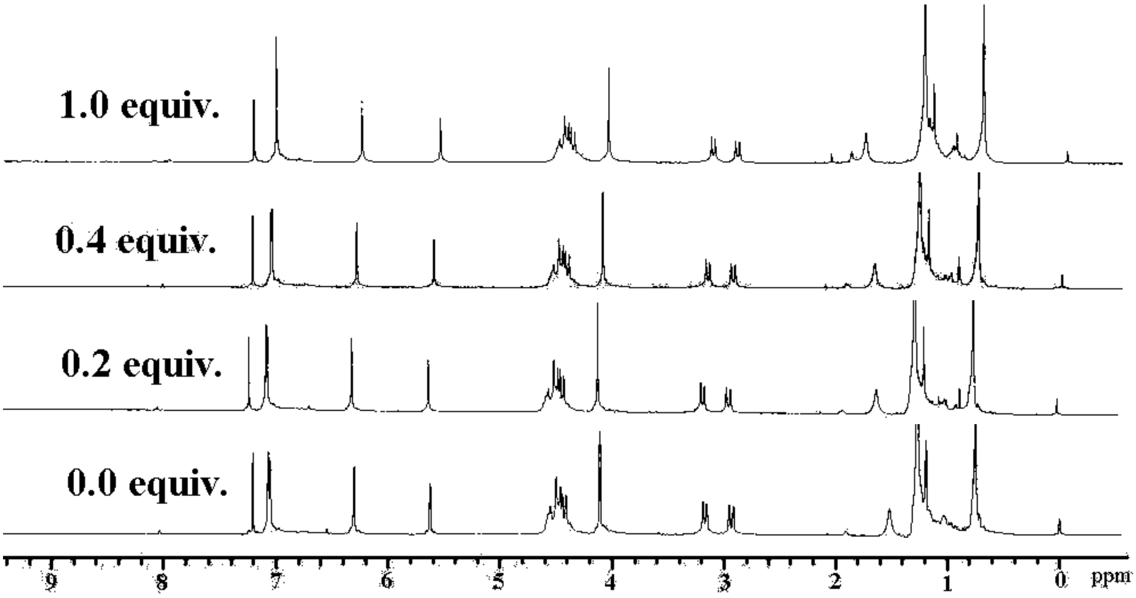

Figure 3.19 : ^{1}H-NMR ($CDCl_3$, 400 MHz) spectra of ligand **5c** with $CsPF_6$

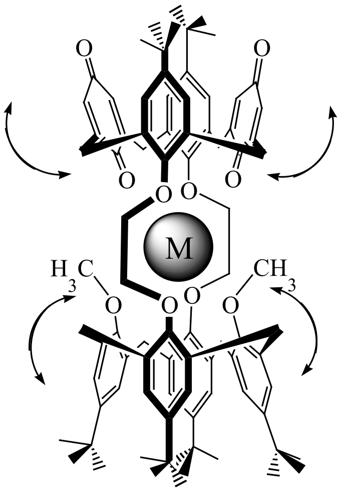

M = Li^+, Na^+ and K^+

Figure 3.20 : A proposed structure of complexation between ligand **5c** with various cations

3.2.4 Calculation of the Complexation Constant [45]

Nuclear magnetic resonance (NMR) spectroscopy is one of the most useful techniques available to chemists for the investigation of dynamic molecular process. Most basic treatments of NMR include at least a qualitative description of the effect of "exchange", reversible dynamic processes, on the appearance of NMR spectra.

One of the most active areas in modern chemical research involves "molecular recognition", the formation of so-called host-guest (or H-G) complexes (C).

$$\mathrm{H} + \mathrm{G} \underset{k_{-1}}{\overset{k_1}{\rightleftarrows}} \mathrm{C} \qquad \textbf{(1)}$$

$$K = \frac{k_1}{k_{-1}} = \frac{[\mathrm{C}]}{[\mathrm{H}]\,[\mathrm{G}]} = \frac{n_c}{n_h\,[\mathrm{G}]} = \frac{n_c}{(1-n_c)\,[\mathrm{G}]} \qquad \textbf{(2)}$$

Where n_h is the mole fraction of uncomplexed host and n_c is the mole fraction of complexed host.

To use NMR methods to study such complexation phenomena, at least one site in the uncomplexed host (or guest) molecule must give rise to a signal at a chemical shift δ_h that is significantly different from the same site in the complexed host (or guest) molecule (δ_c). The magnitude of this difference ($\Delta\delta = \delta_h - \delta_c$) often gives information about the structure of the complex, and may be as large as several ppm.

With this information, we can determine the value of K under slow-exchange conditions by first rewriting equation **2** as

$$K = \frac{[\mathrm{C}]}{([\mathrm{H}]_o - [\mathrm{C}])\,([\mathrm{G}]_o - [\mathrm{C}])} \qquad \textbf{(3)}$$

Where $[\mathrm{H}]_o$ and $[\mathrm{G}]_o$ are the formal (i.e., initial) concentration of host and guest ($[\mathrm{C}]_o = 0$). The relative signal integrals at δ_h and δ_c give

$$\frac{I_c}{I_c + I_h} = n_c \qquad \text{(slow exchange)} \qquad \textbf{(4)}$$

and

$$[\mathrm{C}] = n_c\,[\mathrm{H}]_o \qquad \textbf{(5)}$$

Thus, equation **3** can be rewritten as

$$K = \frac{n_c / [\mathrm{H}]_o}{(1 - n_c)\,(R - n_c)} \qquad \textbf{(6)}$$

Where R is the ratio $[\mathrm{G}]_o/[\mathrm{H}]_o$.

By using equation **6**, the complexation constant (K) can be calculated as shown in Table 3.1

Table 3.1 : Complexation Constant between double calix[4]arenequinones **5a**, **5b** and **5c** with alkali cations.

Alkaline cation	Ligand **5a**	Ligand **5b**	Ligand **5c**
Li^+	30415	897	860
Na^+	44335	9771	5112
K^+	1421	12993	458
Cs^+	NC**	13748	NC**

NC** = No evidence of complexation was observed.

According to the results shown in Table 3.1, ligand **5a** and **5c** form a very stable complexes with Na^+ and exhibit the selectivity trend as $Na^+ > Li^+ >> K^+$ and $Na^+ >> Li^+ > K^+$ respectively. Both ligands **5a** and **5c** show high selectivity to Na^+ due to the optimal spacial fit of the sodium cation within the cavity of the ligands. In contrast, both ligands **5a** and **5c** exhibit low complexation constant with K^+ and no complexation with Cs^+ which could explain by the size of the cation which is larger than Na^+ and Li^+ and larger than the cavity size. The smaller cavity size of ligand **5c** due to the steric from two methyl groups causes the complexation constants of ligand **5c** with various cations lower than those of ligand **5a**. In the case of ligand **5b**, it forms the most stable complex with Cs^+ and the least stable complex with Li^+. Its selectivity with larger cations such as K^+ and Cs^+ occurred due to the large cavity of the ligand and showed the binding trend as $Cs^+ > K^+ >$

Na^+ >> Li^+. We expect that **5a**, **5b** and **5c** would be good sensors for Li^+, Na^+, K^+ and Cs^+. These sensoring properties will be studied by cyclic voltammetry and square wave voltammetry.

3.3 Electrochemical studies

Quinones are commonly used as a reflection of its importance in natural electron transfer systems. In nonaqueous aprotic solvents, quinones undergo two consecutive one-electron transfer processes. In addition, the reduced form of quinone can undergo a chemical reaction to produce hydroquinone according to the following equations.

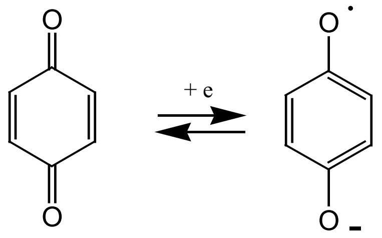

(3.1)

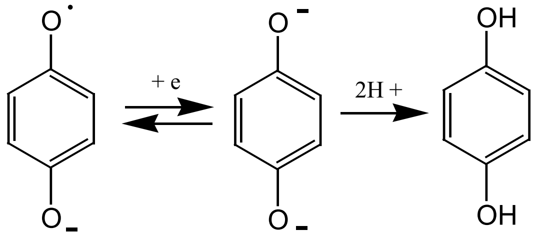

(3.2)

From cation complexation studies, double calix[4]arenequinones **5a**, **5b** and **5c** have been tested for the recognition of alkali cations. In this section, it is of interest to study their interactions with guest cations, in connection with the possibility of electrochemically recognizing alkali cations.

3.3.1 Electrochemical studies of ligand 5a with Li^+, Na^+ and K^+

In the light of the results from NMR titration experiments, ligand **5a** can form complexes with Li^+, Na^+ and K^+; therefore, we investigate the electrochemical properties of **5a** in the presence of Li^+, Na^+ and K^+.

The cyclic voltammogram of ligand **5a** in the mixture of CH_2Cl_2 and CH_3CN (4:1) are presented in Figure 3.21(A). Ligand **5a** exhibits essentially three broad redox waves at -1269, -1394 and -1510 mV, which implies multielectron transfers. Although ligand **5a** has four quinone molecules, one would expect to see 8 one-electron transfer signals in the voltammogram. By taking into account the known behavior of a calix[4]diquinone which can accept a total of four electrons by sequential two-electron reduction process,[26,30-31] the first large quasi-reversible redox wave designated as Ic (cathodic), with a related anodic peak Ia may be attributed to a four-electron reduction process in which a one-electron transfer takes place to each of the quinone moieties present in the ligand to form radical anions. The second and the third more cathodic waves, quasi-reversible reduction IIc and IIIc (related to anodic peak IIa and IIIa, respectively) are consistent with another two-electron reduction process which leads to the formation of dianions. Addition of $LiClO_4$ to electrochemical solution of ligand **5a**, Figure 3.21, led in all cases to the evolution of two new redox waves at -756 and -998 mV, IVc and Vc (related to anodic peak IVa and Va) that were substantially positively shifted relative to wave Ic, which diminished in current height concomitant with the growth of the new waves. Addition of 1.0 equiv. of $LiClO_4$ causes redox waves Ic, IIc and IIIc disappeared and found wave VIc at -1528 mV with a related anodic peak Va instead. The difference in peak potential between the complex and free ligand **5a** is shown in Table 3.3. Squarewave voltammograms also support the result that not only the new waves (IVc and Vc) gradually appears at less negative potential and increases but also the initial wave (Ic, IIc and IIc) decreases and disappears completely as shown in Figure 3.25.

In the case of Na^+, addition of 1.0 equiv. of $NaClO_4$ causes redox waves Ic, IIc and IIIc disappeared as shown in Figure 3.22. Three new redox waves at -1187, -1037 and -933 mV, VIc, Vc and IVc (related to anodic peak VIa, Va and IVa, respectively) appeared and suggested for the complex between ligand **5a** and sodium ion. The difference in peak potential between the complex and the free ligand **5a** is shown in Table 3.3. Square wave voltammograms also support the result that not only the new waves (IVc, Vc and VIc) gradually appear at less negative potential and increase but also the initial wave (Ic, IIc and IIIc) decreases and disappears completely as shown in Figure 3.26.

Upon addition of 1.0 equiv. of KPF_6 to the solution causes redox waves IIc and IIIc disappear as shown in Figure 3.23. A new irreversible redox wave at -1187 mV, Vc and one quasi-reversible wave at -994 mV, IVc (related to anodic peak IVa) appear and suggest the complex between ligand **5a** and potassium cation takes place. Quasi-reversible initial wave Ic became irreversible. The difference in peak potential between the complex and free ligand **5a** is shown in Table 3.3. The squarewave voltammograms (Figure 3.27) support the result that not only the new waves (IVc and Vc) gradually appear at less negative potential and increase but also the initial waves (IIc and IIIc) decrease and disappear completely.

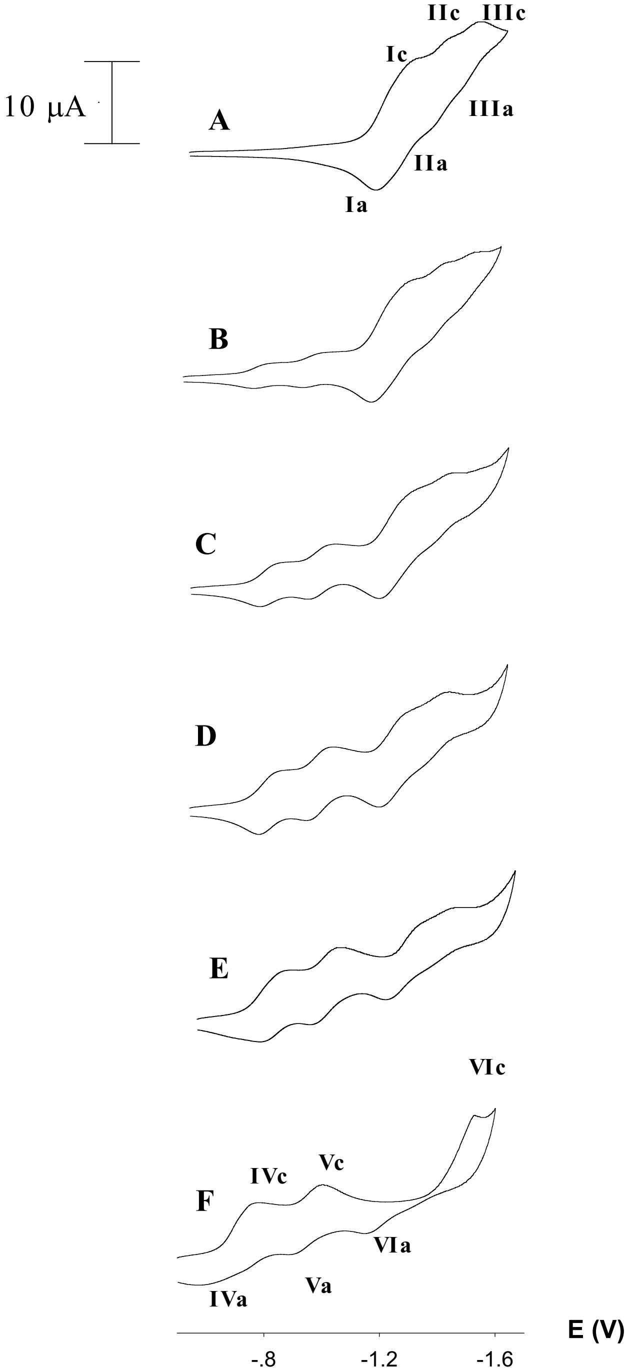

Figure 3.21 : CV of ligand **5a** + Li^+ (A) 0.0 equiv. (B) 0.2 equiv. (C) 0.4 equiv. (D) 0.6 equiv. (E) 0.8 equiv. (F) 1.0 equiv.

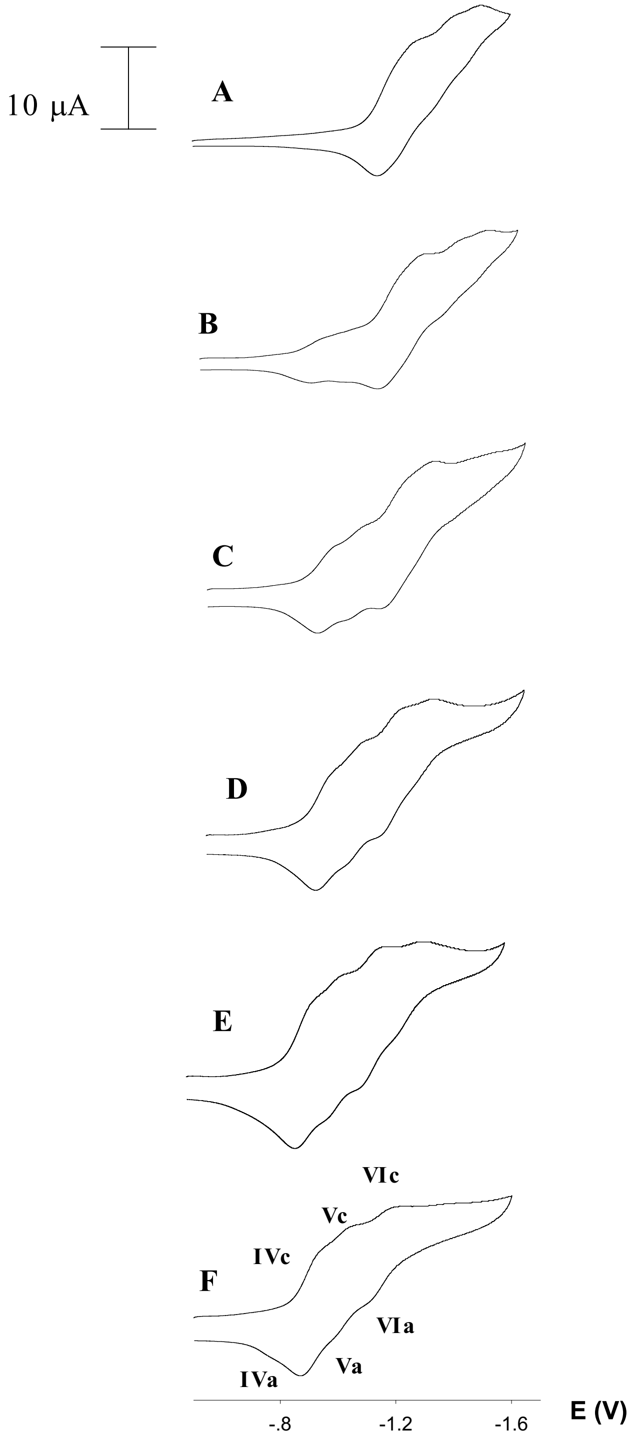

Figure 3.22 : CV of ligand **5a** + Na^+ (A) 0.0 equiv. (B) 0.2 equiv. (C) 0.4 equiv. (D) 0.6 equiv. (E) 0.8 equiv. (F) 1.0 equiv.

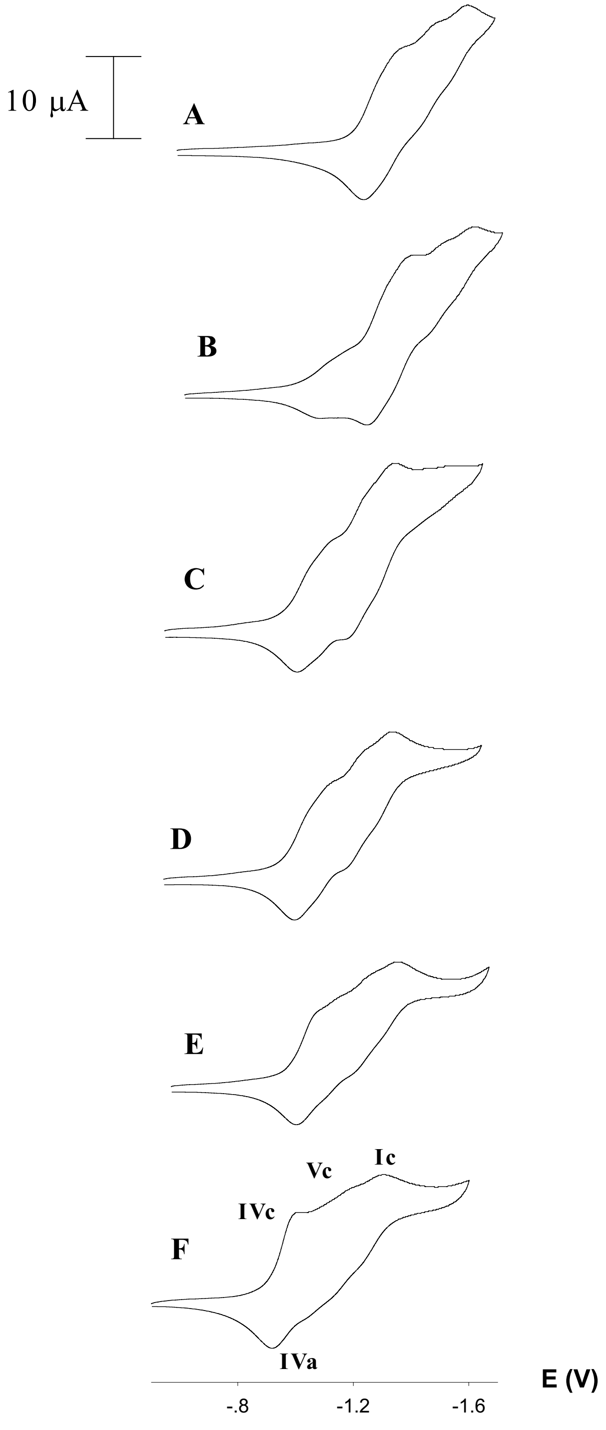

Figure 3.23 : CV of ligand **5a** + K^+ (A) 0.0 equiv. (B) 0.2 equiv. (C) 0.4 equiv. (D) 0.6 equiv. (E) 0.8 equiv. (F) 1.0 equiv.

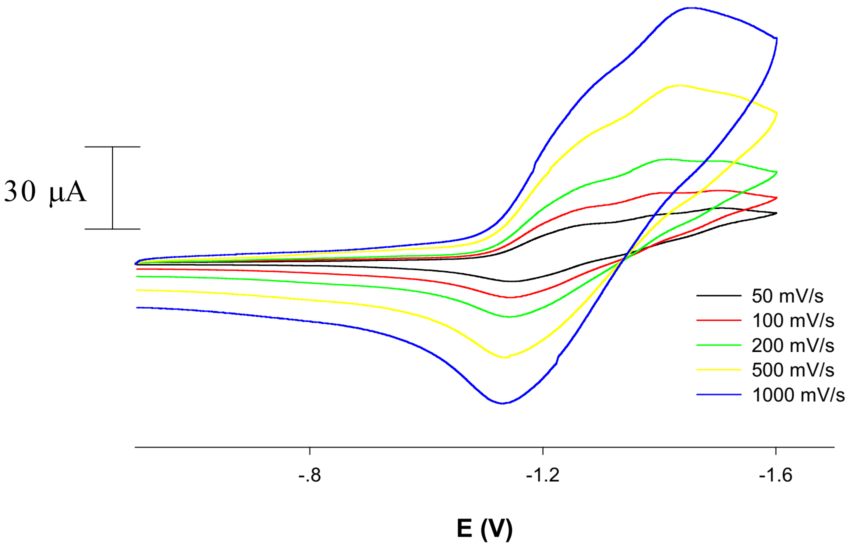

Figure 3.24 : CV of ligand **5a** at various scan rates

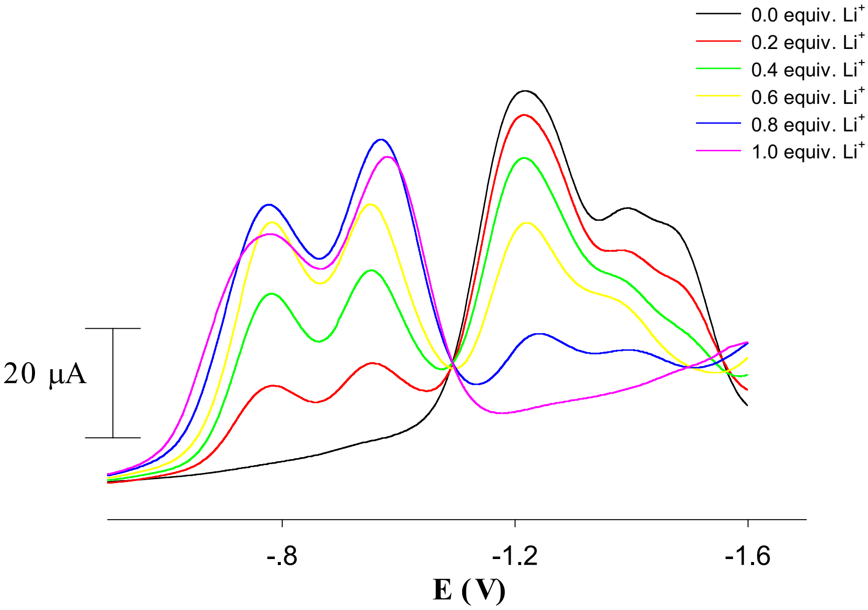

Figure 3.25 : SWV of ligand **5a** + Li$^+$

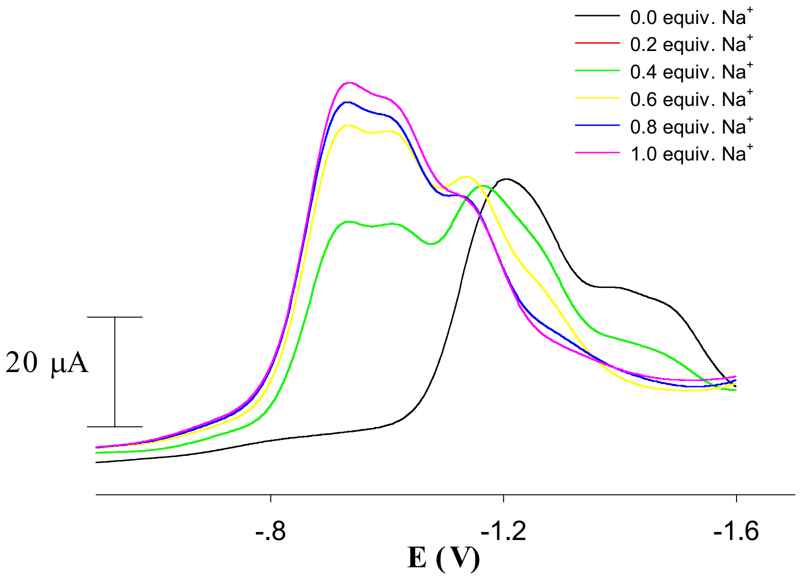

Figure 3.26 : SWV of ligand **5a** + Na^+

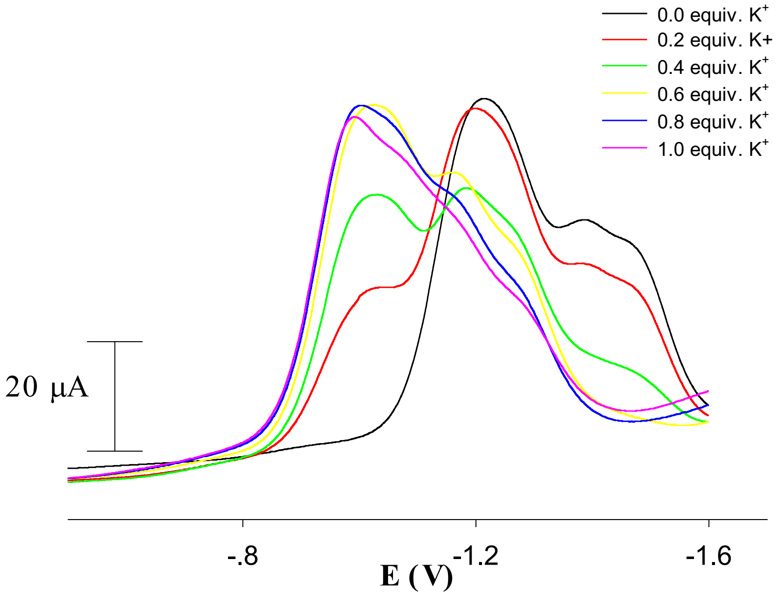

Figure 3.27 : SWV of ligand **5a** + K^+

3.3.2 Electrochemical studies of ligand 5b with Li^+, Na^+, K^+ and Cs^+

In the light of the results from NMR titration experiments, ligand **5b** can form complexes with Li^+, Na^+, K^+ and Cs^+; therefore, we investigate the electrochemical properties of **5b** in the presence of Li^+, Na^+, K^+ and Cs^+.

The cyclic voltammogram of ligand **5b** in the mixture of CH_2Cl_2 and CH_3CN (4:1) are presented in Figure 3.28(A). Compared to the ligand **5a**, ligand **5b** exhibits essentially two broad redox waves at -1269 and -1370 mV, which implies multielectron transfers. The first quasi-reversible redox wave designated as Ic (cathodic), with a related anodic peak Ia may be attributed to a four-electron reduction process in which a one-electron transfer takes place to each of the quinone moieties present in the ligand to form radical anions. The second more cathodic wave, quasi-reversible reduction IIc (related to anodic peak IIa) is consistent with another four-electron reduction process which leads to the formation of dianions. Addition of $LiClO_4$ to electrochemical solution of ligand **5b**, Figure 3.28, led in all cases to the evolution of two new redox waves at -765 and -936 mV, IIIc and IVc (related to anodic peak IIIa and IVa, respectively) that were substantially positively shifted relative to wave Ic, which diminished in current height concomitant with the growth of the new waves. Addition of 1.0 equiv. of $LiClO_4$ causes redox waves Ic and IIc reduced. The difference in peak potential between the complex and free ligand **5b** is shown in Table 3.3. Squarewave voltammograms also support the result that not only the new waves (IIIc and IVc) gradually appear at less negative potential and increase but also the initial waves (Ic and IIc) decrease as shown in Figure 3.33.

In the case of Na^+, addition of 1.0 equiv. of $NaClO_4$ causes redox waves Ic and IIc reduced as shown in Figure 3.29. Two new redox waves at -906 and -1040, IIIc and IVc (related to anodic peak IIIa and IVa, respectively) appeared and suggested for the complex between ligand **5b** and sodium cation. The difference in peak potential between the complex and the free ligand **5b** is shown in Table 3.3. Square wave voltammograms also support the result that not only the new waves (IIIc and IVc) gradually appear at less negative potential and increase but also the initial waves (Ic and IIc) decrease as shown in Figure 3.34.

Upon addition of 1.0 equiv. of KPF_6 to the solution causes redox waves Ic and IIc decreased as shown in Figure 3.30. Two new redox waves at -1016 and -1150 mV, IIIc and IVc (related to anodic peak IIIa and IVa, respectively) appear and suggest the complex between ligand **5b** and potassium cation takes place. The difference in peak potential between the complex and free ligand **5b** is shown in Table 3.3. The squarewave voltammograms (Figure 3.35) support the result that not only the new waves (IIIc and IVc) gradually appear at less negative potential and increase but also the initial waves (Ic and IIc) decrease.

With Cs^+, addition to 1.0 equiv. $CsPF_6$ causes redox waves Ic and IIc decreased as shown in Figure 3.31. Two new redox waves at -1022 and -1156 mV, IIIc and IVc (related to anodic peak IIIa and IVa, respectively) appear and suggest the complex between ligand **5b** and cesium cation takes place. The difference in peak potential between the complex and free ligand **5b** is shown in Table 3.3. The squarewave voltammograms (Figure 3.36) support the result that not only the new waves (IIIc and IVc) gradually appear at less negative potential and increase but also the initial waves (Ic and IIc) decrease.

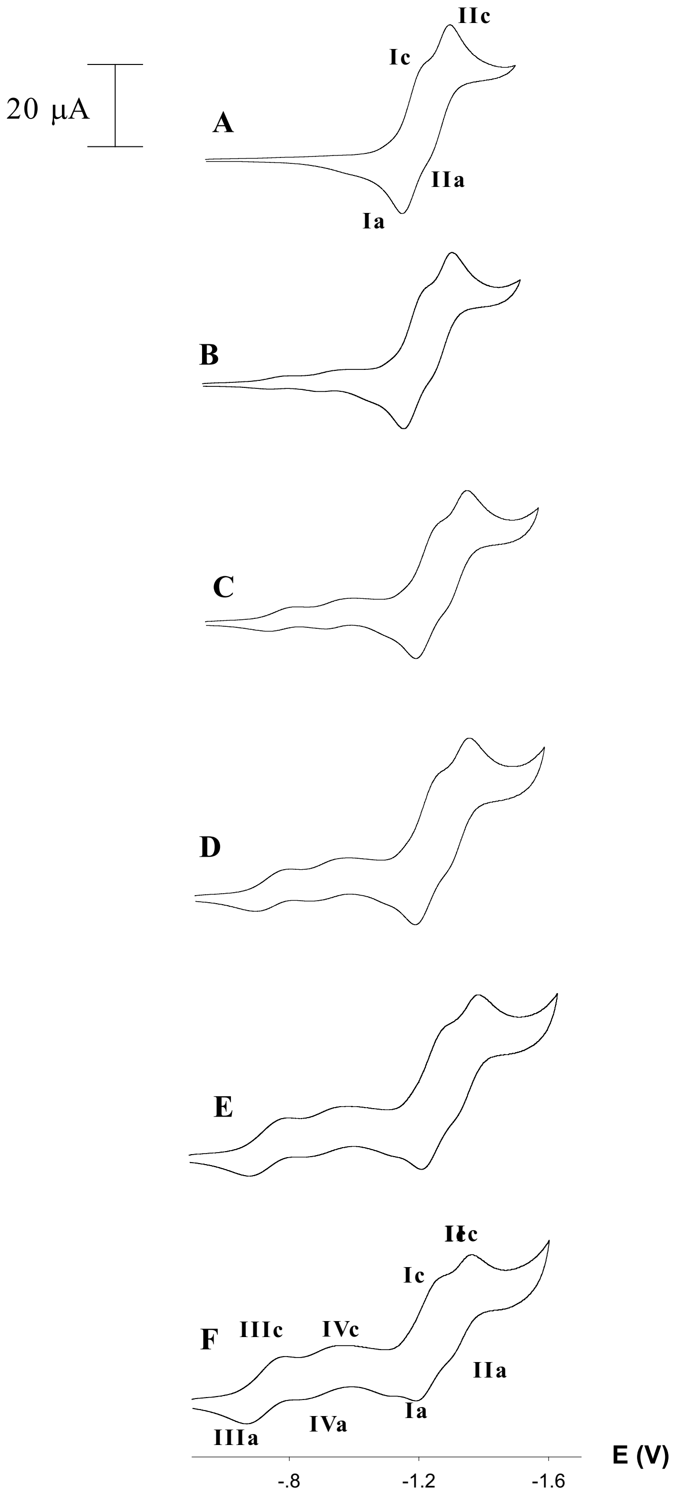

Figure 3.28 : CV of ligand **5b** + Li$^+$ (A) 0.0 equiv. (B) 0.2 equiv. (C) 0.4 equiv. (D) 0.6 equiv. (E) 0.8 equiv. (F) 1.0 equiv.

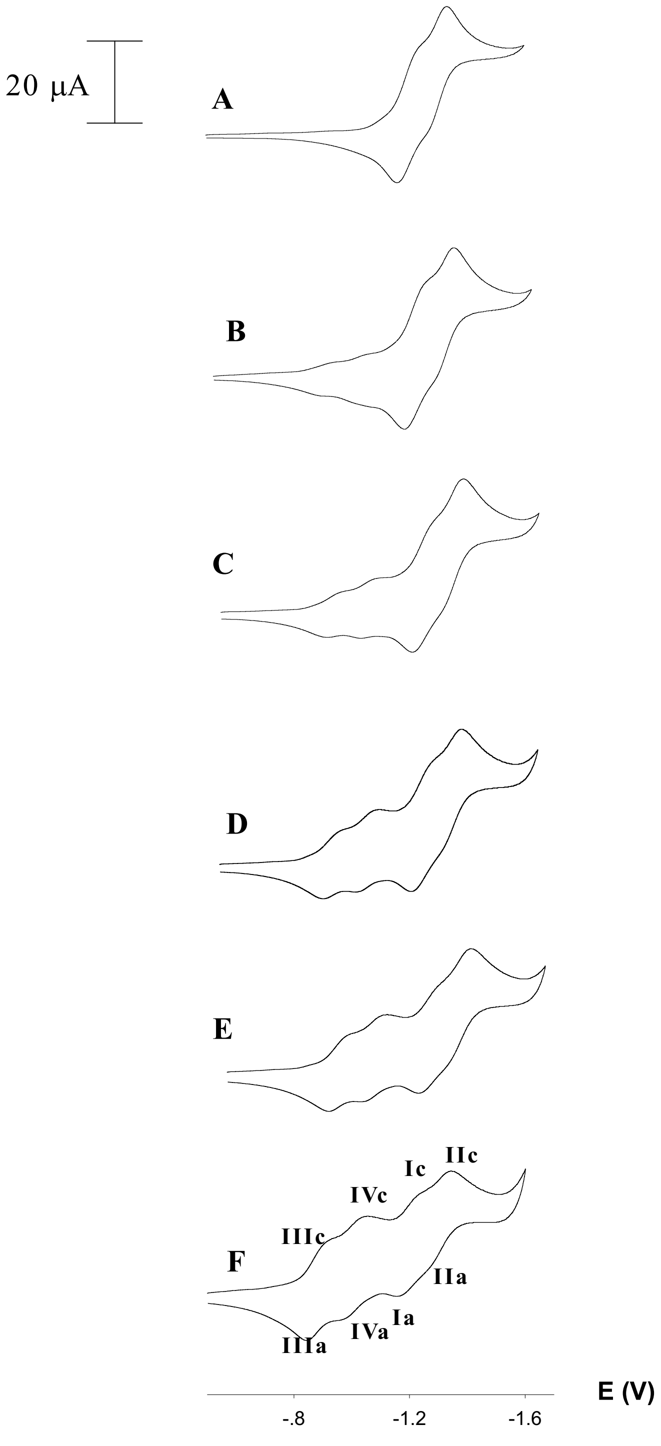

Figure 3.29 : CV of ligand **5b** + Na^+ (A) 0.0 equiv. (B) 0.2 equiv. (C) 0.4 equiv. (D) 0.6 equiv. (E) 0.8 equiv. (F) 1.0 equiv.

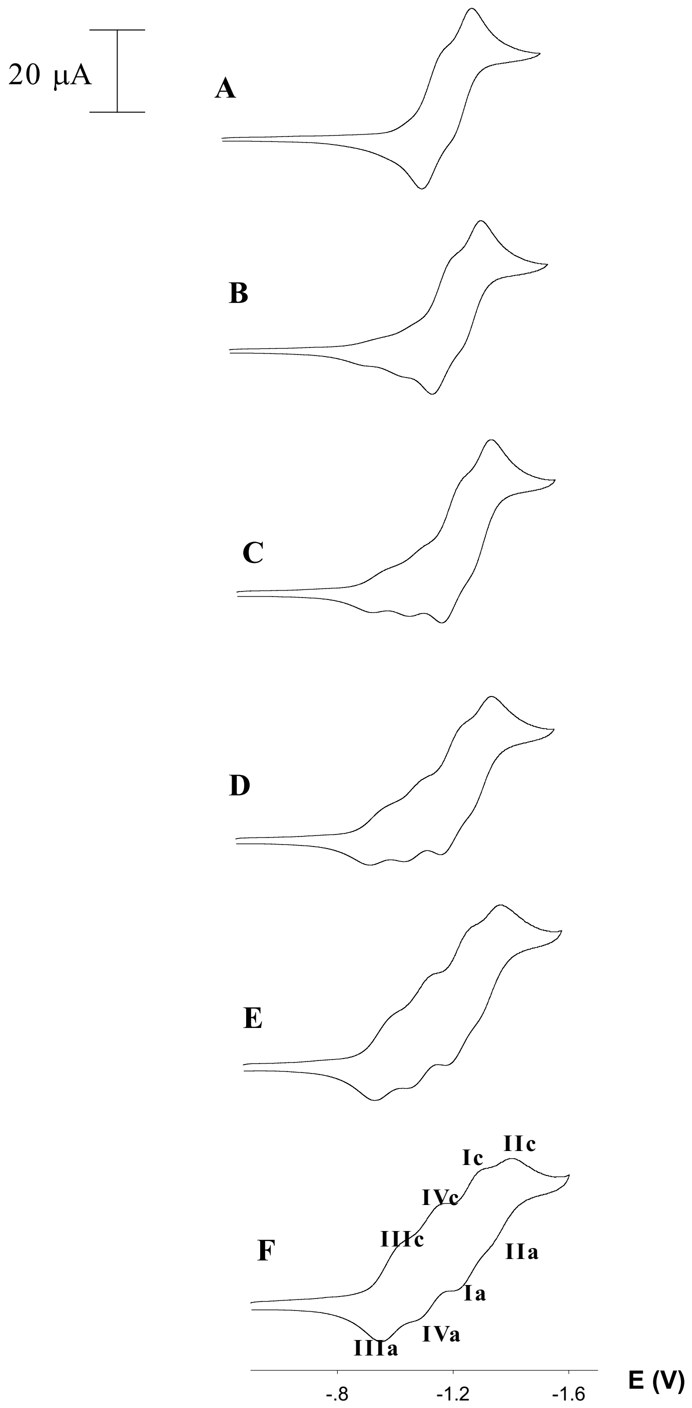

Figure 3.30 : CV of ligand **5b** + K$^+$ (A) 0.0 equiv. (B) 0.2 equiv. (C) 0.4 equiv. (D) 0.6 equiv. (E) 0.8 equiv. (F) 1.0 equiv.

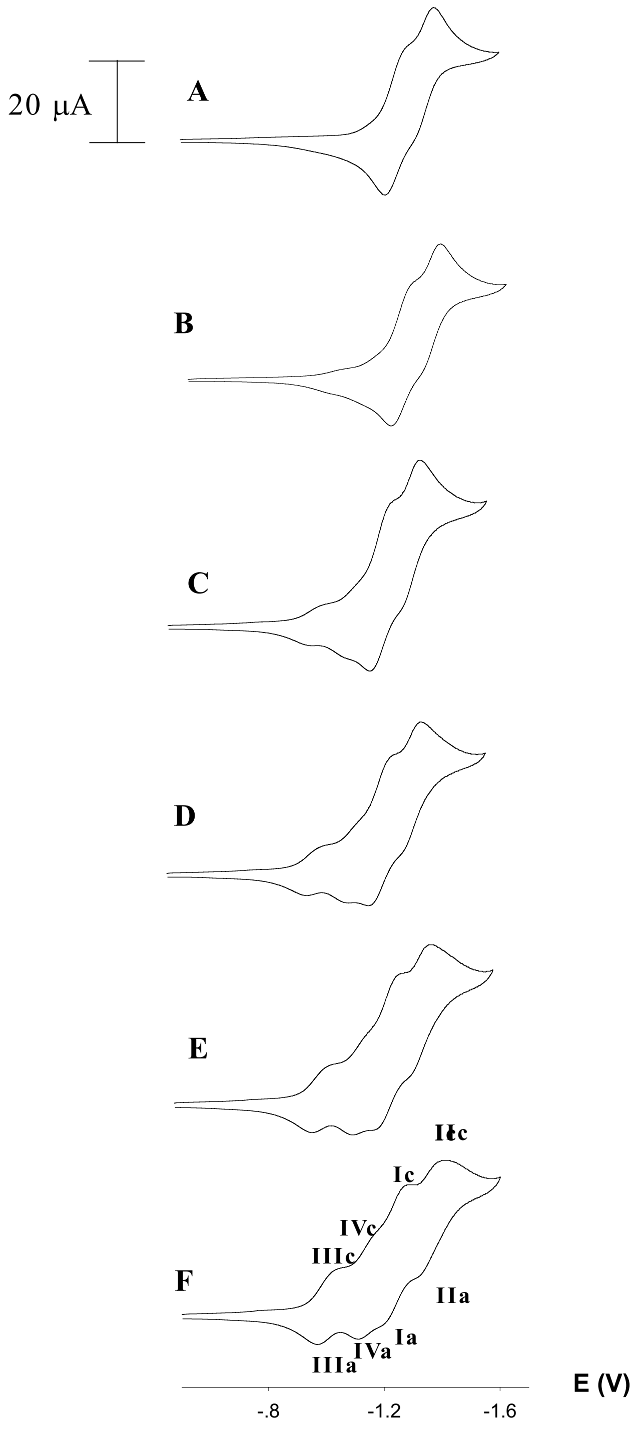

Figure 3.31 : CV of ligand **5b** + Cs$^+$ (A) 0.0 equiv. (B) 0.2 equiv. (C) 0.4 equiv. (D) 0.6 equiv. (E) 0.8 equiv. (F) 1.0 equiv.

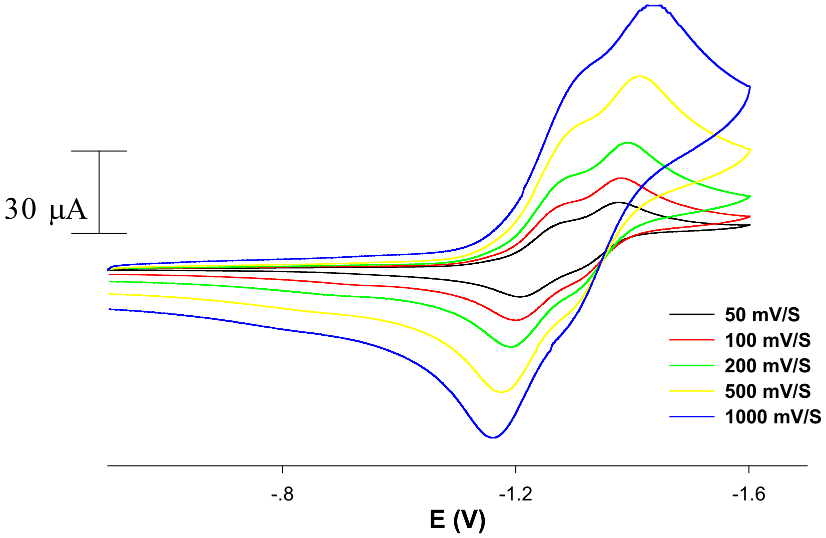

Figure 3.32 : CV of ligand **5b** at various scan rates

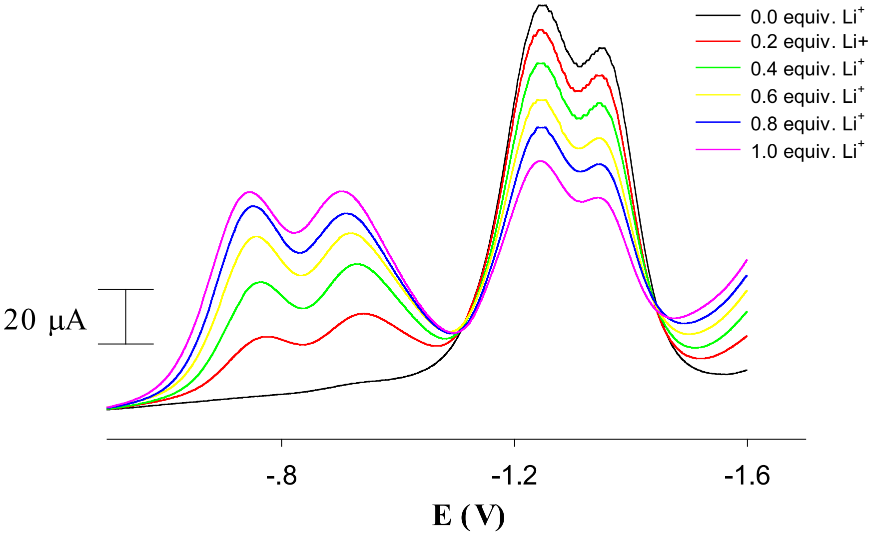

Figure 3.33 : SWV of ligand **5b** + Li^+

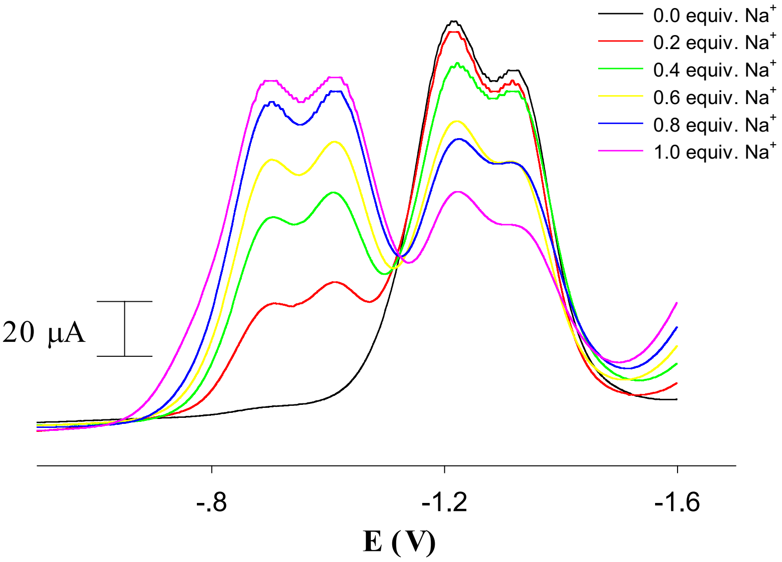

Figure 3.34 : SWV of ligand **5b** + Na$^+$

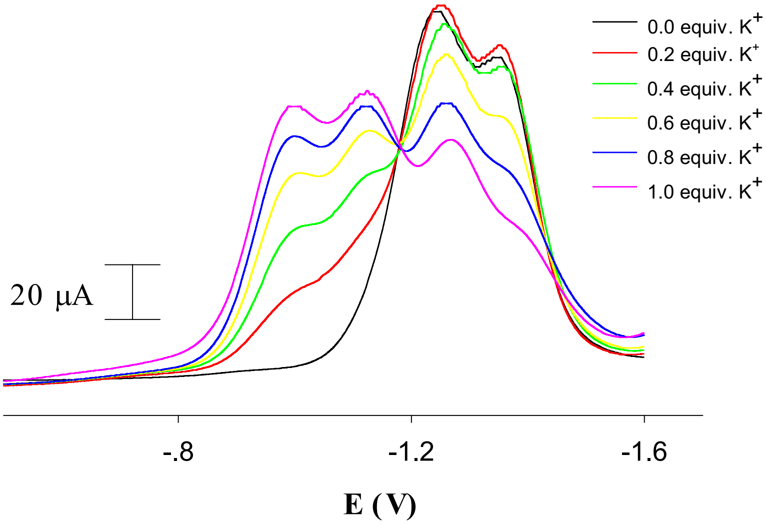

Figure 3.35 : SWV of ligand **5b** + K$^+$

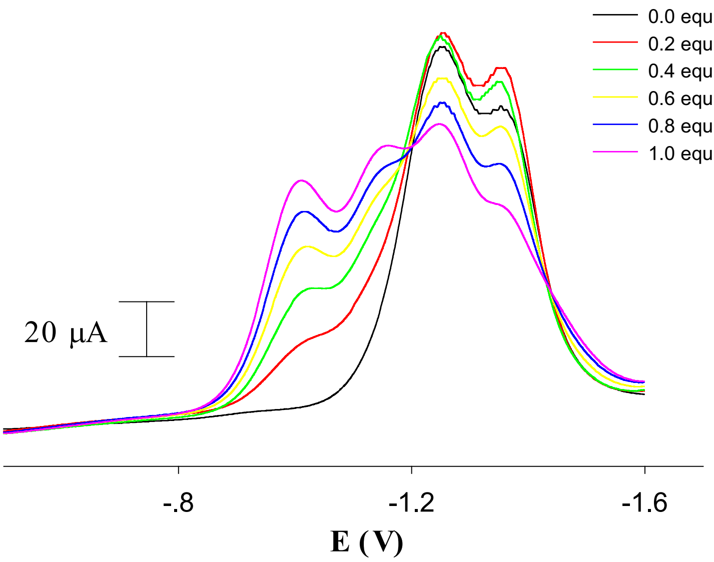

Figure 3.36 : SWV of ligand **5b** + Cs$^+$

3.3.3. Electrochemical studies of ligand 5c with Li^+, Na^+ and K^+

In the light of the results from NMR titration experiments, ligand **5c** can form complexes with Li^+, Na^+ and K^+; therefore, we investigate the electrochemical properties of **5c** in the presence of Li^+, Na^+ and K^+.

The cyclic voltammogram of ligand **5c** in the mixture of CH_2Cl_2 and CH_3CN (4:1) are presented in Figure 3.37(A). Ligand **5c** exhibits essentially two broad redox waves at -1300 and -1477 mV, which implies multielectron transfers. Althought ligand **5c** has two quinone molecules, one would expect to see 4 one-electron transfer signals in the voltammogram. By taking into account the known behavior of a calix[4]diquinone which can accept a total of four electrons by sequential two-electron reduction process. [26,30-31], the first quasi-reversible redox wave designated as Ic (cathodic), with a related anodic peak Ia may be attributed to a two-electron reduction process in which a one-electron transfer takes place to each of the quinone moieties present in the ligand to form radical anions. The second more cathodic wave, quasi-reversible reduction IIc (related to anodic peak IIa) is consistent with another two-electron reduction process which leads to the formation of dianions. Addition of $LiClO_4$ to electrochemical solution of ligand **5c**, Figure 3.37, led in all cases to the evolution of new quasi-reversible wave at -1049 mV, IIIc (related to anodic peak IIIa) that was substantially positively shifted relative to wave Ic, which diminished in current height concomitant with the growth of the new wave. Addition of 1.0 equiv. of $LiClO_4$ causes redox waves IIc disappeared and found Ic became an irreversible wave. The difference in peak potential between the complex and free ligand **5c** is shown in Table 3.3. Squarewave voltammograms also support the result that not only the new wave IIIc gradually appears at less negative potential and increases but also the initial wave IIc decreases and disappears completely as shown in Figure 3.41.

In the case of Na^+, addition of 1.0 equiv. of $NaClO_4$ causes redox waves Ic and IIc disappeare as shown in Figure 3.38. Two new redox waves at -906 and -1040, IIIc and IVc (related to anodic peak IIIa and IVa, respectively) appeared and suggested for the complex between ligand **5b** and sodium cation. The difference in peak potential between the complex and the free ligand **5b** is shown in Table 3.3. Square wave voltammograms also support the result that not only the new waves (IIIc and IVc) gradually appear at less negative potential and increase but also the initial waves (Ic and IIc) decrease and disappear as shown in Figure 3.42.

Upon addition of 1.0 equiv. of KPF_6 to the solution causes redox waves Ic and IIc disappeared as shown in Figure 3.39. Two new redox waves at -946 and -1110 mV, IIIc and IVc (related to anodic peak IIIa and IVa, respectively) appear and suggest the complex between ligand **5c** and potassium cation takes place. The difference in peak potential between the complex and free ligand **5c** is shown in Table 3.3. The squarewave voltammograms (Figure 3.43) support the result that not only the new waves (IIIc and IVc) gradually appear at less negative potential and increase but also the initial waves (Ic and IIc) decrease and disappear completely.

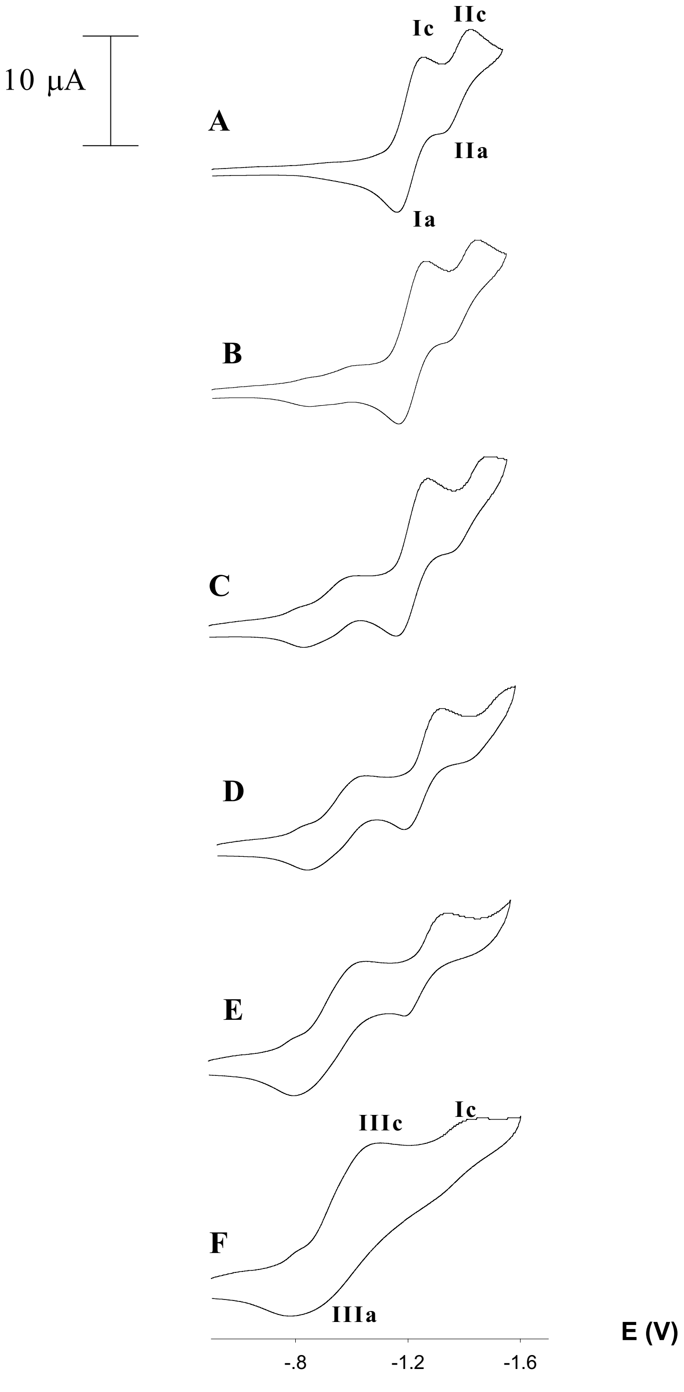

Figure 3.37 : CV of ligand **5c** + Li^+ (A) 0.0 equiv. (B) 0.2 equiv. (C) 0.4 equiv. (D) 0.6 equiv. (E) 0.8 equiv. (F) 1.0 equiv.

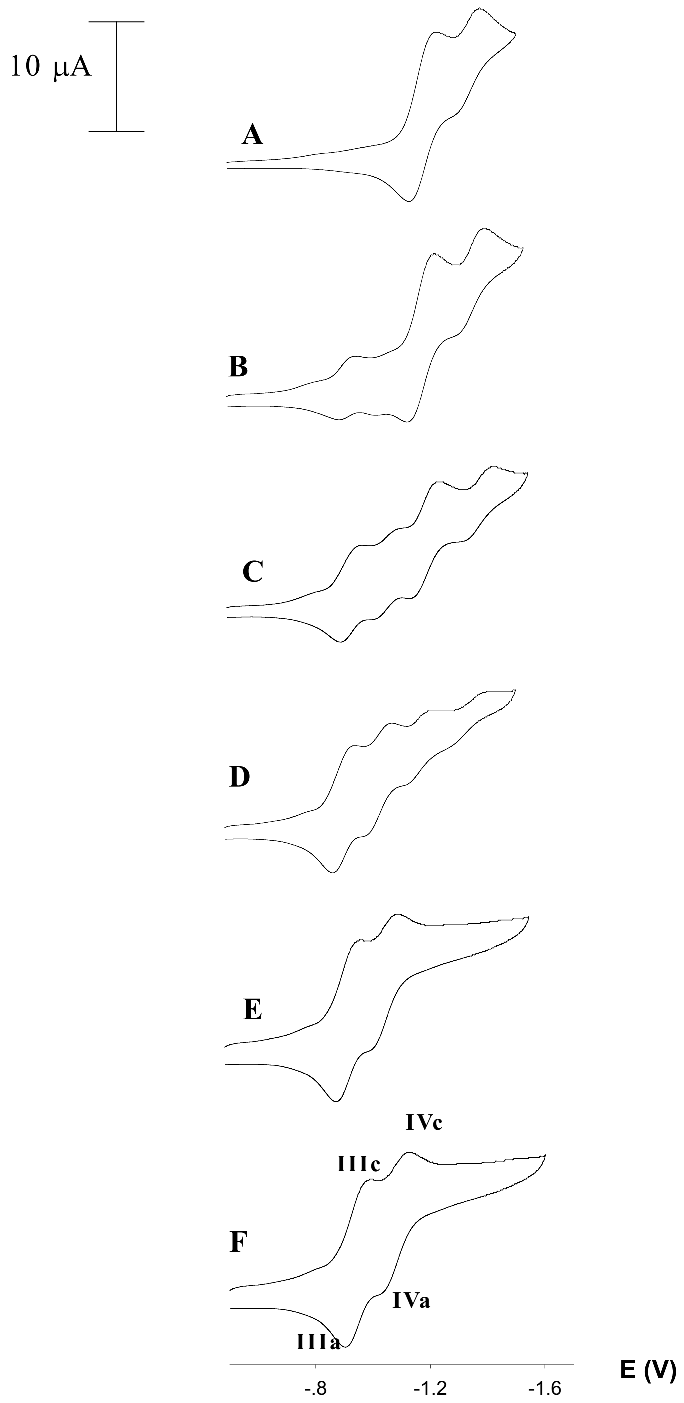

Figure 3.38 : CV of ligand **5c** + Na^+ (A) 0.0 equiv. (B) 0.2 equiv. (C) 0.4 equiv. (D) 0.6 equiv. (E) 0.8 equiv. (F) 1.0 equiv.

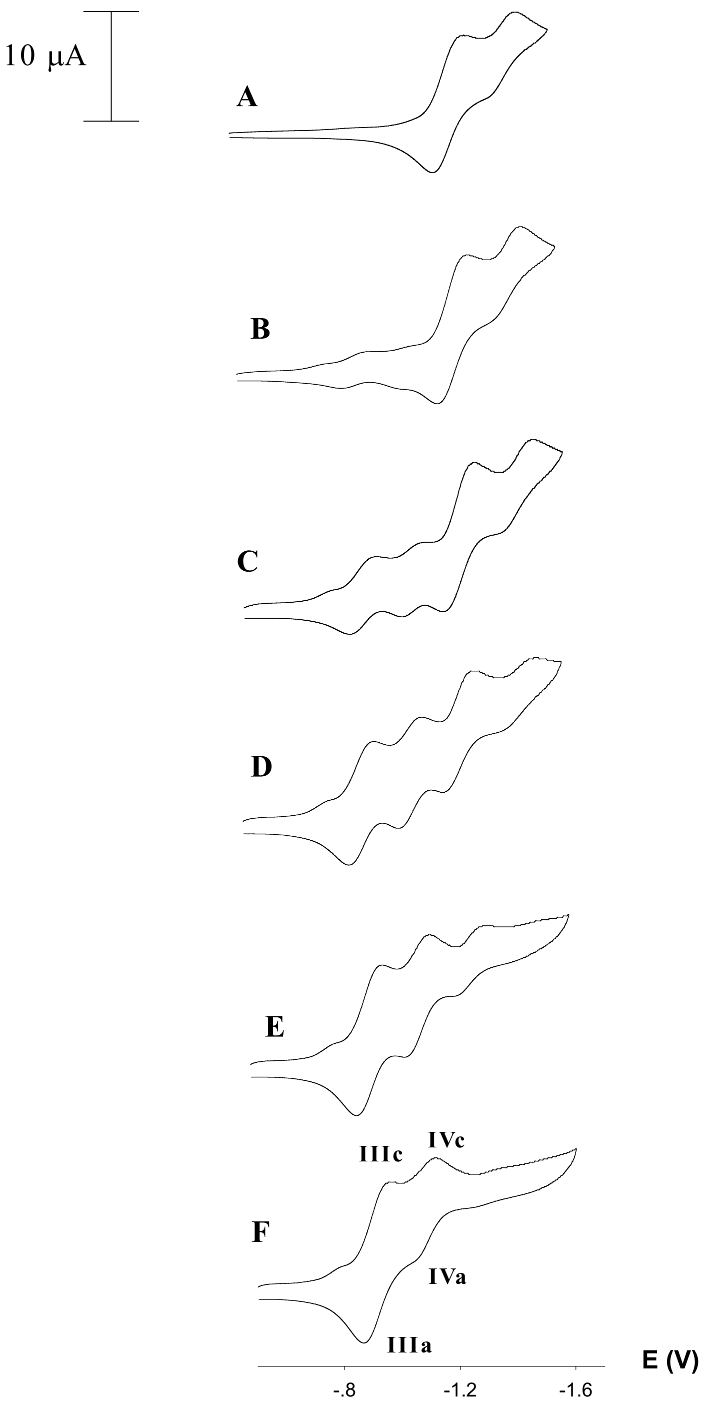

Figure 3.39 : CV of ligand **5c** + K^+ (A) 0.0 equiv. (B) 0.2 equiv. (C) 0.4 equiv. (D) 0.6 equiv. (E) 0.8 equiv. (F) 1.0 equiv.

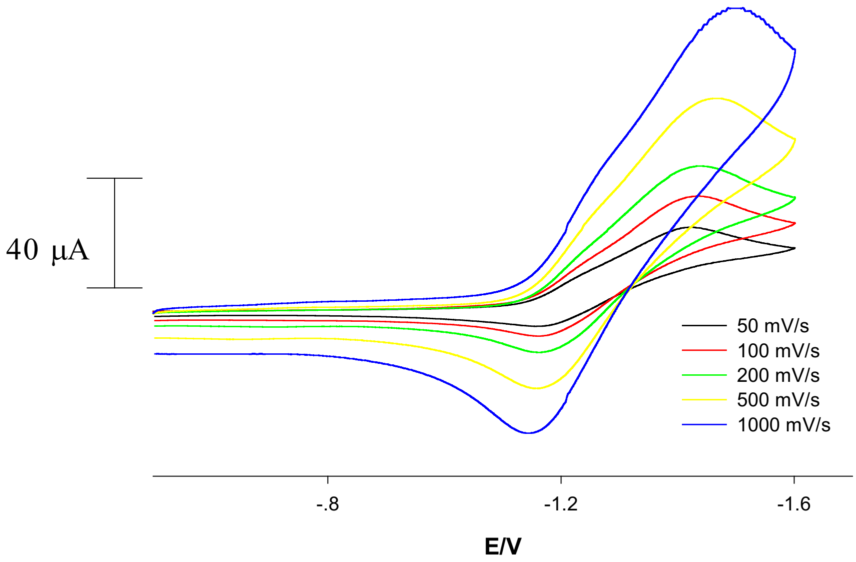

Figure 3.40 : CV of ligand **5c** at various scan rates

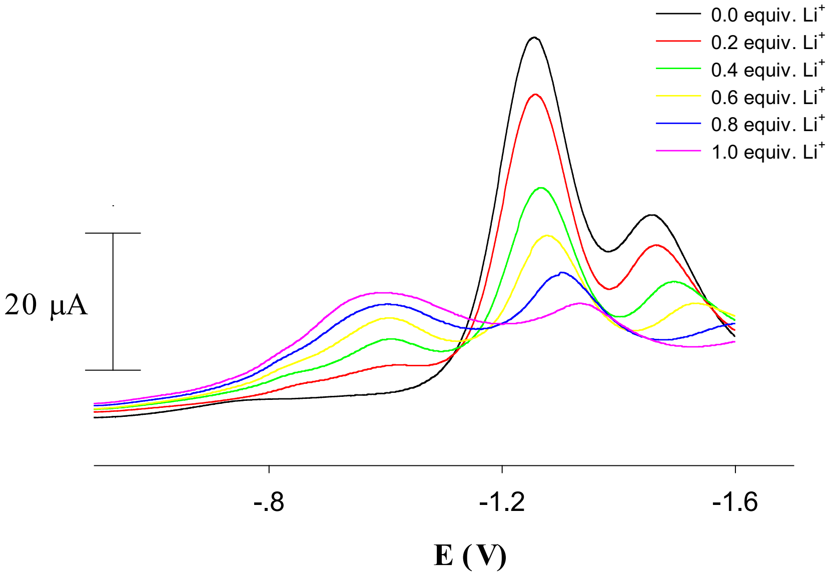

Figure 3.41 : SWV of ligand **5c** + Li^+

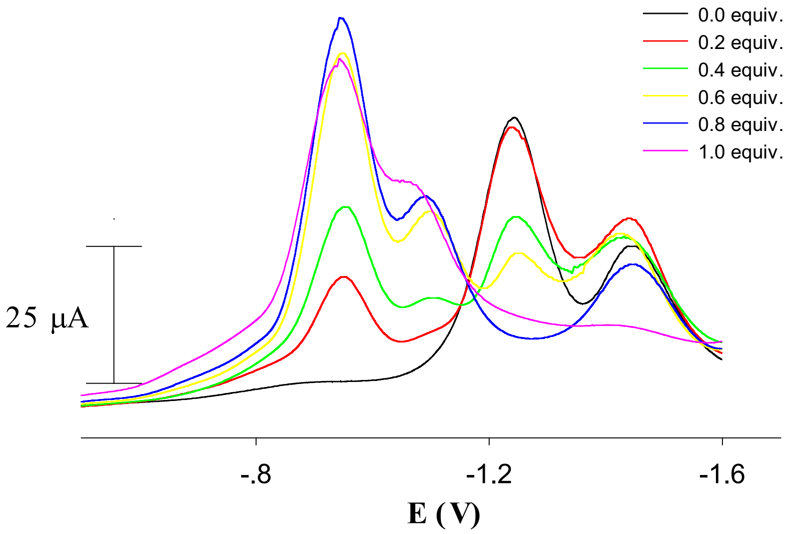

Figure 3.42 : SWV of ligand **5c** + Na$^+$

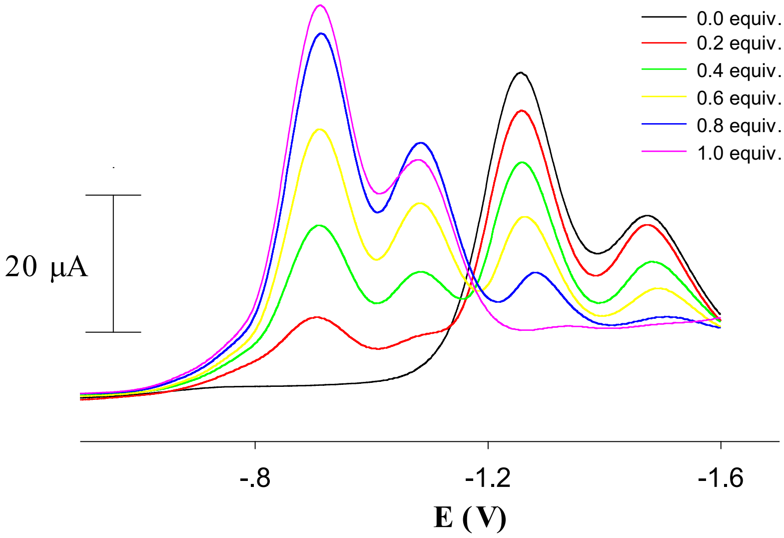

Figure 3.43 : SWV of ligand **5c** + K$^+$

Table 3.2 : Electrochemical data of ligands **5a**, **5b** and **5c** and their complexes with alkali cations from Figure 3.21-3.39.

	E(V) of each redox couple (mV)
Free ligand **5a**	Ic (q, -1269), IIc (q, -1394), IIIc (q, -1510)
	Ia (q, -1147), IIa (q, -1345), IIIa (q, -1443)
+ Li$^+$ 1.0 equiv.	IVc (q, -756), Vc (q, -998), VIc (q, -1528)
	IVa (q, -579), Va (q, -909), VIa (q, -1165)
+ Na$^+$ 1.0 equiv.	IVc (q, -933), Vc (q, -1037), VIc (q, -1187)
	IVa (q, -872), Va (q, -991), VIa (q, -1116)
+ K$^+$ 1.0 equiv.	IVc (q, -994), Vc (ir, -1187), Ic (ir, -1503)
	IVa (q, -921)
Free ligand **5b**	Ic (q, -1269), IIc (q, -1370)
	Ia (q, -1202), IIa (q, -1303)
+ Li$^+$ 1.0 equiv.	IIIc (q, -762), IVc (q, -936), Ic (q, -1254), IIc (q, -1361)
	IIIa (q, -674), IVa (q, -863), Ia (q, -1193), IIa (q, -1303)
+ Na$^+$ 1.0 equiv.	IIIc (q, -906), IVc (q, -1040), Ic (q, -1226), IIc (q, -1342)
	IIIa (q, -845), IVa (q, -979), Ia (q, -1165), IIa (q, -1284)
+ K$^+$ 1.0 equiv.	IIIc (q, -1016), IVc (q, -1150), Ic (q, -1290), IIc (q, -1400)
	IIIa (q, -952), IVa (q, -1086), Ia (q, -1220), IIa (q, -1336)
+ Cs$^+$ 1.0 equiv.	IIIc (q, -1022), IVc (q, -1156), Ic (q, -1269), IIc (q, -1400)
	IIIa (q, -970), IVa (q, -1110), Ia (q, -1205), IIa (q, -1327)
Free ligand **5c**	Ic (q, -1300), IIc (q, -1477)
	Ia (q, -1202), IIa (q, -1388)
+ Li$^+$ 1.0 equiv.	IIIc (q, -1049), Ic (ir, -1388)
	IIIa (q, -790)
+ Na$^+$ 1.0 equiv.	IIIc (q, -976), IVc (q, -1123)
	IIIa (q, -903), IVa (q, -1040)
+ K$^+$ 1.0 equiv.	IIIc (q, -946), IVc (q, -1110)
	IIIa (q, -866), IVa (q, -1052)

Definitions: c, cathodic peak potential; a, anodic peak potential; q, quasi-reversible; ir, irreversible.

Table 3.3: Peak potential shifts for cation complexes with ligand **5a**, **5b** and **5c**.

		Peak potential shifts (mV)
Ligand **5a**	+ Li^+ 1.0 equiv.	I-IV (513), II-V (396), III-VI (18)
	+ Na^+ 1.0 equiv.	I-IV (336), II-V (357), III-VI (323)
	+ K^+ 1.0 equiv.	I-IV (275), II-V (207)
Ligand **5b**	+ Li^+ 1.0 equiv.	I-III (507), II-IV (434)
	+ Na^+ 1.0 equiv.	I-III (363), II-IV (330)
	+ K^+ 1.0 equiv.	I-III (253), II-IV (220)
	+ Cs^+ 1.0 equiv.	I-III (247), II-IV (214)
Ligand **5c**	+ Li^+ 1.0 equiv.	I-III (251)
	+ Na^+ 1.0 equiv.	I-III (324), II-IV (354)
	+ K^+ 1.0 equiv.	I-III (354), II-IV (367)

Definition: X-Y, different cathodic peak potential between ligand at position X and complex at position Y from Figure 3.21-3.39.

In conclusion, ligand **5a**, which has four quinone units, exhibit three redox waves. Unlike ligand **5a**, ligands **5b** and **5c**, which have four and two quinone units exhibit two redox waves. Although ligand **5a** has the same structure as ligand **5b** except the glycolic linkages that are shorter, but cyclic voltammograms show the different redox wave signals. These phenomena can be described due to the poor solubility of ligand **5a** in the mixed solvent during experiments. On addition of alkali cations such as Li^+, Na^+, K^+ or Cs^+, a new set of peaks which indicated for the complex between ligand and cation are observed at a less negative potential than the original free ligand wave. This reflects the stabilization of the reduced form of dianion and the stabilization of the complex as a result of the intramolecular interaction with ring-bound cation. From Table 3.3, the potential difference between the complex peak and the first peak of ligand is as large as

513 and 507 mV for ligand **5a** and **5b** with Li^+. Anodic shifts from ligand **5a**, **5b** and **5c** with another alkali cations also have high value in the range of 220-440 mV. The ΔE value of ligand **5a** and **5b** after complexation with a series of alkali cations exhibit the trend as $Li^+ > Na^+ > K^+ > Cs^+$ while **5c** exhibits the trend as $K^+ > Na^+ > Li^+$. Ligands **5a** and **5b** possess 4 quinone oxygens while **5c** contains only two quinone oxygens and two etheral oxygens. Therefore, **5a** and **5b** are harder acid than **5c** in the reduced forms and can form more stable complexes with smaller cations (Figure 3.44). This results in a larger shifts of cyclic voltammograms to less negative potential upon addition of metal ions. This suggests that hard-soft acid base shows important role in redox chemistry of the quinone moiety. All these phenomena imply double calix[4]arenequinones **5a**, **5b** and **5c** may be applicable to the fabrication of a molecular device that selectively recognizes a specific cation.

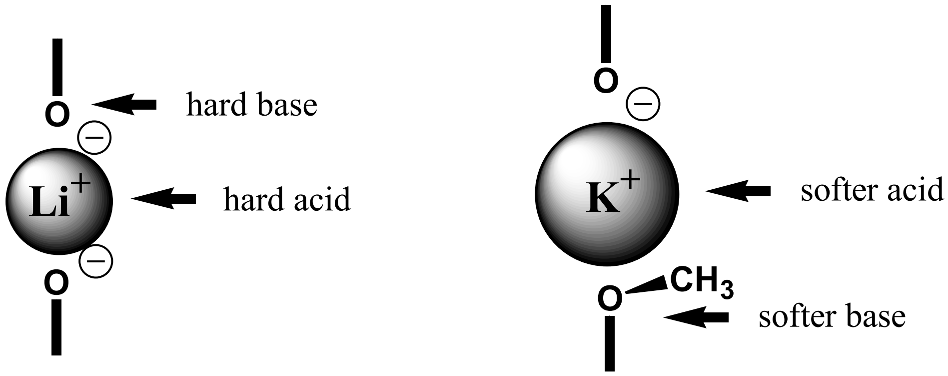

Figure 3.44: Effect of hard-soft acid base to peak potential shifts.

3.3.4 Calculation of binding enhancement factor

In a case when the formal potentials of both free (E_f) and complexed (E_c) forms of a redox active component can be obtained, the ratio of complex formation constants for reduced (K_{red}) and oxidized (K_{ox}) states of this component can be calculated from the difference between the formal potentials. From the cycle shown in Figure 3.44, where M represents the redox-active component and L is the ligand, it follows that [36,46-47]

$$RT\ln K_{ox} + nFE_c = nFE_f + RT\ln K_{red} \qquad (7)$$

and

$$\Delta E = E_{\mathrm{c}} - E_{\mathrm{f}} = (\mathrm{RT}/n\mathrm{F})\ln(K_{\mathrm{red}}/K_{\mathrm{ox}}) \tag{8}$$

or

$$K_{\mathrm{red}}/K_{\mathrm{ox}} = \exp\{\Delta E n\mathrm{F}/\mathrm{RT}\} \tag{9}$$

$$\begin{tikzcd}
\mathrm{M}^{\mathrm{m}} + \mathrm{L} \arrow[r, shift left, harpoon, "-\mathrm{RT}\ln K_{\mathrm{ox}}"] \arrow[d, shift left, harpoon, "-n\mathrm{F}E_{\mathrm{f}}"] & \mathrm{M}^{\mathrm{m}}\mathrm{L} \arrow[l, shift left, harpoon] \arrow[d, shift left, harpoon, "-n\mathrm{F}E_{\mathrm{c}}"] \\
\mathrm{M}^{\mathrm{m-n}} + \mathrm{L} \arrow[u, shift left, harpoon, "\pm \mathrm{ne}^-"] \arrow[r, shift left, harpoon, "-\mathrm{RT}\ln K_{\mathrm{red}}"] & \mathrm{M}^{\mathrm{m-n}}\mathrm{L} \arrow[u, shift left, harpoon, "\pm \mathrm{ne}^-"] \arrow[l, shift left, harpoon]
\end{tikzcd}$$

Figure 3.45 : Redox and complexation equilibria with a redox-active component M.

From cyclic voltammogram studies of complexes between ligands **5a**, **5b** and **5c** with cations suggested that only CV of ligand **5c** with Na^+ and K^+ can be used to calculated binding enhancement factors. This is due to cyclic voltammograms of ligands **5a** and **5b** with cations were too complicate to describe the mechanism. For ligand **5c** with Na^+ and K^+, the mechanism can described by the process shown in Figure 3.45.

$$\begin{tikzcd}
\mathrm{CQ}_2 \arrow[r, shift left, harpoon, "K_1"] \arrow[d, shift left, harpoon, "2\mathrm{e}^-"] & \mathrm{MCQ}_2 \arrow[l, shift left, harpoon, "+\mathrm{M}^+"] \arrow[d, shift left, harpoon, "2\mathrm{e}^-"] \\
\mathrm{CQ}_2^{2-\bullet} \arrow[u, shift left, harpoon] \arrow[r, shift left, harpoon, "K_2"] & \mathrm{MCQ}_2^{2-\bullet} \arrow[u, shift left, harpoon] \arrow[l, shift left, harpoon, "+\mathrm{M}^+"]
\end{tikzcd}$$

Figure 3.46 : A square sheme for cation binding redox mechanism of ligand **5c**

By using equation **9**, binding enhancement factor of ligand **5c** with Na^+ and K^+ can be calculated. K_2/K_1 values for Na^+ and K^+ complexes with ligand **5c** are 2.08 x 10^5 and 6.53 x 10^5, respectively. This reflects the binding enhancement through electrostatic attractions in the reduced forms. As mentioned above, we can conclude that the reduced forms of quinone prefer to bind cations more than the unreduced form.

4. Conclusion

Three double calix[4]arenes, 25,27-di(ethyleneglycol)-bis-*p*-*tert*-butylcalix[4]arene, **1**, 25,27-di(diethyleneglycol)-bis-*p*-*tert*-butylcalix[4]arene, **2b**, and 25,27-di(methoxy)-26,28-di(ethyleneglycol)-bis-*p*-*tert*-butylcalix[4]arene, **4d**, have been synthesized by coupling reactions between *p*-*tert*-butylcalix[4]arene and 1,2-dibromoethane, diethylene glycol ditosylate (**2a**) and 25,27-di(methoxy)-26,28-di(methanesulfonyl)ethoxy-*p*-*tert*-butylcalix[4]arene (**4c**) in 12%, 14%, 52% yields, respectively. Coupling reactions to synthesize compounds **5b** and **5c** were carried out under high pressure. Three quinone derivatives, 25,27-di(ethyleneglycol)-bis-*p*-*tert*-butylcalix[4]tetraquinone, **5a**, 25,27-di (diethyleneglycol)-bis-*p*-*tert*-butylcalix[4]tetraquinone, **5b**, and 25,27-di(methoxy)-26,28-di(ethyleneglycol)-bis-*p*-*tert*-butylcalix[4]diquinone, **5c**, were synthesized by oxidizing compounds **1**, **2b** and **4d** with $Tl(CF_3COO)_3$ in CF_3COOH and were obtained in 52%, 68% and 38% yields, respectively.

^{1}H-NMR titrations show that **5a** and **5c** can form complexes with Li^+, Na^+ and K^+ ions. Compounds **5a** and **5c** selectively bind Na^+. However, the cavity in compound **5c** is possibly smaller than **5a**. Therefore, the stability constant of **5c**+Na^+ is much lower than that of **5a**+Na^+. The binding trends for **5a** and **5c** are as follows; $Na^+ > Li^+ >> K^+$ and $Na^+ >> Li^+ > K^+$. Compound **5b** which has a bigger cavity than **5a** and **5c** shows selectivity for Cs^+. The binding trend for **5b** is as $Cs^+ > K^+ > Na^+ >> Li^+$.

Electrochemical studies using cyclic voltammetry and square wave voltammetry showed significant changing of voltammogram of **5a**, **5b** and **5c** upon addition of alkali cations such as Li^+, Na^+, K^+ or Cs^+. A new set of peaks which indicate the complex between ligands and cations are observed at less negative potentials than the original free ligand waves. Anodic shift for ligands **5a** and **5b** upon addition of alkali cations exhibits the same trend as $Li^+ > Na^+ > K^+ > Cs^+$ while **5c** exhibits the trend as $K^+ > Na^+ > Li^+$. Compounds **5a** and **5b** possess 4 quinone oxygens while **5c** contains only two quinone oxygens and two etheral oxygens. Therefore, **5a** and **5b** are harder acid than **5c** in the reduced forms and can form more stable complexes with smaller cations. This results in a larger shifts of cyclic voltammograms to less negative potential upon addition of metal ions. This suggests that hard-soft acid base shows important role in redox chemistry of the quinone moiety. All these phenomena imply that double calix[4]arenequinones **5a**, **5b** and **5c** may possibly be used as alkali metal ion sensors.

Suggestion for future works

From all obtained results and discussion, future works should be focused on;

1. X-ray crystal structures of ligands **5a**, **5b** and **5c** and their alkali metal complexes should be obtained in order to understand the structure of the synthetic receptors and their coordination chemistry with alkali metal ions.
2. UV-Visible and Fluorescence titrations of ligands **5a**, **5b** and **5c** with alkali metal ions should be investigated to obtain complexation constants and structural behaviors upon complexation.
3. Synthesize other derivatives of double calix[4]arenequinones such as a mono- or a triquinone to compare and study their complexation and electrochemistry.

5. References

1. Kaifer, A.; Gómez-Kaifer, M. *Supramolecular Electrochemistry*. New York: Wiley-VCH Publishers, **1999**, p.103.

2. Asfari, Z.; Böhmer, V.; Harrowfield, J.; Vicens, J., Ed. *Calixarenes 2001*. London: Kluwer academic publishers, **2001**, p.627.

3. Beer, P. D. Transition-metal receptor systems for the selective recognition and sensing of anionic guest species. *Acc. Chem. Res*. **1998**, *31*, 71-80.

4. Arnaud-Neu, F.; Barrett, G.; Cremin, S.; Deasy, M.; Ferguson, G.; Harris, S. J.; Lough, A. J.; Guerra, L.; McKervey, M. A.; Schwing-Weill, M. J.; Schwinte, P. Cation complexation by chemically modified calixarenes. Part 10.Thioamide derivatives of *p-tert*-butylcalix[4]-, [5]- and [6]-arenes with selectivity for copper, silver, cadmium and lead. X-ray molecular structure of calix[4]arene thioamide-lead(II) and calix[4]arene amide-copper(II) complexed. *J. Chem. Soc., Perkin Trans.2* **1992**, 1119-1125.

5. Bocchi, V.; Foina, D.; Pochini, A.; Ungaro, R.; Andreetti, C. D. Synthesis, ^{1}H-NMR, ^{13}C-NMR spectra and conformational preference of open chain ligands on lipophilic macrocycles. *Tetrahedron* **1982**, *38*, 373-378.

6. Ferguson, G.; Kaiter, B.; McKervey, M. A.; Seward, E. M. Synthesis x-ray crystal structure and cation transfer properties of a calix[4]arene tetraketone. A new versatile molecular receptor. *J. Chem. Soc., Chem. Commum*. **1987**, 584-585.

7. Arnaud-Neu, F.; Barrett, G.; Harris, J.; McKervey, M. A.; Owens, M.; Schwing-Weill, M. J.; Schwinte, P. Cation complexation by chemically modified calixarene. 5. Protonation constants for calixarene carboxylates and stability constants of their alkali and alkaline-earth complexes. *Inorg. Chem*. **1993**, *32*, 2644-2650.

8. Muzet, N.; Wipff, G.; Casnati, A.; Domiano, L.; Ungaro, R.; Ugozzoli, F. Alkaline earth and uranyl cation complexes of a calix[4]arene-tetraamide MD and FEP simulations in aqueous and acetonitrile solutions and x-ray structure of its Sr (Picrate)$_2$ complex. *J. Chem. Soc., Perkin Trans.2* **1996**, 1065-1075.

9. Ghidini, E.; Ugozzoli F.; Ungaro, R.; Harkema, S.; Abu-El-Fadl, A.; Reinhoudt, D. N. Complexation of alkali metal cations by conformationally rigid, stereoisomeric calix[4]arene crown ethers : a quantitative evaluation of preorganization. *J. Am. Chem. Soc*. **1990**, *112*, 6979-6985.

10. Reinhoudt, D. N.; Dijkstra, P. J.; in't Veld, P. J. A.; Bugge, K. E.; Harkema, S.; Ungaro, R.; Ghidini, E. Kinetically stable complexes of alkali cations with rigidified calix[4]arenes. X-ray structure of a calixspherard sodium picrate complex. *J. Am. Chem. Soc*. **1987**, *109*, 4761-4762.

11. Gutsche, C. D. Calixarenes. *Acc. Chem. Res*. **1983**, *16*, 162-170.

12. Böhmer, V. Calixarenes, macrocycles with (almost) unlimited possibilities. *Angew. Chem. Int. Ed. Engl.* **1995**, *34*, 713-745.

13. Gutsche, C. D. *'Calixarene'-Monograph in Supramolecular Chemistry*, The Royal Society of Chemistry, Cambridge **1989**, p.36.

14. Ikeda, A. and Shinkai, S. Novel cavity design using calix[*n*]arene skeletons : Toward molecular recognition and metal binding. *Chem. Rev*. **1997**, *97*, 1713-1734.

15. Gutsche, C. D.; Muthukrishnan, R. Calixarenes. 1. Analysis of the product mixtures produced by the base-catalyzed condensation of formaldehyde with para-substituted phenols. *J. Org. Chem*. **1978**, *43*, 4905-4906.

16. Gutsche, C. D.; Dhawan, B.; No, K. H.; Muthukrishnan, R. Calixarenes. 4. The synthesis, characterization, and properties of the calixarenes from *p-tert*-butylphenol. *J. Am. Chem. Soc*. **1981**, *103*, 3782-3792.

17. Shinkai, S. Calixarenes-the third generation of supramolecules. *Tetrahedron* **1993**, *49*, 8933-8968.

18. Van Dienst, E.; Iwema-Bakker, W. I.; Engberson, J. F. J.; Verboom, W.; Reinhoudt, D. N. Calixarenes, chemical chameleons. *Pure & Appl. Chem.* **1993**, *65*, 387-392.

19. Pochini, A. and Ungaro, R. *Calixarenes and Related Hosts-Comprehensive Supramolecular Chemistry*. London: Elservier Science Ltd., **1996**, p.103.

20. Gutsche, C. D.; Dhawan, B.; Levine, J. A.; No, K. H.; Bauer, L. J. Calixarenes. 9. Conformational isomers of the ethers and esters of calix[4]arenes. *Tetrahedron* **1983**, *39*, 409-426.

21. Iwamoto, K.; Araki, K.; Shinkai, S. Syntheses of all possible conformational isomers of O-alkyl-*p*-*t*-butylcalix[4]arenes. *Tetrahedron* **1991**, *47*, 4325-4342.

22. Schmitt, P.; Beer, P. D.; Drew, M. G. B.; Sheen, P. D. Calix[4]tube : A tubular receptor with remarkable potassium ion selectivity. *Angew. Chem. Int. Ed. Engl.* **1997**, *36*, 1840-1842.

23. Ohseto, F.; Shinkai, S. Syntheses of and metal cation oscillation in ionophoric biscalix[4]arenes. *J. Chem. Soc. Perkin Trans.2* **1995**, 1103-1109.

24. Bethell, D.; Dougherty, G.; Coupertino, D. C. Selectivity in redox-switched calix [4]arene catiophores : Electrochemical detection of a conformational change on cation binding. *J. Chem. Soc. Chem. Commun.* **1995**, 675-676.

25. Akine, S.; Goto, K.; Kawashima, T. Synthesis, structure, and redox properties of a quinone-bridged calix[6]arene. *Tetrahedron Lett*. **2000**, *41*, 897-901.

26. Gómez-Kaifer, M.; Reddy, P. A.; Gutsche, C. D.; Echegoyen, L. Electroactive calixarenes. 1. redox and cation binding properties of calixquinones. *J. Am. Chem. Soc*. **1994**, *116*, 3580-3587.

27. Reddy, P. A.; Gutsche, C. D. Calixarenes : Reactions of calix[4]quinones. *J. Org. Chem*. **1993**, *58*, 3245-3251.

28. Suga, K.; Fugihara, M.; Monta, T.; Agawa, T. Electrochemical study on calix[4] quinone and calix[4]hydroquinone in N,N-dimethylformamide. *J. Chem. Soc. Faraday Trans*. **1991**, *87*, 1575-1578.

29. Beer, P. D.; Chen, Z.; Gale, P. A. Diester-calix[4]arenediquinone complexation and electrochemical recognition of group-1 and group-2, ammonium and alkyl ammonium guest cations. *Tetrahedron* **1994**, *50*, 931-940.

30. Beer, P. D.; Gale, P. A.; Chen, Z.; Drew, M. G. B., Heath, J. A.; Ogden, M. I.; Powell, H. R. New Ionophoric Calix[4]diquinones: coordination chemistry, electrochemistry, and x-ray crystal structure. *Inorg. Chem*. **1997**, *36*, 5880-5893.

31. Chung, T. D.; Choi, D.; Kang, S. K.; Lee, S. K.; Chang, S. K.; Kim, H. Electrochemical behavior of calix[4]arenediquinones and their cation binding properties. *J. Electroanal. Chem* **1995**, *396*, 431-439.

32. Bettega, H. C.; Moutet, J.; Ulrich, G.; Ziessel, R. Electrochemical cation recognition by novel 2,2'-bipyridine-grafted calix[4]arenequinones. *J. Electroanal. Chem*. **1996**, *406*, 247-250.

33. Webber, P. R. A.; Chen, G. Z.; Drew, M. G. B.; Beer, P. D. Cesium- and rubidium-selective redox-active bis(calix[4]diquinone) ionophores. *Angew. Chem. Int. Ed*. **2001**, *40*, 2265-2268.

34. Wang, J. *Analytical Electrochemistry*. New York: Wiley-VCH Publishers, **1994**, p.38-42, 161-164.

35. Plambeck, J. A. *Electroanalytical chemistry*. New York: Wiley-VCH Publisher, **1982**, p.310-312.

36. Schneider, H., Yatsimirsky, A. K. *Principles and methods in supramolecular chemistry*. New York: Wiley-VCH Publisher, **2000**, p.173-174.

37. Gutsche, C. D.; Iqbal, M. *p-tert*-Butylcalixarene *Org. Synth*. **1990**, *68*, 234-237.

38. Chen, C. F.; Zheng, Q. Y.; Zheng, Y. S.; Huang, Z. T. Functionalization of calix[4] arenes at the lower rim and synthesis of calix[4](aza)crowns. *Synthetic Communications* **2001**, *31*, 2829-2836.

39. Cobben, P. L. H. M.; Egberink, R. J. M.; Bomer, J. G.; Bergveld, P.; Verboom, W.; Reinhoudt, D. N. Transduction of selective recognition of heavy metal ion by chemically modified field effect transistors (CHEMFETs). *J. Am. Chem. Soc.* **1992**, *114*, 10573-10582.

40. Tomapatanaget, B.; Pulpoka, B.; Tuntulani, T. Preparation of diaza dioxa dithiacrown *p-tert*-butylcalix[4]arene by S-alkylation reactions: Use of metallocalix[4]arene complexes as reaction templates. *Chem. Lett*. **1998**, 1037-1038.

41. Tantrakarn, K.; Ratanatawanate, C.; Pinsuk, T.; Chailapakul, O.; Tuntulani, T. Synthesis of redox-active biscalix[4]quinones and their electrochemical properties. *Tetrahedron Lett*. **2003**, *44*, 33-36.

42. Asfari, Z.; Weiss, J.; Pappalardo, S.; Vicens, J. Synthesis and properties of double-calix[4]arenes, doubly-crowned calix[4]arenes, and double-calixcrowns. *Pure & Appl. Chem*. **1993**, *65*, 585-590.

43. Arduini, A.; Domiano, L.; Pochini, A.; Secchi, A.; Ungaro, R.; Ugozzoli, F.; Struck, O.; Verboom, W.; Reinhoudt, D. N. Synthesis of 1,2-bridged calix[4] arene-biscrowns in the 1,2-alternate conformation. *Tetrahedron* **1997**, *53*, 3767-3776.

44. Jaime, C.; Mendoza, J.; Prados, P.; Nieto, P. M.; Sanchez, C. ^{13}C NMR chemical shifts. A single rule to determine the conformation of calix[4]arenes. *J. Org. Chem*. **1991**, *56*, 3372-3376.

45. Macomber, R. S. An introduction to NMR titration for studying rapid reversible complexation. *J. Chem. Educ*. **1992**, *69*, 375-378.

46. Choi, D.; Chung, T. D.; Kang, S. K.; Lee, S. K.; Kim, T.; Chang, S. K.; Kim, H. Electrochemical recognition of ammonium and alkali metal cations with calix [4]arenediquinone. *J. Electroanal. Chem* **1995**, *387*, 133-134.

47. Miller, S. R.; Gustowski, D. A.; Chen, Z.; Gokel, G. W.; Echegoyen, L.; Kaifer, A. E. Rationalization of the unusual electrochemical behavior observed in lariat ethers and other reducible macrocyclic systems. *Anal. Chem.* **1988**, *60*, 2021-2024.

Anion sensory studies of amide ferrocene calix[4]arene derivatives

1. Introduction

Anion recognition is an area of interest in the field of biological systems[1], environmental pollutants[2] and chemical processes. Recently, anion chemical sensors play important roles in fundamental principles of supramolecular chemistry. Artificial molecules were constructed in the part of anion binding site linking to the sensory unit. Generally, designed sensory molecules contain functional groups that have the capacity for hydrogen bonding and electrostatic interactions as well as the sensory units that can gives electrochemical or optical signals.

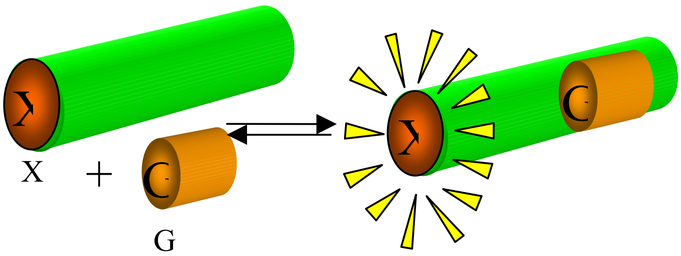

G = Cationic, anionic and Neutral; X = Receptor or signaling Group (Redox / Photo-active)

Figure 1 Depict of concept of electrochemical/optical recognition[2]

Moreover, ditopic receptors have been focused on studying simultaneous cation and anion recognition. Most of them were designed in order to enhance the binding ability using ion pair interactions. Many molecules employed calix[4]arene framework as a building blockin order to augment the binding ability caused by the rigid and preorganized molecule. Calix[4]arene is a popular building block because it can be derivatized on both lower and upper rims. For instance, Ungaro and coworkers[4] reported calix[4]arene-based heteroditopic receptors having the cation binding site of tetraamide on the lower rim and the anion binding site of monothiourea on the upper rim. (**Figure 2**)

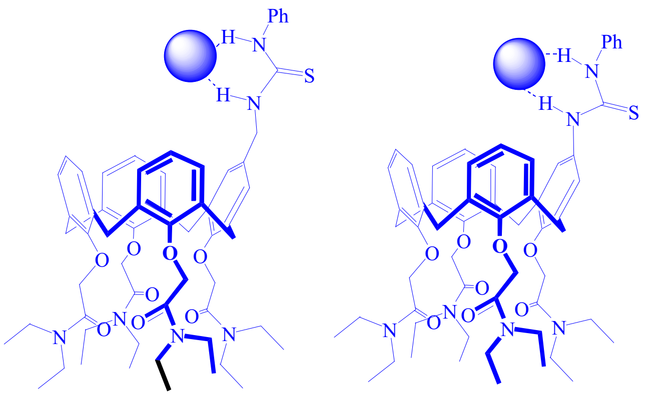

1 **2**

Figure 2 The heteroditopic receptors **1** and **2**

The tetraamide group on the lower rim binds Na^+ selectively. Association constants of ligand **2** in the presence of Na^+ on the tetraamide group have higher value than those of **1** in the absence of Na^+ because the complexes of Na^+ at tetraamide give the influence of electron-withdrawing on NH group directly. In contrast, the complexes of ligand **2** in the presence of Na^+. Ligand **1** has a CH_2 spacer between the aromatic part and the thiourea unit. This spacer prevents the electron-withdrawing effect toward NH proton resulting in no change of anion binding properties compared to the free ligand. Both ligands bind cation and anions simultaneously using the enhancement of binding ability via ion pair interaction. Nevertheless, the heteroditopic calix[4]arene receptors bearing the cationic and anionic binding sites on the same side were synthesized to enhance the binding ability using ion pair interaction. Beer and coworkers[5] designed the heteroditopic rhenium (I) and ruthenium (II) bipyridyl calix[4]arene receptors to bind both cationic and anionic species. (**Figure 3**)

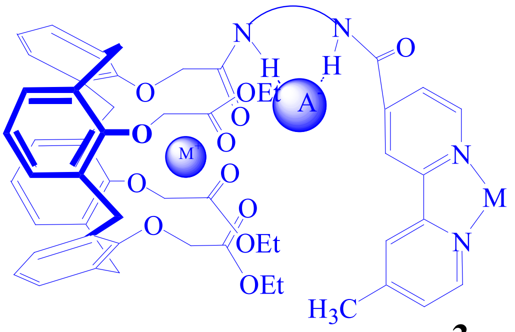

3

M = $Re(CO)_3$, $(bipy)_2Ru^{2+}(PF_6^-)_2$

Figure 3 The heteroditopic receptors based on calix[4]arene

They reported that these ligands bind Li^+ and Na^+ strongly at ethyl ester groups. Moreover, the anion affinity in the presence of lithium and sodium cations was enhanced in case of bromide and iodide, possibly via ion pair interactions. However, the stability constants show higher values in the presence of Na^+.

Many researchers have synthesized anion sensor based on metallocenes which can act as electrochemical sensory devices. In particular, the immobilisation of redox-responsive receptor systems on electrode surfaces.[6-8] In 2002,[9] Barrio and coworkers prepared an anion sensor based on a pyrrole-cobaltocenium receptor (**4 Figure 5**) and studied the electrochemical recognition of anions such as $H_2PO_4^-$, HSO_4^-, Cl^- and Br^-. Electrochemical properties of complexes of ligand and anions in solution and in immobilization on electrode are different. It was found that the electrochemical recognition of anions on the modified electrode showed larger cathodic shift than those of anions in solution and this receptor prefers to bind $H_2PO_4^-$ in both systems.

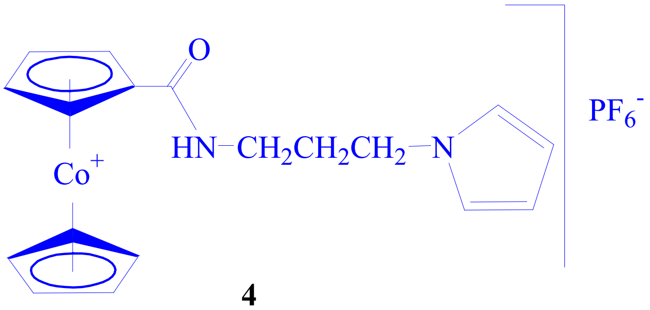

4

Figure 5 The pyrrole-cobaltocenium receptor for electrochemical recognition of anions

Ferrocene units for anionic and cation recognition have been well-known because the ferrocene unit exhibits good electrochemical signals by means of reversible processes. Additionally, the cyclopentadiene ring is easy to be derivetized. These types of compounds can also be used as electrochemical sensor. In 1999, Beer et al.[10] reported the anion recognition of upper-rim cobaltocenium calix[4]arene receptors and found that they formed complexes with carboxylate anions, dihydrogen phosphate and halide anions to a different extent. Recently, ion-pair recognition has been recognized by supramolecular chemists. It is due to its potential applications in metal ion and anion attraction or metal-controlled anion sensing devices.[11] In this dissertation, we synthesized the calix[4]arene derivatives having the amide ferrocene at the upper rim and ethylester at the lower rim for anion and cation recognition, respectively. We also studied electrochemical properties of the synthesized compounds before and after addition of anions.

2. Experimental section

2.1 Synthesis of Calix[4]arene Derivatives

2.1.1 Prepatration of 26, 28-dimethoxycalix[4]arene (1a)[17]

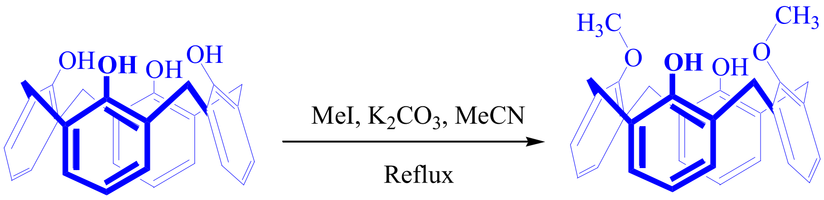

1a

Calix[4]arene (0.425 g, 1.0 mmol) and K_2CO_3 (0.1512 g, 1.09 mmol) was suspended in CH_3CN (10 mL) and the mixture was stirred at room temperature for 1 h. Iodomethane (0.1313 g, 2.20 mmol) was then added and the mixture was heated at reflux overnight. The mixture was cooled to room temperature. The reaction was filtered to take K_2CO_3 off and then the filtrate was concentrated by a rotary evaporator. The residue was dissolved in dichloromethane and washed with 3 M HCl 3 times. The organic layer was dried over anhydrous $NaSO_4$. The volumn of the solvent was reduced by using a rotary evaporator. Upon adding CH_3OH, a white solid of compound **1a** precipitated (0.397 g, 87.77% yield).

Characterization data for 1a

^{1}H-NMR spectrum (200 MHz, $CDCl_3$): δ(in ppm)

δ 7.72 (s, 2H, O*H*), 7.09-6.63 (m, 12H, Ar*H*), 4.33 and 3.42 (d, *J* = 13.2 Hz, 8H, ArCH_2Ar), 3.97 (s, 6H, OCH_3).

2.1.2 Preparation of 26,28-dimethylethylestercalix[4]arene (1b)

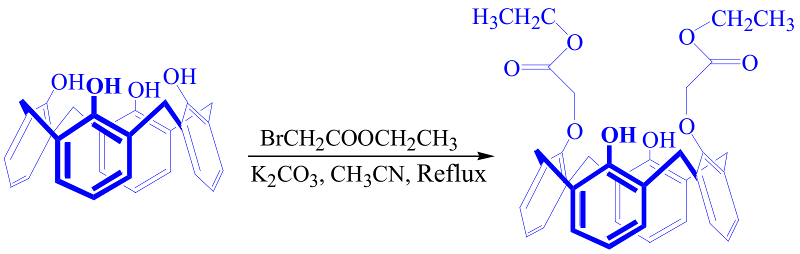

1b

Calix[4]arene (1.0 g, 2.36 mmol) and K_2CO_3 (2.50 g, 23.6 mmol) was suspended in CH_3CN (15 mL) and the mixture was stirred at room temperature for 1 h. Bromoethyl acetate (0.87 g, 5.20 mmol) was then added and the mixture was heated at reflux for 4 h. The mixture was cooled to room temperature. The reaction was filtered to take K_2CO_3 off and then the filtrate was concentrated by rotary evaporator. The residue was dissolved in dichloromethane and washed with saturated NH_4Cl 3 times. The organic layer was dried over anhydrous $NaSO_4$. The volumn of the solvent was reduced by using a rotary evaporator. Upon adding CH_3OH, a white solid of **1b** was obtained (0.801g, 57%).

Characterization data for 1b

^{1}H-NMR spectrum (200 MHz, $CDCl_3$): δ (in ppm)

δ 7.57 (s, 2H, O*H*), 7.04 (d, *J* = 7.47 Hz, 4H, *m*-Ar*H*OR), 6.89 (d, *J* = 7.41 Hz, 4H, *m*-Ar*H*OH), 6.76-6.60 (m, 4H, *p*-Ar*H*OR and *p*-Ar*H*OH), 4.71 (s, 4H, ArOC*H*$_2$-), 4.46 and 3.38 (dd, *J* = 13.3, ArC*H*$_2$Ar), 4.37-4.27 (q, *J* = 7.23 Hz, -OC*H*$_2$CH$_3$), 1.34 (t, *J* = 6.53 Hz, 6H, -OCH$_2$C*H*$_3$)

Melting point: 180 °C

2.1.3 Preparation of 5,7-dinitro-26,28-dimethoxycalix[4]arene (2a)

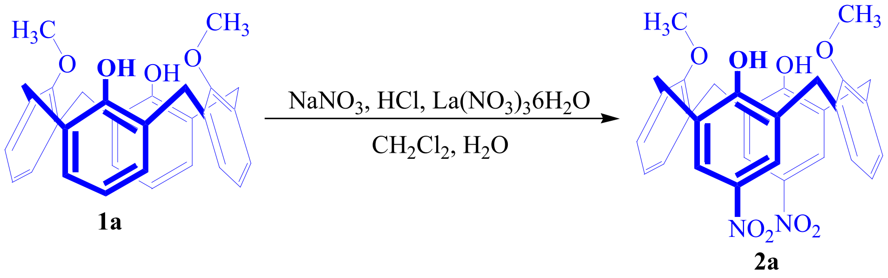

To a solution (CH_2Cl_2, 494 mL) of 26,28-dimethoxycalix[4]arene (**1a**) (10 g, 22.1 mmol) was added $NaNO_3$ (5.64 g ; 66.3 mmol) and a catalytic amount of $La(NO_3)_3.6H_2O$ in a mixture of H_2O (304 mL) and concentrated HCl (55 mL). The mixture was stirred overnight at room temperature. The colour of the mixture turned yellow. The aqueous layers were then separated and extracted with CH_2Cl_2 (250x2). The organic layer was combined and washed with saturated aqueous NH_4Cl (250x2) and dried over anhydrous Na_2SO_4. The solvent was removed by a rotary evaporator and the product was crytallized by adding hexane to give a white solid (8.51 g, 71% yield). mp > 320 ^{O}C decomposed.

Characterization data for 2a

^{1}H-NMR spectrum (200 MHz, $CDCl_3$): δ (in ppm) δ 8.93(s, 2H, -O*H*), 8.04 (s, 4H, *H*Ar-NO_2), 6.94 (d, 4H, *m*-*H*Ar-OCH_3, *J* = 7.2 Hz), 6.85-6.77 (t, 2H, *p*-*H*Ar-OCH_3, *J* = 7.4), 4.28 and 3.52 (dd, 8H, *H*AB system, *J* = 13.3 Hz), 4.02 (s, 6H, -OC*H*3).

Melting point: >320 °C decomposed

2.1.4 Preparation of 5,7-dinitro-26,28-dimethylethylestercalix[4]arene (2b)

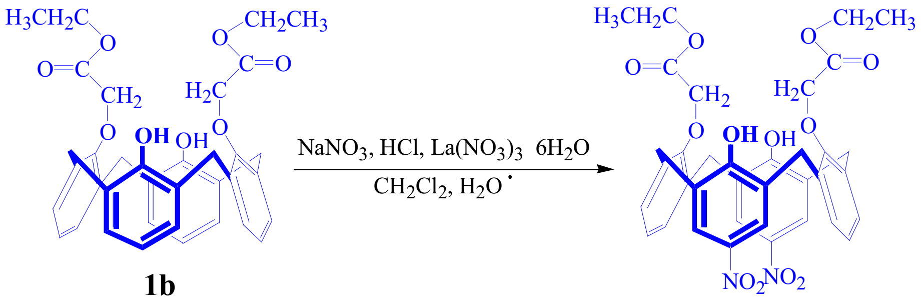

1b

2b

To a solution (CH_2Cl_2, 140 mL) of 26,28-dimethylethylestercalix[4]arene (**1b**) (3.15 g, 5.26 mmol) was added $NaNO_3$ (2.70 g, 31.74 mmol) and a catalytic amount of $La(NO_3)_3.6H_2O$ in a mixture of H_2O (88 mL) and concentrated HCl (14.3 mL). The mixture was stirred overnight at room temperature and then worked up in a similar fashion as **2a** to give a yellow solid **2b** (3.17 g, 88% yield).

Characterization data for 2b

^{1}H-NMR spectrum (200 MHz, $CDCl_3$): δ (in ppm)

δ 8.90 (s, 2H, -O*H*), 8.01 (s, 4H, *O*-Ar*H*-NO_2), 6.91 (d, *J* = 8.34 Hz, *m*-Ar*H*-OH), 6.84 (t, *J* = 6.44 Hz, 2H, *p*-Ar*H*-OR), 4.67 (s, 4H, OC*H*2CO), 4.45, and 3.49 (dd, *J* = 13.32 Hz, 8H, AB system), 4.35 (q, *J* = 7.14 Hz, 4H, OC*H*2CH_3), 1.39 (t, *J* = 8.7 Hz, 6H, -CH_2C*H*3)

Melting point : 250 °C

2.1.5 Preparation of 5,7-dinitro-25,26,27,28-tetramethoxycalix[4]arene (3a)

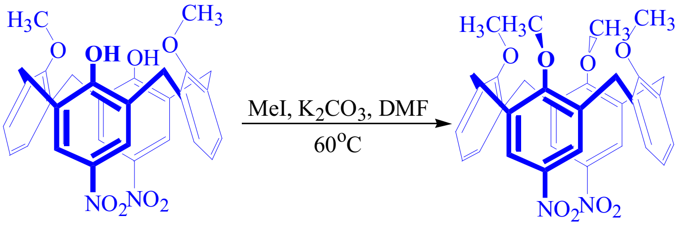

2a

3a

A solution (DMF, 10 mL) of 5,7-dinitro-26,28-dimethoxycalix[4]arene **(2a)** (0.2713 g, 0.5 mmol) and K_2CO_3 (0.695 g, 5 mmol) was stirred at room temperature for 1 h. CH_3I

(0.50 mL, 8.00 mmol) was then added and the mixture was heated at 60 °C for 7 days. After the mixture was cooled to room temperature, the solvent was removed under reduced pressure. The residue was dissolved in CH_2Cl_2 (30 mL) and washed with water and brine (2x30 mL) and then dried over anhydrous Na_2SO_4. The solvent was removed by using a rotary evaporator. Upon addition of CH_3OH, a white solid **3a** precipitated (0.203g.;71% yield).

Characterization data for 3a

^{1}H-NMR spectrum (200 MHz, $CDCl_3$): δ (in ppm)

δ 8.19-6.43 (m, 10H, Ar*H*), 4.37, 4.05, 3.28 and 3.17 (d, each *J* = 13.3 Hz, 8H, ArC*H*₂Ar), 3.85-3.72 (m, 12H, -OC*H*₃).

ESI-TOF mass spectrum: $C_{32}H_{30}N_2O_8$ = 571.30 ([M+H$^+$]) m/z.

Melting point: 260 °C

2.1.6. 5,7-dinitro-25,26,27,28-dimethoxydimethylethylestercalix[4]arene (3b)

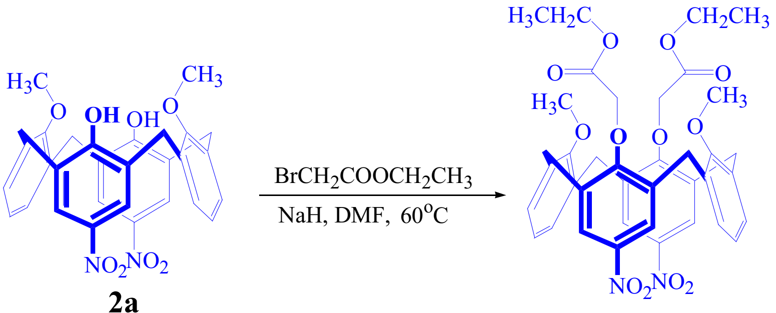

2a

3b

A solution (DMF, 20 mL) of 5,7-dinitro-26,28-dimethoxy dimethylethyl ester calix[4] arene (**2a**) (0.543 g, 1.0 mmol) and NaH (0.12 g, 5.0 mmol) was stirred at room temperature for 1 h. Bromoethyl acetate (0.40 mL, 3.0 mmol) was then added and the mixture was heated at 60 °C overnight. The reaction was worked up corresponding to the procedure for **3a** to provide a pale yellow solid **3b** (0.436g, 61%)

Characterization data for 3b

^{1}H-NMR spectrum (200 MHz, $CDCl_3$): δ (in ppm)

δ 7.83-7.08 (m, 10H, *H*-Aromatic), 4.45 (s, 4H, -OC*H*₂CO-), 4.32-4.21 (q, 4H, -OC*H*₂CH₃, *J* = 7.2 Hz), 3.96-2.99 (m, 14H, -OC*H*₃ and *H*AB system), 1.34-1.27 (td, 6H, -CH₂C*H*₃, *J* = 7.1 and 1.5 Hz).

Elemental Analysis:

Anal. Calcd for $C_{38}H_{38}O_{12}N_2$: C, 63.86 ; H, 5.36 ; N, 3.92

Found : C, 63.85 ; H, 5.29 ; N, 3.88

2.1.7 Preparation of 5,7-dinitro-25,26,27,28-dimethylethylestercalix[4]arene (3c)

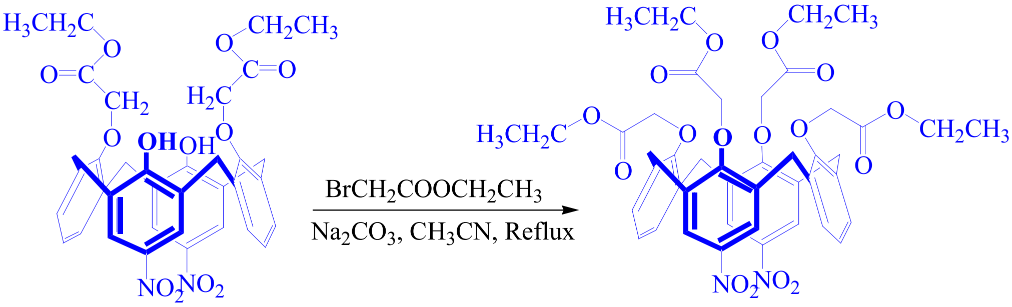

2b

3c

A solution (CH_3CN, 30 mL) of 5,7-dinitro-26,28-dimethylethylestercalix[4]arene **(2b)** (0.60 g, 1.0 mmol) and Na_2CO_3 (1.14 g, 10.4 mmol) was stirred at room temperature for 1 h. Bromoethyl acetate (1.20 mL, 1.67 mmol) was then added and the mixture was refluxed overnight. The mixture was allowed to cool to room temperature and Na_2CO_3 was removed by filtration. The mixture was evaporated using a rotary evaporator. The residue was dissolved in CH_2Cl_2 (20 mL). The organic phase was then washed with saturated NH_4Cl 3 times. The organic layer was dried over anhydrous Na_2SO_4. The solvent was removed under reduced pressure. Finally, compound **3c** precipitated as a yellow solid upon addition of CH_3OH (0.524 g, 61%).

Characterization data for 3c

^{1}H-NMR spectrum (200 MHz, $CDCl_3$): δ (in ppm)

δ 8.90 (s, 2H, O*H*), 8.01 (s, 4H, *m*-Ar*H*OH), 6.99 (d, *J* = 6.97 Hz, *m*-Ar*H*OR), 6.89-6.80 (m, 2H, *p*-Ar*H*OR), 4.71 (s, 4H, -OC*H*₂CO-), 4.45 and 3.49 (dd, *J* = 13.3 Hz, 8H, ArC*H*₂Ar), 4.40-4.29 (q, *J* = 7.17 Hz, -OC*H*₂CH₃), 1.35 (t, *J* = 7.13 Hz, 6H, OCH₂C*H*₃)

Melting point: 190 °C

2.1.8 Preparation of 5,7-diamino-25,26,27,28-tetramethoxycalix[4]arene (4a)

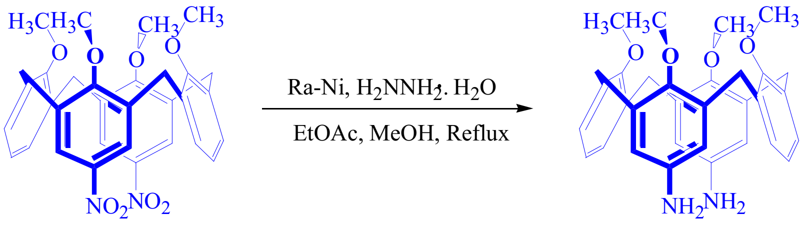

3a **4a**

5,7-Dinitro-25,26,27,28-tetramethoxycalix[4]arene (1.3928 g, 1.95 mmol) and Raney Ni (2.0951 g) were suspended in the mixture of ethylacetate (80 mL) and CH_3OH (40 mL). Hydrazine (4 mL) was then added into the mixture. The mixture was refluxed for 2 h. and allowed to cool to room temperature. The solvent was subsequently removed under reduced pressure. The residue was dissolved in CH_2Cl_2 and extracted and washed with several portions of H_2O. The organic layer was separated, combined and dried over anhydrous Na_2SO_4. The solvent was removed under reduced pressure to give a pale-white solid **4a** (0.976 g, 98% yield).

Characterization data for 4a

^{1}H-NMR spectrum (200 MHz, $CDCl_3$): δ (in ppm)

δ 7.04-6.43 (m-br, 6H, Ar*H*), 6.09 (s, br, 4H, *o*-Ar*H*-NH_2), 4.26-2.91 (m, br, 20H, OCH_3 and AB system).

ES-TOF mass spectrum: $C_{32}H_{34}N_2O_4$ = 511.30 ([M+H$^+$]) m/z.

2.1.9 Preparation of 5,7-diamino-25,26,27,28-dimethoxy dimethylethyl ester calix[4]arene (4b)

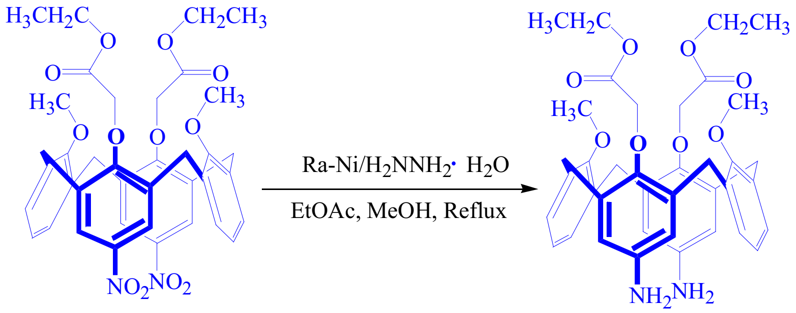

3b **4b**

5,7-Dinitro-25,26,27,28-dimethoxydimethylethylestercalix[4]arene (**3b**) (0.714 g, 1.0 mmol) and Raney Ni (1.0 g) were suspended in the mixture of ethylacetate (38 mL) and

CH_3OH (28 mL). Hydrazine (4 mL) was subsequently added. The mixture was refluxed for 2 h and allowed to cool to room temperature. The reaction was worked up as described previously (**4a**). Compound **4b** was obtained as a white solid (0.628 g, 96%).

Characterization data for 4b

^{1}H-NMR spectrum (200 MHz, $CDCl_3$): δ (in ppm)

δ 7.22 (d, 4H, *m*-*H*Ar-OCH_3, *J* = 6.9 Hz), 6.93-6.86 (t, 2H, *p*-*H*Ar-OCH_3, *J* = 7.2 Hz), 5.69 (s, 4H, *o*-*H*Ar-NH_2), 4.40 (d, 4H, AB system, *J* = 13.1 Hz and s, 4H, *o*-C*H*$_2$CO-), 4.30-4.20 (q, 4H, -OC*H*$_2$$CH_3$, *J* = 7.1 Hz), 3.96 and 3.46 (s, 6H, -OC*H*$_3$), 3.10 (d, 4H, AB system, *J* = 12.8 Hz), 1.33-1.26 (t, 6H,-OCH_2C*H*$_3$, *J* = 7.1 Hz).

ESI-TOF mass spectrum: $C_{38}H_{42}N_2O_8$ = 655.70 ($[M+H^+]$) m/z.

Elemental Analysis:

Anal. Calcd.for $C_{38}H_{42}N_2O_8$: C, 69.71 ; H, 6.47 ; N, 4.28

Found : C, 69.71 ; H, 6.25 ; N, 4.26.

2.1.10 Preparation of 5,7-diamino-25,26,27,28-tetramethylethylestercalix[4]arene (4c)

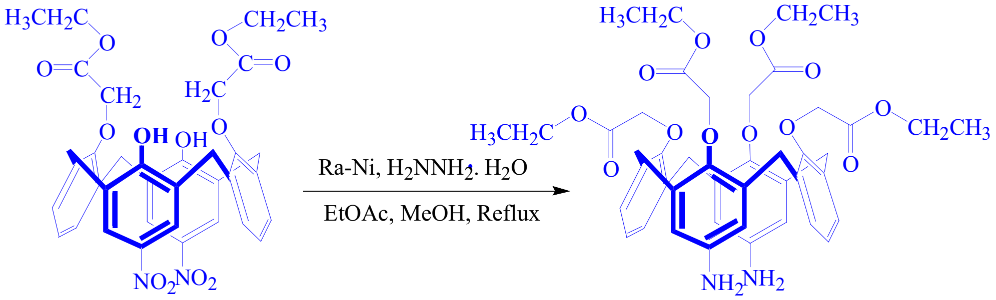

3c **4c**

5,7-Dinitro-25,26,27,28-tetramethylethylestercalix[4]arene (1.47 g, 1.52 mmol) (**3c**) and Raney Ni (1.52 g) were suspended in the mixture of ethylacetate (58 mL) and CH_3OH (42 mL). Hydrazine (6 mL) was subsequently added. The mixture was refluxed for 2 h. and allowed to cool to room temperature. The reaction was worked up as described previously (**4a**). Compound **4c** was obtained as a white solid (1.15g, 95%).

Characterization data for 4c

^{1}H-NMR spectrum (200 MHz, $CDCl_3$): δ (in ppm)

δ 6.69-6.59 (m, 6H, m-Ar*H*-OR), 6.01 (s, 4H, *o*-Ar*H*-NH_2), 4.78 and 3.10 (d, *J* = 13.1 Hz, 8H, AB system), 4.70 (s, 4H, ArOC*H*$_2$-), 4.61 (s, 4H, NH_2-Ar-OC*H*$_2$-), 4.18 (q, *J* = 7.1 Hz, 8H, *o*-C*H*$_2$$CH_3$), 1.26 (t, *J* = 7.2 Hz, 12 H, -C*H*$_3$)

ESI-TOF mass spectrum: $C_{44}H_{50}N_2O_{12}$ = 799.13 ([M+H$^+$]) m/z.

2.1.11 Preparation of 5,7-diamideferrocenyl-25,26,27,28-tetramethoxycalix [4]arene (5a)

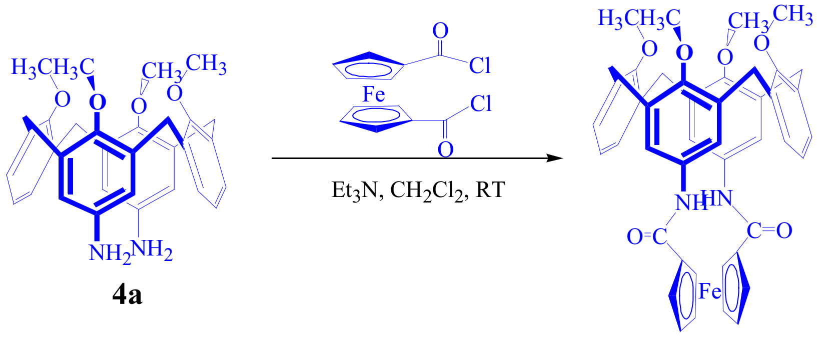

4a

5a

Into a two-necked round-bottomed flask, the mixture of tetramethoxy-diaminocalix [4]arene (**4a**) (0.786 g, 1.54 mmol) and triethylamine (0.5 mL) in dichloromethane (30 mL) was stirred at room temperature under N_2. 1,1-Bis(chlorocabonyl)ferrocene (0.6201g, 2.0 mmol) in dichloromethane (30 mL) was transferred into the mixture via cannula. The mixture was stirred at room temperature under N_2 for 4 h. It was then washed with several portions of H_2O. The organic layer was dried with anhydrous $NaSO_4$. The solvent was removed under reduced pressure to afford a dark red residue which was then placed on a silica gel chromotography column. Compound **5a** was eluted from the column using 10% EtOAc in CH_2Cl_2 as eluant. Compound **5a** is an orange solid (0.576 g., 50%). Orange crystals pf **5a** were obtained by slow diffusion of hexane into CH_2Cl_2 and CH_3OH solution of compound **5a**.

Characterization data for 5a

^{1}H-NMR spectrum (500 MHz, d^6-Acetone): δ (in ppm)

.δ 8.09 (s, 2H, -N*H*-(pc)), 7.86 (s, 2H,-N*H*-(c)), 7.59 and 6.46 (d, *J* =3 Hz, 4H, -Ar*H*-NH-(pc)), 7.22 (d, *J* = 8 Hz, 4H, *m*-Ar*H* (c)) 7.18 and 7.10 (d, *J* = 7.5 Hz, 4H, *m*-Ar*H*, (pc)), 7.01 (t, *J* = 7.5 Hz, 2H, *p*-Ar*H* (c)), 6.93 and 6.81 (t, *J* = 7.5 Hz, 2H, *p*-Ar*H* (pc)), 6.47 (s, 4H, -NH-Ar*H*- (c)) 5.00 and 4.83 (m, 4H, *o*-Cp*H* (pc)), 4.75 (t, *J* = 2.5 Hz, 4H, *o*-Cp*H* (c)), 4.41 and 4.36 (m, 4H, m-Cp*H* (pc)), 4.36 and 3.14 (d, *J* =13.5, 8H, AB system(c)), 4.313 (t, *J* = 2

Hz, 4H-Cp*H* (c)), 4.04 and 3.06 (d, *J* = 14 Hz, 8H, AB system), 3.92-3.65 (m, 21H, -OC*H*$_3$ (pc and c)), 2.86 (s, 3H, -OC*H*$_3$ (pc)).

ESI-TOF mass spectrum: $C_{44}H_{40}N_2O_6Fe$ = 749.50 ([M+H$^+$]) m/z.

Elemental Analysis:

Anal. Calcd. for $C_{44}H_{40}N_2O_6Fe\cdot0.5\ CH_2Cl_2$: C, 67.56; H, 5.22; N, 3.45.

Found : C, 67.72; H, 5.24; N, 3.55.

Melting point: 200 °C decomposed

2.1.12 Preparation of 5,7-diamideferrocenyl-25,26,27,28-dimethoxy dimethylethylestercalix[4] arene (5b)

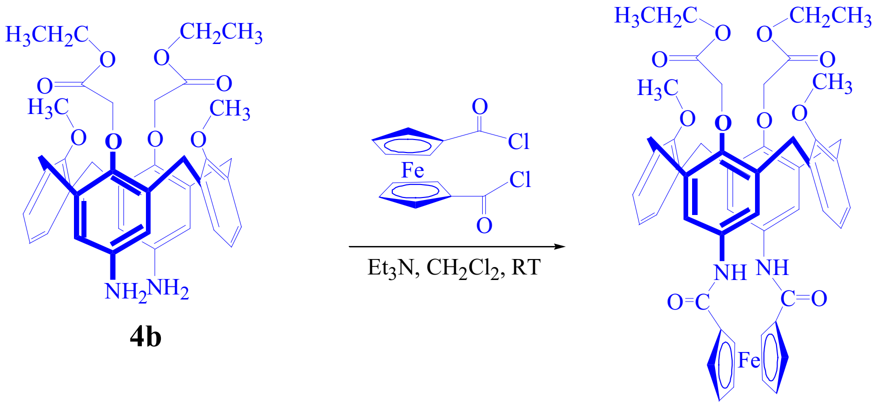

4b

5b

Into a two-necked round-bottomed flask, the mixture of dimethoxy dimethyl ethylester-diaminocalix[4]arene(**4b**) (1.31 g, 2.0 mmol) and triethylamine (1.0 mL) in dichloromethane (40 mL) was stirred at room temperature under N_2. 1,1-Bis(chlorocabonyl) ferrocene (0.620 g, 2.1 mmol) in dichloromethane (20 mL) was transferred into the mixture via cannula. The mixture was stirred at room temperature under N_2 for 4 h. It was then washed with several portions of H_2O. The organic layer was dried with anhydrous $NaSO_4$. The solvent was removed under reduced pressure to afford a dark red residue which was then placed on a silica gel chromotography column. Compound **5c** was eluted from the column using 10% EtOAc in CH_2Cl_2 as eluant. Compound **5b** is an orange solid (0.576 g., 50%). Orange crystals of **5b** was obtained by slow diffusion of hexane into CH_2Cl_2 and CH_3OH solution of compound **5b**.

Characterization data for 5b

^{1}H-NMR spectrum (500 MHz, acetane-d^6): δ (in ppm) δ 8.10 (s, 2H, -N*H*-(pc)) and 7.88 (s, 2H, -N*H*-(c)), 7.58 and 6.45 (d, *J* = 2.5 Hz, 4H, -Ar*H*-NH-(pc)), 7.43 and 7.04 (d, *J* = 7.5 Hz, 4H, *m*-Ar*H*, (pc)), 7.12 (d, *J* = 7.5 Hz, 4H, *m*-Ar*H* (c)), 6.95 (t, *J* = 7.5 Hz, 2H, *p*-Ar*H* (c)), 6.89 and 6.82 (t, *J* = 7.5 Hz, 2H, *p*-Ar*H* (pc)), 6.46 (s, 4H, -NH-Ar*H*- (c)) 5.03 and 4.86 (m, 4H, *o*-Cp*H* (pc)), 4.78 (t, *J* = 2 Hz, 4H, *o*-Cp*H* (c)), 4.39-4.37 (m, 4H (m-Cp*H* (pc)), 4H (m-Cp*H* (c)), 8H (-OCH_2-CO-(c and pc)), 4H (AB system(c))), 4.26-4.21 (m, 4H, -OCH_2CH$_3$). 4.07 and 3.05 (d, *J* = 14 Hz, 4H, AB system (pc)), 3.83 and 3.59 (d, *J* = 12.5 Hz, 4H, AB system (pc)), 2.97 (s, 3H, -OCH_3), 1.28 (m, 6H, -CH_3).

ESI-TOF mass spectrum: $C_{50}H_{48}N_2O_{10}Fe$ = 893.51 ([M+H$^+$]) m/z.

Elemental Analysis:

Anal. Calcd. for $C_{50}H_{48}N_2O_{10}Fe{\cdot}0.5\ CH_2Cl_2$: C, 64.85; H, 5.28; N, 3.00.

Found: C, 65.28; H, 5.51; N, 3.19.

Melting point: 150 °C

2.1.13 Preparation of 5,7-diamideferrocenyl-25,26,27,28-tetramethyl ethylestercalix[4]arene (5c)

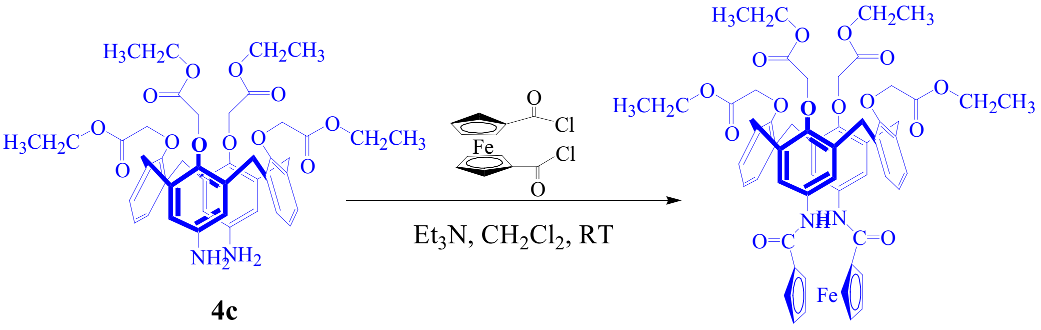

4c

5c

Into a two-necked round-bottomed flask, the mixture of tetramethylethylester-diaminocalix[4]arene(**4c**) (1.13 g, 1.53 mmol) and triethylamine (1.0 mL) in dichloromethane (40 mL) were stirred at room temperature under N_2. 1,1-Bis(chlorocabonyl)ferrocene (0.481 g, 1.55 mmol) in dichloromethane (20 mL) was transferred into the mixture via cannula. The mixture was stirred at room temperature under N_2 for 4 h. The work-up procedure is similar to the procedure described previously. Crude product was purified on a silica gel column using 10% EtOAc in CH_2Cl_2 as eluant to afford an orange solid **5c** (0.666 g, 42%).

Characterization data for 5c

^{1}H-NMR spectrum (200 MHz, $CDCl_3$): δ (in ppm) δ 7.25 (s, 2H, -NH-), 7.20 (d, *J* = 6.7 Hz, 4H, m-Ar*H*-OR), 7.09 (t, *J* = 6.4 Hz, 2H, *p*-Ar*H*OR), 6.43 (s, 4H, *o*-Ar*H*-NH-), 4.87 and 3.22 (d, *J* = 13.0, 8H, AB system), 4.90 (s, 4H, -NH-ArHOCH_2-), 4.77 (s, br, 4H,Cp*H*), 4.45 (s, 4H, ArH-OCH_2-), 4.33 (s, br, 4H, Cp*H*), 4.17 (q, *J* = 7.1 Hz, 8H, -OCH_2CH$_3$), 1.33-1.22 (m, 12H, -OCH$_2$CH_3).

ES-TOF mass spectrum: $C_{56}H_{56}N_2O_{14}Fe$ = 1037.20 ([M+H$^+$]) m/z.

Elemental Analysis:

Anal. Calcd. for $C_{56}H_{56}N_2O_{14}Fe$: C, 64.87; H, 5.44; N, 2.70.

Found: C, 64.84; H, 5.40; N, 2.63.

Melting point: 227 °C

3. Results and discussion

3.1 Synthesis and characterization of calix[4]arene derivatives

3.1.1 Design and syntheses

We have designed anion receptors containing ferrocene units connecting to the amide moieties. The amide groups bind with anion guests using hydrogen bonding interactions: O=C-N-H---X, where X = anions. Nevertheless, we have attached ethyl ester groups on the lower rim of calix[4]arene to function as rotation-inhibitors as well as binding sites for cations. The designed molecules are shown in **Figure 6**.

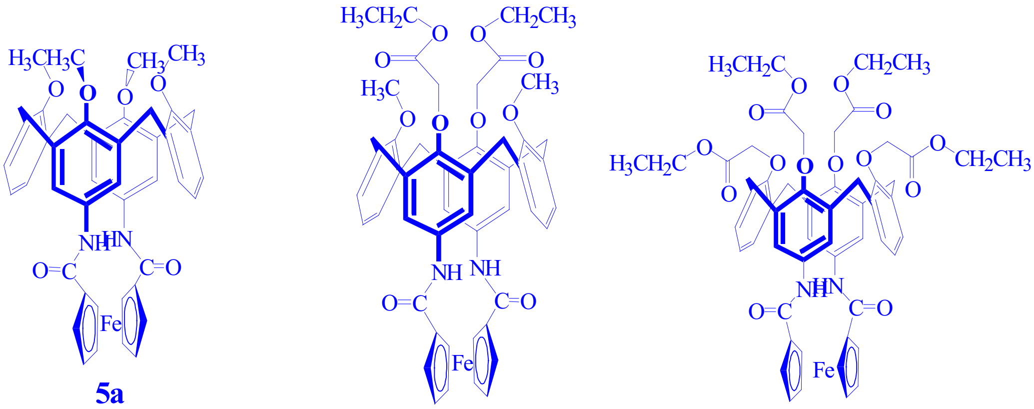

5a **5b** **5c**

Figure 6 Target molecules contain cation and anion binding sites

Syntheses of ethyl ester ferrocene amide and methoxy ferrocene amide calix[4]arene **5a**, **5b** and **5c** are summarized in **Scheme 1**. Nitrations of dimethoxy calix[4]arene**1a**[17] and diethyl ester calix[4]arene **1b**[24] were accomplished using a phase transfer strategy[25] between organic and water phase. $NaNO_3$, concentrated HCl and $La(NO_3)_3$ as catalyst were dissolved in water while compounds **1a** and **1b** were dissolved in dichloromethane. The solution mixture was kept stirring vigorously at room temperature until thesolution turned yellow. The mixture were worked up to afford yellow powders of dimethoxy dinitrocalix[4]arene (**2a)** and diethyl ester dinitrocalix[4]arene **(2b)** in 71% and 88%, respectively. Reagents used in this reaction are mind and appropriate for producing selectively nitro substituents on the *para* position of phenol rings . Compound **2a** hardly dissolves in common solvents such as CH_2Cl_2, CH_3OH, EtOAc and CH_3CN, but dissolves very well in DMF. Thus, the nucleophilic substitutions of compound **2a** with CH_3I and ethyl bromoacetate in the presence of NaH and K_2CO_3, respectively, were carried out in DMF at 60 ^oC. Controlling the temperature for this reaction is quite important because DMF can decompose at higher temperature. The tetra-substituted dinitrocalix[4]arene, **3a** and **3b,** were obtained as pale-yellow powders at 71% and 61% yields, respectively. On the other hand, diethyl ester dinitrocalix[4]arene dissolves easily in common organic solvents. Nucleophilic substitution of **2b** with ethyl bromoacetate was carried out in acetonitrile in the presence of Na_2CO_3. Pale-yellow solid of tetraethyl esterdinitrocalix[4]arene (**3c**) was obtained in 61% yield. Essentially, the hydroxy groups at the *para* position to the nitro groups must be protected prior to the reduction of nitro groups to amino groups because *p*-hydroxy aniline unit is easy to be oxidized and transformed to quinone. Reduction of nitro groups (**3a**, **3b** and **3c**) was carried out using Raney Ni and $N_2H_4{\cdot}H_2O$ in the mixture of CH_3OH and EtOAc to yield diamino compounds **4a**, **4b** and **4c** in 98%, 95%, and 96% yields, respectively.[26] Coupling reactions were performed using the freshly synthesized diamino compounds (**4a**, **4b** and **4c**) and 1,1-bis(chlorocarbonyl)ferrocene[27-28] This reaction should be refrained from the moisture because the hydroxy group can replace the Cl atom of chlorocarbonylferrocene to give carboxylic ferrocene. Therefore, 1,1-bis(chlorocarbonyl)ferrocene were maintained under N_2 and transferred via cannula to the solution of diamino calix[4]arene in the presence of NEt_3 in CH_2Cl_2. The mixture was stirred at room temperature under N_2 for 4 h to produce orange solids of ferrocene amide calix[4]arenes **5a**, **5b** and **5c** in 50%, 42%, and 40% yields, respectively. The main by-product from this reaction is Bisamideferrocene calix[4]arene. In order to achieve higher yields of the desired compounds, reactions should be carried out in dilute solutions.

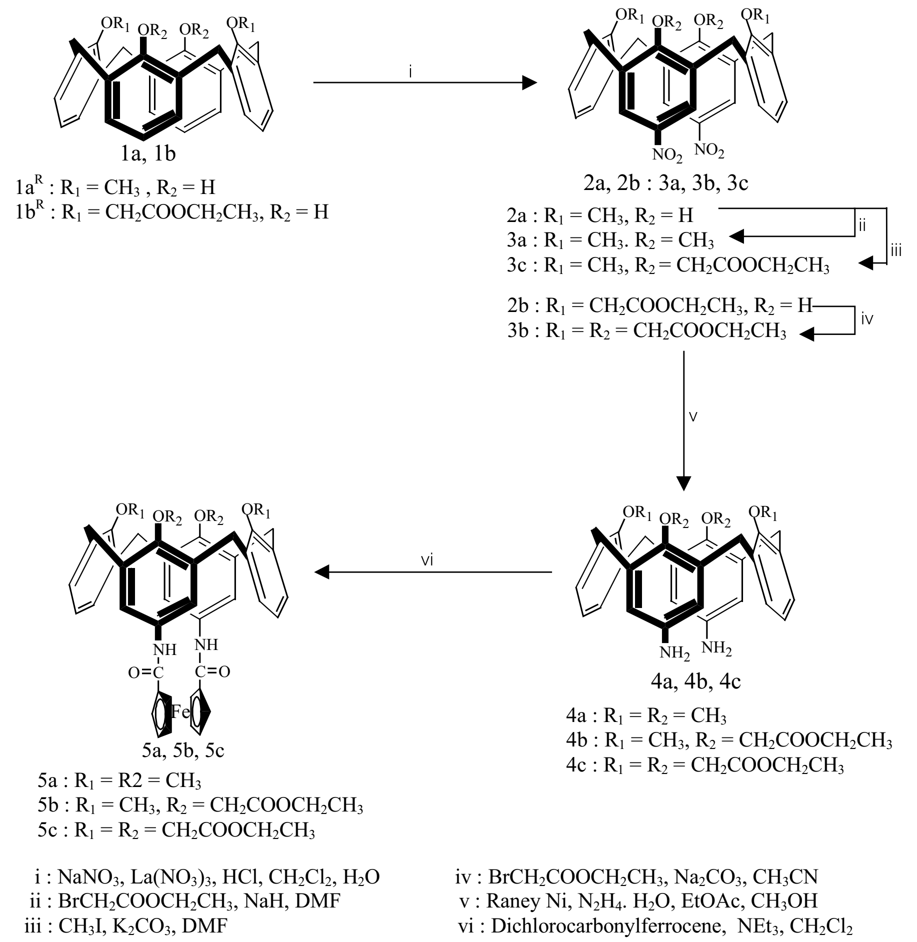

1a, 1b
$1a^R$: $R_1 = CH_3$, $R_2 = H$
$1b^R$: $R_1 = CH_2COOCH_2CH_3$, $R_2 = H$

2a, 2b : 3a, 3b, 3c
2a : $R_1 = CH_3$, $R_2 = H$
3a : $R_1 = CH_3$. $R_2 = CH_3$
3c : $R_1 = CH_3$, $R_2 = CH_2COOCH_2CH_3$

2b : $R_1 = CH_2COOCH_2CH_3$, $R_2 = H$
3b : $R_1 = R_2 = CH_2COOCH_2CH_3$

4a, 4b, 4c
4a : $R_1 = R_2 = CH_3$
4b : $R_1 = CH_3$, $R_2 = CH_2COOCH_2CH_3$
4c : $R_1 = R_2 = CH_2COOCH_2CH_3$

5a, 5b, 5c
5a : $R_1 = R2 = CH_3$
5b : $R_1 = CH_3$, $R_2 = CH_2COOCH_2CH_3$
5c : $R_1 = R_2 = CH_2COOCH_2CH_3$

i : $NaNO_3$, $La(NO_3)_3$, HCl, CH_2Cl_2, H_2O
ii : $BrCH_2COOCH_2CH_3$, NaH, DMF
iii : CH_3I, K_2CO_3, DMF
iv : $BrCH_2COOCH_2CH_3$, Na_2CO_3, CH_3CN
v : Raney Ni, N_2H_4. H_2O, EtOAc, CH_3OH
vi : Dichlorocarbonylferrocene, NEt_3, CH_2Cl_2

Scheme 1 Pathway of syntheses **5a**, **5b** and **5c**

3.2 Structure in Solution and Solid State

The structures of calix[4]areneare are normally classified into four basic conformations according to the possible ‘up’ and ‘down’ arrangement of the phenol rings: cone, partial cone, 1,2-alternate and 1,3-alternate. The most stable conformation is cone conformation due to intramolecular hydrogen bonding among hydroxy groups at the lower rim. However, calix [4]arene compounds are found in other conformations depending on the base used in substitution reactions and functional groups attached on the lower rim oxygen atoms.[29] In the case of compounds **5a** and **5b**, NMR spectra at room temperature showed complicated signals suggesting a mixed conformation of the calix[4]arene unit. Both compounds have two opposite anisole rings in a rigid fashion linking by amide ferrocene and the remianed phenyl rings are flexible for free rotation. ^{1}H-NMR spectra of both **5a** and **5b** exhibited sharp peaks at room temperature (**Figure 8 and 9)** suggesting that the conformational interconversion took place in a slow exchange manner on NMR time scale.[30] According to COSY, NOESY, ROESY, HMQC, HMBC and DEPT, both cone and partial cone conformation were seen in the spectrum. For the most advantage of the mentioned 2D-NMR techniques above, the correlation cross peaks of NOESY can be used to identify corresponding 2 different conformations in the spectrum. The correlation of signals can be assigned either cone or partial cone conformation. The correlation protons were assigned in **Figure 7** according to the results of NOESY shown in **Figure 8 and 9.**

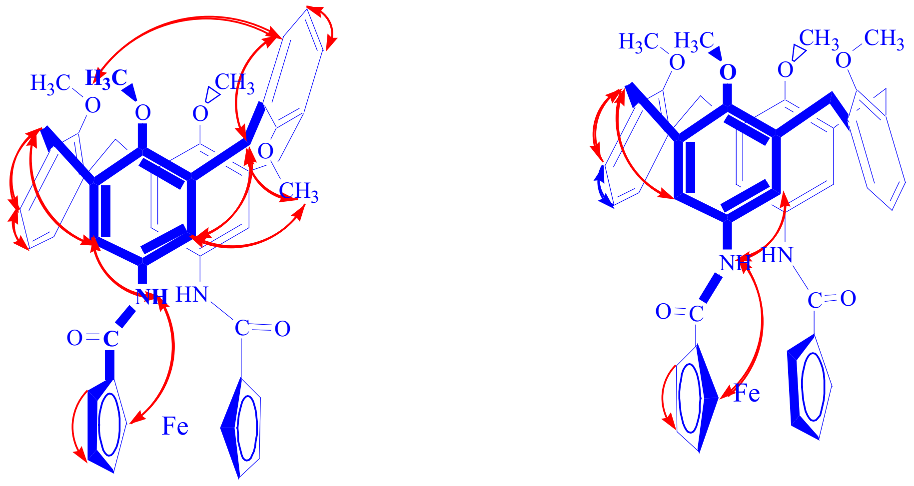

Partial Cone conformation

Cone conformation

Figure 7 NOESY correlation of Partial Cone and Cone conformation of **5a**

From the 2D-NOESY correlation of the partial cone conformation, the methoxy group at 2.87 ppm on the rotated phenol ring displays a cross peak with *o*-Ar*H*NHCO aromatic proton at 6.379 ppm. The other methoxy groups correlates to the inversed aromatic protons (doublet signals at 7.20 and 7.06 ppm and triplet signals at 6.90 and 6.63 ppm).

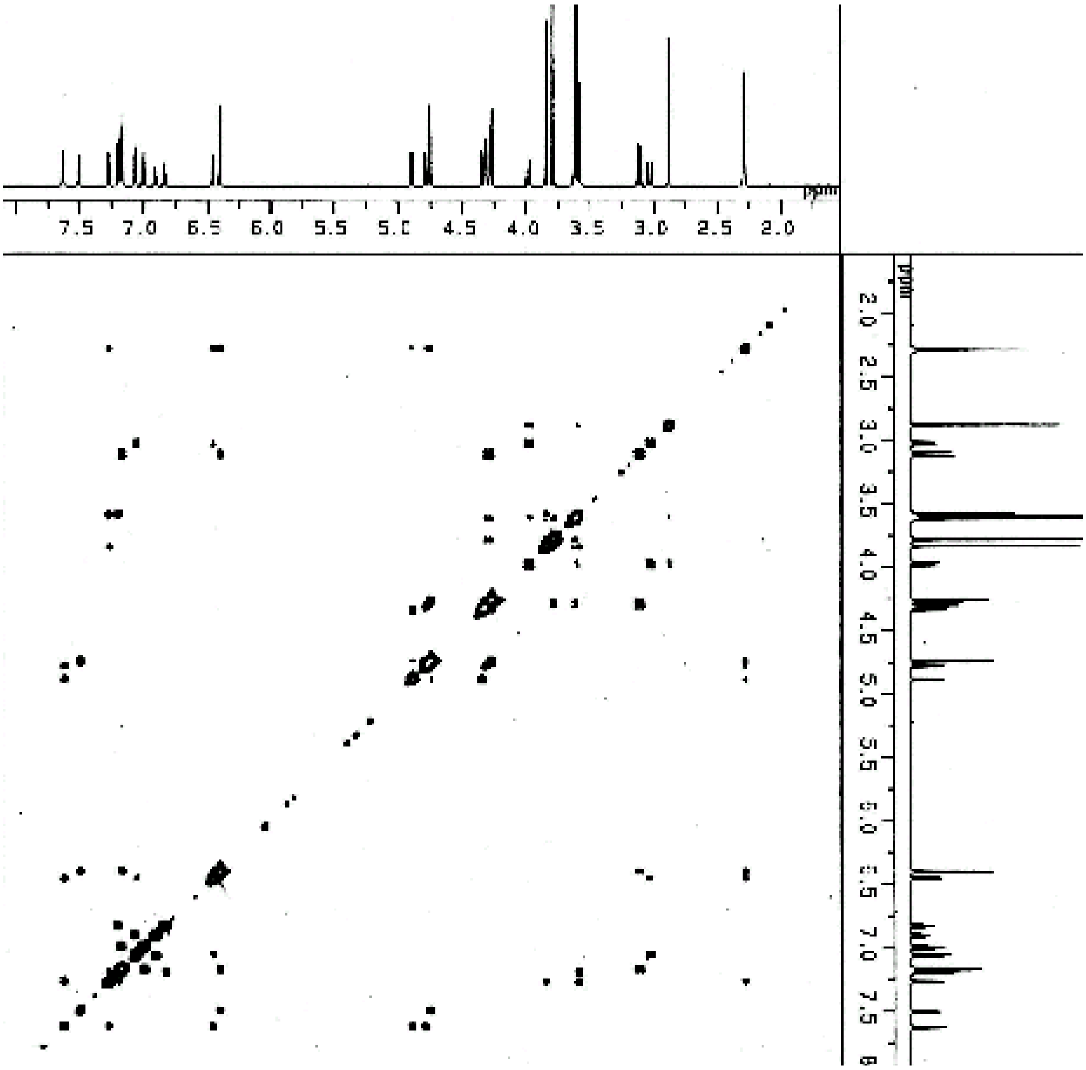

Figure 7 NOESY spectrum of 5,7-diamideferrocenyl-25,26,27,28-tetramethoxycalix[4]arene (**5a**) in $CDCl_3$ with 400 MHz

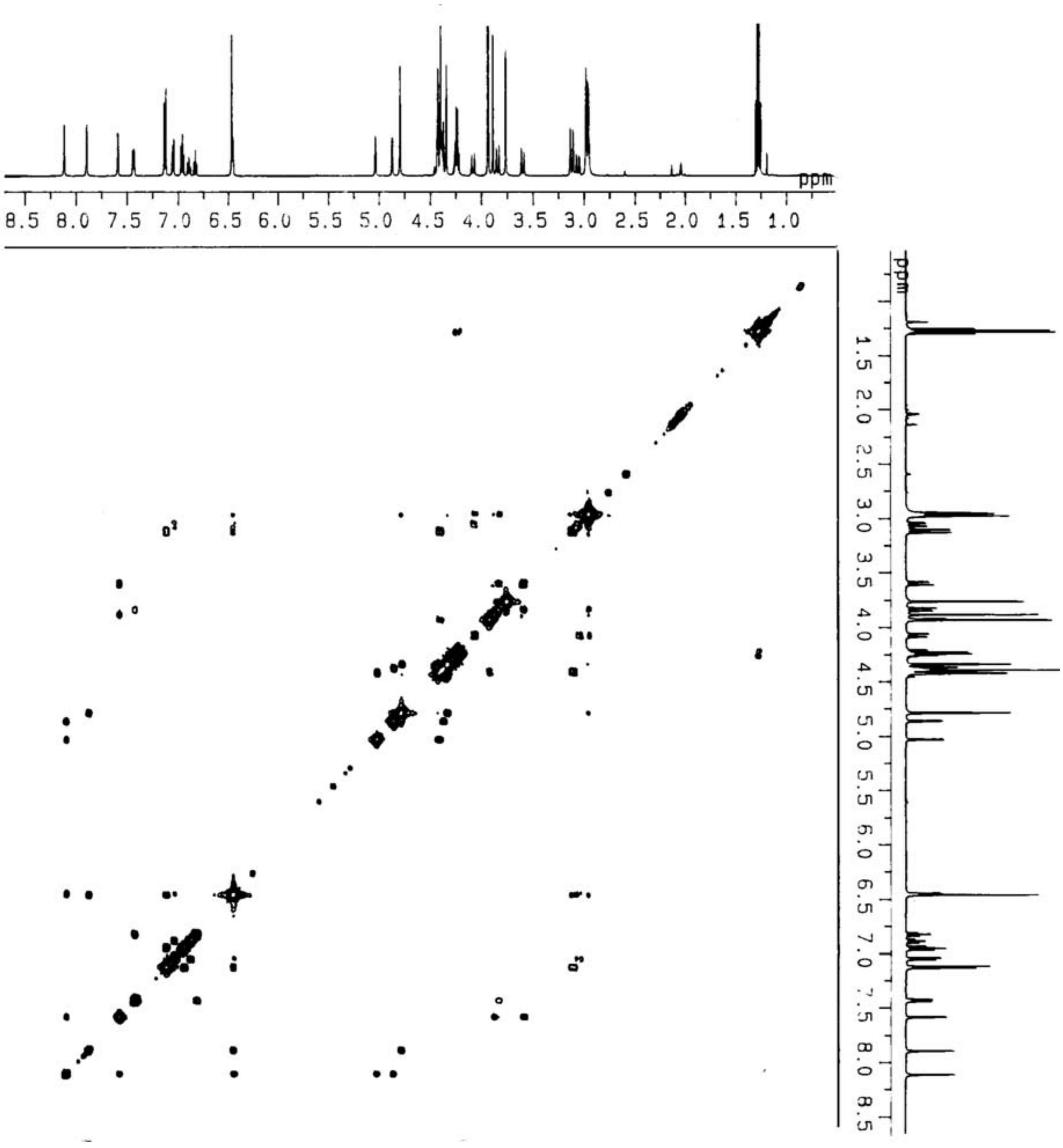

Figure 8 NOESY spectrum of 5,7-diamideferrocenyl-25,26,27,28-dimethoxy dimethyl ethylestercalix[4]arene (**5b**) in Acetone-d^6 with 500 MHz

The methylene protons at 3.98 ppm correlate to the methoxy group on the inversed aryl ring. On the other hand for cone conformation, the methoxy groups have no correlation with the aromatic protons and with the methylene protons. In contrast to **5a** and **5b**, tetraethylester calix[4]arene (**5c**) was found to be in a cone conformation only in the solution state. Four bulky ethylester groups at the lower rim thus inhibit the ring rotation.

Considering the ^{1}H-NMR spectra of **5a** and **5b** in acetone-d^6, 500 MHz, the cone conformation has two planes of symmetry. The aromatic protons exhibit a triplet for *p*-Ar*H*OCH$_3$ at 7.01 ppm for **5a** and at 6.95 ppm for **5b**, a doublet of *m*-Ar*H*OCH$_3$ at 7.22 ppm for **5a** and at 7.12 ppm for **5b** and a singlet for meta protons substituted aromatic ring on upper rim at 6.47 ppm for **5a** and at 6.46 ppm for **5b**. In addition, the methylene bridge protons in cone conformation appear as two sets of doublets at 4.36 and 3.14 ppm for **5a** and at 4.04 and 3.06 ppm for **5b** while partial cone conformation has 4 sets of doublets at 4.29, 3.98, 3.11 and 3.03 ppm for **5a** and at 4.09, 3.82, 3.32 and 3.19 ppm for **5b**. It is notable that peaks due to methyl protons of the partial cone conformation shift more up-field shift than those of the cone conformation. This probably stems from the effect of ring currents from aryl units of calix[4]arene when one of the methoxy group point into the calix[4]arene cavity (**Figure 10 and 11**) Additionally, ^{13}C NMR spectra of compounds **5a** and **5b** show characteristic peaks of methylene bridge carbon at ca. 31 ppm for the cone conformation and at ca. 31 ppm and ca. 37 ppm for partial cone conformation.[31]

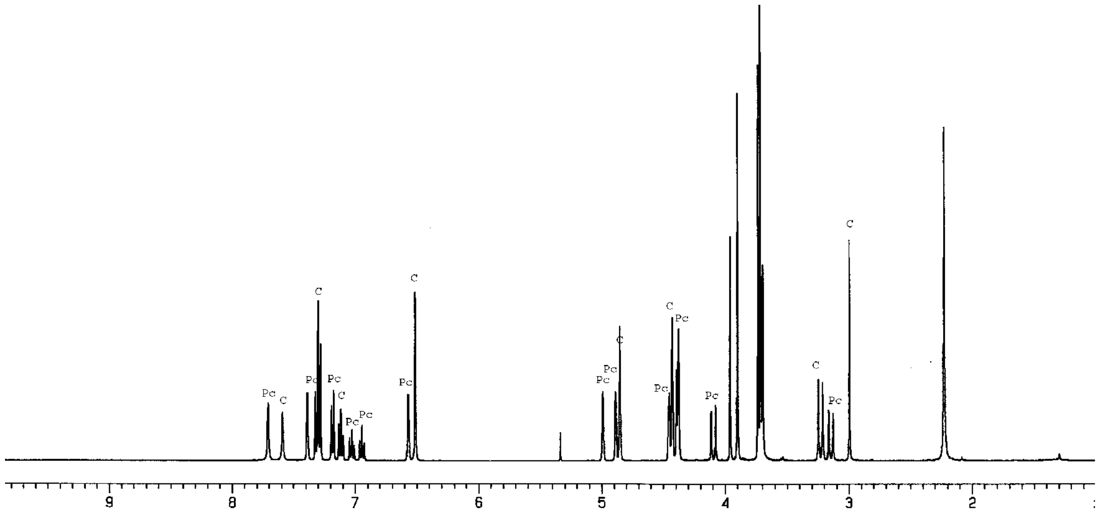

Figure 10 ^{1}H-NMR spectrum of 5,7-diamideferrocenyl-25,26,27,28-tetramethoxycalix[4] arene (**5a**) in CDCl$_3$ with 400 MHz

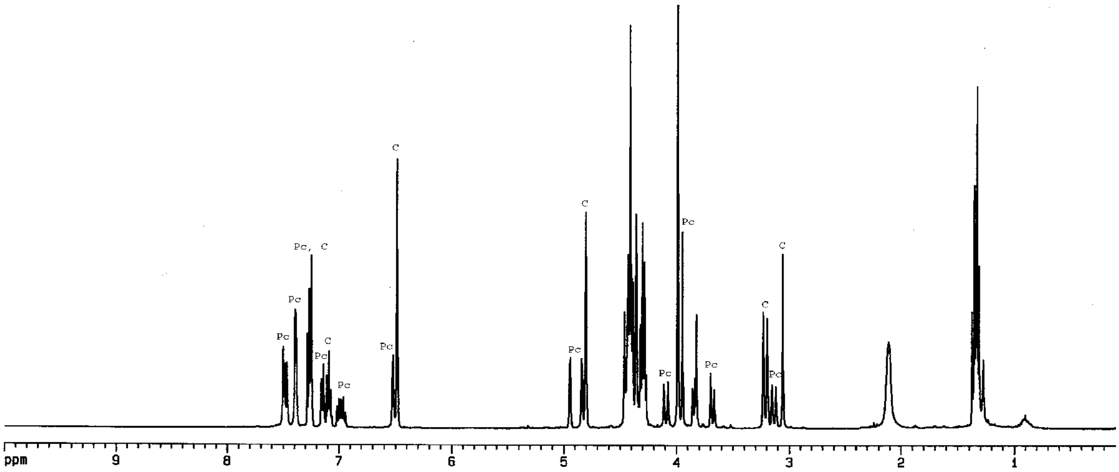

Figure 11 ^{1}H-NMR spectrum of 5,7-diamideferrocenyl-25,26,27,28-dimethoxy dimethyl ethylestercalix[4]arene (**5b**) in $CDCl_3$ with 400 MHz

^{1}H-NMR spectra of **5a** and **5b** in the different solvents show the different intensity of cone and partial cone conformation ratio depending on the polarity of solvent. (Shown in **Table 1)**

Table 1 Show the intensity of cone and partial cone conformation ratio

	5a C:PC	**5b** C:PC
$CDCl_3$	1:1	1:1
CD_2Cl_2	1:1	1:1
Acetone-d^6	1:2	1:1
DMSO-d^6	1:2	1:1
CD_3CN-d^3	1:1	1:1

Elucidation of ^{1}H-NMR spectra of **5a** and **5b** in DMSO-*d*^{6} and acetone-*d*^{6} was found that compound **5a** exists in partial cone and cone conformation in 2:1 ratio, whereas compound **5b** in 1:1 ratio. The ratio of cone to partial cone conformation for **5a** and **5b** is 1:1 in CD_3Cl

and CD_2Cl_2. This is opposite to that reported by Shikai where the concentration of cone conformation of tetramethoxy calix[4]arene was found to increase upon increasing solvent polarity.[32] From the ^{1}H-NMR spectrum of **5c**, it shows only cone conformation containing a triplet for *p*-Ar*H*OCH_3 at 7.09 ppm, a doublet of *m*-Ar*H*OR at 7.20 ppm and a singlet for meta protons substituted aromatic ring on upper rim at 6.43 ppm as well as the methylene bridge proton at 4.87 and 3.22 ppm as shown in **Figure 12**.

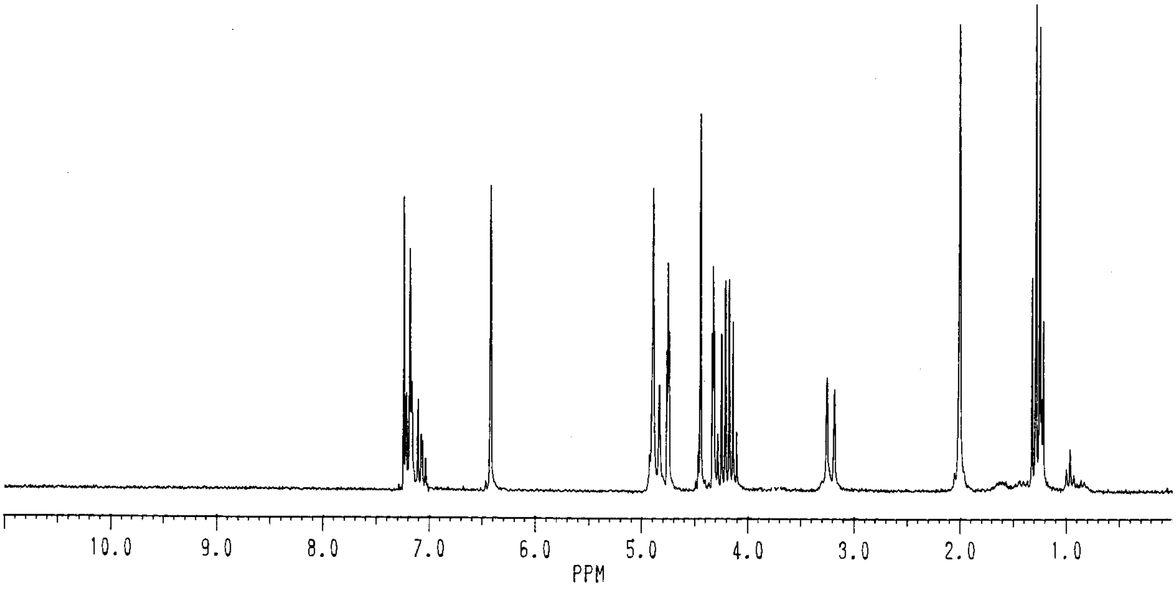

Figure 12 ^{1}H-NMR spectrum of 5,7-diamideferrocenyl-25,26,27,28-tetramethyl ethylestercalix[4]arene (**5c**) in $CDCl_3$ with 200 MHz

3.3 VT NMR experiments

Conformational interconversion can be studied by variable temperature NMR spectroscopy in order to investigate the inversion barrier energy between cone and partial cone conformation.[33-36] ^{1}H-NMR spectra of **5a** and **5c** exhibit sharp signals at room temperature indicating a slow exchange of conformation on the NMR time scale.[37] In order to study thermodynamic properties of these receptors (**5a** and **5b**), they should, thus, be determined by measuring dynamic ^{1}H-NMR at high temperature in DMSO-d^6 ranging from 25 to 150 °C (which is the limitation of the NMR machine and solvent properties). Variable temperature ^{1}H-NMR spectra is illustrated in **Figure 13**. No coalescence signals were observed in the range of 25-150 °C.

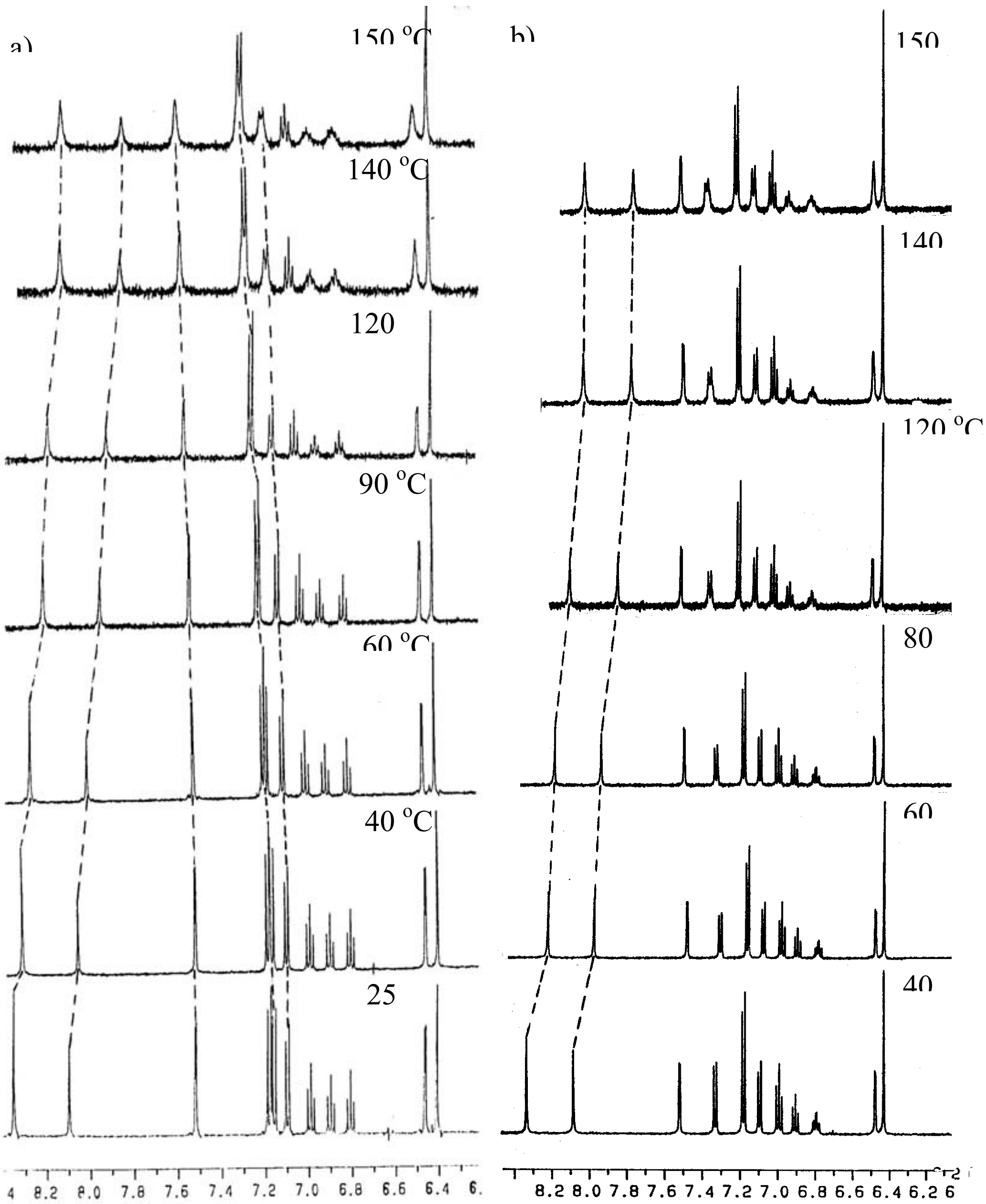

Figure 13 Variable high temperatures of **5a** (a) and **5b** (b) in DMSO-d^6

The NH peaks of **5a** and **5b** in cone and partial cone conformation move up field (**5a**; $\Delta\delta = 0.438$ and 0.441 ppm for C and Pc, respectively, **5b**; $\Delta\delta = 0.43$ for both C and PC) and doublet peaks at ArCH_2Ar of partial cone conformation shifted downfield slightly ($\Delta\delta \sim 0.1$ ppm). All peak assignments of partial cone conformation for **5a** became board at 110 °C and their intensities decreased while those of **5b** took place at 140 °C. This signified that the methoxy aromatic rings of **5b** rotated around methylene bridge more slowly than those of **5a** since compound **5b** had two bulky ethyl ester groups to inhibit the rotation. In contrast, cone conformation for both **5a** and **5b** retained sharp signals even at higher temperature. It implies that cone conformation is stable and does not undergo interconversion at high temperature.[38] According to integrated signals, partial cone conformation gradually changed to cone conformation observed from reduction of mole fractions of PC whereas those of C increased at higher temperature. **(Figure 14)**

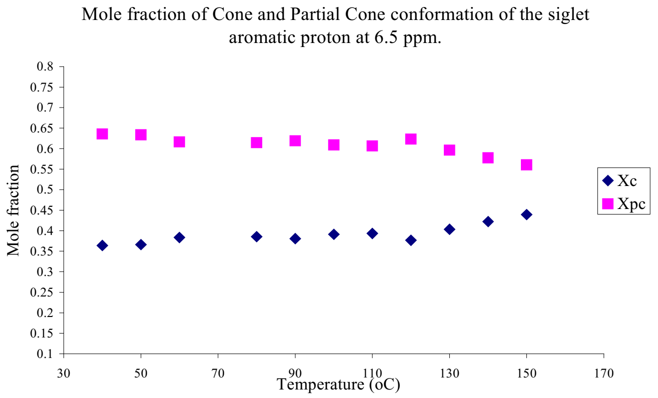
Mole fraction of Cone and Partial Cone conformation of the siglet aromatic proton at 6.5 ppm.

(a) Mole fraction of Tetramethoxyamideferrocenecalix[4]arene **5a**

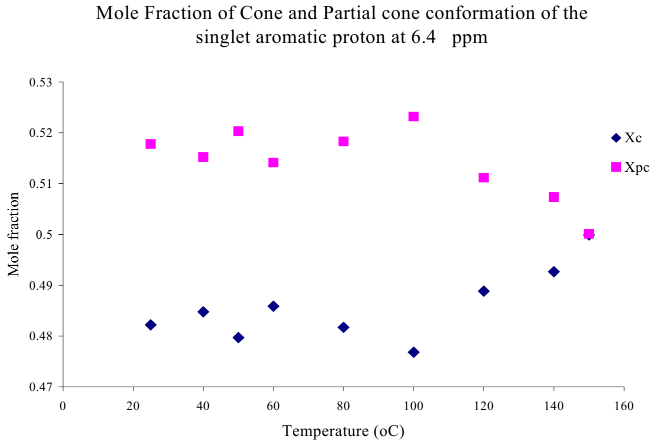
Mole Fraction of Cone and Partial cone conformation of the singlet aromatic proton at 6.4 ppm

(b) Mole fraction of Dimethoxydimethylethylesteramideferrocenecalix[4]arene **5c**

Figure 14 Mole fraction of cone and partial cone conformation at variable temperature from 25 °C to 150 °C

Reinhoudt et al.[38] studied the mechanism of conformational interconversion of calix [4]arene derivatives containing tetramethoxy at lower rim and crown-ether at upper rim by quantitative 2-D EXSY NMR spectroscopy.(**Figure 15**)

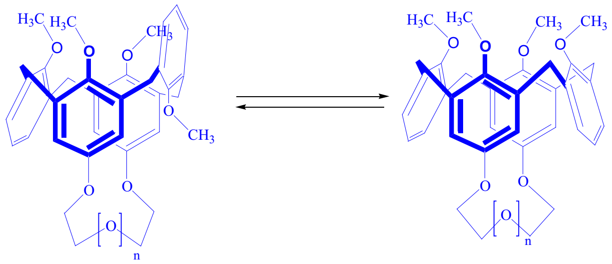

Partial Cone Conformation

Cone Conformation

Figure 15 Tetramethoxy calix[4]crown in cone and partial cone conformation

Behaviors of ^{1}H-NMR spectra of their compounds are similar to ^{1}H-NMR spectra of both **5a** and **5b** shich showrd sharp signals of the mixture of cone and partial cone conformation at room temperature. Surprisingly, the results of 2-D EXSY NMR spectrum showed that the conformational interconversion processes occur via the intermediate of 1,3-alternate conformation following the equilibrium shown in **3.3.1**.

$$C \underset{k_{PC}}{\overset{k_{CP}}{\rightleftarrows}} A \underset{k_{AP}}{\overset{k_{PA}}{\rightleftarrows}} P \qquad \textbf{(1)}$$

Reinhoudt stated that this mechanism cannot be observed by ^{1}H-NMR and 2D-NOSEY results. It is worthwhile to propose that the mechanism of **5a** and **5b** may occur pass the 1,3-alternate conformation. Otherwise the conformational interconversion took place possibly between cone and partial cone conformation directly. Variable high temperature results give enough information to deduce that the conformational interconversion of **5a** and **5b** took place between cone to partial cone without the intermediate 1,3-alternate conformation. (**Figure 16**)

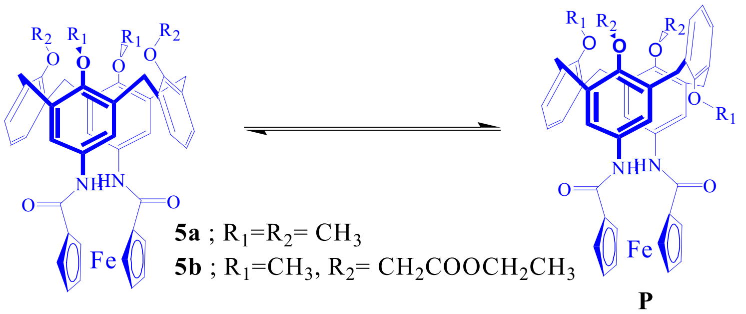

5a ; R_1=R_2= CH_3

5b ; R_1=CH_3, R_2= $CH_2COOCH_2CH_3$

C

P

Figure 16 The proposed mechanism of conformational interconversion of **5a** and **5c**

3.4 X-ray structure analysis

Crystals of **5a** and **5b** were obtained by slow diffusion of hexane to the solution of compounds **5a** and **5b** in mixed CH_2Cl_2 and CH_3OH. Crystallographic data are listed in **Table 2**

Table 2 Crystallographic data for the X-ray Diffraction Studies of **5a** and **5b**

Compounds	**5a**	**5b**
Empirical Formula	$C_{46}H_{48}FeN_2O_8$	$C_{52}H_{56}FeN_2O_{12}$
Formula weight	812.71	956.84
Temperature (K)	120 (2)	120(2)
Radiation (λ, Å)	Mo Kα (0.71073)	Mo Kα (0.71073)
Crystal system	Monoclinic	Monoclinic
Space group	$P2_1$	$C2/c$
a, (Å)	12.813(3)	13.008(3)
b, (Å)	13.337(3)	21.775(4)
c, (Å)	12.983(3)	16.105(3)
$\alpha = \gamma$, deg	90	90
β, deg	118.73(3)	95.48(3)
V, $Å^3$	1945.5(7)	4540.9
Z	2	4
ρ(cal), g/cm^3	1.387	1.400
Abs coeff, (mm^{-1})	0.447	0.401
Crystal size (mm^3)	0.20 x 0.18 x 0.14	0.26 x 0.14 x 0.12
Reflection collected	15395	20610
$R(F)^a$, %	5.69	4.59
$Rw(F^2)^a$, %	14.17	11.39

[a] Residuals: $R(F) = \Sigma|F_o - F_c|/\Sigma F_o$; $R_w(F^2) = \{[\Sigma w(F_o^2 - F_c^2)^2]/[\Sigma w(F_o^4)^2]\}^{1/2}$.

Compound **5a** has 2 molecules of CH_3OH as a solvent of crystallization while **5b** contains 1 molecule of CH_3OH. There are hydrogen bonding interactions between C=O of the amide group and hydrogen atom of methanol and also between NH of the amide group and oxygen atom of methanol as shown in **Figure 17**.

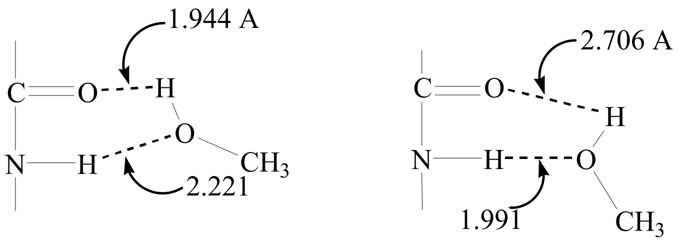

Hydrogen bond interactions between methanols and amide group of **5a**

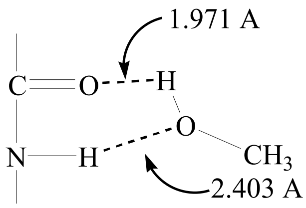

Hydrogen bond interactions between methanol and amide group of **5b**

Figure 17 The distance of hydrogen bond interaction between methanol and amide group of **5a** and **5c**

X-ray structures showed that the compound **5a** adopts a partial cone conformation in the solid state, in which all methoxy groups point out of cavity. This reduces the steric crowdedness of the calix[4]arene units.[39-40]

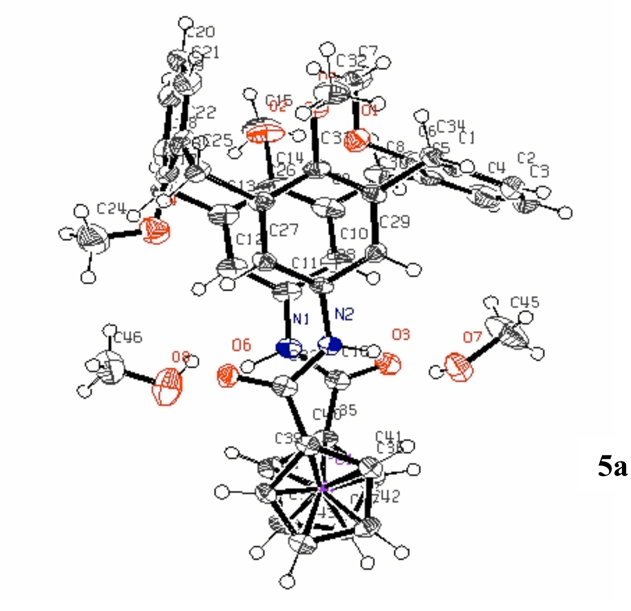

5a

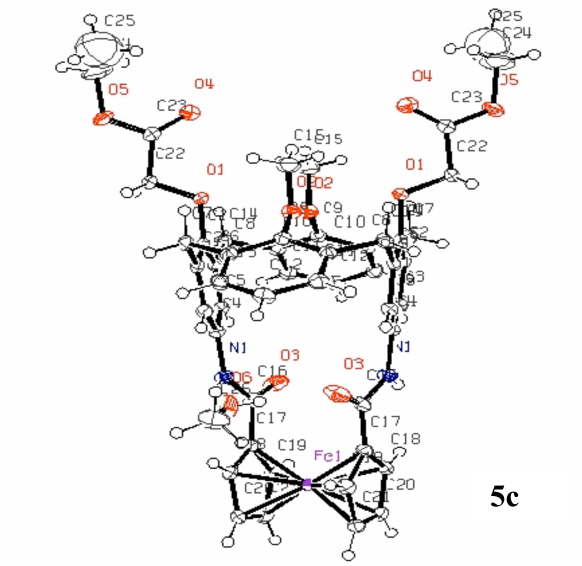

5c

Figure 18 Crystal structure of compound **5a** and **5c**

The stable structure of **5b** is in cone conformation in solid state due to the steric hindrance of 2 ethyl ester groups. As observed from x-ray structure of **5a**, one methoxy group on C7 was subjected to the anisotropic effect from inversed anisole ring. Therefore, the ^{1}H-NMR chemical shift of this methoxy group appears at high field ($\delta = 2.87$ ppm). The molecule **5b** has one plane of symmetry between calix[4]arene rings while **5a** lacks the plane of symmetry caused by an inversed phenyl unit. Dihedral angles[41-43] between the phenyl rings and the plan of the four methylene groups are 79.17°, 75.85°, -100.83° and 24.31° for **5a** and those of **5b** are 83.97° and 35.24°. The anisole ring opposite the inversed aryl ring of **5a** is in a flattened phenyl unit attributed by the dihedral angle at 24.31° and also both unsubstituted phenyl rings of **5b** are in flatted units corresponding to dihedral angles at 35.24°. It was suggested that it is in a 'pinch cone' conformation. In the principle of calix[4]arene conformation mentioned above, cone conformation has the symmetrical C_{4v} structure while pinch cone conformation is in C_{2v} symmetry containing two opposite aromatic rings almost parallel and the other two adopted a flattened conformation.[44-45] The previous studies on the interconversion of tetra-*o*-alkylated calix[4]arene by computational study. It was predicted that a structure with C_{2v} symmetry is more stable than the more symmetrical C_{4v} structure.[39,43] Considering **5a** and **5b**, the distances between the equatorial calix[4]arene bridging methylene hydrogens (H_{eq}) and the two adjacent aromatic hydrogens (H_1, H_2 and H_3

in **chart 1**) were determined from x-ray structure identifying either the conformation is in a partial cone or a pinch cone conformation. The distance of H_{eq}-H_1 is longer than that of H_{eq}-H_2 for the pinch cone conformation. In addition, the distance of H_{eq}-H_3 is longest compared to the former distances. Undoubtedly, it was concluded that **5b** exists in a pinch cone conformation and **5a** in a partial cone conformation.[44]

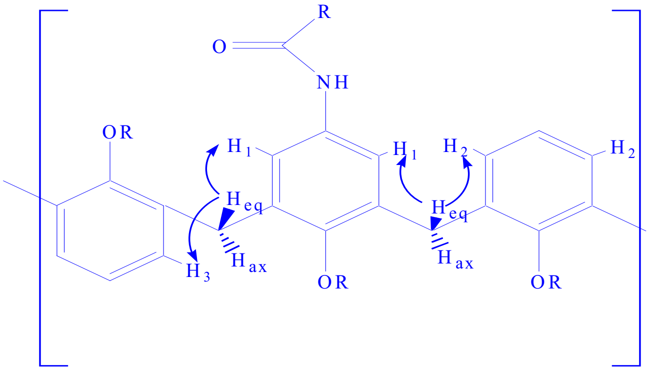

Chart 1 Correlation of proton at aromatic and methylene bridge of C and PC

Table 3 Show the distances between the H_{eq} at methylene bridge and aromatic protons.

Distance (Å)	**5a**	**5b**
H_{eq}-H_1	2.743	2.741
H_{eq}-H_2	2.348	2.421
H_{eq}-H_3	3.495	

The crystal structure of **5a** exhibited a CH_3····HC- interaction between hydrogen of methoxy groups and aromatic protons on the inversed phenyl ring with the distance around 3.425 Å which corresponds to the correlation in the NOSEY spectrum. Interestingly, the 2 oxygen atoms on amide groups point in the opposite direction when they have no interaction with guest molecules. When complexes with guests, 2 oxygen atoms on amide groups point into the same orientation. Consequently, the NH- groups were preorganized prior to bind with anion using hydrogen bonding interaction.[45] This evidence is supported by x-ray structure of bridge-cobaltocenium amide calix[4]arene.

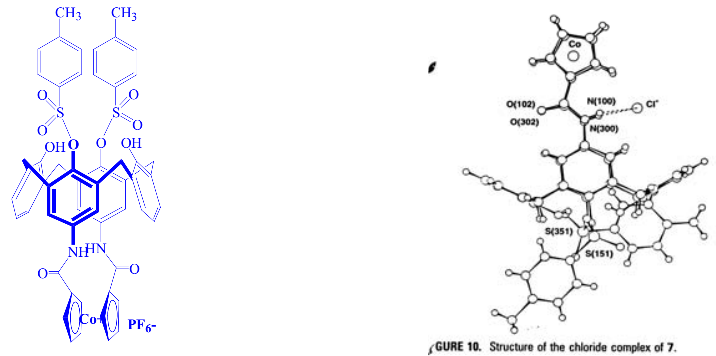

Bridge-cobaltoceniumamide calix[4]arene

FIGURE 10. Structure of the chloride complex of 7.

Figure 19 Show crystal structure of cobaltoceniumcalix[4]arene and Cl^-.

From the previous works, most ferrocene units is in the eclipsed geometry.[46-47] X-ray structures of **5a** and **5b** show the distorted eclipsed geometry of the ferrocene units possesing dihedral angles of 21.075°and 15°, respectively. For **5b**, two substituted phenyl rings is not parallel. The upper rim is tappered resualting from the ferrocene bridge. Therefore, two diethylester groups on the lower rim point away from each other resulting in the distances of O1-O1^i around 5.192 Å and O4-O4^i around 5.782 Å while diamide ferrocene on upper rim having the distances of N1-N1^i and C4-C4^i of 4.234 Å and 4.907 Å, respectively.

Table 4 Selected Bond Distances (Å) and Angles (deg) for **5a**

O1-C6	1.376(5)	N1-C11	1.428(5)	Fe1-C39	2.053(4)
O1-C7	1.448(5)	N1-C16	1.361(6)	C1-C34	1.523(6)
O2-C14	1.398(5)	N1-H1N	1.12(4)	C5-C8	1.507(8)
O2-C15	1.437(5)	N2-C28	1.429(5)	C8-C9	1.522(7)
O3-C16	1.225(5)	N2-C33	1.369(5)	C13-C17	1.505(7)
O4-C23	1.396(5)	N2-H2N	0.96(6)	C16-C35	1.490(6)
O4-C24	1.390(5)	Fe1-C35	2.043(4)	C33-C40	1.482(6)
O5-C31	1.385(4)	Fe1-C36	2.053(4)	C17-C18	1.511(7)
O5-C32	1.436(5)	Fe1-C37	2.061(4)	C22-C25	1.463(6)
O6-C33	1.234(5)	Fe1-C38	2.059(4)	C25-C26	1.513(6)
				C30-C34	1.526(5)
C6-C1-C34	120.2(4)	N1-C16-C35	115.6(3)	C27-C28-N2	124.2(3)
C2-C1-C34	122.0(4)	C13-C17-C18	110.5(3)	C29-C28-N2	115.6(3)
C5-C8-C9	112.6(4)	C13-C17-H17A	109.6	C31-C30-C34	121.3(3)
C5-C8-H8A	109.1	H17A-C17-H17B	108.1	O6-C33-N2	123.3(3)

H8A-C8-H8B	107.8	C23-C18-C17	121.6(4)	N2-C33-C40	115.3(3)
C14-C9-C8	123.0(4)	C19-C18-C17	120.7(4)	C30-C34-C1	110.6(3)
C10-C9-C8	117.9(4)	C23-C22-C25	120.8(4)	C30-C34-A34A	109.5
C10-C11-N2	123.6(4)	C21-C22-C25	122.5(4)	H34A-C34-H34B	108.1
C12-C11-N1	116.1(4)	C22-C25-C26	109.4(3)	C16-C35-Fe1	126.6(3)
C12-C13-C17	121.1(4)	C22-C25-H25A	109.8	C41-C40-C33	131.6(4)
C14-C13-C17	122.1(4)	H25A-C25-H25B	108.3	C44-C40-C33	121.8(4)
O3-C16-N1	124.2(4)	C31-C26-C25	119.6(3)	C16-N1-C11	127.4(4)
O3-C16-C35	120.1(4)	C27-C26-C25	120.6(3)	C16-N1-H1N	115(2)
C11-N1-H1N	116(2)	C40-Fe1-C44	41.49	C40-Fe1-C42	68.24(7)
C33-N2-C28	127.3(3)	C40-Fe1- C35	112.4(3)	C40-Fe1-C37	171.57(19)
C33-N2-H2N	124(3)	C40-Fe1-C36	134.35	C40-Fe1-C38	148.68(17)
C28-N2-H2N	108(3)	C40-Fe1-C39	118.12		

Table 5 Selected Bond Distances (Å) and Angles (deg) for **5c**

O1-C1	1.400(3)	O4-C23	1.195(4)	N1-C4	1.418(3)
O1-C22	1.414(3)	O5-C23	1.341(4)	N1-C16	1.350(4)
O2-C9	1.380(3)	O5-C24	1.436(5)	N1-H1	0.760(4)
O2-C13	1.428(4)	O6-C26	1.401(4)	Fe1-C17	2.046
O3-C16	1.235(4)	O6-H6	0.8400		
C3-C2-C7	118.0(2)	C8-C7-H7A	109.7	C18-C17-C16	129.6(3)
C1-C2-C7	122.4(2)	H7A-C7-H7B	108.2	C21-C17-Fe1	69.57(16)
C5-C4-N1	118.1(2)	O2-C9-C8	119.1(2)	C16-C17-Fe1	127.3(2)
C3-C4-N1	122.3(2)	C12-C15-C14^{i}	122.4	O1-C22-C23	108.8(2)
C1-C6-C14	122.3(2)	O3-C16-N1	123.3(3)	O4-C23-O5	124.5(3)
C5-C6-C14	118.9(2)	O3-C16-C17	120.6(3)	O4-C23-C22	126.6(3)
C8-C7-C2	109.7(2)	C21-C17-C16	122.3(3)	O5-C23-C22	108.9(3)

3.5 Binding properties of 5a, 5b and 5c towards anions and cations

3.5.1 Binding properties with anions for 5a, 5b and 5c

In the past decade, many artificial molecules were synthesized for binding anions. There are 2 types of anion receptors: charged receptors and neutral receptors. Charged receptors are –NH- group or ammonium[48-50], guanidinium and amidinium[51-52], as well as pyridinium.[53] Neutral receptors possess calixpyrroles[54-55], amide (-CONH-)[56-57] and thiourea (-NHCSNH-) or urea (-NHCONH-)[58-59] for binding anions. Our molecules consist of both anion and cation binding sites. Compounds **5a**, **5b** and **5c** containing CONH group as hydrogen bond donor were subjected to study their ability to bind various shapes and charges of anions such as spherical geometry (Cl^-, Br^- and I^-), planar or Y-shape (NO_3^-, CH_3COO^- and $C_6H_5COO^-$) and tetrahedral geometry ($H_2PO_4^-$, HSO_4^-). In addition, compounds **5b** and **5c** have the ethyl ester groups (for binding cation), attached on the lower rim of calix[4] arene. We would like to study the effect of cations to anion binding properties of **5b** and **5c**. The recognition of three ligands with tetrabutylammonium salts, Cl^-, Br^-, I^-, NO_3^-, HSO_4^-, $H_2PO_4^-$, acetate and benzoate, was measured by ^{1}H-NMR titrations. Firstly, binding studies of three ligands were carried out in $CDCl_3$. Interestingly, the ratio of cone to partial cone conformation of **5a** in $CDCl_3$ changes upon addition of Cl^- and $H_2PO_4^-$. From the integration of signals of Cp ring protons, we can estimate the ratios of cone and partial cone conformation as shown in **Table 6** The results implies that **5a** can recognize Cl^- and $H_2PO_4^-$ by changing its conformation. Due to the unconformity of the ratio of cone and partial cone conformation of **5a** during anion titration, vide infra, the stability constants of **5a** toward anions, however, cannot be estimated.

Table 6 Mole fraction (X) of cone (C) and partial cone (PC) conformation when increasing the ratio of anion to **5a**

Anion	X_c/X_{pc} with various **5a** : anions ratios		
	1:0	1:1	1:4
Cl^-	0.452/0.548	0.427/0.573	0.395/0.605
$H_2PO_4^-$	0.452/0.548	0.448/0.552	0.427/0.573

The association constants depend on the solvent system. The acceptor number (AN) of solvents should be realized in term of anion recognition. Solvents that have the high acceptor number (AN) will have the high affinity for anionic species. Consequently, the ability of receptors to complex anion decreased. The acceptor numbers of $CHCl_3$ and CD_3CN are 23.1 and 12.5, respectively.[60] The K values of complexes measured in $CDCl_3$ are very low. We, therefore, measure binding constants of compounds **5a**, **5b** and **5c** with anions in CD_3CN. The binding constants of **5a**, **5b** and **5c** were carried out by ^{1}H-NMR titration upon the addition of anion guest molecules at room temperature. The ^{1}H-NMR spectra were recorded until no peak shift appeared upon adding anions. The titration curves between **5a**, **5b** and **5c** with acetate are shown in **Figure 20**

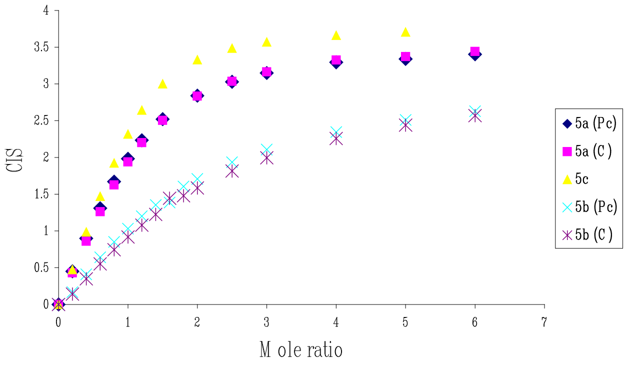

Figure 20 Titration curves between **5a**, **5b** and **5c** with acetate in CD_3CN

And the titration curves between **5a** with various anions are shown in **Figure 21**

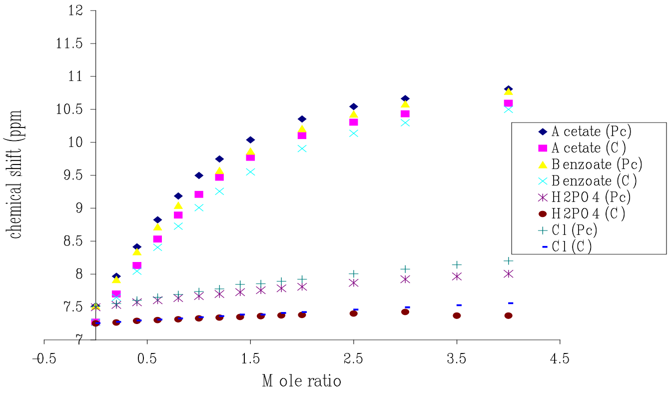

Figure 21 Titration curves between **5a** and various anions in CD_3CN

Curve **5c** exhibited larger chemical shift than other ligands. These behaviors implies a high stability constant. The titration curves display the 1:1 stoichiometry. Obviously, titration curves between compound **5a** and various anions show that in the large shifts occur for carboxylate anion but smaller shifts for $H_2PO_4^-$ and Cl^-. Compounds **5a**, **5b** and **5c** possessing the amide NH groups forming a bi-dentate hydrogen bonding array that are complementary to carboxylate anions and $H_2PO_4^-$. Therefore, halide anions give smaller K values. However, all ligands give a slight shift for $H_2PO_4^-$ comparing to carboxylate anion due to the low basicity of $H_2PO_4^-$.[61] The stability constants of compounds **5a**, **5b** and **5c** are summarized in **Table 7**.

Table 7 The stability constants of compound **5a**, **5b** and **5c** toward various anions at room temperature in CD_3CN-*d*^{3} (M^{-1})

Anions	**5a**		**5c**		**5b**
	PC	C	PC	C	C
$PhCOO^-$	540	472	139	100	915
CH_3COO^-	826	741	227	174	1200
$H_2PO_4^-$	34	a	91	94	a
Cl^-	32	a	49	86	29

PC = partial cone conformation ; C = cone conformation

a, K values could not refined.

All association constants have errors less than 10%.

As mentioned previously, compounds **5a** and **5b** exist in cone and partial cone conformation in solution at room temperature. Two different N*H* signals were observed at 8.09 and 7.86 ppm for **5a** and at 8.10 and 7.88 ppm for **5b** belonging to partial cone conformation and cone conformation, respectively. In CD_3CN, both cone and partial cone conformations ratios of **5a** and **5b** are constant. K values showed that all compounds in cone and partial cone conformations preferably formed with acetate anion. Unfortunately, all ligands have no interaction with Br$^-$, I$^-$, NO_3^- and HSO_4^- observing from no NH signal shifts upon addition of these anions possibly due to unmatched size or charge density of anions. In the case of HSO_4^-, it can preferentially bind with molecules containing a basic amine functionality because the acidic hydrogen sulfate ion is capable of protonation the amine groups and the positively charged receptor strongly binds the produced SO_4^-. [61] Futhermore, all ligands bind preferentially with acetate over benzoate due to the basicity order of acetate and benzoate.[62] Plots of chemical shift (*vide supra*) between **5a**, **5b** as well as **5c** and acetate signified the high K values. Anion binding constants of compounds **5a** and **5b** of partial cone conformation are superior to those of cone conformation. All ligands give the favorite to anions in a Y-shape geometry, espectially acetate and benzoate. The association constants with anions are in order of **5c** > **5a** > **5b**. All ligands selectively bind carboxylate over halide anions and $H_2PO_4^-$. The previous works of Beer and coworkers[63-64] studied the association constants of the molecules containing cobaltocenium at the upper rim of calix[4]arene. The anion-coordination properties of cobaltocenium bridge calix[4]arene receptors are dependent upon the degree of preorganization of the upper rim.

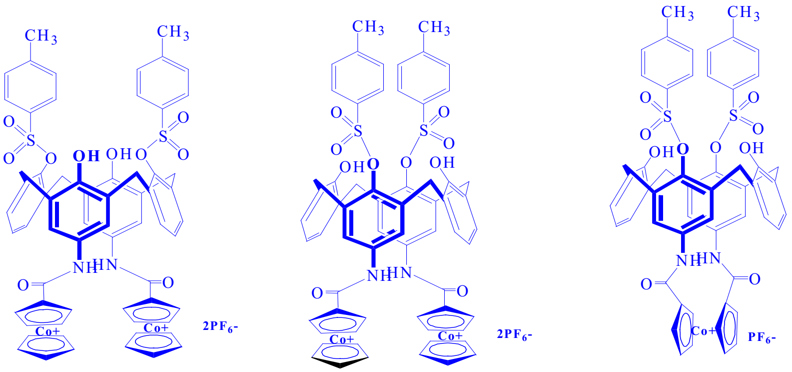

A **B** **C**

Figure 22 Calix[4]arenes contain cobaltocenium and tosyl groups

It was found that the position of tosyl substituent on lower rim of calix[4]arene has a dramatic influence on the anion coordination properties of upper rim. For instances, compound **A** binds with acetate much better than $H_2PO_4^-$, whereas the selective preference is reversed with an isomeric **B**. In the case of compound **C,** it formed thermodynamically stronger anions complexes with carboxylate than either compound **A** or **B**, and with a notable selectivity for acetate. The electron withdrawing tosyl-substituents at the *para* position on phenyl group bearing amide moieties induced the increasing in acidity of the NH protons and resulted in the higher affinity for acetate which is more basic than $H_2PO_4^-$. (pK_a of CH_3COOH = 1.7x10^{-7}, pK_a of H_3PO_4 = 7.1x10^{-3}).[65] It is the worthwhile to point out why the association constants of **5a**, **5b** and **5c** with carboxylate anions are much higher than other anions due to the substituent groups on lower rim. However, the predicted association constants with acetate should be in order of **5c**, **5b** and **5a**. Receptor **5b** and **5c** posses the electron withdrawing ethyl ester substituents at *para* position on phenyl units with amide groups. However, **5c** has more affinity for anions comparing to **5b** since **5c** is rigidified from four ethyl ester bulky groups to give a high degree of preorganization.[66] In contrast, **5a** has the electron donating methoxy group at the anisole rings bearing amide groups. This is the reason that it displays lower anion recognition than **5c** related the K values but higher binding ability than **5b**. Presumably, the effect of water in the deuterated solvent competed the binding with anions.[65] Water is competitive to bind with NH using hydrogen bonding interaction resulting in less K values of complexes between host and guest molecules even the traces of water in deuterated solvent. The higher intensity of water signals was observed in titration spectra of **5b** due to moisture. Predictable formation between amide calix[4]arene and acetate was related to the work's Beer.[10] The structure of bridge-cobaltocenium amide calix[4]rene are similar to our compounds and therefore, the complexes with carboxylate should have a similar structure. The proposed structure is shown in **Figure 23**.

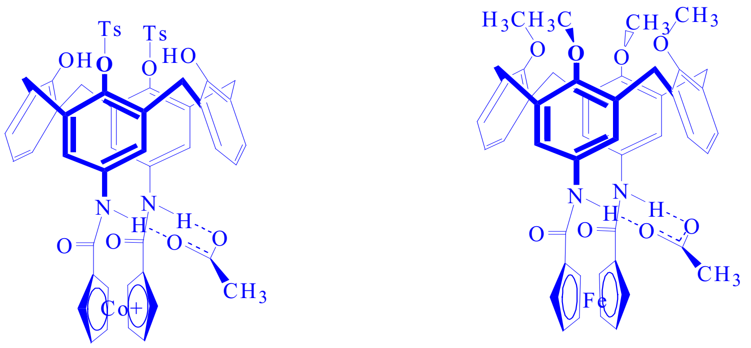

Bridg-cobalttocenium calix[4]arene

5a

Figure 23 The proposed structure of complex between bridge-ferrocene amide calix[4]arene and acetate

Additionally, aromatic signals in ^{1}H-NMR spectra of titration between **5a** with benzoate significantly shifted as shown in **Table 8**.

Table 8 Chemical shift of complex between **5a** and Benzoate

Ratio of Ligand:anions	0.0	1.0	1.5	2.0	Δδ
NH (PC)	7.515	9.321	9.865	10.207	2.692
NH (C)	7.267	9.008	9.552	9.905	2.638
m-Ar*H*OCH$_3$ (C) d, *J* = 7.8 Hz	7.254	7.121	7.083	7.059	-0.195
m-Ar*H*OCH$_3$ (PC) d, *J* = 7.2 Hz	7.141	7.093	7.073	7.059	-0.082
p-Ar*H*OCH$_3$ (C) t, *J* = 6.9 Hz	7.054	6.720	6.609	6.547	-0.507
p-Ar*H*OCH$_3$ (PC) t, *J* = 6.9 Hz	6.977	6.834	6.805	6.764	-0.213
o-Ar*H*NHCO (PC)	6.559	6.801	6.874	6.918	0.359
o-Ar*H*NHCO (C)	6.428	6.566	6.609	6.637	0.209
o-Cp*H*CONH (PC)	4.928, 4.836	5.229, 4.916	5.317, 4.935	5.379, 4.947	0.451, 0.111
o-Cp*H*CONH (C)	4.755	4.945	5.004	5.042	0.287

It is noteworthy that the complexes give the influence on aromatic rings of receptors. This behavior is possibly similar to the previous work. Cameron and Loeb[66] have synthesized calix[4]arene derivatives containing amide group with different number of electron withdrawing chloro-substituents at 1 and 3 position of upper rim. It was found that these receptors could bind strongly with benzoate. The formation is attributed to the calixarene adopting a ‘pinched cone’ conformation resulting in not only the two amide groups becoming parallel but also one phenyl ring of calix[4]arene is parallel to benzoate ring.

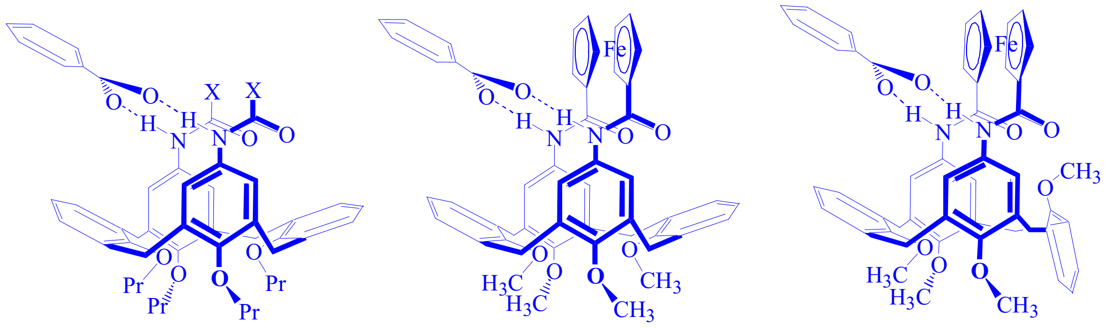

I $X = CH_2Cl$
II $X = CHCl_2$
III $X = CCl_3$

5a (C) and benzoate

5a (Pc) and benzoate

Figure 24 The proposed structure of complex with benzoate

This phenomenon is analogous to **5b** and **5c**. Elucidation by NMR spectra for PC signals indicates that aromatic protons of the non-inversed phenyl ring showed larger shifts over those of the inversed phenyl ring. The results are obtained by the ring current effect from benzoate. For the instances, protons of *p*-Ar*H*OCH$_3$ (PC) pointed into the ring current and shifted to more upfield. On the other hand, protons of *o*-Ar*H*NHCO- (PC) appeared more downfield because they are outside the ring current from the non-inversed phenyl ring of the building block. The downfield shift of the Cp*H* protons took place significantly by means of the effect of hydrogen bond interaction between NH--$^-$OOCC$_6$H$_5$. The proposed structure is shown in **Chart 2**.

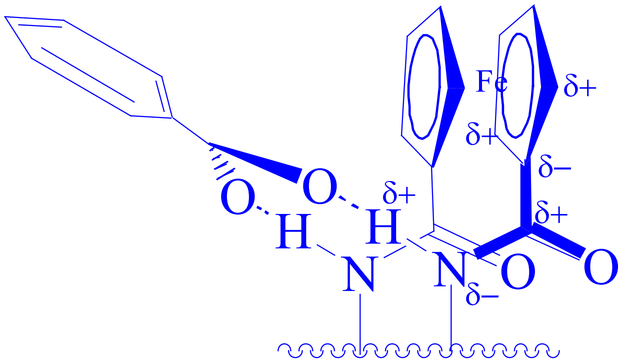

Chart 2 Show the effect of hydrogen bond interaction on Cp*H* signals

We took attempts to grow single crystals of these complexes but unfortunately, the complexes decomposed whilst they were left in solution over 3 days. Furthermore, the NOESY and ROESY of these complexes were carried but no more data supported the assumption according to no cross peak correlation observed clearly in the spectra.

3.5.2 Binding properties of cations with 5b and 5c

As mentioned above, the designed molecules consist of 2 binding sites, one for anion recognition from amide moieties and the other for cation recognition from ethyl ester groups. Compounds **5b** and **5c** contain the ethyl ester groups, which are able to bind alkaline metals.[67-69] The difference between both ligands is the number of ethyl ester groups. The points of study are to compare the affinity for cation and the effects of cation binding towards anion binding strength. Previously, the simultaneous complexation of cation and anion guest species by bifunctional receptors were studied and found that the presence of cation enhanced the anionic binding abilities in terms of ion-pair recognition.[70-76] Recently, many ditopic receptors employed the calix[4]arene as building block. These receptors were classified into two types: cation and anion binding sites are in the same side of calix[4]arene and both binding sites are in the opposite side of the building block. Basically, the anion binding constants were enhanced significantly from cation binding in the case of ditopic receptors which have cation binding and aion binding sites in the same side of the framework. Beer and co-workers[77] studied the simultaneous stability constant of cations and anions. Their compounds were shon in **Figure 25**. The simultaneous co-ordination of a cation and an anion is at the benzo crown amide substituted at the lower rim of calix[4]arene.

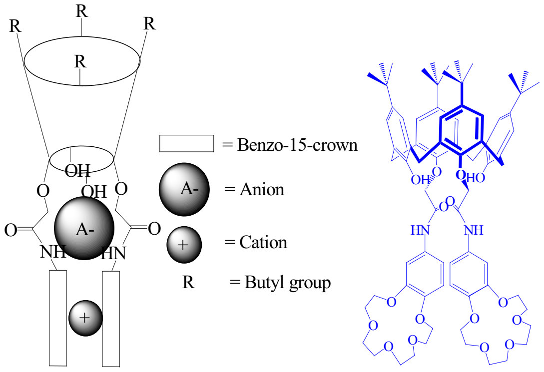

Figure 25 Show the ditopic receptor for both cationic and anionic species

They suggested that the K values of this ligand with K^+ ion and either $H_2PO_4^-$ or HSO_4^- are much higher compared to those of ligand without K^+. The electrostatic interaction of the ion-pair is directly attributable the complexation. Our receptors have the cation binding site at the lower rim and the anion binding site at the upper rim. The binding enhancement occurred from the effect of cation through phenyl bonds and ion-paired enhancement.

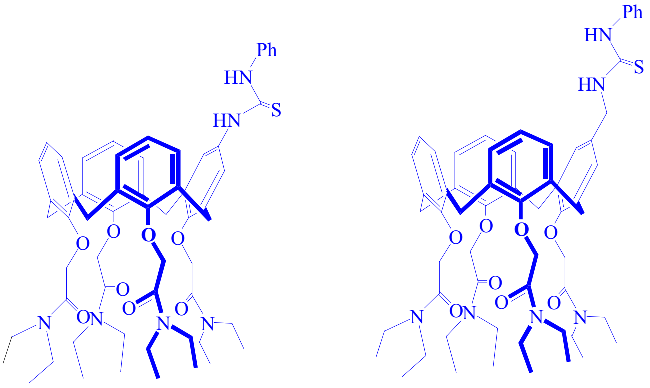

A **B**

Figure 26 Show the ditopic receptors having cation and anion binding sites not the same side

Ungaro and co-workers[4] designed ligands **A** and **B** in order to compare their binding enhancements due to the simultaneous binding with cations and anions. The anionic association constant indicated that receptor **A** with K^+ increased the K values. On the other hand, this behavior is reversed with receptor **B**. It was assumed that the urea group at the upper rim for receptor B obtained a little effect of the amide group at the lower rim due to a CH_2 spacer. Our receptors containing ethyl ester moieties were expected to bind with alkali metals and to give the influence on anion binding properties. The methodology of study the effect of cation complexation on anion binding is the preparation of the saturated cation binding site by adding one equivalent of alkali salts and then the association constants with anions were evaluated by adding variable amounts of tetrabutylammonium salts (TBA). The titration experiments were recorded by ^{1}H-NMR spectrometer. Unfortunately, no signals shift under complexes with alkali salts. Moreover, the results of ^{1}H-NMR spectra show no peaks shift during adding the amount of tetraammonium salt. Upon adding more anion salts, not only NH signal shifted gradually but also the precipitate was observed in on NMR tube. It suggested that **5c** have ability to bind weakly to alkali metals (Na^+ and K^+). The metal ion is labile and forms salt with added anion. Therefore, we cannot evaluate the stability constants for the complexes of ligand with metal and anion guests. We presumed that the upper rims were rigidified by ferrocene bridge which locks the position of the aryl rings and the ethyl ester groups at lower rims are too far apart to form comples with cation. (**Figure 27**)

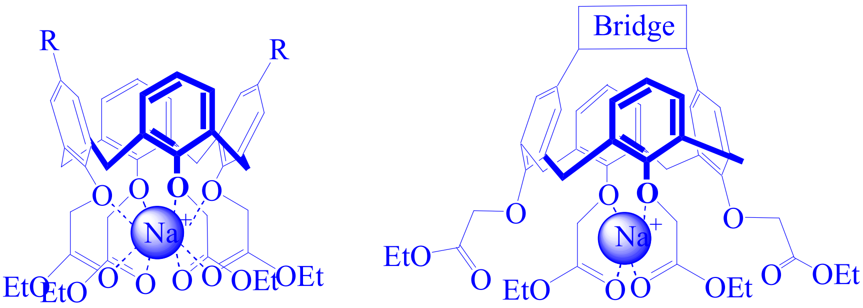

(a) (b)

Figure 27 Proposed Na^+ cation binding for calix[4]arene tetraethylester derivatived : (a) normal Na^+ binding (b) lower rim binding site disrupted by the upper rim bridge.

The distances between 2 ethyl ester groups on the substituted aryl rings were mentioned in x-ray part. The rest of ethyl ester groups on the unsubstituted aromatic rings are capable of binding with cation with weak interactions in the case of **5c** but not for **5b.** These are the reason of the precipitation of sodium or potassium states upon addition of anion. Similarly, Reinhoudt and co-workers[78] studied the bifunctional receptors containing the urea moieties at upper rim and tetraethyl ester at lower rim of calix[4]arene.

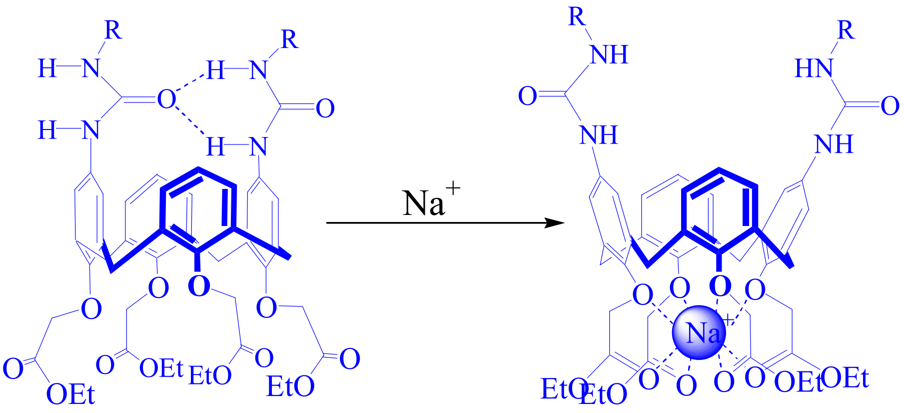

Figure 28 Complexation of Na^+ ions with ditopic receptor

This ligand cannot bind with anion in the absence of Na^+ since the intramolecular hydrogen bond interaction of urea moiety blocks anionic molecules. In the presence of Na^+ cation, four ethyl ester groups can adjust themselves to bind Na^+ ions and destroy the hydrogen bond interaction of the urea groups. Unrigidified molecule is able to bound with anions. Unlike **5c**, due to the ferrocene bridge, ethyl ester groups cannot be rearranged in a suitable orientation for binding cations. However, the weak binding of metal by the ligand can be determined by electrospray ionization mass spectrometry.

Mass Spectroscopy. ESI-MS $C_{56}H_{56}O_{14}N_2Fe$ = 1036.31 [M, 1036.91]

$C_{56}H_{56}O_{14}N_2FeNa$ = 1059.90 [M+Na]

$C_{56}H_{56}O_{14}N_2FeK$ = 1076.00 [M+K]

$C_{56}H_{56}O_{14}N_2FeRb$ = 1122.39 [M,+Rb]

$C_{56}H_{56}O_{14}N_2FeCs$ = 1169.81 [M+Cs]

The results of mass spectrometry displayed the major peak of **5c** with Na^+ but the rest of alkali metals showed only small peaks. It is assumed that **5c** binds selectively with Na^+ according to the hard-soft acid-base principle. The ethyl ester groups have oxygen donor atoms as hard bases which prefer to form complex with hard acids such as Na^+.[79]

1.5.3 Electrochemical studies

As mentioned above, three ligands, **5a**, **5b** and **5c** contain ferrocene units at the upper rim of the calix[4]arene building block. Naturally, ferrocene unit has ability to display the electrochemical signal. Therefore, the electrochemical properties of these ligands can be studied by techniques such as cyclic voltammetry and square wave voltammetry. The cyclic voltammetry and the square wave techniques were performed using solutions of **5a**, **5b** and **5c** (**1** x 10^{-3} M) in distilled anhydrous acetonitrile with 0.1 M Bu_4NPF_6 as supporting electrolyte and using a glassy carbon working electrode, a Ag/Ag^+ reference electrode and a Pt wire counter electrode. All solutions were purged with N_2 before measurements. The potential was scanned in the range of 0.15 to 0.55 V at 50 mV/s. The cyclic voltammograms of **5a**, **5b** and **5c** give reversibly redox couples as shown in the **Figure 29**. The values of the potential for the redox couples were shown in **Table 9**.

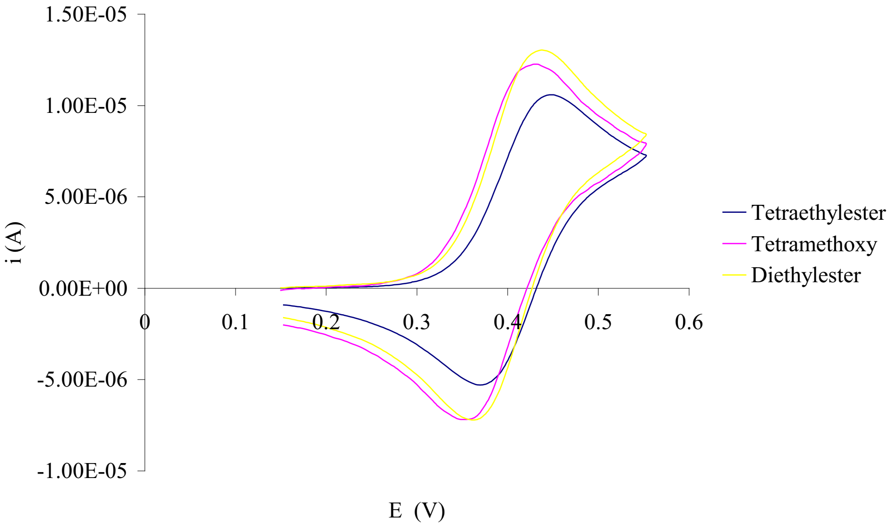

Figure 29 Cyclic voltammograms of **5a**, **5b** and **5c** in acetonitrile with 0.1 M TBAPF

Table 9 The characteristic values of **5a**, **5b** and **5c**

Ligands	E_{pa} (V)	E_{pc} (V)	$E_{1/2}$	ΔE (V)	I_{pa}/I_{pc}
5a	0.412	0.354	0.383	0.058	1.01
5b	0.428	0.370	0.399	0.058	1.02
5c	0.448	0.385	0.414	0.058	1.02

All CVs measurements of the free ligands were carried out by varied scan rates at 20, 50, 80, 100, 200, 500, 800 and 1000 mV/s. Cyclic voltammograms of **5a**, **5b** and **5c** at various scan rates in acetonitrile are depicted in **Figure 30**. The correlation between current (i) and square root of scan rates ($\nu^{1/2}$) was plotted and shown in **Figure 31**.

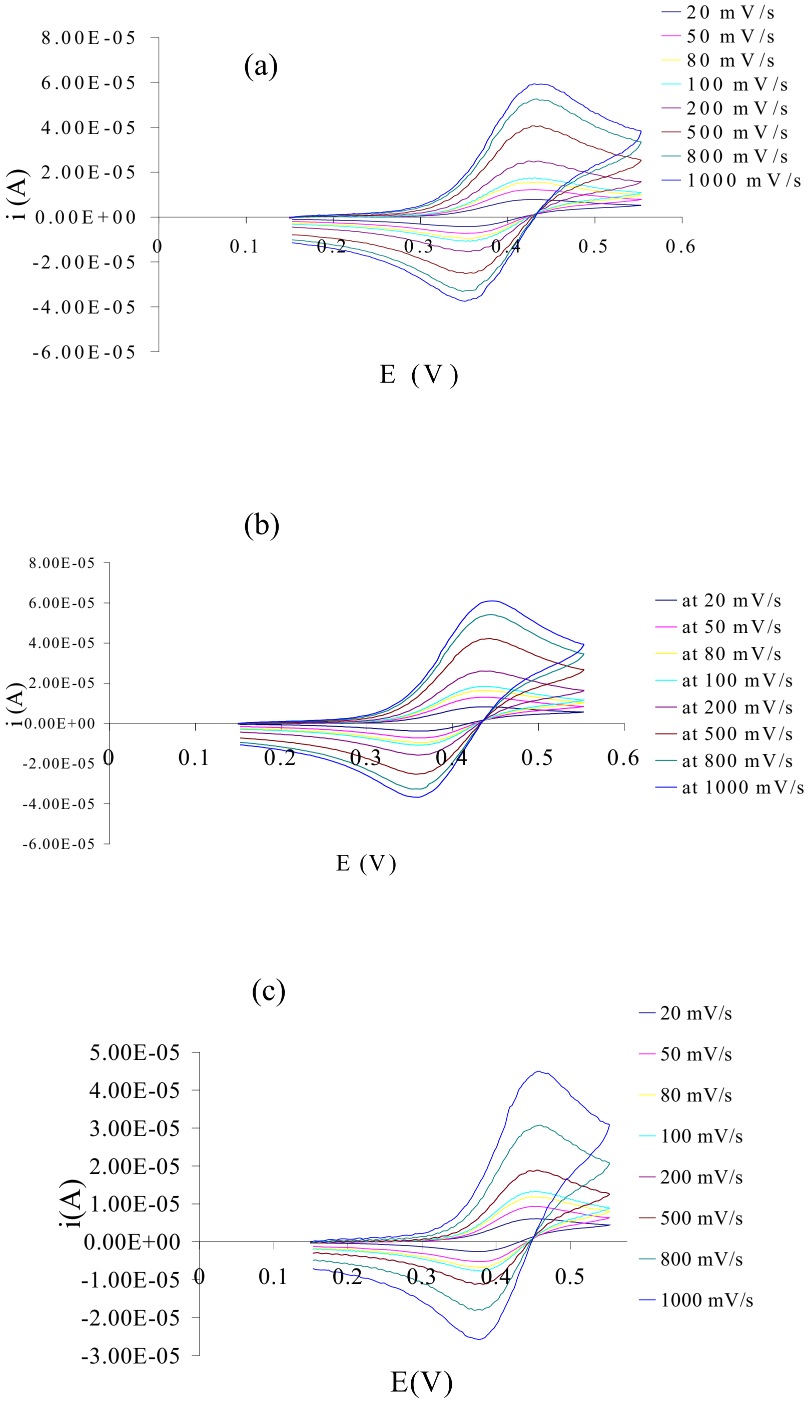

Figure 30 Cyclic voltammograms of **5a** (a) **5b** (b) and **5c** (c) in acetonitrile with 0.1 M TBAPF at different scan rates

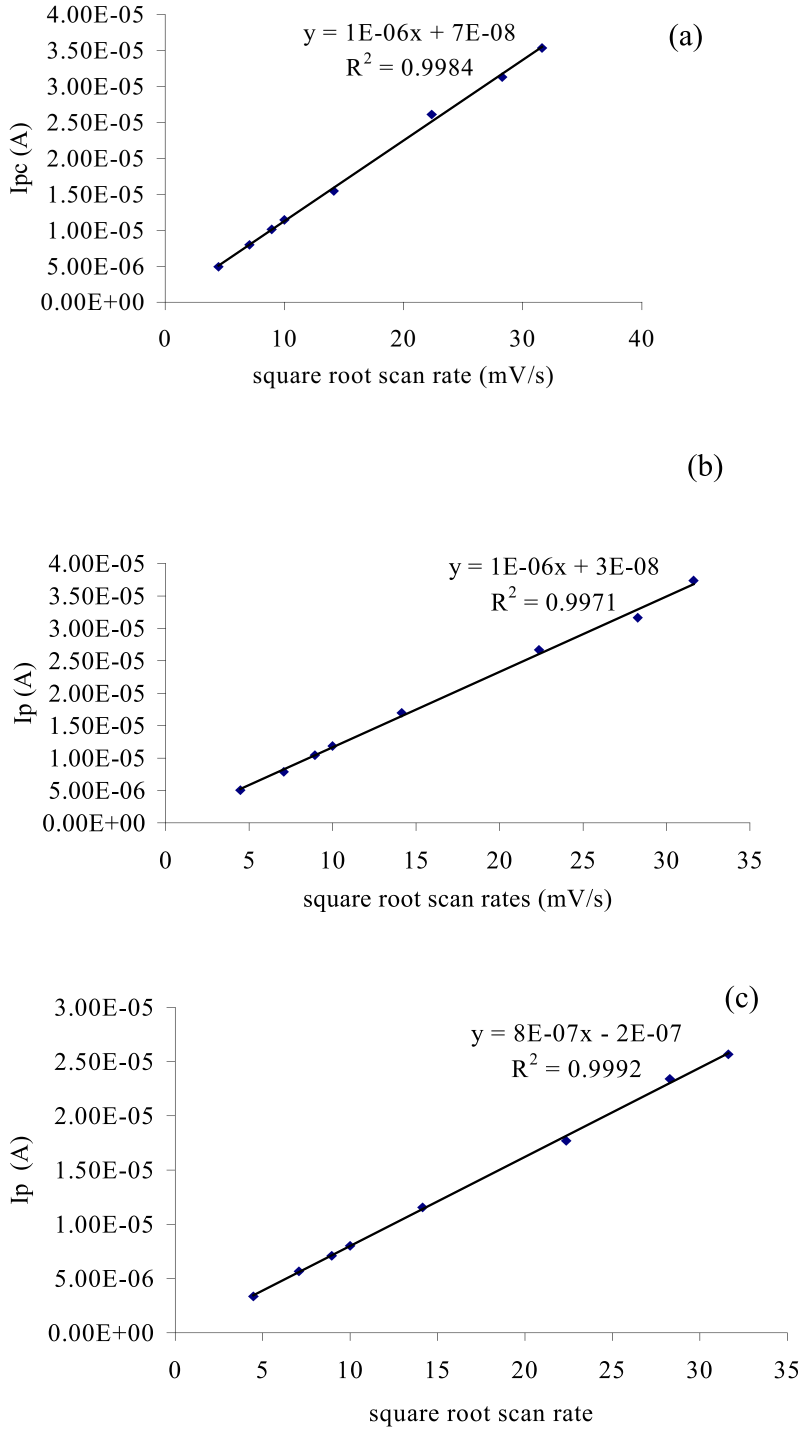

Figure 31 Plots of currents and square root of scan rates ($\nu^{1/2}$) for **5a** (a) **5b** (b) and **5c** (c)

All ligands have the anodic and cathodic intensities ratios close to the unity and the ΔE is equal to 58 mV corresponding to a one electron transfer process. The plot of i_p and $\nu^{1/2}$ is a straight line passing though the origin. This indicates that i_p is proportional to $\nu^{1/2}$, a characteristic of the reversible electron transfer. The redox couples of **5a**, **5b** and **5c** are conceptually reversible system of Fe^{II}/Fe^{III} redox centers. Additionally, the proportion of i_p and $\nu^{1/2}$ displays the diffusion system. Interestingly, in the case of potentials carried out in the range of 0.15 – 1.25 V, another irreversible peak appeared at the potential range of 0.85-1.22 V. It was the one-electron electrochemical oxidation of aryl ether units of calix[4] arene.[80-81] (**Figure 32**)

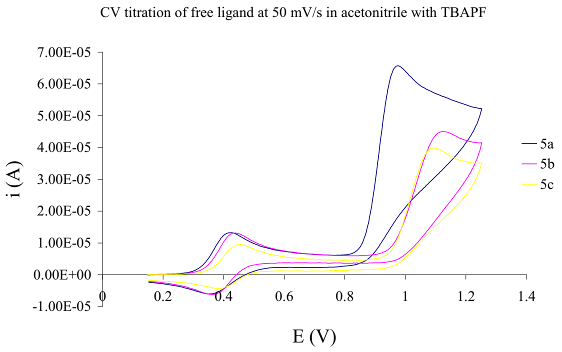

Figure 32 Cyclic voltammograms of **5a**, **5b** and **5c** at 50 mV/s in acetonitrile with 0.1 M TBAPF

The ethyl ester substituents on hydroxy oxygens are electron withdrawing groups and destabilize the positive charge of the oxidized oxygen atom as shown in **Figure 33** It is thus support the higher oxidation potential for **5b** and **5c** compared to **5a** bearing the methoxy groups.

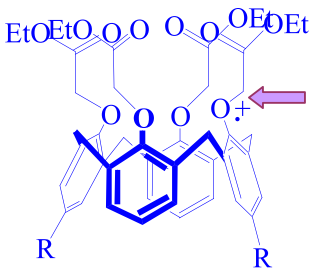

Figure 33 Show the oxidized oxygen atom of aryl ether unit

At various scan rates (shown in **Figure 34**), there was no oxidation peak appeared in the voltammograms. This implied that the characteristic of these electron transfer is an *EC* mechanism.[77] The deposition of the oxidized species may also occurred since not only the disappearance of reductive wave intensities but also the decrease of intensities of oxidation wave belonging to the ferrocenium unit. The species obtained from the oxidation of aryl ether unit were possibly adsorbed on the surface of the working electrode.

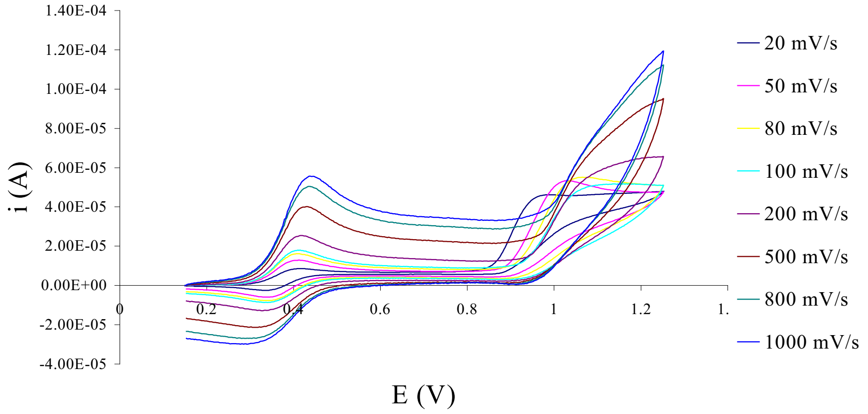

Figure 34 Cyclic voltammograms of **5a** at different scan rates

We focused our attention on the potential in the range of 0.15-0.55 V because we would like to study the effect of anion to the electron transfer process of the ferrocene unit. Titrations were carried out by addition of aliquots of tetrabutylammonium salts of benzoate, acetate, $H_2PO_4^-$ and Cl^- and followed by measurements at the scan rates of 50 mV/s. Addition of anion was varied from 0.2 to 4.0 equivalents. The feature of cyclic voltammograms of **5a** with benzoate was shown in **Figure 35 (a)**. Titrations of **5a**, **5b** and **5c** with caboxylate anion display the progressive appearance of a new wave at a less positive potential and a progressive disappearance of the initial wave. Titrations were also carried out in the square wave mode. It was found that not only the new wave gradually appears at less positive potential but also the initial wave decreases and disappears completely as shown in **Figure 35 (b)** and the K(+) and ΔE values shown in **Table 10**. The replacement of initial wave by the new one is complete after addition of excess anions (4.00 equivalents). Furthermore, the complexes of all ligands and anions show irreversible electrochemical systems. Presumably, the Fc^+ unit enhanced binding with anionic species using the electrostatic interactions.

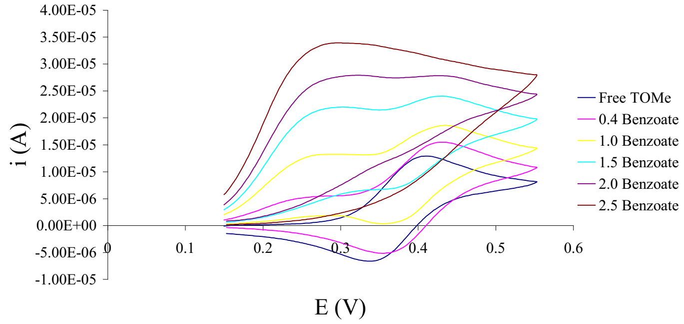

(a) Cyclic voltammograms titration with 0.1 M TBAPF in acetonitrile at 50 mV/s

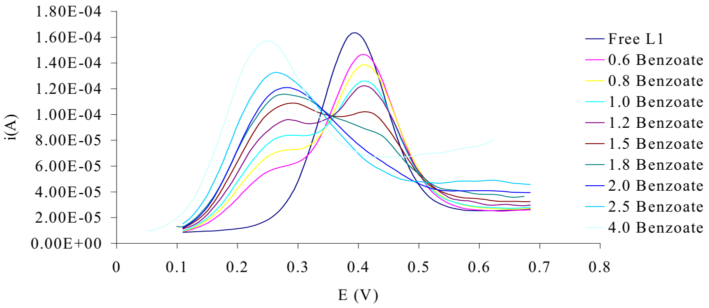

(b) Square wave titration at 50 mV/s and at frequency 60 Hz

Figure 35 Titration between **5a** and NBu_4PhCOO in acetonitrile with 0.1 M TBAPF

The ion-pairing associations are accompanied by adsorption phenomena according to the poor solubility of ion pair in solution. On the other hand, when an anion forms complex with amide ferrocenium unit, it probably blocks the electron released by the oxidation cycle. The result was observed by a loss of reversibility of Fc/Fc^+ redox wave. In contrast, cyclic voltammogram behaviors for Fc center of ligands and $H_2PO_4^-$ and Cl^- display small cathodic shift in Fc/Fc^+ redox potential (one wave behavior), indicating the weak interaction of $H_2PO_4^-$ and Cl^- with ligands (**Figure 36** and **37**)

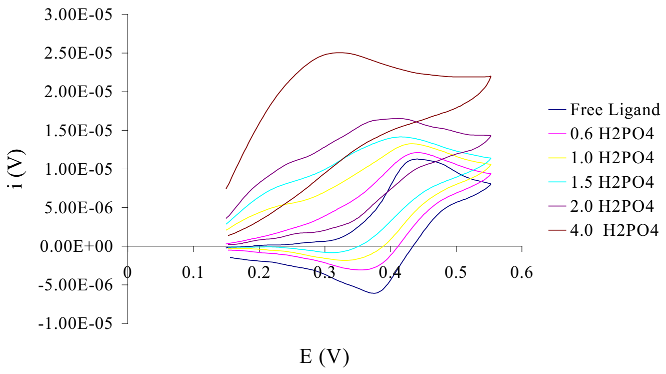

(a) Cyclic voltammogram titration at 50 mV/s.

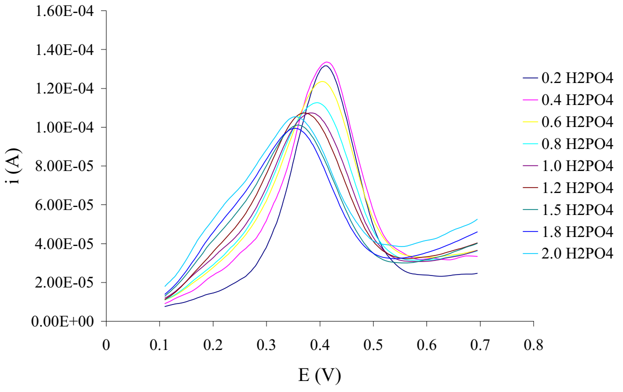

(b) Square wave titration at 50 mV/s and at 60 Hz.

Figure 36 Titration of **5b** and $NBu_4H_2PO_4$ in CH_3CN with 0.1 M TBAPF

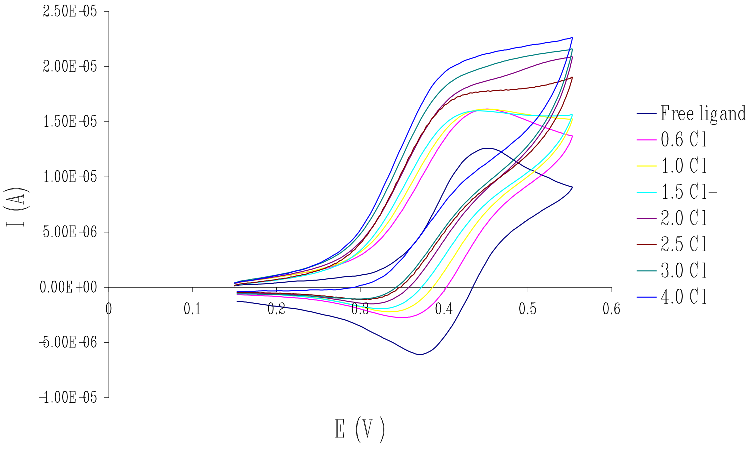

Figure 37 Titration of **5b** and NBu_4Cl in CH_3CN with 0.1 M TBAPF

Considerably, the cyclic voltammograms of complexes is conceptually similar to Astruc's works. In principle, Kaifer[81] studied the switching between binding states which can be classified broadly into two categories, *binary* and *incremental*. The binary case refers to the situation without the affinity between either cation or anion and the neutral ligand, but an interaction occurring under the redox-system. The incremental case refers to all situations observed by a finite binding between cation or anion and the neutral ligand and an interaction enhancement upon the redox ligand. The electrochemical properties of our works are classified into the incremental case because the incremental behavior is more suiltable for rapid interconversions of molecular structure due to kinetic availability of the bound species in both binding states exhibiting two waves upon addition of guest molecules. As the same rationalization, we can deduce the mechanism of electrochemical properties of complexes as shown in **Scheme 2**. [83-84]

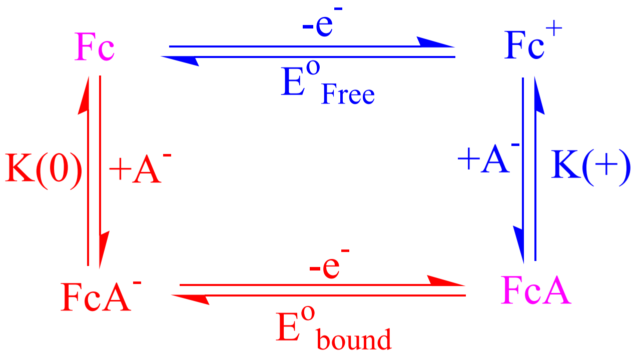

Scheme 2 The mechanism of electrochemical properties for complexes

The mechanism consists of four reactions in a square path, the total Gibbs free energy change (ΔG) in this cycle is thus zero. Importantly, the equilibrium is possibly approached via 2 routes, which cannot prove the exact machanism. The clock-wise route takes the pathway of oxidation of ferrocene unit to ferrocenium unit prior to bind with anionic species. Otherwise, the other route was described that the neutal ligands form complexes with anionic species and the Fe^{II} in complexes were oxidized to be Fe^{III} species. However, we assumed the equilibrium via a clock-wise route. The stability constant K of host/guest (1:1) complex is mathematically defined by equilibrium shown in **Scheme 2** where Fc and A$^-$ represent the ferrocene unit and anions, respectively.

The total Gibbs free change energy.;

$$\Sigma\Delta G = \Delta G_{free} + \Delta G_{(+)} + \Delta G_{bound} + \Delta G_{L} = 0 \qquad (1)$$

By considering ΔG in term of thermodynamic energy: $\Delta G = RT\ln K$ and in the case of thermodynamic potential in reaction expressed in $\Delta G = -nFE^{o}_{cell}$.

Thus, put ΔG parameter into the equation 1

$$-nF(E^{o}_{free}-E) - RT\ln K_{(+)} + nF(E^{o}_{bound}-E) + RT\ln K_{(L)} = 0 \qquad (2)$$

$$nF(E^{o}_{bound}-E^{o}_{free}) = RT\ln K_{(+)} - RT\ln K_{(L)} \qquad (3)$$

$$\frac{K_{(+)}}{K_{(L)}} = e^{[-nF(E^{\circ}bound-E^{\circ}free)/RT]}$$

$$K_{(+)} = K_{(L)}e^{[-nF(E^{\circ}bound-E^{\circ}free)/RT]} \qquad (4)$$

$K_{(+)}$ = association constant of anion with ferricinium

$K_{(L)}$ = association constant of anion with ferrocene

The ratio $K_{(+)}/K_{(L)}$ is a theoretically useful parameter because it allows not only the calculation of $K_{(+)}$ but also the evaluation of the effect of electron transfer on the complexation. In some cases, the relationship of $K_{(+)}/K_{(L)}$ is described in terms of the binding enhancement factor or BEF.[85] The stoichiometry of complexes is 1:1 between ligand and anion however, the binding enhancement factors were evaluated at 4.0 equivalents of anions which is the saturated point observed by no more potential shifted further. As the former refined equation, the enhancement association constants of all complexes were shown in **Table 10**.

Table 10 The association constants of ligands in ferricinium forms with anions

Anions	**5a**			**5b**			**5c**		
	ΔE (V)	**K(+)**	**BEF**	**ΔE** (V)	**K(+)**	**BEF**	**ΔE** (V)	**K(+)**	**BEF**
Acetate	0.08	18618	22.5	0.118	22470	99	0.130	189677	158
Benzoate	0.114	45755	84.7	0.136	27744	200	0.136	182631	200
$H_2PO_4^-$	a	-	-	0.084	2473	26.3	a	-	-
Cl^-	a	-	-	a	-		a	-	-

a; the uncertainties on ΔE values are estimated.

The stability constants measured by cyclic voltammetry give higher K values which are enhanced through the synergy between $X^{-}\cdots H$-N hydrogen bonding and electrostatic attraction in the oxidized forms. As mentioned above, the oxidized forms of ferrocene are in ferricinium form which prefers to bind anion species, especially for benzoate. The electrons on -COO^- of benzoate are stabilized by aromatic ring resulting in the stable higher negative charge and the electron crowd of aromatic ring also enhanced the electrostatic interaction with ferricinium. According to the cyclic voltammograms of the titration between **5b** and $H_2PO_4^-$ and Cl^-, the initial peak shifts slightly to the lower positive potential. The results of $H_2PO_4^-$ and Cl^- measured by cyclic voltammetry are pertinent to those by ^{1}H-NMR titrations. It can be concluded that all ligands are unfavorable to bind with these anions.

Moreover, the cation binding ability studied by cyclic voltammetry are carried out by titrations between **5c** and $NaClO_4$ in acetonitrile with 0.1 M TBAPF. The potentials were measured in the range of 0.15 V to 1.3 V. As mentioned previously, the oxidation wave at 1.1 V belongs to aryl ether of ethyl ester groups.[86-87] This potential range is of interest in order to study changes upon the addition of cations. Cyclic voltammograms of titration experiments were depicted in **Figure 38**.

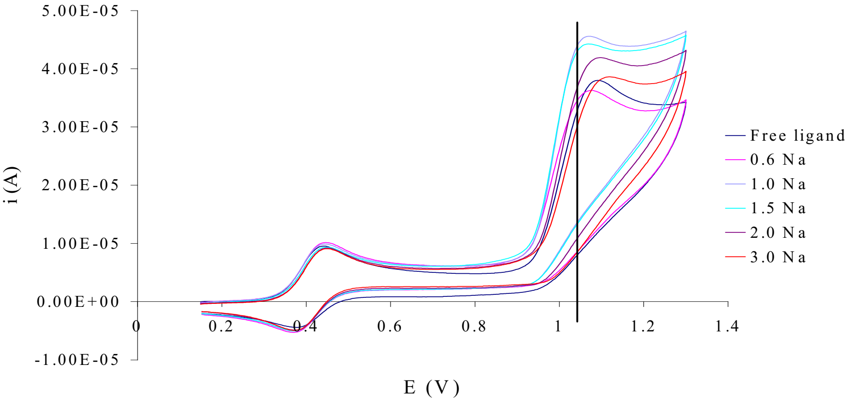

Figure 38 CV titrations of **5c** and $NaClO_4$ in acetonitrile using 0.1 M TBAPF as supporting electrolyte

The cyclic voltammograms can be separated into 2 sets depending upon the amount of added Na^+. In the first set, the cyclic voltammograms upon addition of $NaClO_4$ from 0 to 1.5 equivalents showed a slight shift of the oxidation wave to less oxidative potential. In the second set, the addition of Na^+ in the amount of 2.0 and 3.0 equivalents resulted in potential shift to higher oxidative potentials. However, we focused on the cyclic voltammogram of the free ligand with addition of excess cation (3.0 equivalent) in which the oxidative wave at 1.093 V shifted to the higher oxidative potential. (**Figure 39)** Additionally, the backward current belonging to ferrocene unit, increased significantly and caused the reduction of the i_{pa}/i_{pc} ratio as shown in **Table 11**.

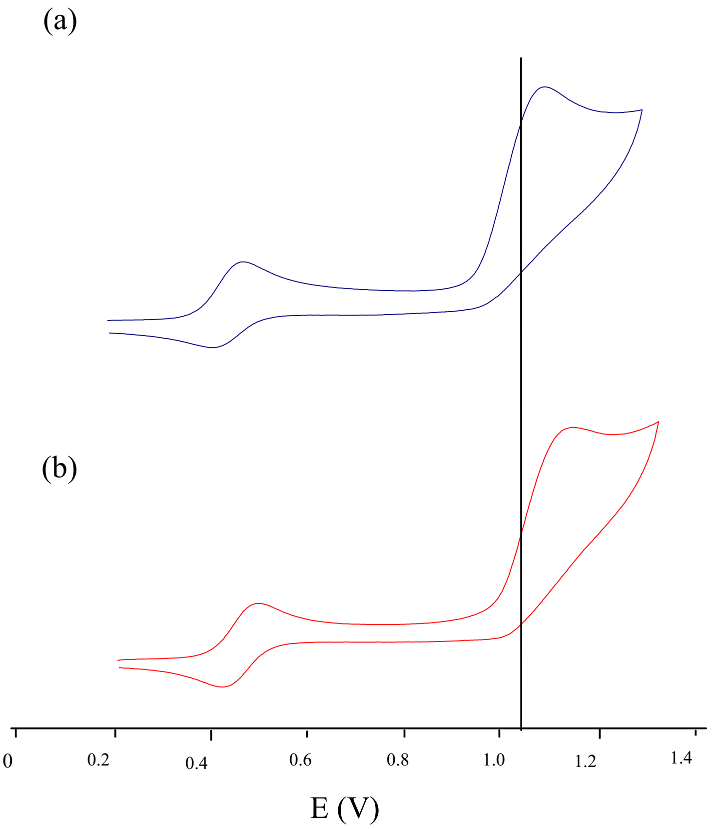

Figure 39 Cyclic votammograms of **5c** (a) and complex of **5c** with Na^+ (b) in acetonitril with 0.1 M TBAPF

Table 11 The i_{pa}/i_{pc} ratios of ferrocene couple upon the addition of $NaClO_4$

ligand: Na	i_{pa}/i_{pc}
1.0:0	2.005
1.0:0.6	1.445
1.0:1.0	1.372
1.0:1.5	1.319
1.0:2.0	1.267
1.0:3.0	1.159

According to the movement of the oxidation wave at 1.1 V to higher potential upon adding excess $NaClO_4$, it may imply that the aryl ether units of **5c** in the presence of $NaClO_4$ are oxidized harder than those of **5c** in the absence of $NaClO_4$ since the cation binding at ethyl ester groups destabilize the aryl ether units in their oxidized forms. Additionally, the decrease of oxidatized species reduced the deposition on the surface of the electrode and resulted in the increase of the backward currents belonging to the ferricinium unit. From the results of cation titration by cyclic voltammetry, it supported the results from electrospary ionization mass spectroscopy that **5c** has ability to bind cation, even weak interactions. Unfortunately, the effects of cation towards anion recognition cannot be carried out by cyclic voltammetry because no changes upon addition anions in the presence of $NaClO_4$ took place obviously and the precipitate occurred during the addition of anions. We assumed that Na^+ bounded with ethyl ester group was removed and formed the precipitates.

4. Conclusion

5,7-Diamideferrocenyl-25,26,27,28-tetramethoxycalix[4]arene (**5a**), 5,7-diamide ferrocenyl-25,26,27,28-dimethoxy dimethyl ethylestercalix[4]arene (**5b**) and 5,7-diamide ferrocenyl-25,26,27,28-tetramethyl ethylestercalix[4]arene (**5c**) have been synthesized by coupling reactions between 1,1-di(chlorocabonyl)ferrocene and tetramethoxy-diaminocalix [4]arene (**4a**), dimethoxy dimethylethylester-diaminocalix[4]arene (**4b**) and tetramethyl ethylester-diaminocalix[4]arene (**4c**), respectively. Characterizations by NMR and X-ray structures show that **5a** and **5b** are in the mixture of cone and partial cone conformation in solutions while **5c** is in cone conformation only. In the case of solid state structures, **5a** is in partial cone conformation while **5b** is in cone conformation. The stability constants measured by ^{1}H-NMR titration in CD_3CN show the **5a**, **5b** and **5c** bind acetate selectively and display the anion binding affinity in order of **5c** > **5a** > **5b**. Electrochemical studies of the three ligands carried out by cyclic voltammetry exhibit the binding enhancement for benzoate over acetate, $H_2PO_4^-$ and Cl^-. Binding abilities of **5c** towards cations have been investigated by electrospray ionization mass spectrometry. The results support the binding abilities of **5c** with cations such as Na^+, K^+, Rb^+ and Cs^+. However, binding constants are probably low, therefore, they cannot be calculated by ^{1}H-NMR titrations. Interestingly, cyclic voltammetry can show the difference of voltammograms between the free ligand and its cation complex. This technique supports that **5c** can form a complex with Na^+ with weak interactions.

5. References

1. I. Alfonso, F. Rebolledo, V. Gotor, *Chem. Eur. J.* **2000**, *6*. 3331.
2. M. Rothmaier, W. Simon, *Anal. Chim. Acta.* **1993**, *271*, 135.
3. P. D. Beer, *Acc. Chem. Res*. **1998**, *31*, 71.
4. N. Pelizzi, A. Casnati, A. Friggeri, R. Ungaro, *J. Chem. Soc., Perkin Trans. 2* **1998**, 1307.
5. J. B. Cooper, M. G. B. Drew, P. D. Beer, *J. Chem. Soc., Dalton Trans.* **2001**, 392.
6. L. A. J. Chrisstoffels, F. de Jong, D. N. Reinhoudt, S. Sivelli, L. Gazzola, A. Casnati, R. Ungaro, *J. Am. Chem. Soc.,***1999**, *121*, 10142.
7. J-C. Moutet, E. Saint-Aman, M. Ungureanu, T. Visan, *J. Electroanal. Chem*. **1996**, *410*, 79.
8. C. M. Casado, I. Cuadrado, B. Alonso, M. Moran, J. Losada, *J. Electroanal.Chem.* **1999**, *463*, 87.
9. I. del Peso, B. Alonso, F. Lobete, C. M. Casado, I. Cuadrado, J. L. del Barrio, *Inorg. Chem. Commun*., **2002**, *5*, 288.
10. P. D. Beer, M. G. B. Drew, D. Hesek, K. C. Nam, *Organomettallics* **1999**, *18*, 3933.
11. P. D. Beer, S. W. Dent, *Chem. Commun*. **1998**, 825.
12. Z. Otwinowski & W. Minor, *Methods in Enzymology* (**1997**), Vol *276* : *Macromolecular Crystrallography*, part A, pp. 307-326,C. W. Carter. Jr. & R. M. Sweet, Eds., Academic Press.
13. R. H. Blessing, *Acta Cryst.* **1995**, *A51* , 33.
14. R. H. Blessing, *J. Appl. Cryst*., **1997**, 30421.
15. G. M. Sheldrick, *Acta Cryst*., **1990**, *A46*, 467.
16. C. D. Gutsche and M. Iqbal, *Org. Synth.* **1989**, *68*, 234.
17. V. J-D. Loon, A. Arduini, L. Coppi, W. Verboom, A. Pochini, R. Ungaro, S. Harkema, D. Reinhoudt, *J. Org. Chem.* **1990**, *55*, 5539.
18. I. Ando, H. Miyake, Y. Ohki, K. Ujimoto, H. Kurihara, *Bull. Chem. Soc. Jpn*. **2000**, *73*, 2753.
19. A. Chesney, M. R. Bryce, A. S. Batsanov, J. A. K. Howard, L. M. Goldenberg, *Chem. Commun*. **1998**, 677.

20. H. Plenio, d. Burth, *Organometallics*, **1996**, *15*, 1151.

21. P. R. A. Webber, G. Z. Chen, M. G. B. Drew, P. D. Beer, *Angew., Chem. Int. Ed.*, **2001**, *40*, 2265.

22. K. Ogasawara, T. Ishiguro, S. Horiuchi, H. Yamochi, Y. Nogami, *J. Phys. Chem. Solids* **1997**, *58*, 39.

23. W. Ong, A. E. Kaifer, *J. Am. Chem. Soc.* **2002**, *124*, 9358.

24. P. L. H. M. Cobben, R. J. M. Egberink, J. G. Bomer, P. Bergreld, W. Verboom, D. N. Reinhoudt, *J. Am. Chem. Soc.* 1992, 114, 10573.

25. O. Struck, J. P. M. van Duynhoren, W. Verbiim, D. N. Reinhoudt, H. Sybolt, J. G. van Hummel, *J. Org. Chem.* **1997**, *62*, 2487.

26. D. Gutsche and S.K. Sharma, *J. Org. Chem*., **1999**, *64*, 998-1003.

27. F. W. Knobloeh, W. H. Rausher, *J. Polym. Sci.* **1961**, *54*, 651.

28. H. J. Lorkowski, R. Pannier, A. Wende, *J. Prakt. Chem.* **1967**, *35*, 149.

29 H. Otsuka, S. Shinkai, *Supramolecular science* **1996**, *3*, 189.

30. J-D. V. Loon, L. C. Groenen, S. S. Wijmenga, W. Verboom and D. N. Reinhoudt, *J. Am. Chem. Soc.* **1991**, *113*, 2378.

31. C. Jaime, J. de Mendoza, P. Prados, P. M. Nieto, C. Sanchez, *J. Org. Chem.* **1991**, *56*, 3372.

32. S. Shinkai, K. Iwamoto, K. Araki, T. Matsuda, *Chem. Lett.* **1990**, 1263.

33. S. T. Cantrill, G. J. Youn, J. F. Stddart, D. J. Williams, *J. Org. Chem.* **2001**, *66*, 6857.

34. D. M. Pawar, K. L. Davis, B. L. Brown, S. V. Smith and E. A. Noe, *J. Org. Chem.* **1999**, *64*, 4580.

35. C. Jaime, J. de Mendoza, P. Prados, P. M. Nieto, C. Sanchez, *J. Org. Chem.* **1991**, *56*, 3372.

36. C. D. Gutsche, B. Dhawan, J. A. Levine, K. H. No, L. J. Bauer, *Tetrahedron*, **1983**, *39*, 409.

37. S. E. Biali, V. Bohmer, S. Cohen, G. Ferguson, C. GrÜttner, F. Grynszpan, E. F. Paulus, I. Thondorf, W. Vogt, *J. Am. Chem. Soc*. **1996**, *118*, 12938.

38. L. C. Groenen, J-D, van Loon, W. Verboom, S, Harkema, A. Casnati, R. Ungaro, A. Pochini, F. Ugozzoli and D. N. Reinhoudt, *J. Am. Chem. Soc.* **1991**, *113*, 2385.

39. P. D. J. Grootenhuis, P. A. Kollman, L. C. Groenen, D. N. Reinhoudt, G. J. van Hummel, F. Ugozzoli and G. D. Andreetti, *J. Am. Chem. Soc.* **1990**, *112*, 4165.
40. K. Iwamoto, K. Araki and S. Shinkai, *J. Org. Chem.* **1991**, *56*, 4955.
41. A. Yamada, T. Murase, K. Kikukawa, T. Mutsuda, S. Shinkai, *Chem. Lett.* **1990**, 455.
42. A. Yamada, T. Murase, K. Kikukawa, T. Arimura, S. Shinkai*, J. Chem. Soc. Perkin Trans. 2* **1991**, 793.
43. T. Harada, J. M. Rudzinski, E. Osawa, S. Shinkai, *Tetrahedron Lett.* **1993**, *49*, 5941.
44. J. Scheerder, R. H. Vreekamp, J. F. J. Engbersen, W. Verboom, J. P. M. van Duynhoven, D. N. Reinhoudt, *J. Org. Chem.*, **1996**, *61*, 3476.
45. P. D. Beer, *Acc. Chem. Res.* **1998**, *31*, 71.
46. J. M. Lloris, R. Martinez-Máñez,M. E. Padilla-Tosta, T. Pardo, J. Soto, P. D. Beer, J. Caddman and D. K. Smith, *J. Chem. Soc., Dalton Trans.* **1999**, 2359.
47. M. Scherer, J. L. Sessler, A. Gebauer and V. Lynch, *Chem. Commun.* **1998**, 85.
48. L. Fabbrizzi, P. Pallavicini, L. Parodi and A. Taglietti, *Inorganica. Chimica Acta*, **1995**, *238*. 5.
49. L. Fabbrizzi, A. Leone and A. Taglietti, *Ang. Chem. Int. Ed.* **2001**, *40*, 3066.
50. L. Fabbrizzi, I. Faravelli, G. Francese, M. Licchelli, A. Perotti and A. Taglietti, *Chem. Commun*., **1998**, 971.
51. A. Metzger, E. V. Anslyn, *Angew. Chem. Int. Ed. Engl.* **1998**, *37*, 649.
52. M. Segura, V. Alcazar, P. Prados, J. de Mendoza, *Tetrahedron*, **1997**, *53*, 13119.
53. K.-S. Jeong, Y. L. Cho, *Tetrahedrom Lett*. **1997**, *38*, 3279.
54. P. A. Gale, J. L. Sessler and V. Kral, *Chem. Commun*., **1998**, 1.
55. B. Turner, M. Botoshansky, and Y. Eichen, *Angew. Chem. Int. Ed. Engl.* **1998**, *35*, 2782.
56. A. P. Bisson, V. M. Lynch, M. K. C. Monahan, E. V. Anslyn*, Angew. Chem. Int. Ed. Engl.* **1997**, *36*, 2340.
57. A. Szumna and J. Jurczak, *Eur. J. Org. Chem.* **2001**, 4031.
58. D. H. Lee, K. H. lee and J-I. Hong, *Org, Lett.* **2001**, *3*, 5.
59. V. Stastny, P. Lhotak, V. Michlova, I. Stibor and J. Sykora, *Tetrahedron* **2002**, *58*, 7207.

60. C. Reichardt, “*Solvents and Solvent Effects in Organic Chemistry*” 2nd, rev. and enl. Ed., Weinheim ; Basel (Schweiz) ; Cambridge ; New York, NY : VCH, **1988**, 20-24.

61. K. Izutsu, *Acid-Base Dissocation Constants in Dipolar Aprotic Solvents*, Blackwell Scientific Publications, Oxford, **1990**.

62. P. D. Beer, A. R. Graydon, A. O. M. Johnson, D. K. Smith, *Inorg. Chem.* **1997**, *36*, 2112.

63. P. D. Beer, M. G. B. Draw, D. Hesek, M. Shade, F. Szemes, *Chem. Commun.* **1996**, 2161.

64. P. D. Beer, M. G. B. Draw, D. Hesek, K. C. Nam, *Chem. Commun.* **1997**,107.

65. J. C. Jr. Adrian and C. S. Wilcox, *J. Am. Chem Soc.* **1991**, *113*, 678.

66. P. Bülmnn, S. Nishizawa, K. P. Xiao, Y. Umezawa, *Tetrahedron* **1997**, *53*, 1647.

67. B. R. Cameron, S. J. Loeb, *Chem. Commun.* **1997**, 573.

68. K. Iwamoto, S. Shinkai. *J. Org. Chem*. **1992**, *57*, 7066.

69. F. Arnaud-Neu, E. M. Collins, M. Deasy, G. Ferguson, S. J. Harris, B. Kaitner, A. J. Lough, M. A. McKervey, E. Marques, B. L. Ruhl, M. J. Schwing-Weill, E. M. Seward, *J. Am, Chem, Soc.*, **1989**, *111*, 8681.

70. Y. Israëli, C. Detellier, *J. Phys. Chem. B*, **1997**, *101*, 1897

71. A. Echvarren, A. Galan, J. de Mendoza, A. Salmeron, J.-M. Lehn, *J. Am. Chem. Soc*. **1989**, *111*, 4994.

72. D. M. Rudkevich, Z. Brzozka, M. Pllys, H. C. Viser, W. Verboom, D. N. Reinhoudt, *Angew. Chem*. **1994**, *106*, 480.

73. D. M. Rudkevich, Z. Brzozka, M. Pllys, H. C. Viser, W. Verboom, D. N. Reinhoudt *Angew. Chem. Int. Ed. Engl*. **1994**, *33*, 467.

74. P. D. Beer, P. K. Hopkins, J. D. McKinney, *Chem. Commun*. **1999**, 1273.

75. D. J. White, N. Laing, H. Miller, S. Parsons, S. Coles, P. A. Tasker, *Chem. Commun*. **1999**, 2077.

76. P. D. Beer, M. G. B. Drew, R. J. Knubley, M. I. Ogden, *J. Chem. Soc. Dalton Trans*. **1995**, 3117.

77. P. Monk ‘*Fundamentals of Electroanalytical Chemistry*” JOHN WILEY & SONS LTD, **2001**, pages 169-173.

78. J. Scheerder, J. P. M. van Duynhoven, J. F. J. Engbersen, D. N. Reinhoudt, *Angew. Chem. Int. Ed. Engl.* **1996**, *35*, 1090.

79. G. L. Miessler, D.A. Tarr, “Inorganic Chemistry”; Prentice-Vall, Inc., A DIVision of Simon&chuster EnglewoodCliffs, New Jersey, 1991, 197-202 pp.

80. A. Pailleret, D. W. H. Arrign, Electrochem. Commun., **2001**, *3*, 24-27.

81. A. Pailleret, D. W. H. Arrign, J. K. Browne, M. Anthony, *J. Mater. Chem*., **2002**, *12*, 2665.

82. S. R. Miller, D. A. Gustowski, Z-H. Chen, G. W. Gokel, L. Echegoyen, A. E. Kaifer, *Anal. Chem.* **1988**, *60*, 2021.

83. C. Valerio, J-L. Fillllaut, J. Ruiw, J. Guittard, D. Astruc, *J. Am. Chem. Soc.* **1997**, *119*, 2588.

84. P. D. Beer, P.A. Gale, G. Z. Chen, *J. Chem. Soc., Dalton Trans.* **1999**, 1897.

85. J. C Medina, T. T. Goodnow, M. T. Rojas, J. L. Atwood, B.C. Lynn, A. E. Kaifer, G. W. Gokel*, J. Am. Chem. Soc.* **1992**, *114*, 10583.

86. A. Pailleret, D. W. H. Arrign, *Electrochem. Commun.* **2001**, *3*, 24.

87. L. J. Li, X. P. Ni, K. Leong, *Angew. Chem. Int. Ed., Engl*, **2003**, *42*, 69.

Output

1. Publications

There are 4 publications obtained from this project.

1. Tomapatanaget, B.; Tuntulani, T. “Lower Rim Tetra-Substituted and Upper Rim Ferrocene Amide Calix[4]Arenes: Synthesis, Conformation and Anion Binding Properties” *Tetrahedron Lett*. **2001**, *42*, 8105.
2. Tongraung, P; Chantarasiri, N.; Tuntulani, T. “Calix[4]arenes Containing Urea and Crown/Urea Moieties: Effects of the Crown Ether Unit and Na^+ towards Anion Binding Ability” *Tetrahedron Lett*. **2003**, *44*, 29-32.
3. Tantrakarn, K.; Ratanatawanate, C.; Pinsuk, T.; Chailapakul, O.; Tuntulani, T. “Synthesis of Redox-Active Biscalix[4]quinones and Their Electrochemical Properties” *Tetrahedron Lett*. **2003**, *44*, 33-36.
4. Tomapatanaget, B.; Tuntulani, T.; Chailapakul, O. “Calix[4]arenes Containing Ferrocene Amide as Carboxylate Anion Receptors and Sensors” *Org. Lett*. **2003**, *5*, 1539-1542.

2. Production of new researchers

1. Miss Boosayarat Tomapatanaget, Ph.D.
2. Mr. Pan Tongraung, Ph.D.
3. Mr. Kriengkamol Tantrakarn, M.Sc.
4. Mr. Nattavut Kerdpaiboon, M.Sc.

3. Conferences

1. “Synthesis of Diethoxy Bis-Calix[4]quinone for Alkali Metal Ion Sensors” 26th International Symposium on Macrocyclic Chemistry, Fukuoka, Japan, 15-20 July, 2001.
2. “Calix[4]arene Containing Ferrocene as Anion Sensor” 26th International Symposium on Macrocyclic Chemistry, Fukuoka, Japan, 15-20 July, 2001.
3. “Synthesis of Calix Crown Urea for Anion Recognition” International Conference & Exhibition on Pure and Applied Chemistry 2002, Bangkok, 29-31 May 2002.
4. “Synthesis, Conformation Studies and Anion Sensing Properties of Ferrocene Amide Calix[4]arene” 3rd Tateshina Conference on Organic Chemistry, Chino, Japan 14-16 November 2003.

Appendix

Publications from This Project

Pergamon

Tetrahedron Letters 42 (2001) 8105–8109

TETRAHEDRON
LETTERS

Lower rim tetra-substituted and upper rim ferrocene amide calix[4]arenes: synthesis, conformation and anion-binding properties

Boosayarat Tomapatanaget and Thawatchai Tuntulani*

Department of Chemistry, Faculty of Science, Chulalongkorn University, Bangkok 10330, Thailand

Received 29 July 2001; revised 5 September 2001; accepted 13 September 2001

Abstract—Calix[4]arenes containing ferrocene amide at the upper rim and methoxy or ethoxycarbonylmethoxy (ethyl ester) groups at the lower rim (**5a**, **5b** and **5c**) have been synthesized. It was found that tetramethoxy **5a** and dimethoxy diethyl ester **5c** were conformationally labile and existed in both cone and partial cone conformation in solution. Anion-binding studies by ^{1}H NMR titration in $CDCl_3$ showed that **5b** bound Cl^- selectively with high stability. Compound **5c** formed complexes with Cl^- and $H_2PO_4^-$ where the former was more stable. The ratio of cone to partial cone conformation in compound **5a** was found to decrease upon binding Cl^- and $H_2PO_4^-$ and in a polar solvent. © 2001 Elsevier Science Ltd. All rights reserved.

Anion recognition and sensing is now an increasingly important research topic in supramolecular chemistry due to the entanglement of various anions in biological and environmental subjects. Chemists employ either electrostatic or hydrogen bonding interactions as binding tools for constructing anion receptors.[1] Beer and co-workers have been pioneers in making metallocene amide receptors for binding anions.[2] These types of compound can also be used as electrochemical sensors. In 1999, Beer et al. reported the anion recognition of upper rim cobaltocenium calix[4]arene receptors and found that they formed complexes with carboxylate anions, dihydrogen phosphate and halide anions to a different extent.[3] Recently, ion-pair recognition has been recognized by supramolecular chemists due to its potential applications in metal ion and anion attraction or metal-controlled anion sensing devices.[4] Beer and colleague have synthesized hetero ditopic ferrocene receptors containing two ethyl ester calix[4]arene units bridged by a ferrocene amide moiety.[5] It was found that the binding ability of this ligand toward halide anions increased in the presence of Na^+.

We have synthesized tripodal aza crown ether calix[4]arenes containing simultaneous cation- and anion-binding sites and found out that the binding ability toward Br^- is enhanced in the presence of K^+.[6] We are interested in constructing ion-pair receptors and sensors using calix[4]arene as building block and attaching the ferrocene amide functional group on the upper rim and ethyl ester groups on the lower rim.

Syntheses of ethyl ester ferrocene amide and methoxy ferrocene amide calix[4]arenes **5a**, **5b** and **5c** are summarized in Scheme 1. Dinitro derivatives of dimethoxy and diethyl ester calix[4]arenes, **1a**[7] and **1b**,[8] respectively were synthesized from a catalytic nitration reaction using $NaNO_3$ and HCl in H_2O as reagent and $La(NO_3)_3$ as catalyst. This reaction is appropriate for producing nitro substituents on the *para* position of phenol rings. The dinitro compounds **2a** and **2b** were obtained in 71 and 88% yields, respectively.[9] Compound **2a** hardly dissolves in CH_2Cl_2, but dissolves very well in DMF. Nucleophilic substitution reactions of **2a** with CH_3I in the presence of K_2CO_3 in DMF and ethyl bromoacetate in the presence of NaH in DMF yielded the tetra-substituted dinitrocalix[4]arenes, **3a**[10] (71%) and **3c**[11] (61%), respectively. Tetraethyl ester dinitrocalix[4]arene, **3b**, was obtained in 61% yield from the reaction of **2b** with ethyl bromoacetate in the presence of Na_2CO_3 in CH_3CN.[8] Reduction of **3a**, **3b** and **3c** with Raney Ni and $N_2H_4{\cdot}H_2O$ resulted in diamino compounds **4a** (98%), **4b** (95%) and **4c** (96%), respectively.[12] Upon coupling with freshly synthesized 1,1-bis(chlorocarbonyl)ferrocene[13] in the presence of NEt_3 in CH_2Cl_2, compounds **4a**, **4b** and **4c** gave the desired ferrocene amide calix[4]arenes **5a** (50%), **5b** (42%) and **5c** (40%), respectively.[14] All spectroscopic data and elemental analysis results support the existence of all synthesized compounds.

Keywords: ferrocene; calix[4]arene; conformation; anion binding.

* Corresponding author.

PII: S0040-4039(01)01722-1

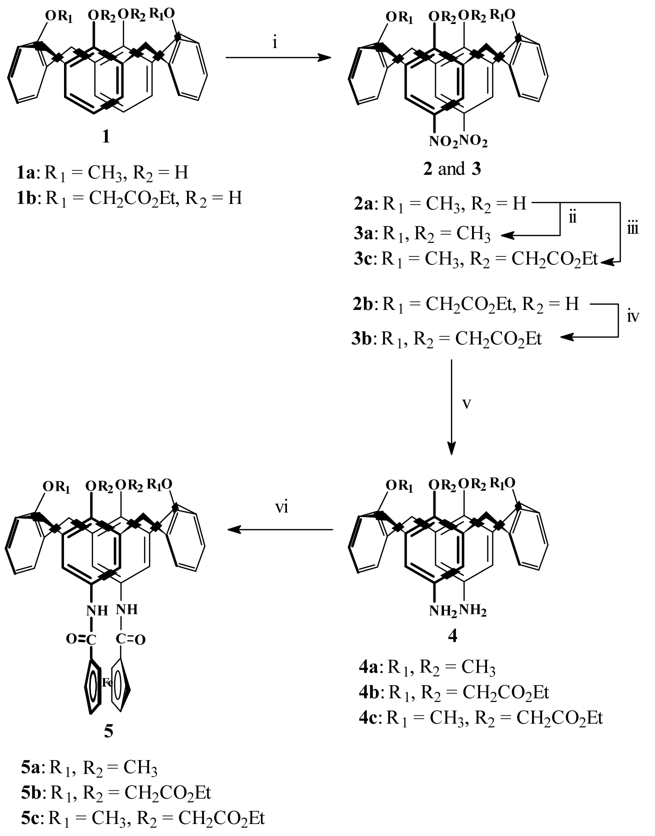

Scheme 1. *Reagents and conditions*: (i) $NaNO_3$, $La(NO_3)_3$, HCl, H_2O in CH_2Cl_2; (ii) CH_3I, K_2CO_3 in DMF; (iii) $BrCH_2CO_2Et$, NaH in DMF; (iv) $BrCH_2CO_2Et$, Na_2CO_3 in CH_3CN; (v) Raney Ni, $N_2H_4{\cdot}H_2O$, EtOAc in CH_3OH; (vi) 1,1-bis(chlorocarbonyl)ferrocene, NEt_3 in CH_2Cl_2.

The structure of calix[4]arene is usually classified into four basic conformations according to the possible 'up' and 'down' arrangement of phenol rings: cone, partial cone, 1,2-alternate and 1,3-alternate. Due to the lack of intramolecular hydrogen bonding among OH groups of the aryl rings, compounds **5a**, **5b** and **5c** should be conformationally labile at room temperature. However, **5b** is found to exist only in cone conformation in solution because four bulky ethyl ester groups at lower rim inhibit the phenyl ring rotation. Although **5a** and **5c** show complicated ^1H and ^{13}C NMR spectra at room temperature suggesting mixed conformations of the calix[4]arene unit, the upper rim connection to ferrocene limits possible conformations to be cone, partial cone and 1,3-alternate. Using NOESY, COSY and HMBC spectroscopy, we have found that **5a** and **5c** exist in both cone and partial cone conformations in an approximately 1:1 ratio in $CDCl_3$. ^1H NMR spectra (500 MHz, acetone-d_6) of **5a** and **5c** and the conformation assignment are shown in Fig. 1.

The methylene bridge protons in cone conformation appear as two sets of doublets at 4.04 and 3.06 ppm for **5a** and at 4.04 and 3.06 ppm for **5c** while partial cone conformation has 4 sets of doublets at 4.29, 3.98, 3.11 and 3.03 ppm for **5a** and at 4.09, 3.82, 3.32 and 3.19 ppm for **5c**. It should be noted that peaks due to methyl protons of the partial cone conformation shift more upfield than those of the cone conformation. This probably stems from the effect of ring currents from aryl units of calix[4]arene when one of the methoxy group points into the calix[4]arene cavity (Fig. 1). In addition, ^{13}C NMR spectra of compounds **5a** and **5c** show characteristic peaks of methylene bridge carbons at ca. 31 ppm for the cone conformation and at ca. 31 ppm and ca. 37 ppm for the partial cone conformation.[15]

We are interested in the binding ability of compounds **5a**, **5b** and **5c** toward anions. Halide anions and dihydrogen phosphate are quite interesting in terms of their relevance to the biological systems. ^1H NMR (200 MHz) titration has thus been employed in complexation studies of **5a**, **5b** and **5c** toward halide anions (Cl^-, Br^- and I^-) and $H_2PO_4^-$ using Bu_4N^+ as countercation in $CDCl_3$.[16] There is no displacement of any proton signals of **5a**, **5b** and **5c** observed upon addition of Br^- and I^-. The result suggests that **5a**, **5b** and **5c** do not form complexes with $Br^-$and I^-. Addition of Cl^- to **5a**, **5b** and **5c** results in the displacement of signals due to -OCN***H***-. Job plot analysis indicates that **5b** and **5c** bind Cl^- in a 1:1 ligand/anion ratio. However, in the presence of $H_2PO_4^-$, only signals due to -OCN***H***- of **5a** and **5c** shift downfield while those of **5b** do not move.

Unfortunately, due to the unconformity of the ratio of cone and partial cone conformation of **5a** during anion titration, vide infra, the stability constant of **5a** toward anions cannot be estimated. Association constants of **5b** and **5c** toward various anions calculated by the program EQNMR[17] are collected in Table 1. The result shows that **5b** binds Cl^- selectively with high stability. This is similar to the tetraethyl ester urea calix[4]arene that can bind Cl^- efficiently in the presence of Na^+.[18] Compound **5c** can bind both Cl^- and $H_2PO_4^-$ in which the former gives a more stable complex. As compared to **5b**, the flexibility of the calix[4]arene unit may reduce the anion-binding ability of **5c**.

Interestingly, the ratio of cone to partial cone conformation of **5a** in $CDCl_3$ changes upon addition of Cl^- and $H_2PO_4^-$. From the integration of signals of cp ring protons, we can estimate the ratio of cone to partial cone conformation as shown in Table 2. The result implies that the concentration of the partial cone conformation of **5a** increases upon increasing the concentration of Cl^- and $H_2PO_4^-$. Another example of conformational change of calix[4]arene from cone to partial cone upon binding anions has recently been found by us.[19] In addition, in a polar solvent such as acetone-d_6, the cone to partial cone ratio of compound **5a** becomes approximately 1:2 signifying the increase of partial cone conformation. This is opposite to that reported by Shinkai where the concentration of the cone conformation of tetramethoxy calix[4]arene was found to increase upon increasing solvent polarity.[20] Our results thus suggest that besides solvent polarity, the conformation ratio of the calix[4]arene unit in **5a** may depend upon the degree of hydrogen bond interactions between its -CONH- groups and solvents and anions.

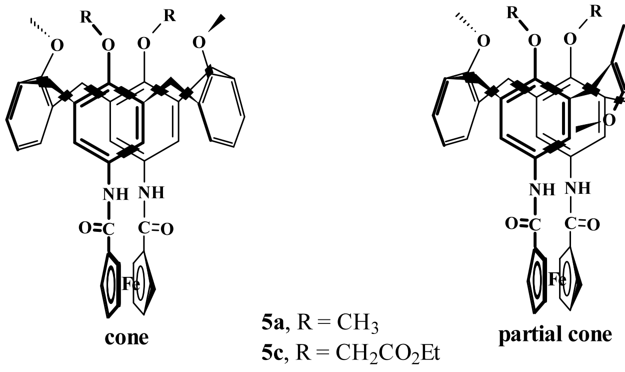

5a, R = CH_3
5c, R = CH_2CO_2Et

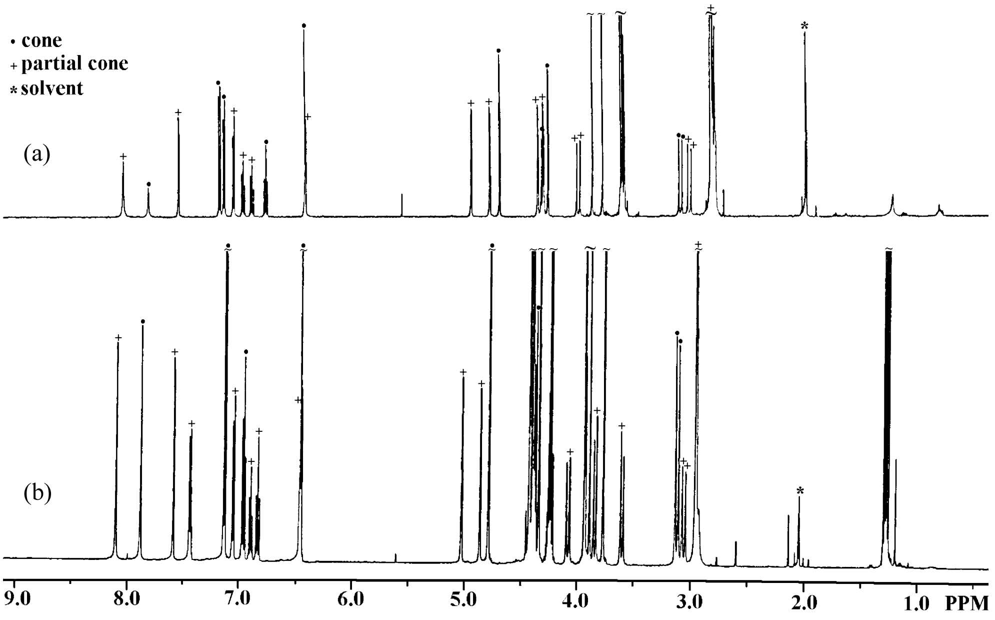

Figure 1. ^1H NMR spectra of (a) **5a** and (b) **5c** and their conformation assignment.

Table 1. Association constants of **5a**, **5b** and **5c** with various anions[a]

Anion[b]	K_{assoc} (M^{-1})		
	5a	**5b**	**5c**
Cl^-	[d]	1800.1	513.6
Br^-	[c]	[c]	[c]
I^-	[c]	[c]	[c]
$H_2PO_4^-$	[d]	[c]	244.0

[a] All experiment were carried out at 298 K; errors estimated to be less than 15%.

[b] Using Bu_4N^+ as countercation.

[c] No peak shift of -OCN*H* protons was observed.

[d] K_{assoc} cannot be calculated due to conformational unconformity.

In conclusion, we have synthesized three derivatives of calix[4]arene containing bifunctional substituents at both upper and lower rim (**5a**, **5b** and **5c**), and their preliminary anion-binding and conformational properties have been reported. We are investigating ion-pair binding ability of ligands **5a**, **5b** and **5c**, the detail of their conformational and redox properties. The results will be reported in due course.

Table 2. Mole fraction (X) of cone (c) and partial cone (pc) conformation when increasing the ratio of **5a** to anions

Anion	X_c/X_{pc} with various **5a**:anion ratios		
	1:0	1:1	1:4
Cl^-	0.452/0.548	0.427/0.573	0.395/0.605
$H_2PO_4^-$	0.452/0.548	0.448/0.552	0.427/0.573

Acknowledgements

This work was supported financially by the Thailand Research Fund (RSA/06/2544 and PHD/0182/2542). B.T. is a Ph.D. student supported by the Royal Golden Jubilee Program. The authors thank the Science and Technology Equipment Center of Chulalongkorn University for the 500 MHz NMR measurements.

References

1. Steed, J. W.; Atwood, J. L. *Supramolecular Chemistry*; John Wiley & Sons: New York, 2000; pp. 197–249.
2. Beer, P. D. *Acc. Chem. Res.* **1998**, *31*, 71.
3. Beer, P. D.; Hesek, D.; Nam, K. C.; Drew, M. G. B. *Organometallics* **1999**, *18*, 3933.
4. Beer, P. D.; Gale, P. A. *Angew. Chem., Int. Ed.* **2001**, *40*, 486.
5. Cooper, J. B.; Drew, M. G. B.; Beer, P. D. *J. Chem. Soc., Dalton Trans.* **2000**, 2721.
6. Tuntulani, T.; Poompradub, S.; Thavornyutikarn, P.; Jaiboon, N.; Chaichit, N.; Ruangpornvisuti, V.; Asfari, Z.; Vicens, J. *Tetrahedron Lett.* **2001**, *42*, 5541.
7. Van Loon, J.-D.; Arduni, A.; Coppi, L.; Verboom, W.; Pochini, A.; Ungaro, R.; Harkema, S.; Reinhoudt, D. N. *J. Org. Chem.* **1990**, *55*, 5639.
8. Rudkevich, D. M.; Verboom, W.; Reinhoudt, D. N. *J. Org. Chem.* **1994**, *59*, 3683. Compound **3b** was synthesized and characterized by the method described in this article.
9. Typical procedure: To a solution of **1** (22.1 mmol) in CH_2Cl_2 (494 mL) was added a solution of $NaNO_3$ (5.64 g, 66.3 mmol) and a catalytic amount of $La(NO_3)_3{\cdot}6H_2O$ in a mixture of H_2O (304 mL) and concentrated HCl (55 mL). The mixture was stirred overnight at room temperature. The color of the mixture changed to yellow. The aqueous layer was then separated and extracted with CH_2Cl_2 (2×250 mL). The organic layer was combined and washed with saturated aqueous NH_4Cl (2×250 mL) and dried over anhydrous Na_2SO_4. The solvent was removed by a rotary evaporator and the product was crystallized by adding hexane. Compound **2a**: ^{1}H NMR (200 MHz, $CDCl_3$) δ 8.93 (s, 2H, -O*H*), 8.04 (s, 4H, *H*Ar-NO_2), 6.94 (d *J*=7.2 Hz, 4H, *m-H*Ar-OCH_3), 6.85–6.77 (t *J*=7.4, 2H, *p-H*Ar-OCH_3), 4.28 and 3.52 (d each *J*=13.3 Hz, 8H, ArCH_2Ar), 4.02 (s, 6H, -OCH_3). Compound **2b**: ^{1}H NMR (200 MHz, $CDCl_3$) δ 8.90 (s, 2H, -O*H*), 8.01 (s, 4H, *O*-Ar*H*-NO_2), 6.91 (d *J*=8.3 Hz, 4H, *m*-Ar*H*-OH), 6.84 (t *J*=6.4 Hz, 2H, *p*-Ar*H*-OR), 4.67 (s, 4H, OCH_2CO), 4.45, and 3.49 (d each *J*=13.3 Hz, 8H, ArCH_2Ar), 4.35 (q *J*=7.1 Hz, 4H, OC$H_2$$CH_3$), 1.39 (t *J*=8.7 Hz, 6H, -CH_2CH_3).
10. Compound **2a** (0.271 g, 0.500 mmol) in the presence of K_2CO_3 (0.695 g, 5.000 mmol) in DMF (10 mL) was stirred at room temperature for 1 h. CH_3I (0.500 mL, 8.000 mmol) was then added and the mixture was heated at 60°C for 7 days. After the mixture cooled to room temperature, the solvent was removed under reduced pressure. The residue was dissolved in CH_2Cl_2 (30 mL) and extracted with aqueous NH_4Cl (2×30 mL). The combined organic phase was washed with water and brine (2×30 mL) and then dried over anhydrous Na_2SO_4. The solvent was removed under reduced pressure. Upon addition of CH_3OH, a white solid of **3a** precipitated. ^{1}H NMR (200 MHz, $CDCl_3$) δ 8.19–6.43 (m, 10H, Ar*H*), 4.37, 4.05, 3.28 and 3.17 (d each *J*=13.3 Hz, 8H, ArCH_2Ar), 3.85–3.72 (m, 12H, -OCH_3). ESI-TOF *m/z* 571.30 [M+H$^+$] (M, 570.30).
11. Compound **2c** (1.001 g, 1.840 mmol) and NaH (0.222 g, 9.250 mmol) in DMF (20 mL) were stirred at room temperature for 1 h and ethyl bromoacetate (1 mL) was then added. The mixture was stirred and heated at 60°C overnight. The work-up procedure is the same as for compound **3a**. Compound **3c** was obtained as white solid. ^{1}H NMR (200 MHz, $CDCl_3$) δ 7.83–7.08 (m, 10H, *H*Ar), 4.45 (s, 4H, -OCH_2CO-), 4.37 (q *J*=7.2 Hz, 4H, -OC$H_2$$CH_3$), 3.96–2.99 (m, 14H, -OCH_3 and ArCH_2Ar), 1.30 (t *J*=7.1, 6H, -CH_2CH_3). Anal. calcd for $C_{38}H_{38}N_2O_{12}$: C, 63.86; H, 5.36; N, 3.92. Found: C, 63.85; H, 5.29; N, 3.88.
12. Typical procedure: To a solution of **3** (1.950 mmol) and Raney Ni (2.095 g) in a mixture of ethyl acetate (80 mL) and CH_3OH (40 mL) was added $N_2H_4{\cdot}H_2O$ (4 mL). The mixture was refluxed for 2 h and allowed to cool to room temperature. The solvent was subsequently removed under reduced pressure. The residue was dissolved in CH_2Cl_2 and extracted with several portions of H_2O. The organic layer was separated and dried over anhydrous Na_2SO_4. The solvent was then removed under reduced pressure to give **4** as white solid. In order to avoid the decomposition, **4** was used immediately (without further purification) for synthesizing compound **5**. Compound **4a**: ^{1}H NMR (200 MHz, $CDCl_3$) δ 7.04–6.43 (m br, 6H, Ar*H*), 6.09 (s br, 4H, *o*-Ar*H*-NH_2), 4.26–2.91 (m br, 20H, -OCH_3 and ArCH_2Ar); ESI-TOF *m/z* 511.30 [M+H$^+$] (M, 510.63). Compound **4b**: ^{1}H NMR (200 MHz, $CDCl_3$) δ 6.69–6.59 (m, 6H, m-Ar*H*-OR), 6.01 (s, 4H, *o*-Ar*H*-NH_2), 4.78 and 3.10 (d each *J*=13.1 Hz, 8H, ArCH_2Ar), 4.70 (s, 4H, ArOCH_2-), 4.61 (s, 4H, NH_2-Ar-OCH_2-), 4.18 (q *J*=7.1 Hz, 8H, -C$H_2$$CH_3$), 1.26 (t *J*=7.2 Hz, 12 H, -CH_2CH_3); ESI-TOF *m/z* 799.13 [M+H$^+$] (M, 798.89). Compound **4c**: ^{1}H NMR (200 MHz, $CDCl_3$) δ 7.22 (d *J*=6.9 Hz, 4H, *m-H*Ar-OCH_3), 6.90 (t *J*=7.2 Hz, 2H, *p-H*Ar-OCH_3), 5.69 (s, 4H, *o-H*Ar-NH_2), 4.40 (d *J*=13.1 Hz, 4H, ArCH_2Ar, and s, 4H, -CH_2CO-), 4.25 (q *J*=7.1 Hz, 4H, -OC$H_2$$CH_3$), 3.96 and 3.46 (s, 6H, -OCH_3), 3.10 (d *J*=12.8 Hz, 4H, ArCH_2Ar), 1.30 (t *J*=7.1 Hz, 6H, -OCH_2CH_3); ESI-TOF *m/z* 655.70 [M+ H$^+$] (M, 654.76); Anal. calcd for $C_{38}H_{42}N_2O_8$: C, 69.71; H, 6.47; N, 4.28 Found: C, 69.71; H, 6.25; N, 4.26.
13. (a) Knobloeh, F. W.; Rausher, W. H. *J. Polym. Sci.* **1961**, *54*, 651; (b) Lorkowski, H. J.; Pannier, R.; Wende, A. *J. Prakt. Chem.* **1967**, *35*, 149.
14. Typical procedure: Into a two-necked round-bottomed flask, compound **4** (1.54 mmol) and triethylamine in dichloromethane (30 mL) were stirred at room temperature under a nitrogen atmosphere. A solution of 1,1-bis-(chlorocarbonyl)ferrocene (0.6201g, 2.0 mmol) in dichloromethane (30 mL) was transferred into the mixture via cannula. The mixture was stirred continuously at room temperature under a nitrogen atmosphere for 4 h. It was washed with several portions of H_2O and the organic layer was dried with anhydrous $NaSO_4$. The solvent was removed under reduced pressure to afford a dark red residue which was then placed on a SiO_2 chromatography column. Compound **5** was eluted from the column using 10% EtOAc in CH_2Cl_2 as eluant. Compound **5a**: ^{1}H NMR (acetone-*d*$_6$, 500 MHz) δ 8.09 (s, 2H, -N*H*- (pc)), 7.86 (s, 2H, -N*H*- (c)), 7.59 and 6.46 (d *J*=3.0 Hz, 4H, -Ar*H*-NH- (pc)), 7.22 (d *J*=8.0 Hz, 4H, *m*-Ar*H* (c)) 7.18 and 7.10 (d *J*=7.5 Hz, 4H, *m*-Ar*H* (pc)), 7.01 (t *J*=7.5 Hz, 2H, *p*-Ar*H* (c)), 6.93 and 6.81 (t *J*=7.5 Hz, 2H, *p*-Ar*H* (pc)), 6.47 (s, 4H, -NH-Ar*H*- (c)), 5.00 and 4.83 (m, 4H, -Cp*H* (pc)), 4.75 (t *J*=2.5 Hz, 4H,

-Cp*H* (c)), 4.41 and 4.36 (m, 4H, *m*-Cp*H* (pc)), 4.36 and 3.14 (d $J=13.5$, 12H, ArCH_2Ar (c and pc)), 4.31 (t $J=2.0$ Hz, 4H, Cp*H* (c)), 4.04 and 3.06 (d each $J=14.0$ Hz, 4H, ArCH_2Ar (pc)), 3.92–3.65 (m, 21H, -OCH_3 (pc and c)), 2.86 (s, 3H, -OCH_3 (pc)); ESI-TOF *m*/*z* 749.50 [M+H$^+$] (M, 748.66); Anal. calcd for $C_{44}H_{40}FeN_2O_6$·0.5CH_2Cl_2: C, 67.56; H, 5.22; N, 3.54 Found: C, 67.72; H, 5.24; N, 3.55. Compound **5b**: ^{1}H NMR (200 MHz, $CDCl_3$) δ 7.25 (s, 2H, -N*H*-), 7.20 (d $J=6.7$ Hz, 4H, *m*-Ar*H*-OR), 7.09 (t $J=6.4$ Hz, 2H, *p*-Ar*H*OR), 6.43 (s, 4H, *o*-Ar*H*-NH-), 4.87 and 3.22 (d each $J=13.0$ Hz, 8H, ArCH_2Ar), 4.90 (s, 4H, -NH-ArHOCH_2-), 4.77 (s br, 4H, Cp*H*), 4.45 (s, 4H, ArH-OCH_2-), 4.33 (s, br, 4H, Cp*H*), 4.17 (q $J=7.1$ Hz, 8H, -OCH_2CH$_3$), 1.33–1.22 (m, 12H, -OCH$_2$CH_3); ESI-TOF *m*/*z* 1037.20 [M+H$^+$] (M, 1036.91); Anal. calcd for $C_{56}H_{56}FeN_2O_{14}$: C, 64.87; H, 5.44; N, 2.70 Found: C, 64.84; H, 5.40; N, 2.63. Compound **5c**: ^{1}H NMR (acetone-d_6, 500 MHz) δ 8.10 (s, 2H, -N*H*- (pc)) and 7.88 (s, 2H, -N*H*- (c)), 7.58 and 6.45 (d $J=2.5$ Hz, 4H, -Ar*H*-NH- (pc)), 7.43 and 7.04 (d $J=7.5$ Hz, 4H, *m*-Ar*H* (pc)), 7.12 (d $J=7.5$ Hz, 4H, *m*-Ar*H* (c)), 6.95 (t $J=7.5$ Hz, 2H, *p*-Ar*H* (c)), 6.89 and 6.82 (t $J=7.5$ Hz, 2H, *p*-Ar*H* (pc)), 6.46 (s, 4H, -NH-Ar*H*- (c)) 5.03 and 4.86 (m, 4H, *o*-Cp*H* (pc)), 4.78 (t $J=2.0$ Hz, 4H, *o*-Cp*H* (c)), 4.39–4.37 (m, 4H, *m*-Cp*H* (pc) and 4H, *m*-Cp*H* (c) and 8H, -OCH_2-CO- (c and pc) and 8H, ArCH_2Ar (c)), 4.26–4.21 (m, 4H, -OCH_2CH$_3$), 4.07 and 3.05 (d $J=14.0$ Hz, 4H, ArCH_2Ar (pc)), 3.83 and 3.59 (d each $J=12.5$ Hz, 4H, ArCH_2Ar (pc)), 3.93–3.76 (m, 9H, -OCH_3 (c and pc)), 2.97 (s, 3H, -OCH_3 (pc)), 1.28 (m, 12H, -CH$_2$CH_3 (c and pc)); ESI-TOF *m*/*z* 893.51 [M+H$^+$] (M, 892.79); Anal. calcd for $C_{50}H_{48}FeN_2O_{10}$·0.5CH_2Cl_2: C, 64.85; H, 5.28; N, 3.00 Found: C, 65.28; H, 5.51; N, 3.19.

15. Jaime, C.; de Mendoza, J.; Prados, P.; Nieto, P. M.; Sánchez, C. *J. Org. Chem.* **1991**, *56*, 3372.
16. Solutions of **5a**, **5b** and **5c** (0.01M) in $CDCl_3$ were prepared. To a solution of a ligand in each NMR tube was added 0.0–4.0 equiv. of 0.25 M tetrabutylammonium salt of an anion. Spectra were recorded every 24 h until the complexation reached the equilibrium. The result of the experiment was a plot of displacement in chemical shift as a function of the amount of added anion. The program EQNMR was then used to analyze the resulting titration curves and calculate stability constant values in M^{-1}. Titration experiments were repeated twice with at least 12 data points for each anion.
17. Hynes, M. J. *J. Chem. Soc., Dalton Trans.* **1993**, 311.
18. Scheerder, J.; van Duynhoven, J. P. M.; Engbersen, J. F. J.; Reinhoudt, D. N. *Angew. Chem., Int. Ed. Engl.* **1996**, *35*, 1090.
19. Pothsree, T.; Seangprasertkij-Magee, R.; Tuntulani, T. *J. Incl. Phenom.* **1997**, *29*, 99.
20. Shinkai, S.; Iwamoto, K.; Araki, K.; Matsuda, T. *Chem. Lett.* **1990**, 1263.

Pergamon

SCIENCE DIRECT

Tetrahedron Letters 44 (2003) 29–32

TETRAHEDRON
LETTERS

Calix[4]arenes containing urea and crown/urea moieties: effects of the crown ether unit and Na^+ towards anion binding ability

Pan Tongraung, Nuanphun Chantarasiri and Thawatchai Tuntulani*

Department of Chemistry, Faculty of Science, Chulalongkorn University, Bangkok 10330, Thailand

Received 16 September 2002; revised 28 October 2002; accepted 8 November 2002

Abstract—Calix[4]arenes containing urea and crown/urea moieties, **7** and **10**, respectively have been synthesized. ^1H NMR titrations of **7** and **10** with anions in DMSO-d_6 showed that **7** and **10** formed complexes with Cl^-, Br^-, NO_3^- and $H_2PO_4^-$ to a different extent. The association constants of **7** and **10** towards anions were calculated and found to vary as $H_2PO_4^- > Cl^- > Br^- > NO_3^-$. However, compared to **7** the presence of the crown unit in **10** resulted in a slightly higher affinity to Cl^- and Br^-, but a lower affinity to $H_2PO_4^-$. Upon addition of Na^+, the binding ability of **10** towards $H_2PO_4^-$ is increased due to ion-pair enhancement. © 2002 Elsevier Science Ltd. All rights reserved.

Anion recognition is an increasingly important research topic in supramolecular chemistry due to possible applications in selective ion receptors and sensors in biological and environmental systems.[1,2] Urea is used dominantly in neutral anion receptors because of its strong hydrogen bonding towards anions.[3,4] Umezawa and co-workers showed that urea receptors with a rigid xanthene spacer formed strong complexes with dihydrogen phosphate.[5] Very recently, cystine-based symmetrical cyclic oligoureas have been synthesized and found to bind Cl^-, Br^- and NO_3^- to a different extent.[6]

Calix[4]arene is one of the most important supramolecular building blocks because of its capability of being modified at both the wide and narrow rims. Recently, derivatives of calix[4]arene have been used as receptors for cations, anions and neutral molecules.[7] Budka et al. have synthesized a tetra-urea derivative of calix[4]arene in a 1,3-alternate conformation. It was found that this receptor, with two possible binding sites, exhibited a strong negative allosteric effect which led to the exclusive complexation of only one anion.[8] Reinhoudt and co-workers demonstrated that a calix[4]arene derivative containing ethyl ester groups and urea moieties on the narrow rim and on the wider rim, respectively, was able to bind Cl^- efficiently in the presence of Na^+.[9]

We are interested in synthesizing neutral anion receptors using calix[4]arene as the building block and attaching urea units as receptors for anions at the wider rim. In addition, in one of the target molecules, a crown ether group is attached to a calix[4]arene urea on the narrow rim. Anion binding studies of the hosts synthesized with various anions have been performed to investigate the effect of the crown ether unit and different cations towards anion binding ability.

Protection and deprotection strategies have been employed to generate a specifically functionalized calix[4]crown urea. Syntheses of calix[4]crown ureas were carried out as shown in Scheme 1. Calix[4]arene was reacted with 2 equiv. of benzoyl chloride in CH_3CN in the presence of Na_2CO_3 as base under N_2, and the reaction was heated at reflux for 2 h to give dibenzoyl calix[4]arene **2** in 90% yield.[10] Nitration of **2** with 65% HNO_3 and CH_3COOH in CH_2Cl_2 at room temperature yielded the dinitro compound **3** in 45% yield.[11] Methylation of **3** with CH_3I in CH_3CN using Na_2CO_3 as base and refluxing the reaction for 5 days resulted in the dimethyldinitro calix[4]arene **4** in 85% yield.[12] Removal of the benzoyl groups from **4** by excess NaOH resulted in a dimethyldinitro calix[4]arene building block **5** in 50% yield.[13] Reduction of the nitro groups in **5** with $SnCl_2 \cdot 2H_2O$ gave the dimethyldiamino calix[4]arene **6** in 70% yield.[14] The presence of the methyl groups at the positions *para* to the amine groups aids in stabilizing compound **6**. Nevertheless, compound **6** was immediately coupled with phenyl isocyanate in CH_2Cl_2 at room temperature. The white solid **7** precipitated out of the reaction in 60% yield.[15] The dimethoxydiurea calix[4]arene **7** is highly polar and dissolves only in polar solvents such as DMF and DMSO.

Keywords: calix[4]arene; anion binding; ion-pair enhancement.

* Corresponding author.

PII: S0040-4039(02)02530-3

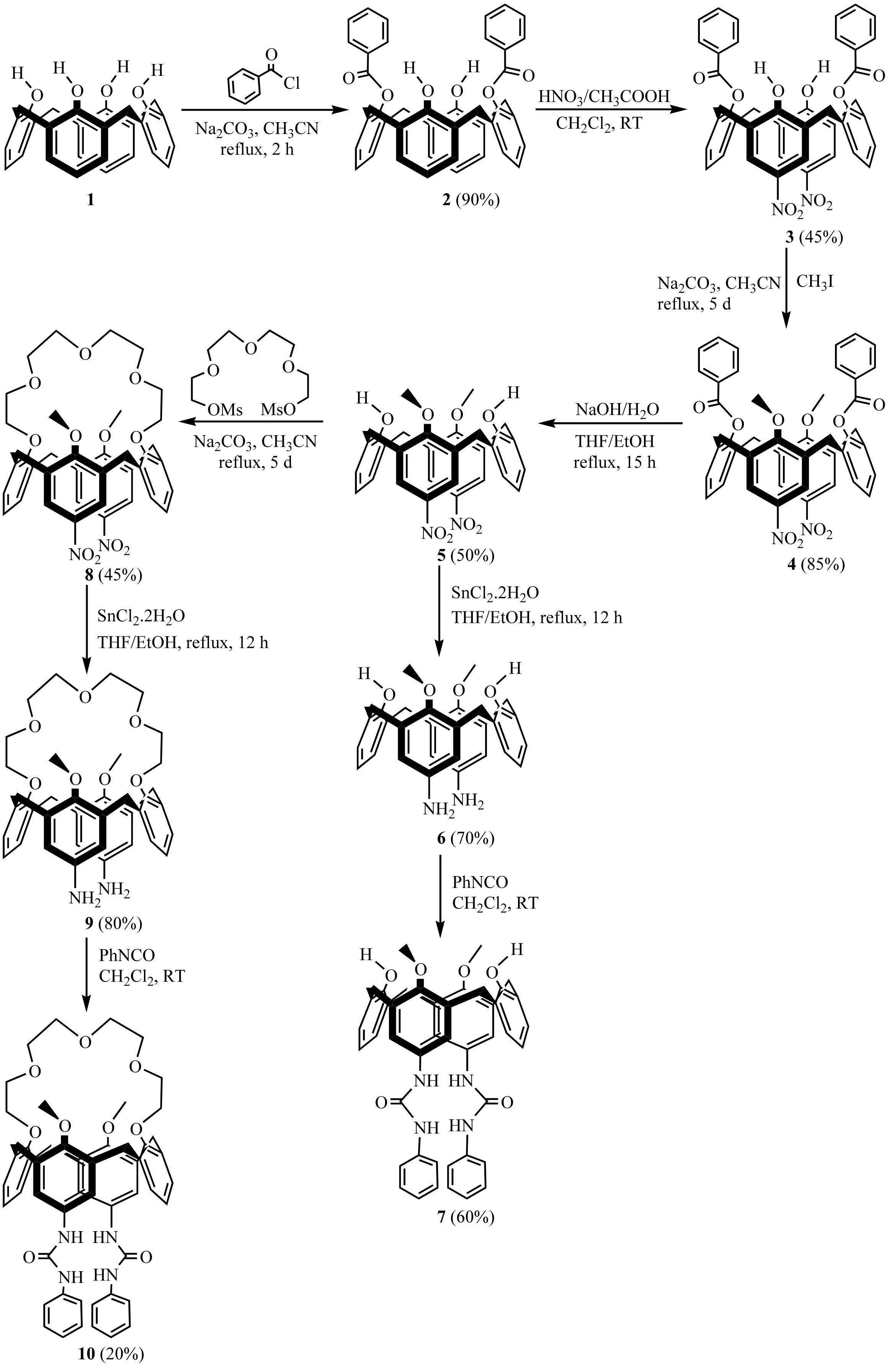
1
Na₂CO₃, CH₃CN
reflux, 2 h
2 (90%)
HNO₃/CH₃COOH
CH₂Cl₂, RT
NO₂ NO₂
3 (45%)
Na₂CO₃, CH₃CN
reflux, 5 d
CH₃I
4 (85%)
NaOH/H₂O
THF/EtOH
reflux, 15 h
5 (50%)
OMs MsO
Na₂CO₃, CH₃CN
reflux, 5 d
8 (45%)
SnCl₂.2H₂O
THF/EtOH, reflux, 12 h
6 (70%)
NH₂ NH₂
PhNCO
CH₂Cl₂, RT
7 (60%)
SnCl₂.2H₂O
THF/EtOH, reflux, 12 h
9 (80%)
PhNCO
CH₂Cl₂, RT
10 (20%)

Scheme 1.

Compound **5** underwent nucleophilic substitution with tetraethylene glycol dimethanesulfonate in CH_3CN using Na_2CO_3 as base and heating at reflux for 5 days to yield the dimethyldinitro crown calix[4]arene **8** in 45% yield.[16]

Reduction of the nitro groups of **8** with $SnCl_2{\cdot}2H_2O$ gave the crown dimethyldiamino calix[4]arene **9** in 80% yield.[17] The ^1H NMR spectra of compounds **8** and **9** showed very complicated signals in the aromatic and alkyl proton regions that signified aryl ring inversion in the calix[4]arene unit.[18] This behavior stems from the lack of intramolecular hydrogen bonding in **8** and **9**. The coupling reaction between **9** and phenylisocyanate at room temperature resulted in the precipitation of the calix[4]arene crown urea **10** in 20% yield.[19] Although **10** lacks intramolecular hydrogen bonding, the substituents on the urea nitrogen prohibit the ring inversion. Compound **10** is hardly soluble in common organic solvents such as CH_2Cl_2 and $CHCl_3$. It dissolves only in highly polar solvents such as DMSO. Spectroscopic data and elemental analysis support the structures of all the compounds synthesized.

We aimed to compare the binding ability of compounds **7** and **10** towards anions. Because of their importance in environmental and biological systems, anions such as $H_2PO_4^-$, NO_3^-, Cl^-, Br^- and I^-, were chosen for study. The anion binding studies of compounds **7** and **10** were carried out by ^1H NMR titrations.[20] Addition of tetrabutylammonium iodide anion to a DMSO-d_6 solution of the receptors **7** and **10** did not cause any shifts of the NH or other proton resonances which indicated that **7** and **10** could not form complexes with I^-. However, addition of a tetrabutylammonium salt of a guest anion such as $H_2PO_4^-$, Cl^-, Br^- and NO_3^- to a DMSO-d_6 solution of the receptors **7** and **10** resulted in significant downfield shifts of the NH resonances at room temperature, which is consistent with the formation of hydrogen-bonded complexes. The plots between the mole ratios of anion: **7** and the NH chemical shift of compound **7** are illustrated in Figure 1. Job plot analysis indicates that **7** and **10** bind $H_2PO_4^-$, Cl^-, Br^- and NO_3^- in a 1:1 ligand/anion ratio. Association constants of **7** and **10** towards $H_2PO_4^-$, Cl^-, Br^- and NO_3^- calculated by the program EQNMR[21] are collected in Table 1.

The results in Table 1 indicate that both compounds **7** and **10** bind Cl^-, Br^-, NO_3^- and $H_2PO_4^-$ albeit to a different extent. Both compounds form most stable complexes with $H_2PO_4^-$ and least stable complexes with NO_3^-. Compound **10** binds Cl^- and Br^- more strongly than **7** does. However, **7** forms a more stable complex with $H_2PO_4^-$ than compound **10**. These results indicate that the presence of the crown bridging group in compound **10** has increased the binding ability towards Cl^- and Br^- slightly and decreased the binding ability towards $H_2PO_4^-$.

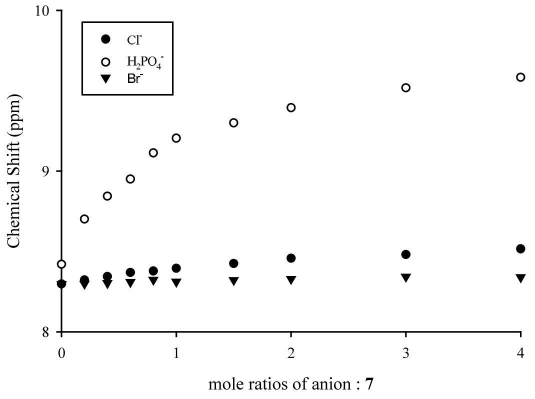

Figure 1. Plots between mole ratios of anion **7** and the NH chemical shifts.

Table 1. Association constants of ligands **7** and **10** towards $H_2PO_4^-$, Cl^-, Br^- and NO_3^- using $n\mathrm{Bu}_4\mathrm{N}^+$ as countercation[a]

Anion	Association constants (M^{-1})	
	7	**10**
$H_2PO_4^-$	250	200
Cl^-	43	60
Br^-	30	31
I^-	No binding	No binding
NO_3^-	13	11

[a] All experiment were carried out at 298 K, errors estimated to be less than 15%.

Recently, ion-pair recognition has attracted chemists' attention. Beer and colleagues have discovered that the presence of a suitable cation increases the binding ability of anion receptors containing cation binding units.[22] Compound **10** includes a crown-5 unit which is well known to form stable complexes with Na^+.[7] We are also interested to see the effect of the ion-pair enhancement in the binding ability of compound **10** towards $H_2PO_4^-$. Upon adding 1.2 equiv. of $NaPF_6$ to a DMSO-d_6 solution of the receptor **10**, we observed large chemical shifts in the region of the proton resonance of the crown ether unit suggesting complex formation between Na^+ and the crown ether unit. Addition of $n\mathrm{Bu}_4\mathrm{NH}_2\mathrm{PO}_4$ to the solution caused the NH peak to shift downfield. The association constant was then calculated by the program EQNMR to be 1028.4 M^-.[1] The presence of Na^+ thus increases the binding ability of **10** towards $H_2PO_4^-$. Potentially, this type of receptor can be modified to be a metal-ion controlled anion receptor or sensor in the future.

In summary, we have synthesized calix[4]arene ureas **7** and **10**. Anion binding studies by ^1H NMR showed that both **7** and **10** bind $H_2PO_4^-$ selectively. The incorporation of the crown ether unit in the calix[4]urea results in a slightly higher affinity of **10** for Cl^- and Br^-, but a lower affinity for $H_2PO_4^-$. The presence of Na^+ is found to enhance the affinity of **10** for $H_2PO_4^-$. We are currently synthesizing other derivatives of calix[4]arene containing crowns/ureas and studying their anion binding and sensing ability. These results will be reported in due course.

Acknowledgements

This work was financially supported by the Thailand Research Fund (RSA/06/2544). PT is a Ph.D. student supported by the National Science and Technology Development Agency. We thank Professor Jeremy Kilburn for mass spectrometry results.

References

1. Beer, P. D.; Gale, P. A. *Angew. Chem., Int. Ed. Engl.* **2001**, *40*, 486.
2. Anslyn, E. V. *Curr. Opin. Chem. Biol.* **1999**, *3*, 740.
3. Schmidtchen, F. P.; Berger, M. *Chem. Rev.* **1997**, *97*, 1609.
4. Antonisse, M. M. G.; Reinhoudt, D. N. *Chem. Commun.* **1998**, 443.
5. Bühlmann, P.; Nishizawa, S.; Xiao, K. P.; Umezawa, Y. *Tetrahedron* **1997**, *53*, 1647.
6. Ranganathan, D.; Lakshmi, C. *Chem. Commun.* **2001**, 1250.
7. Asfari, Z.; Böhmer, V.; Harrowfield, J.; Vicens, J. *Calixarenes*; Kluwer Academic Publishers: Dordrecht, 2001; p. 2001.
8. Budka, J.; Lhoták, P.; Michlová, V.; Stibor, I. *Tetrahdron Lett.* **2001**, *42*, 1583.
9. Scheerder, J.; van Duynhoven, J. P. M.; Engbersen, J. F. J.; Reinhoudt, D. N. *Angew. Chem., Int. Ed. Engl.* **1996**, *35*, 1090.
10. **2**: ^{1}H NMR spectrum (200 MHz, CDCl$_3$) δ 8.36 (d, $J=8$ Hz, 4H, Ar***H***$_{\text{benzoyl}}$), 7.72 (t, $J=8$ Hz, 2H, Ar***H***$_{\text{benzoyl}}$), 7.53 (t, $J=8$ Hz, 4H, Ar***H***$_{\text{benzoyl}}$), 7.07 (d, $J=4$ Hz, 4H, Ar***H***), 6.66–6.94 (m, 8H, Ar***H***), 5.50 (s, 2H, ArO***H***), 3.98 (d, $J=14$ Hz, 4H, ArC***H***$_2$Ar), 3.52 (d, $J=14$ Hz, 4H, ArC***H***$_2$Ar).
11. **3**: ^{1}H NMR spectrum (200 MHz, CDCl$_3$) δ 8.21 (d, $J=8$ Hz, 4H, Ar***H***), 7.97 (s, 4H, Ar***H***), 7.76 (t, $J=7$ Hz, 2H, Ar***H***), 7.53 (t, $J=7$ Hz, 4H, Ar***H***), 7.01 (m, 6H, Ar***H***), 6.33 (s, 2H, ArO***H***), 3.99 (d, $J=14$ Hz, 4H, ArC***H***$_2$Ar), 3.66 (d, $J=14$ Hz, 4H, ArC***H***$_2$Ar).
12. **4**: ^{1}H NMR spectrum (200 MHz, CDCl$_3$) δ 6.75–8.19 (m, 20H, Ar***H***), 3.35–3.82 (m, 14H, ArOC***H***$_3$, ArC***H***$_2$Ar).
13. **5**: ^{1}H NMR spectrum (200 MHz, CDCl$_3$) δ 7.80 (s, 4H, Ar***H***), 7.52 (s, 2H, ArO***H***), 7.14 (d, $J=7$ Hz, 4H, Ar***H***), 6.75 (t, $J=6$ Hz, 2H, Ar***H***), 4.33 (d, $J=13$ Hz, 4H, ArC***H***$_2$Ar), 4.05 (s, 6H, ArOC***H***$_3$), 3.51 (d, $J=13$ Hz, 4H, ArC***H***$_2$Ar). FAB MS (*m*/*z*): 542.84 [M$^+$].
14. **6**: ^{1}H NMR spectrum (200 MHz, CDCl$_3$) δ 7.88 (s, 2H, ArOH), 7.02 (d, $J=7$ Hz, 4H, Ar***H***), 6.64 (t, $J=7$ Hz, 2H, Ar***H***), 6.18 (s, 4H, Ar***H***), 4.21 (d, $J=14$ Hz, 4H, ArC***H***$_2$Ar), 3.89 (s, 6H, ArOC***H***$_3$), 3.27 (d, $J=14$ Hz, 4H, ArC***H***$_2$Ar), 1.78 (br, 4H, -N***H***$_2$).
15. **7**: ^{1}H NMR spectrum (200 MHz, DMSO-*d*$_6$) δ 8.42 (s, 2H, ArN***H***-), 8.30 (s, 2H, ArN***H***-), 8.17 (s, 2H, ArO***H***), 7.08–7.33 (m, 16H, Ar***H***), 6.89 (t, $J=7$ Hz, 2H, Ar***H***), 6.60 (t, $J=7$ Hz, 2H, Ar***H***), 4.15 (d, $J=13$ Hz, 4H, ArC***H***$_2$Ar), 3.89 (s, 6H, ArOC***H***$_3$), 3.46 (d, $J=13$ Hz, 4H, ArC***H***$_2$Ar). ESI MS (*m*/*z*): 720.99 [M$^+$]. Anal. calcd for **7** ($C_{44}H_{40}$ N_4O_6): C, 73.32; H, 5.59; N, 7.77. Found: C, 73.16; H, 5.63; N, 7.74.
16. **8**: ^{1}H NMR spectrum (200 MHz, CDCl$_3$) δ 8.28–8.04 (m, 4H, Ar***H***), 6.50–6.94 (m, 6H, Ar***H***), 4.42 (d, $J=13$ Hz, 4H, ArC***H***$_2$Ar), 3.24–4.20 (m, 26H, ArOC***H***$_3$, -OC***H***$_2$C***H***$_2$O- and ArC***H***$_2$Ar). ESI MS (*m*/*z*): 723.40 [M$^+$+Na$^+$].
17. **9**: ^{1}H NMR spectrum (200 MHz, CDCl$_3$) δ 6.47–6.97 (m, 10H, Ar***H***), 4.33 (d, $J=12$ Hz, 4H, ArC*H*$_2$Ar), 4.01 (s, 6H, ArOC*H*$_3$), 3.28–3.92 (m, 16H, -OC*H*$_2$C*H*$_2$O-), 2.99 (d, $J=12$ Hz, 4H, ArC*H*$_2$Ar), 2.74 (br, 4H, ArN***H***$_2$).
18. Veravong, S.; Ruangpornvisuti, V.; Pipoosananakaton, B.; Sukwattanasinitt, M.; Tuntulani, T. *ScienceAsia* **2000**, *26*, 163.
19. **10**: ^{1}H NMR spectrum (200 MHz, DMSO-*d*$_6$) δ 8.59 (s, 2H, ArN***H***-), 8.37 (s, 2H, ArN***H***-), 7.44 (d, $J=8$ Hz, 4H, ArH$_{\text{ph}}$), 7.26 (t, $J=8$ Hz, 6H, Ar***H***$_{\text{Ph}}$), 6.94 (t, $J=7$ Hz, 2H, Ar***H***), 6.45–6.59 (m, 8H, Ar*H*), 4.30 (d, $J=12$ Hz, 4H, ArC***H***$_2$Ar), 4.03 (s, 6H, ArOC***H***$_3$), 3.34–3.84 (m, 16H, -OC***H***$_2$C***H***$_2$O-), 3.13 (d, $J=13$ Hz, 4H, ArC***H***$_2$Ar). ESI MS (*m*/*z*): 901.69 [M$^+$+Na$^+$]. Anal. calcd for **10**·2H$_2$O ($C_{52}H_{58}N_4O_{11}$): C, 68.26; H, 6.39; N, 6.12. Found: C, 68.05; H, 5.96; N, 6.65.
20. Solutions of **7** and **10** (0.01 M) in DMSO-*d*$_6$ were prepared. To a solution of a ligand in each NMR tube was added 0.0–4.0 equiv. of a 0.25 M tetrabutylammonium salt of the anion. The result of the experiment was a plot of displacement in chemical shift as a function of the amount of added anion. The program EQNMR was then used to analyze the resulting titration curves and to calculate stability constant values in M^{-1}.
21. Hynes, M. J. *J. Chem. Soc., Dalton Trans.* **1993**, 311.
22. (a) Redman, J. E.; Beer, P. D.; Dent, S. W.; Drew, M. G. B. *Chem. Commun.* **1998**, 231; (b) Beer, P. D.; Hopkins, P. K.; McKinney, J. D. *Chem. Commun.* **1999**, 253; (c) Cooper, J. B.; Drew, M. G. B.; Beer, P. D. *J. Chem. Soc., Dalton Trans.* **2000**, 2721.

Pergamon

SCIENCE DIRECT®

Tetrahedron Letters 44 (2003) 33–36

TETRAHEDRON
LETTERS

Synthesis of redox-active biscalix[4]quinones and their electrochemical properties

Kriengkamol Tantrakarn, Chalita Ratanatawanate, Tipsukhon Pinsuk, Orawon Chailapakul and Thawatchai Tuntulani*

Department of Chemistry, Faculty of Science, Chulalongkorn University, Bangkok 10330, Thailand

Received 15 September 2002; revised 28 October 2002; accepted 8 November 2002

Abstract—Biscalix[4]arenes, **7** and **8**, have been synthesized by a one-pot coupling method and a stepwise approach, respectively. A one-pot reaction in a pressurized vessel resulted in the symmetric biscalix[4]arene **7** in high yield. Oxidation of compounds **7** and **8** by $Tl(CO_2CF_3)_3$ in CF_3COOH yielded biscalix[4]quinones, **9** and **10**, respectively. Preliminary electrochemical studies by cyclic voltammetry of **9** and **10** show significant changes of their voltammograms upon addition of Na^+. © 2002 Elsevier Science Ltd. All rights reserved.

Sensing technology and sensors have advanced in the past decade.[1] Chemists play a very important role in the development of chemical sensors. Typically, a chemical sensor composes of two important parts: a receptor unit and a signaling unit.[2] The signaling unit can give either electrochemical or optical responses. The most popular signaling units used by chemists are ferrocene and *p*-quinone.[3,4] The fabrication of sensory units and sensors can be carried out in a suitable way for sensing metal ions, anions or organic molecules.

Calix[4]arene is one of the most versatile molecular building blocks suitable for attaching both receptor and sensory units to the same molecules. Many calix[4]arene derivatives containing ferrocene[3] and *p*-quinone[4] have been synthesized and their binding and sensing properties towards metal ions and anions have been studied. However, calix[4]quinones, in particular, are superior to ferrocenes because of the direct involvement of the calixarene framework. Therefore, one can design and construct a molecular sensor from a calix[4]quinone using its available oxygen atoms as donors for binding alkali cations.[5] This should enhance both the selectivity and sensitivity of the sensors. A number of biscalixarenes have been synthesized and their binding studies with metal ions have been reported.[6] It is of interest to synthesize different biscalix[4]arenes using ethylene bridges connecting lower rim phenoxy groups. The substituents at the other *o*-phenoxy groups can also be varied. Upon oxidation, we expect to obtain various kinds of biscalix[4]quinones possessing a different number and various positions for the quinone moieties. This should lead to new selectivity and sensitivity for the compounds.

Biscalix[4]arene **7** has been synthesized in one step. Nucleophilic substitution reactions of *p*-*tert*-butylcalix[4]arene (**1**) with bromoethyl tosylate (**3**) using K_2CO_3 as base yielded compound **7** in 41% yield.[7] This reaction also produced bisbromoethoxy calix[4]arene in 23% yield. This result implies that the coupling process occurred in a stepwise manner in which bisbromoethoxy calix[4]arene was produced in the first step. Subsequent nucleophilic substitution with another unit of calix[4]arene resulted in **7**. Janssen et al. found that the use of pressure for selective alkylation of calix[6]arene resulted in a high yield of the alkylated products.[8] Ostaszewski and Jurczak also reported the use of high pressure in the synthesis of simple and chiral bicyclic cryptands and diazacoronands that produced the desired products in high yield.[9] The high-pressure approach was thus used in the synthesis of **7** aiming to increase the cyclization rate. The reaction between **1** and bromoethyl tosylate (**3**) in acetonitrile in the presence of K_2CO_3 in a pressurized vessel which was compressed with N_2 at 50 psi and heated at 100°C yielded **7** in 69% yield as shown in Eq. (1).[10] Compound **7** was thus obtained in a very high yield upon applying high pressure, and bisbromoethoxy calix[4]arene was not found in the reaction.

Keywords: biscalixarene; quinone; cyclic voltammetry.

* Corresponding author.

PII: S0040-4039(02)02520-0

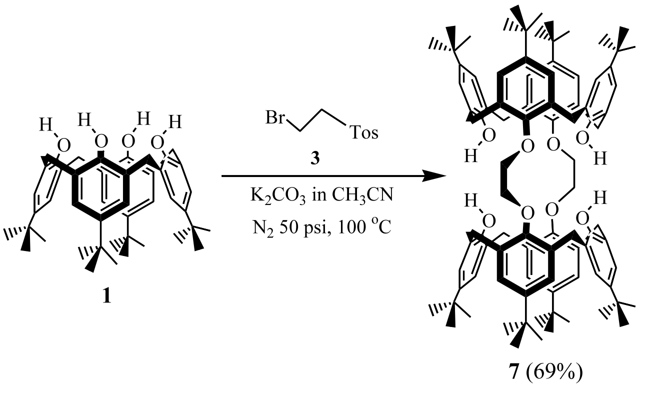

(1)

The one-pot synthesis is only suitable for preparing a symmetric biscalix[4]arene. To synthesize unsymmetric biscalix[4]arenes for further fabrication to biscalix[4]quinones having different quinone moieties, however, needs stepwise synthetic approaches. Compounds **7** and **8** can be prepared in a stepwise manner as shown in Scheme 1.

The diethyl ester calix[4]arene **4** was synthesized according to the published procedure with slight modification.[11] The reaction of **1** with ethyl bromoacetate (2.5 equiv.) in CH_3CN using K_2CO_3 as base and refluxing for 4 h resulted in compound **4** which can be easily separated from the mixture in 85% yield by addition of CH_3OH into its CH_2Cl_2 solution. The compound **4** was subsequently reduced with 3 equiv. of $LiAlH_4$ in dry THF at 0°C to yield the dialcohol **5**[12] in 97% yield. To facilitate the nucleophilic substitution reaction, the –OH groups were changed to methylsufonate (mesyl) groups by the addition of methanesulfonyl chloride (3.0 equiv.) in the presence of Et_3N (3 equiv.) and a catalytic amount of DMAP. The disulfonyl ester **6**[13] was obtained in 96% yield. The compound **6** acts as a building block for constructing both symmetric and unsymmetric biscalix[4]arenes. Finally, the coupling reaction of **1** and **6** in CH_3CN using K_2CO_3 as base resulted in the symmetric biscalix[4]arene **7** in 24% yield. It is clearly seen that in the case of the symmetric biscalix[4]arene, the one-pot synthetic approach gives much higher yields than that of the stepwise synthesis. Nevertheless, the stepwise synthesis is good for preparing unsymmetric biscalixarenes. The coupling reaction of **6** and **2**[14] in THF using NaH as base resulted in the unsymmetric biscalix[4]arene **8**[15] in 18% yield. The oxidation of compounds **7** and **8** using $Tl(CF_3CO_2)_3$ in CF_3COOH resulted in yellowish biscalix[4]tetraquinone, **9** (21%),[16] and biscalix[4]arenediquinone, **10** (56%),[17] respectively.

Echegoyen and co-workers have shown that there are marked perturbations of the quinone redox couples of calix[4]quinones on addition of sodium cations.[5] We thus investigated the electrochemical properties of com-

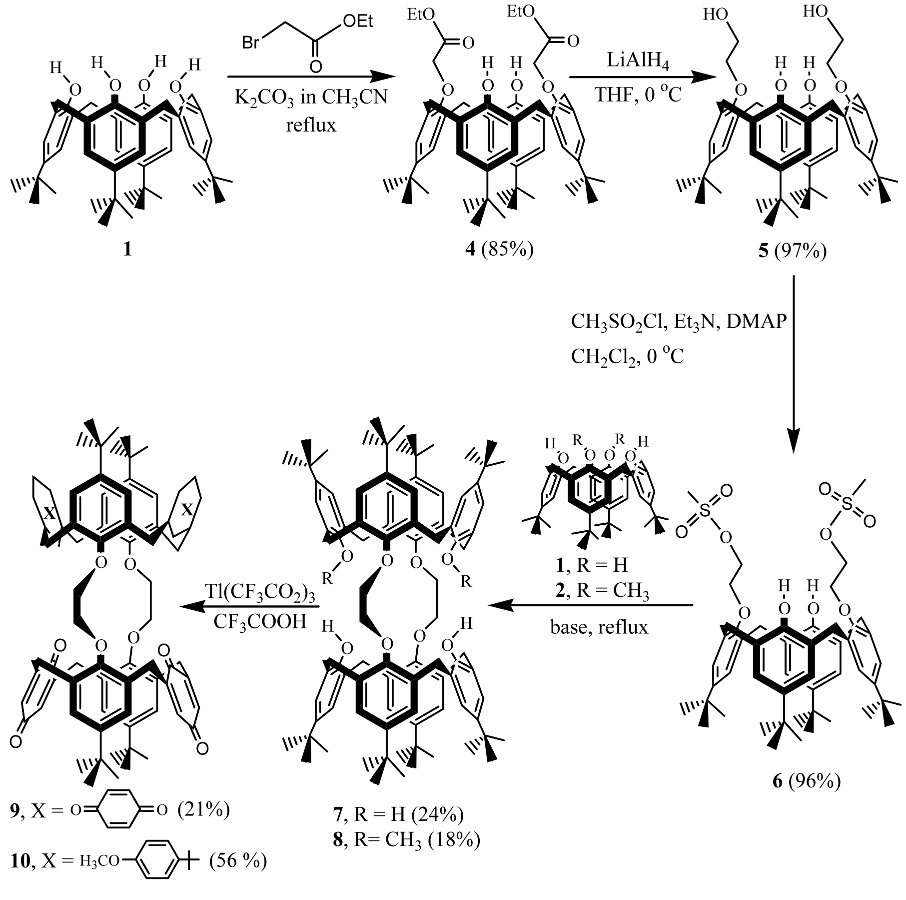

Scheme 1.

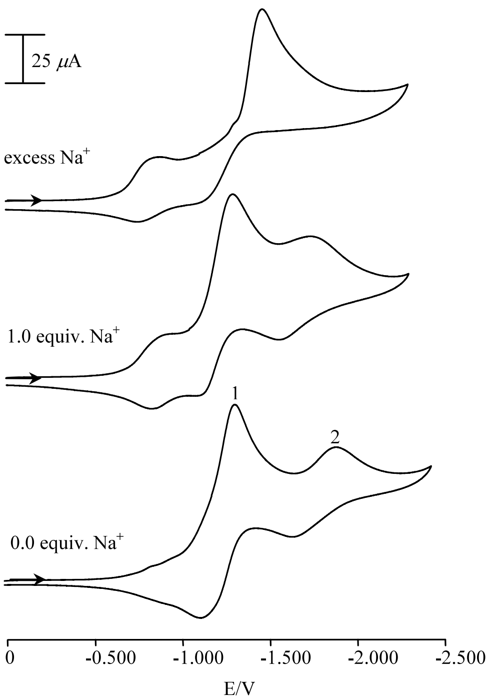

Figure 1. Voltammogram of **9** in 20% DCM in CH_3CN using tetrabutylammonium tetrafluoroborate ($TBABF_4$) as supporting electrolyte at a scan rate of 50 mV/s.

pounds **9** and **10** by cyclic voltammetry in 20% DCM in CH_3CN using tetrabutylammonium tetrafluoroborate ($TBABF_4$) as supporting electrolyte.[18] Compound **9** showed two broad quasi-reversible redox waves 1 and 2 at −1.235 and −1.790 V, respectively (Fig. 1) indicating a complicated electron transfer mechanism which was quite similar to the behavior of the biscalix[4]arene tetraquinone possessing a longer spacer reported by Beer and co-workers.[19] Interestingly, upon addition of 1 equiv. of Na^+ (ClO_4^- as counter cation), a new reversible reduction wave at −0.885 V appears in the voltammogram and the quasi-reversible reduction wave 2 shifts more anodically while wave 1 shifts insignificantly. However, adding excess Na^+ results in the disappearance of both waves 1 and 2 and the appearance of an irreversible wave at −1.466 V. This may indicate that Na^+ forms a more stable complex with the reduced form of **9**.

Cyclic voltammograms (CV) of compound **10** exhibit three waves 1, 2 and 3 at −1.092, −1.201 and −1.754 V, respectively (Fig. 2). This voltammogram is similar to the calixdiquinone esters and amides reported by Beer and colleagues.[20] The first two couples indicate two one-electron transfer processes. Wave 3 is an irreversible wave probably involving a reduction of the quinone to its radical form and subsequent protonation to the hydroquinone. However, upon increasing the scan rate, two new irreversible oxidation waves appear at −0.750 and −0.337 V. This may signify that wave 3 represents a two-electron transfer reduction process. The result suggests that **10** undergoes an electron transfer, electron transfer and chemical reaction (EEC) mechanism.

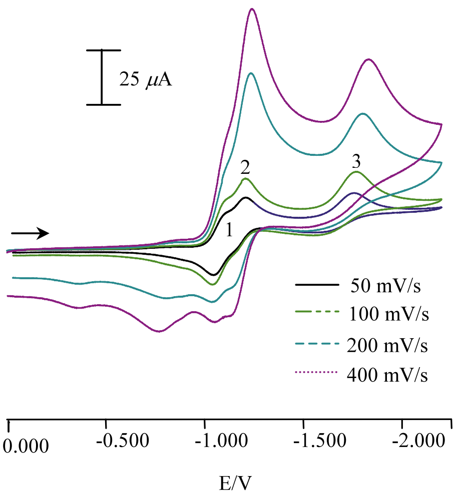

Figure 2. Voltammogram of **10** in 20% DCM in CH_3CN using tetrabutylammonium tetrafluoroborate ($TBABF_4$) as supporting electrolyte at various scan rates.

On addition of Na^+ (1 equiv.) to the solution of **10**, a new wave at −0.880 V appears in the voltammogram. However, upon adding excess Na^+, the current of the wave at −0.880 V increases, waves 1 and 2 disappear and a quasi-reversible wave at −1.334 V appears in the voltammogram (Fig. 3). In addition, wave 3 at −1.754 V becomes reversible. Biscalix[4]quinone **10** thus shows a significant change of its CV waves upon complexing Na^+.

In summary, we have synthesized two new biscalix[4]arenes (**7** and **8**) and two biscalix[4]quinones (**9**

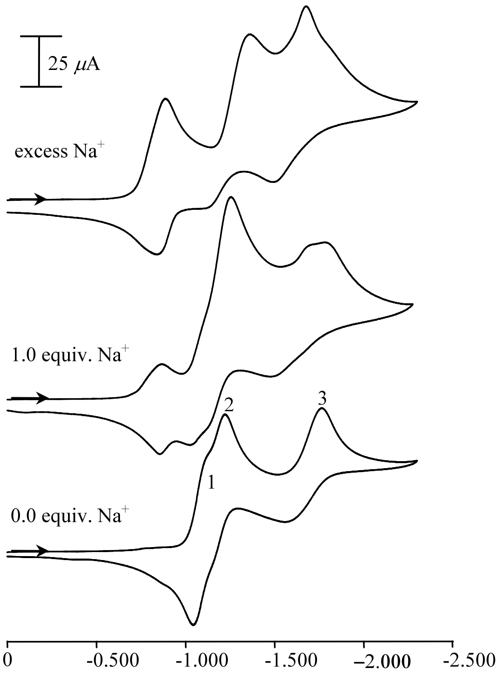

Figure 3. Voltammogram of **10** upon addition of Na^+ in 20% DCM in CH_3CN using tetrabutyl ammonium tetrafluoroborate ($TBABF_4$) as supporting electrolyte at a scan rate of 50 mV/s.

and **10**). We also show that the use of pressure increases the yield of the symmetric biscalix[4]arene **7**. Calixquinones **9** and **10** exhibit interesting electrochemical properties and show a promising ability to sense Na^+. We are currently pursuing electrochemical studies of the compounds synthesized towards other alkali metal ions and the results will be reported in due course.

Acknowledgements

This work was financially supported by the Thailand Research Fund (Grant no. RSA/06/2544). Authors thank Professor Jeremy Kilburn for the ESI MS results.

References

1. Cattrall, R. W. *Chemical Sensors*, *Oxford Chemistry Primers*; Oxford Science Publisher: Oxford, UK, 1997.
2. Beer, P. D. *Acc. Chem. Res.* **1998**, *31*, 71.
3. (a) Cooper, J. B.; Drew, M. G. B.; Beer, P. D. *J. Chem. Soc., Dalton Trans.* **2000**, 2721; (b) Beer, P. D.; Hesek, D.; Nam, K. C.; Drew, M. G. B. *Organometallics* **1999**, *18*, 3933.
4. (a) Chung, T. D.; Kang, S. K.; Kim, H.; Kim, J. R.; Oh, W. S.; Chang, S.-K. *Chem. Lett.* **1998**, 1225; (b) Nam, K. C.; Kang, S. O.; Jeong, H. S.; Jeon, S. *Tetrahedron Lett.* **1999**, *40*, 7343.
5. Gómez-Kaifer, M.; Reddy, P. A.; Gutsche, C. D.; Echegoyen, L. *J. Am. Chem. Soc.* **1994**, *116*, 3580.
6. Asfari, Z.; Weiss, J.; Vicens, J. *Synlett* **1993**, 719.
7. Tomapatanaget, B.; Pulpoka, B.; Tuntulani, T. *Chem. Lett.* **1998**, 1037.
8. Janssen, R. G.; Verboom, W.; Reinhoudt, D. N.; Casnati, A.; Freriks, M.; Pochini, A.; Ugozzoli, F.; Ungaro, R.; Nieto, P. M.; Carramolino, M.; Cuevas, F.; Prados, P.; de Mendoza, J. *Synthesis* **1993**, 380.
9. Jurczak, J.; Ostaszewski, R. *J. Coord. Chem. Part B* **1992**, *27*, 201.
10. In a high pressure tube (Ace Glass Co., Catalog No. 8648-29) equipped with valves and pressure gauge, *p*-*tert*-butylcalix[4]arene, **1**, (3.0 g, 4.62 mmol), catalytic amount of 18-crown-6, bromoethyl tosylate, **3**, (1.3 g, 4.62 mmol) and K_2CO_3 (1.3 g, 9.24 mmol) were suspended in anhydrous acetonitrile (10 mL). The tube was then pressurized with N_2 at 50 psi. The mixture was stirred and heated at 100°C for 4 days. The solution was allowed to cool to room temperature. The pressure in the tube was then released. The solvent was evaporated to dryness to yield a yellow residue. The residue was dissolved in dichloromethane (100 mL) and an aqueous solution of 3 M hydrochloric acid was subsequently added until the pH of the solution reached pH 1. The mixture was extracted with dichloromethane (3×50 mL). The combined organic layer was dried over anhydrous Na_2SO_4, filtered and concentrated on rotary evaporator to obtained a white solid of **7**. The product was recrystallized in dichloromethane upon addition of methanol to afford a white crystalline solid (2.16 g, 69%). **7**: ^{1}H NMR spectrum (200 MHz, $CDCl_3$) δ 7.65 (s, 4H, ArO*H*), 7.00 (s, 8H, *m*-*H*ArOH), 6.82 (s, 8H, *m*-*H*ArOCH$_2$CH$_2$Ar*H*), 4.55 (s, 8H, ArOC*H*$_2$C*H*$_2$OAr), 3.55 and 4.50 (d each, $J_{H-H}=14.0$ Hz, 16H, Ar C*H*$_2$Ar), 1.25 (s, 36H, HOAr-*t*-C$_4$*H*$_9$), 0.99 (s, 36H, ROAr-*t*-C$_4$*H*$_9$). FAB MS (*m*/*z*): 1367.8 [M^++NH_4^+]. Anal. calcd for **7** ($C_{92}H_{116}O_8$): C, 81.86; H, 8.66. Found: C, 81.86; H, 8.86.
11. Collins, E. M.; McKervey, M. A.; Madigan, E.; Moran, M. B.; Owens, M.; Ferguson, G.; Harris, S. J. *J. Chem. Soc., Perkin Trans. 1* **1991**, 3137.
12. **5**: ^{1}H NMR spectrum (200 MHz, $CDCl_3$) δ 9.23 (s, 2H, ArO*H*), 7.07 (s, 4H, *m*-HOAr*H*), 7.01 (s, 4H, *m*-ROAr*H*), 5.2 (s, 2H, -CH$_2$CH$_2$O*H*), 4.29 (t, 8H, ArOC*H*$_2$C*H*$_2$OH), 3.43 and 4.30 (d, $J_{H-H}=14.0$ Hz, 8H, ArC*H*$_2$Ar), 1.20 (s, 18H, ROAr-*t*-C$_4$*H*$_9$), 1.19 (s, 18H, HOAr-*t*-C$_4$*H*$_9$).
13. **6**: ^{1}H NMR spectrum (200 MHz, $CDCl_3$) δ 7.06 (s, 4H, ROAr*H*), 6.74 (s, 4H, HOAr*H*), 6.67 (s, 2H, ArO*H*), 4.64 (m, 4H, MsC*H*$_2$C*H*$_2$O), 3.36 (m, 8H, ArC*H*$_2$Ar and MsOC*H*$_2$C*H*$_2$O), 4.24 (d, $J_{H-H}=13$ Hz, 4H, ArC*H*$_2$Ar), 3.23 (s, 6H, SO$_2$C*H*$_3$), 1.28 (s, 18H, HOAr-*t*-C$_4$*H*$_9$), 0.90 (s, 18H, ROAr-*t*-C$_4$H$_9$).
14. Gutsche, C. D.; Dhawan, B.; Levine, J. A.; No, K. Y.; Bauer, L. J. *Tetrahedron* **1983**, *39*, 409.
15. **8**: ^{1}H NMR spectrum (200 MHz, $CDCl_3$) δ 7.09–6.70 (m, 18H, *H*Ar and ArO*H*), 4.78–4.12 (m, 22H, OC*H*$_2$C*H*$_2$O, ArC*H*$_2$Ar and –OC*H*$_3$), 3.40–3.15 (m, 8H, ArC*H*$_2$Ar), 1.30 (s, 18H, Ar-*t*-C$_4$*H*$_9$), 1.25 (s, 18H, Ar-*t*-C$_4$*H*$_9$), 0.92 (s, 36H, Ar-*t*-C$_4$*H*$_9$). ESI MS (*m*/*z*): 1395.2 (M^++NH_4^+).
16. **9**: ^{1}H NMR spectrum (200 MHz, $CDCl_3$) δ 7.10 (s, 8H, ROAr*H*), 5.86 (s, 8H, $H_{quinone}$), 4.39 (s, 8H, OC*H*$_2$C*H*$_2$O), 4.52 and 3.00 (dd, $J_{H-H}=13.9$ Hz, 16H, ArC*H*$_2$Ar), 1.33 (s, 36H, Ar-*t*-C$_4$*H*$_9$). ESI MS (*m*/*z*): 1203.4 (M^++4H+NH_4^+). IR (ν_{CO}): 1664.86 cm^{-1}. Anal. calcd for **9** ($C_{76}H_{76}O_{12}\cdot 2H_2O$): C, 74.98; H, 6.62. Found: C, 74.99; H, 6.20.
17. **10**: ^{1}H NMR spectrum (200 MHz, $CDCl_3$) δ 7.15 (br s, 12H, *H*ArOR), 6.50 (s, 4H, $H_{quinone}$), 4.70–4.40 (m, 16H, OC*H*$_2$C*H*$_2$O, ArC*H*$_2$Ar), 4.15 (s, 6H, -OC*H*$_3$), 3.38–3.12 (m, 8H, ArC*H*$_2$Ar), 1.30 (s, 36H, Ar-*t*-C$_4$*H*$_9$), 0.80 (s, 18H, Ar-*t*-C$_4$*H*$_9$). ESI MS (*m*/*z*): 1315.8 (M^++4H+NH_4^+). IR (ν_{CO}): 1657.14 cm^{-1}. Anal. calcd for **10** ($C_{86}H_{100}O_{10}\cdot 3H_2O$): C, 76.64; H, 7.93. Found: C, 77.20; H, 8.52.
18. CV experiments were carried out on an AUTOLAB PGSTAT100 potentiostat using a glassy carbon working electrode, a Ag/AgNO$_3$ reference electrode and a platinum auxiliary electrode. All experiments were performed under N_2.
19. Webber, P. R. A.; Chen, G. Z.; Drew, M. G. B.; Beer, P. D. *Angew. Chem., Int. Ed.* **2001**, *40*, 2265.
20. Beer, P. D.; Gale, P. A.; Chen, Z.; Drew, M. G. B.; Heath, J. A.; Ogden, M. I.; Powell, H. R. *Inorg. Chem.* **1997**, *36*, 5880.

ORGANIC
LETTERS

2003
Vol. 5, No. 9
1539−1542

Calix[4]arenes Containing Ferrocene Amide as Carboxylate Anion Receptors and Sensors

Boosayarat Tomapatanaget, Thawatchai Tuntulani,* and Orawon Chailapakul

Department of Chemistry, Faculty of Science, Chulalongkorn University, Bangkok 10330, Thailand

tthawatc@chula.ac.th

Received February 28, 2003

ABSTRACT

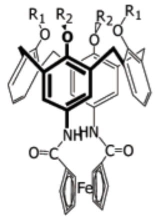

L1 : $R_1 = R_2 = CH_3$
L2 : $R_1 = CH_3$, $R_2 = CH_2COOEt$
L3 : $R_1 = R_2 = CH_2COOEt$

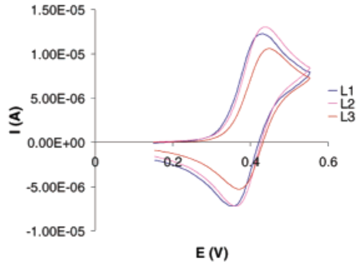

Calix[4]arene derivatives containing amide ferrocene units at the wide rim and ethyl ester groups at the narrow rim, L1–L3, were synthesized and their anion binding and sensing properties were investigated. It was found from ^1H NMR titrations that L1–L3 were able to bind selectively with carboxylate anions. Moreover, cyclic voltammetry and square wave voltammetry showed that L1–L3 were able to act as electrochemical sensors for carboxylate anions.

Anion recognition is an area of interest for biological systems and environmental pollutants. It is thus important to fabricate new anion sensors or develop new techniques for sensing anions. Artificial molecules are constructed to have anion binding sites linked to a sensory unit. Generally, chemists have employed either hydrogen bonding receptors or cationic receptors such as amide, guanidinium, pyridinium, and urea or thiourea groups for binding anions.[1] Ferrocene and cobaltocene have been used as electrochemical responding units, as they give a reversible redox couple in cyclic voltammograms. Additionally, cyclopentadienes can be easily modified. Beer and co-workers are pioneers in making metallocene amide receptors for binding and sensing anions.[2]

Recently, ion-pair recognition has been recognized by supramolecular chemists due to its potential applications in metal ion and anion attraction or metal-controlled anion sensing devices.[3] Beer and co-workers have synthesized a number of ditopic receptors that can undergo selective ion-pair recognition. Rhenium(I) bipyridyl amide crown ether receptors were found to complex KCl ion pairs.[4a] A tripodal tris(amido benzo-15-crown-5) ligand was found to cooperatively bind chloride, iodide, and perrhenate anions via cobound crown ether-complexed sodium cations.[4b] Reinhoudt and co-workers have synthesized an elegant calix[4]arene derivative with cation binding ester groups on the narrow rim and anion binding urea groups on the wide rim. The compound was able to bind Cl^- efficiently in the presence of Na^+.[5]

Our group is interested in synthesizing ion-pair receptors and sensors. Calix[4]arene is an excellent supramolecular

---

[1] Schmidtchen, F. P.; Berger, M. *Chem. Rev.* **1997**, *97*, 1609.

[2] (a) Beer, P. D.; Graydon, A. R.; Johnson, A. O. M.; Smith, D. K. *Inorg. Chem.* **1997**, *36*, 2112. (b) Beer, P. D.; Drew, M. G. B.; Hesek, D.; Nam, K. C. *Organometallics* **1999**, *18*, 3933.

[3] Gale, P. A. *Coord. Chem. Rev.* In press.

[4] (a) Redman, J. E.; Beer, P. D.; Dent, S. W.; Drew, M. G. B. *Chem. Commun.* **1998**, 231−232. (b) Beer, P. D.; Hopkins, P. K.; McKinney, J. D. *Chem. Commun.* **1999**, 1253−1254.

[5] Scheerder, J.; van Duynhoven, J. P. M.; Engbersen, J. F. J.; Reinhoudt, D. N. *Angew. Chem., Int. Ed. Engl.* **1996**, *35*, 1090.

10.1021/ol034355+ CCC: $25.00

building block for this purpose. We synthesized a tripodal amine-capped calix[4]arene. In its ammonium form, the receptor increased its affinity for Br^- in the presence of K^+.[6] In this paper, we report new receptors and sensors for both cations and anions. Our strategy is to attach the cation binding groups, ethyl esters, to the narrow rim of calix[4]-arene and the sensory units, ferrocenes, to the amide units acting as anion receptors at the wider rim. The ethyl ester groups also serve as inhibitors for phenyl ring rotation. We have thus synthesized three calix[4]arene derivatives, **L1**−**L3** (Figure 1).

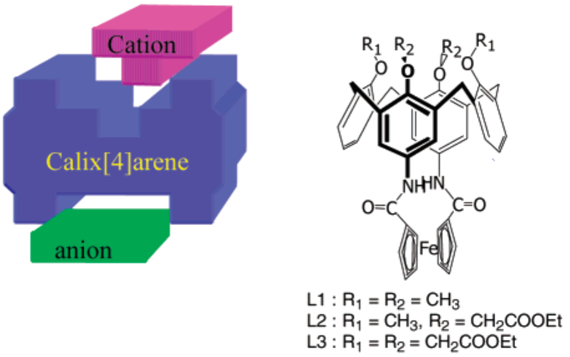

Figure 1. Schematic diagram for designed receptors.

The preparation of ethylester ferrocene amide and methoxy ferrocene amide calix[4]arenes **L1**−**L3** was reported previously.[7] NMR techniques such as COSY, NOESY, HMQC, and HMBC indicated that **L1** and **L2** exist as mixtures of cone and partial cone conformations (Supporting Information), while **L3** is in a cone conformation.

We studied the binding ability of the three ligands toward anions such as $PhCO_2^-$, $CH_3CO_2^-$, $H_2PO_4^-$, HSO_4^-, NO_3^-, Cl^-, Br^-, and I^- as their tetrabutylammonium salts by ^1H NMR titrations in CD_3CN. The NH protons of the amide groups in the three compounds were monitored. For all ligands, the NH signal did not shift upon addition of Br^-, I^-, NO_3^-, or HSO_4^-, signifying that **L1**−**L3** did not form complexes with these anions. Upon addition of $PhCO_2^-$ or $CH_3CO_2^-$, significant downfield shifts of the NH protons of **L1**−**L3** were observed due to hydrogen bonding interactions. Smaller shifts of the NH signals were found in the cases of $H_2PO_4^-$ and Cl^-. The titration curves for **L3** with $PhCO_2^-$, $CH_3CO_2^-$, $H_2PO_4^-$, and Cl^- are shown in Figure 2. Two different N*H* signals were observed at 8.09 and 7.86 ppm for **L1** and at 8.10 and 7.88 ppm for **L2** belonging to the amide NH protons of their partial cone and cone conformations, respectively. In CD_3CN, both cone and partial cone conformation ratios of **L1** and **L2** are constant. Therefore, ^1H NMR titrations can be carried out and *K* values can be calculated for each conformation. Stability constants of compounds **L1**−**L3** toward various anions calculated by the program EQNMR[8] are summarized in Table 1.

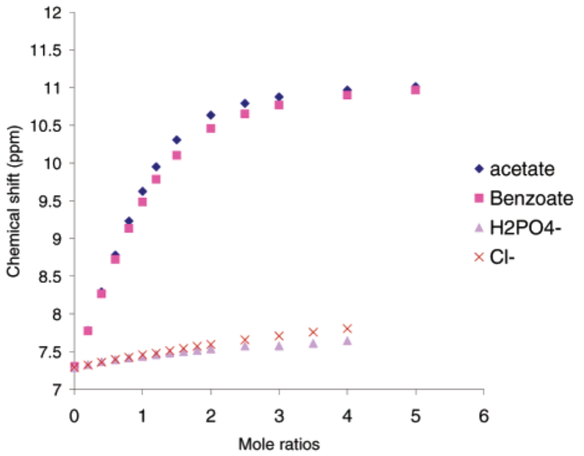

Figure 2. Titration curves of **L3** with various anions in CD_3CN.

Table 1. Stability Constants of Compounds **L1**−**L3** toward Various Anions at Room Temperature in CD_3CN-d^3 (M^{-1})

	L1		**L2**		**L3**
anions	PC	C	PC	C	C
$PhCOO^-$	540	472	139	100	915
CH_3COO^-	826	741	227	174	1200
$H_2PO_4^-$	34	a	91	94	a
Cl^-	32	a	49	86	29

[a] PC = partial cone conformation; C = cone conformation a. *K* values could not be refined. All association constants have errors of less than 10%.

Compounds **L1**−**L3** possess amide NH groups that can form bidentate-like hydrogen bonding interactions with carboxylate anions and $H_2PO_4^-$. Moreover, all ligands bind preferentially with acetate over benzoate because acetate is more basic than benzoate.[9] Interestingly, **L3** has a higher affinity for anions compared to **L1** and **L2** since **L3** is rigidified by four bulky ethyl ester groups to give a high degree of preorganization. Ethyl ester groups on aromatic rings are also electron-withdrawing groups. This enhances the acidity of the amide NH protons. Cl^- and $H_2PO_4^-$ anions give smaller *K* values than acetate and benzoate, probably due to the mismatched structure for spherical and tetrahedral anions.

The effects of alkali metal ions on the anion affinity of compound **L3** have also been studied. Unfortunately, upon

---

(6) Tuntulani, T.; Poompradub, S.; Thavornyutikarn, P.; Jaiboon, N.; Ruangpornvisuti, V.; Chaichit, N.; Asfari, Z.; Vicens, J. *Tetrahedron Lett.* **2001**, *42*, 5541.

(7) Tomapatanaget, B.; Tuntulani, T. *Tetrahedron Lett.* **2001**, *42*, 8105. Details of syntheses and characterization can be found in Supporting Information.

(8) Hynes, M. J. *J. Chem. Soc., Dalton Trans.* **1993**, 311.

(9) Izutsu, K. *Acid−Base Dissocation Constants in Dipolar Aprotic Solvents*; Blackwell Scientific Publications: Oxford, 1990.

addition of metal cations, white precipitates of metal salts always formed and the chemical shift of the NH protons did not change. This suggests that the added metal ions formed complexes with the bound anions and precipitated as salts. This also implies that the metal cations bind loosely in the ethyl ester cavity. However, the complexation of the ligands with alkali metals such as Na^+, K^+, Rb^+, and Cs^+ can be studied by ESI mass spectrometry. The molecular mass peaks of complexes between **L3** and Na^+, K^+, Rb^+, and Cs^+ were found at 1059.90, 1076.00, 1122.39, and 1169.81 *m*/*z*, respectively.

The electrochemical properties of ligands **L1**−**L3** can be studied by cyclic voltammetry and square wave voltammetry. Cyclic voltammetry (CV) and square wave voltammetry (SWV) were performed using solutions of **L1**−**L3** (1×10^{-3} M) prepared in anhydrous acetonitrile with 0.1 M Bu_4NPF_6 as a supporting electrolyte and using a glassy carbon working electrode, a Ag/Ag^+ reference electrode, and a Pt wire counter electrode. The potential was scanned in the range of 0.15−0.55 V at 50 mV/s. Cyclic voltammograms of **L1**−**L3** showed reversible redox couples of ferrocene/ferricinium at $E_{1/2}$ of 0.383, 0.399, and 0.417 mV, respectively, as shown in Figure 3.

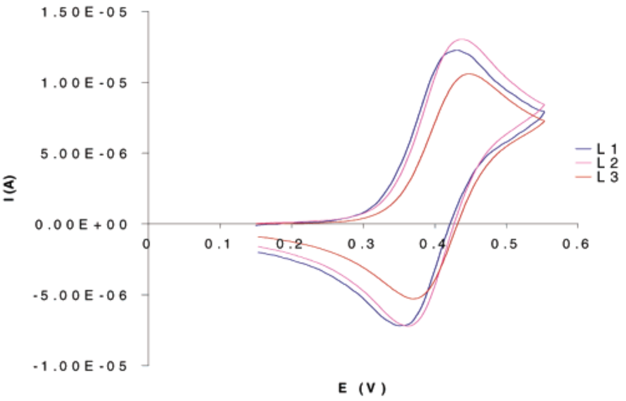

Figure 3. Cyclic voltammograms of **L1**−**L3**.

In light of results from ^1H NMR titrations, acetate, benzoate, $H_2PO_4^-$, and Cl^- were subjected to electrochemical investigation in order to study the effect of anions on the electron-transfer process of the ferrocene units in **L1**−**L3**. Titrations were carried out by addition of aliquots of tetrabutylammonium salts of benzoate, acetate, $H_2PO_4^-$, and Cl^-, followed by CV and SWV measurements at a scan rate of 50 mV/s. Addition of anions was generally varied from 0.2 to 4.0 equiv. Titrations of **L1**−**L3** with benzoate anion display a progressive appearance of a new oxidation wave at a less positive potential and a progressive disappearance of the initial oxidation and reduction wave. In a square wave voltammogram, it has been found that a new wave gradually appears at a less positive potential, while the initial wave decreases and disappears completely. The replacement of the initial wave by the new one is complete after addition of excess anionic species (2.5 equiv). In the case of cyclic voltammograms, the complexes of all ligands and anions (benzoate and acetate) result in quasireversible voltammograms when 0.2−3.0 equiv of anions were added and voltammograms became completely irreversible after adding 4 equiv of anions. Presumably, the ferricinium (Fc^+) unit enhances binding with anionic species through electrostatic interactions (ion-pairing interactions). Anions, then, inhibit the electron-transfer back to ferrocene (Fc). Cyclic voltammograms and square wave voltammograms of **L3** with benzoate are shown in Figure 4.

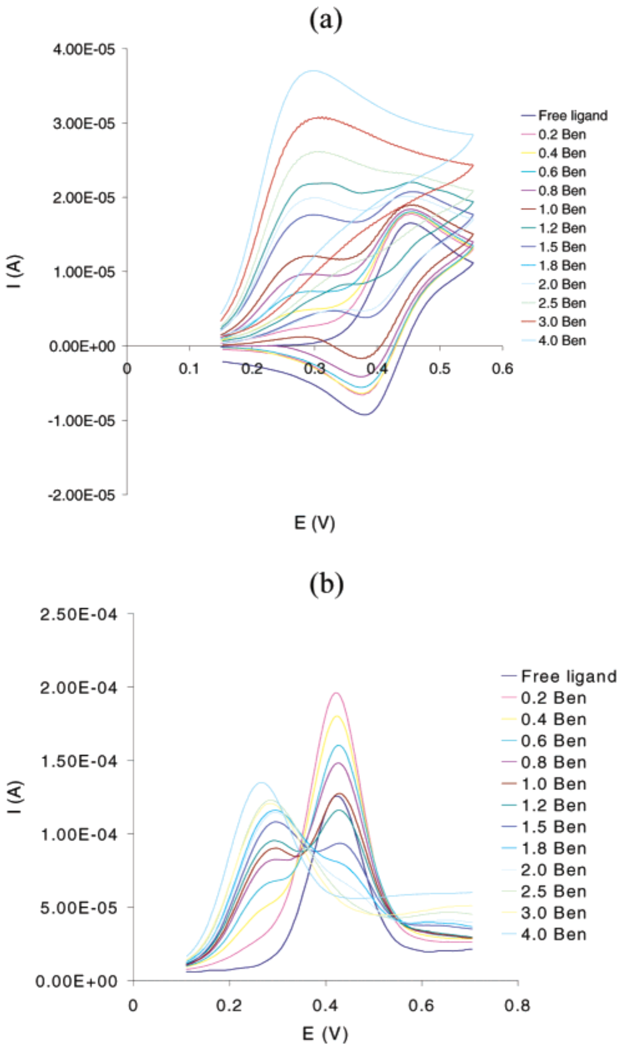

Figure 4. Titrations of **L3** and benzoate in CH_3CN with 0.1 M TBAPF and a scan rate of 50 mV/s: (a) CV titrations and (b) SWV titrations. Ben = benzoate.

The mechanism of electrochemical and anion binding processes can be deduced as shown in Scheme 1 and is similar to the Echegoyen−Kaifer model.[10] The complexes of Fc^+A^- can occur by two pathways. In one pathway, Fc may bind anionic species via amide NH groups by hydrogen bonding interactions to produce the complex of FcA^-, which

Scheme 1. Mechanism of Electrochemical Properties for Complexes

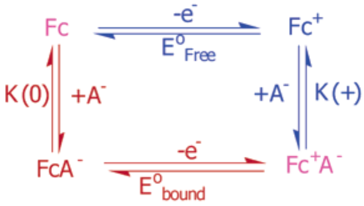

is then oxidized to give Fc^+A^-. Alternatively, a Fc unit is first oxidized to a Fc^+ unit and subsequently binds anions, exploiting the synergy of hydrogen bonding interactions via the NH groups and electrostatic interactions. This causes the enhancement of binding ability of the ferricinium form toward anions.

The enhancement of binding constants ($K_{(+)}/K_{(0)}$) upon complexing anions to the ferricinium forms can be calculated from the relationship shown in eq 1.[10]

$$nF(E^\circ_{\text{bound}} - E^\circ_{\text{free}}) = RT \ln(K_{(+)}/K_{(0)}) \qquad (1)$$

$K_{(+)}$ = association constant of anion with ferricinium

$K_{(L)}$ = association constant of anion with ferrocene

Astruc and co-workers reported the enhancement of the binding constants of ferricinium units toward anions in their ferrocene amide dendrimer upon electrochemical oxidation of the ferrocene units.[11] They found that cyclic voltammogram of their dendrimers showed reversible peak shifts to less positive potentials upon addition of $H_2PO_4^-$ and they could calculate $K_{(+)}$ values. In our case, due to the quasi-reversible behavior of the cyclic voltammograms upon addition of anions, we can calculate only the binding enhancements as shown in Table 2.

Table 2. Binding Enhancements ($K_{(+)}/K_{(0)}$) of **L1**−**L3** with Various Anions Measured by Cyclic Voltammetry Techniques in CH_3CN with 0.1 M TBAPF and a Scan Rate at 50 mV/s

	L1	**L2**	**L3**
$C_6H_5COO^-$	85	200	200
CH_3COO^-	23	99	158
$H_2PO_4^-$	a	a	a
Cl^-	a	a	a

[a] Values could not be calculated.

From the results in Table 2, the ferricinium forms of **L1**−**L3** prefer to bind benzoate. The electrons on benzoate are stabilized by the aromatic ring, resulting in a stable negative charge, and the electron cloud of the aromatic ring also enhances the electrostatic interaction with the ferricinium form. Interestingly, the cyclic voltammograms of titrations of the three ligands with $H_2PO_4^-$ and Cl^- show only a slight shift in potential. The binding enhancement for these anions cannot be calculated. The electrochemical results thus agree with the ^{1}H NMR titration in that all three ligands recognize carboxylate anions better than $H_2PO_4^-$ and Cl^-.

In summary, we synthesized three calix[4]arene derivatives and found that all ligands can be anion receptors and sensors. All three ligands have selectivity for carboxylate anions. Enhancement of binding constants by electrostatic interactions takes place for the ferricinium forms of **L1**−**L3**.

Acknowledgment. This work was financially supported by the Thailand Research Fund (RSA/06/2544 and PHD/0182/2542). B.T. is a Ph.D. student with support from the Royal Golden Jubilee Program.

Supporting Information Available: Detailed experimental procedures, two-dimensional NMR spectra of **L1** and **L2**, ^{1}H NMR titration plots, and CV and SWV plots. This material is available free of charge via the Internet at http://pubs.acs.org.

OL034355+

---

(10) Miller, S. R.; Gustowski, D. A.; Chen, Z.-H.; Gokel, G. W.; Echegoyen, L.; Kaifer, A. E. *Anal. Chem.* **1988**, *60*, 2021.

(11) (a) Valerio, C.; Fillllaut, J.-L.; Ruiz, J.; Guittard, J.; Astruc, D. *J. Am. Chem. Soc.* **1997**, *119*, 2588. (b) Ruiz, J.; Medel, M. J. R.; Daniel, M.-C.; Blais, J.-C.; Astruc, D. *Chem. Commun.* **2003**, 464. (c) Daniel, M.-C.; Ruiz, J.; Astruc, D. *J. Am. Chem. Soc.* **2003**, *125*, 1150.